THE JOURNAL
OF
CHEMICAL PHYSICS

VOLUME 7 OCTOBER, 1939 NUMBER 10

The Infra-Red Absorption Spectrum of Gaseous Cyanogen, C_2N_2

C. R. BAILEY AND S. C. CARSON
University College, London, England

(Received June 12, 1939)

A discussion of the thermodynamic functions of cyanogen recently appeared in this journal. We therefore think it of interest to describe our re-examination of the infra-red spectrum. The structure of the bands is critical in arriving at a satisfactory assignment of the fundamental frequencies and we have been able to obtain some additional evidence on this question.

EXPERIMENTAL

1. Apparatus

THE apparatus has been described in previous communications from this laboratory; a Hilger D42 spectrometer is used furnished with quartz, fluorite, rocksalt, sylvine and potassium bromide prisms all of approximately 60° angle. With regard to the dispersion of potassium bromide the early values given by Gundelach[1] are in error; thus calibration curves constructed for the instrument from these data gave an error of some 26 cm^{-1} in the maximum of the CS_2 fundamental at 25.2μ;[2] the latter values obtained by Korth[3] appear to be more accurate.

We have always taken great care to check our calibrations against well-defined bench marks in the infra-red and to observe temperature and setting corrections where necessary. It should be remarked here that a fictitious accuracy is often accorded to measurements obtained in the short wave regions particularly from about 4μ to 1μ. The effective slit width may vary from say 10 to 70 cm^{-1} in this region under the most favorable conditions, and as a consequence not merely is the determination of the center of a band subject to considerable error, but the experimental contour at this low resolution may be markedly different from that obtained with a grating instrument. The latter effect produces shifts in the apparent maximum of the CO_2 fundamental at 4.25μ with the amount of CO_2 in the air: the shape of envelope is also affected by the presence of foreign gases, slightly different readings being obtained for atmospheric CO_2 compared with a pure sample in the absorption tube.

2. Preparation of the gas

Cyanogen was prepared either by heating mercuric cyanide or from a mixture of potassium cyanide and copper sulphate solutions. The latter method produces spectroscopically large amounts of hydrogen cyanide, a substance which has many very powerful absorption bands. A small proportion was also present in the gas from mercuric cyanide, but a threefold distillation over mercuric oxide was sufficient to remove all traces of the impurity.

EXPERIMENTAL RESULTS

The short wave infra-red spectrum of gaseous cyanogen was previously examined by Bur-

[1] E. Gundelach, Zeits. f. Physik **66**, 775 (1930).
[2] D. M. Dennison and N. Wright, Phys. Rev. **38**, 2077 (1931).
[3] K. Korth, Zeits. f. Physik **84**, 677 (1933).

TABLE I. *The infra-red absorption spectrum of gaseous cyanogen,* C_2N_2.

Band	Wave-Length (μ) B. & C.	Wave-Length (μ) Burmeister	Frequency (cm^{-1}) B. & C.	Relative Intensity	Prism	Slit Width (cm^{-1})
A	3.755	3.79	2663	40; *w*	fluorite	17
B	3.901	3.93	2563	65; *m*	fluorite	15
C	4.651	4.65	2156 2143	100; *vs*	fluorite	9
D	4.778		2093	15; *w*	fluorite	9
E	13.65	13.50	739.6 724.1	90; *s*	rocksalt	3
F	16.18	16.07	617.3	20; *w*	sylvine	4
G	*ca.* 50[7]		*ca.* 200	*s*		
H	*ca.* 94[7]		*ca.* 106	*m*		

meister[4] and his results are incorporated in Table I. In addition Rubens and von Wartenberg[5] found about two percent absorption near 53μ; later work[6] shows this to be more intense and to extend from about 160 to 330 cm^{-1}, maximum near 200 cm^{-1}, with an additional band near 94μ or 106 cm^{-1}.

In addition to the above there were faint traces of absorption near 3010 and 1090 cm^{-1}, but it is important to note that we found complete transmission between 17μ and 26.5μ. The band contours are given in Fig. 1, and any pertinent remarks on their structure will be found in the discussion.

Assignments

A summary of the many attempts to allocate the observed bands to fundamental modes is given by Woo.[7] The difficulty is to find an arrangement which will simultaneously satisfy the selection rules, accord with the experimental values of the heat capacity[8] and provide reasonable values for the force constants. The molecule has the symmetry $D_{\infty h}$; the vibrational modes are well known, but are given with their characteristics for the sake of easy reference in Fig. 2.

The enumeration is that of Dennison[9] who also gives the selection rules. Since the molecule has a center of symmetry no bands should be active both in the infra-red and Raman spectra, and a knowledge of the latter is necessary to complete the assignments. The fullest determination of the Raman spectrum is the most recent[10] and was carried out with the liquid; other results are also available for the gas[11] and for the liquid.[12]

The results of the present discussion are embodied in Table II. The valence modes ω_1 and ω_2 will be taken from the strong Raman lines 2330, 848 and 506 cm^{-1}. Calculation supported by experiment[13] shows that the absolute values of ω_1, ω_2, ω_4 and ω_5 remain remarkedly constant whether there is a triple bond in the middle of the molecule or a single bond in the middle and a triple at each end, i.e., for either

$$m-M\equiv M-m \qquad (1)$$

or

$$m\equiv M-M\equiv m. \qquad (2)$$

It is probable that $\omega_1=848$ (liq.) and $\omega_2=2330$

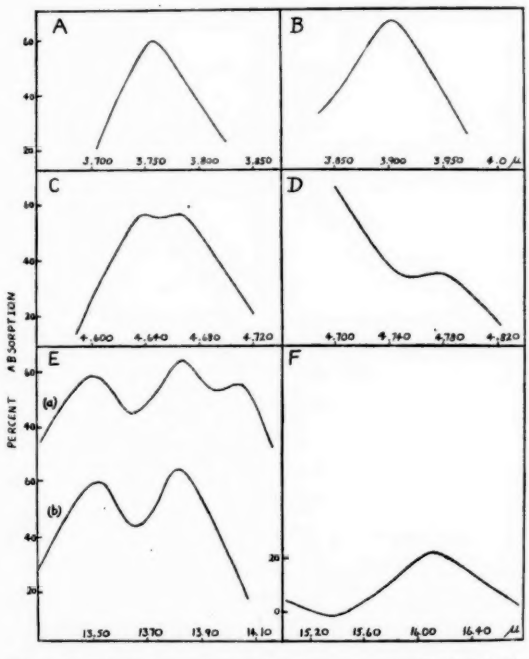

FIG. 1. The infra-red bands of cyanogen: E; (a) before removing HCN, (b) after distilling over HgO. A, $p=70$ cm, B, $p=70$ cm, C, $p=3$ cm, D, $p=70$ cm, E, $p=6$ cm, F, $p=40$ cm.

[4] W. Burmeister, Verh. d. deutsch. physikal. Ges. **15**, 589 (1913).
[5] H. Rubens and H. von Wartenberg, Verh. d. deutsch. physikal. Ges. **13**, 796 (1911).
[6] J. Strong and S.-C. Woo, Phys. Rev. **42**, 267 (1932).
[7] S.-C. Woo, Zeits. f. physik. Chemie **B37**, 399 (1937).
[8] D. P. Stevenson, J. Chem. Phys. **7**, 171 (1939).
[9] D. M. Dennison, Rev. Mod. Phys. **3**, 280 (1931).
[10] A. W. Reitz and R. Sabathy, Wien. Ber. **146**, 577 (1938).
[11] P. Daure and A. Kastler, Comptes rendus **192**, 1721 (1931).
[12] A. Petrikaln and J. Hochberg, Zeits. f. physik. Chemie **B8**, 440 (1930).
[13] F. Trenkler, Physik. Zeits. **36**, 423 (1935).

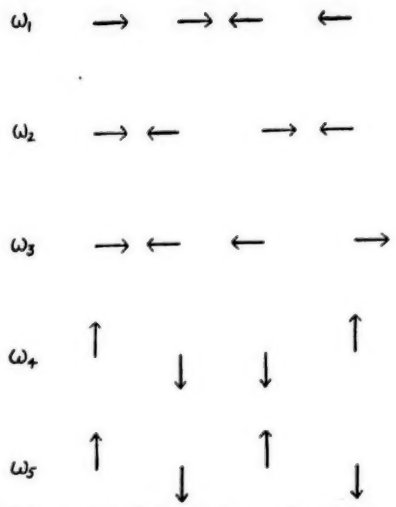

FIG. 2. Fundamental modes of vibration of the rectilinear molecule $X-Y-Y-X$.

cm^{-1} (gas). Some assignments have given $\omega_1=756$; this was found in one case in the liquid[12] although later work[10] does not show it. ω_3 is certainly the powerful infra-red parallel band D at 2150 cm^{-1}, showing only P and R branches ($\Delta\nu\doteq 13$ cm^{-1}). The indications of complexity at E in this band may be due either to $\omega_2-\omega_4$, which if ω_4 is correctly chosen, may be expected at 2082 cm^{-1}, or to the isotope effect. The shift for a $C^{13}-C^{13}$ molecule is given by the relationship

$$2\omega_3\Delta\omega_3=\frac{-K\Delta M\times 10^2}{5.863M},$$

where M is the mass of the C atom and K is the triple bond force constant (*ca.* 17×10^5 dynes/cm) derived from ω_3. This gives $\Delta\omega_3$ as approximately 44 cm^{-1} (the Teller product theorem[14] gives $\Delta\omega_3=45$ cm^{-1}) and one might take the shift for a $C^{12}-C^{13}$ molecule as about half this, with a P branch at about 2120 cm^{-1}, so that the first explanation may be more likely. This fundamental is the only affected to any marked extent by the interchange of triple and single bonds mentioned above and in structure (1) with the same masses and force constants would have a value of about 1000 cm^{-1}.

ω_4 is infra-red active and of the perpendicular type. It is this fundamental which has always proved difficult to assign. As Trenkler's models show,[13] any oversimplified force field gives calculated frequency values which are lower by some 30 percent than those obtained; one therefore changes Lechner's frequency equation for this mode from

$$n_4^2=d(1/M+1/m) \text{ to } n_4^2=(d+\alpha)(1/M+1/m),$$

where d and α are, respectively, angular deformation and interaction force constants. The other bending frequency ω_5 is Raman active, and an expression of the type

$$n_5^2=d(9/M+1/m)$$

gives results which are about six percent too high; if we take ω_5 as the strong Raman line 506 cm^{-1} we may accept d as very close to 0.207×10^5 dynes/cm and $d+\alpha$ as 0.35×10^5 dynes/cm. From this we calculate ω_4 as about 303 cm^{-1}. This result supports reasonably well the assignment of ω_4 to the long wave band located by Rubens and by Strong. We have taken ω_4 as 240 cm^{-1}. The chief difficulty in accepting this allocation is that ω_4 is doubly degenerate and hence the contribution

TABLE II. *Assignments in the spectrum of cyanogen.*

FREQUENCY (CM^{-1})	ACTIVITY	COMBINATION
2663	IR; $\perp$	$\begin{cases}A_u+E_g;\\ \omega_3+\omega_5\end{cases}=2656$
2563	IR; $\perp$	$\begin{cases}A_g+E_u;\\ \omega_2+\omega_4\end{cases}=2562$
2330	R	$A_g;\ \omega_2$
2150	IR; $\parallel$	$A_u;\ \omega_3$
2093	IR; $\perp$	$\begin{cases}A_g-E_u;\\ \omega_2-\omega_4\end{cases}=2082$
1026	R	$\begin{cases}E_g+E_g;\\ 2\omega_5\end{cases}=1012$
848	R	$A_g;\ \omega_1$
732	IR; $\parallel$	$\begin{cases}E_u+E_g;\\ \omega_4+\omega_5\end{cases}=746$
618	IR; $\perp$	$\begin{cases}A_g-E_u;\\ \omega_1-\omega_4\end{cases}=608$
506	R	$E_g;\ \omega_5$
ca. 240	IR; $\perp$	$E_u;\ \omega_4$

[14] Cf. W. R. Angus, C. R. Bailey and others, J. Chem. Soc. 977 (1936).

from such a low frequency to the specific heat is very large; with the above choice of fundamentals we find C_p at 0°C to be 13.2 cal./mole. Thermal determinations give 10.39 cal. at 0°C[15] and again 10.13 cal. at 6°C.[16] Eucken and others reconcile the thermal and spectroscopic values by taking ω_4 as 732 cm^{-1}: a perpendicular band at this frequency would give satisfactory agreement. It will be remembered that careful purification of the cyanogen was found to be necessary; and the change in appearance of this band as hydrogen cyanide is eliminated may be seen in Fig. 1. E, (a) and (b). The band is of the parallel type and the separation of the P and R branches is 15.5 cm^{-1} corresponding to a moment of inertia of approximately 190×10^{-40} g cm^2: Recent electron diffraction measurements[17] give the interatomic distances as $C\equiv N=1.16$ and $C-C=1.37$ A, the corresponding moment of inertia being 180×10^{-40} g cm^2. It may be that the Q branch is very weak; but the analogous vibrations in CO_2 and C_2H_2 do not support this; the doublet structure also forbids its interpretation as $3\omega_4$. Further reasons for not accepting 732 cm^{-1} as ω_4 are that anomalous values are obtained for the bending force constants and also that the combination bands B, D, E and F are more reasonably accounted for with $\omega_4=240$.

Unless the structure suggested is wrong it is difficult to see how any other allocation is possible, and hence the discrepancy in the specific heat values must await further experimental work before a final decision can be made. The final summary of the assignments is given in Table II.

With regard to the force constants it may be stated that the values $K_{CN}=16.95$ and $K_{CC}=5.17$ derived by Reitz and Sabathy[10] accord reasonably well with Pauling's work[17] since the Badger relationship gives 16.8 and 5.6×10^5 dynes/cm. If the electron diffraction results are true then the values obtained by Linnett and Thompson,[18] 17.51 and 6.69×10^5 are too high.

The authors wish to acknowledge the continued help and encouragement received from Professor C. K. Ingold, while one of them (S. C. C.) is indebted to the Carnegie Trust for a Fellowship held during the course of this work.

[15] M. A. Masson, Ann. Chim. Phys. **53**, 257 (1858).
[16] A. Eucken and A. Bertram, Zeits. f. physik. Chemie **B31**, 361 (1935).
[17] L. Pauling and H. D. Springall, J. Am. Chem. Soc. **61**, 927 (1939).
[18] J. W. Linnett and H. W. Thompson, J. Chem. Soc. 1399 (1937).

OCTOBER, 1939 JOURNAL OF CHEMICAL PHYSICS VOLUME 7

The Near Infra-Red Absorption Spectra of Pentaerythritol and Diketopiperazine Obtained with Plane Polarized Light

JOSEPH W. ELLIS AND JEAN BATH
University of California at Los Angeles, Los Angeles, California
(Received June 3, 1939)

Pentaerythritol, $C(CH_2OH)_4$, a crystalline alcohol, and diketopiperazine, $(CH_2NHCO)_2$, also crystalline, have been subjected to an infra-red absorption study with plane polarized waves in the region 1–2.5μ. Pronounced pleochroism is observed, and this dependence of absorption upon the plane of vibration of the electric vector, E_0, is used in identifying the bands associated with the normal vibrations of the methylene groups, CH_2, in each crystal. An interesting example of Fermi resonance arises.

In pentaerythritol the appearance of pronounced absorption by perturbed OH groups when E_0 oscillates along the c axis indicates that the feature of the crystalline structure, deduced from an x-ray diffraction study which orients all of the OH groups at right angles to this axis, must be modified.

The absence of the usual NH absorption near 1.50μ supports Corey's assumption of electron resonance in diketopiperazine.

PENTAERYTHRITOL and diketopiperazine are two dissimilar crystalline materials, which, because of the regularity of arrangements of their molecules with respect to the crystal axes, seemed to offer possibilities for obtaining interesting spectroscopic and further structural information if their infra-red absorption were investigated with plane polarized light. The structures of these two crystals have been deduced by means of x-ray diffraction studies

by Llewellyn, Cox and Goodwin[1] and by Corey,[2] respectively. A study of the spectrum of pentaerythritol, $C(CH_2OH)_4$, was undertaken at the suggestion of Dr. E. G. Cox of the University of Birmingham, England, as a possible means of securing confirmatory evidence for the placements of the four hydroxyl groups per molecule. Spectra of diketopiperazine, $(CH_2NHCO)_2$, were originally recorded in connection with our investigation of substances containing NH groups. The study of this crystal was resumed subsequently to that of pentaerythritol because both crystals have methylene groups, CH_2.

The spectra were obtained with a recording quartz spectrograph and, as shown in reproductions of the original recordings in Fig. 2, were restricted to the range 1–2.6μ. Plane polarized radiation almost free from absorption bands in this region, except for the atmospheric water vapor bands *W* and a slight absorption caused by the quartz prisms, was obtained by sending the beam through a large Glan-Thompson prism. The 5-cm path of calcite in this prism introduces no appreciable bands because the extraordinary wave, which alone is transmitted, has the main component of its electric vector perpendicular to the planes of the CO_3 ions and thus is largely incapable of exciting the intensely absorbing planar oscillations within these ions.

We make no attempt to analyze the complete spectra of pentaerythritol and diketopiperazine nor to identify all of the bands of the restricted overtone region of Fig. 2. Rather, we pick certain features to discuss which we think are of interest. The nature of the specimens which we had to use was such that there was great loss of light. Consequently, the slit was opened so wide that it included at times a $\Delta\lambda$ as great as 0.01μ. It seemed that there was not sufficient justification for reducing the records to a percentage absorption basis, especially since it was difficult to get appropriate comparison curves.

1.5μ OH Absorption of Pentaerythritol

Pentaerythritol is an aliphatic alcohol which forms a tetragonal crystal having the symmetry properties of the space group $I\bar{4}$. Although the $C(CH_2OH)_4$ molecular unit was originally supposed to have pyramidal structure, the work by Llewellyn, Cox and Goodwin[1] is now generally accepted as demonstrating a tetrahedral distribution of valencies around the central carbon atom. The body-centered cell of dimensions $a_0=6.10$ and $c_0=8.73$A contains two molecules of this type, each of which possesses a fourfold alternating axis of symmetry parallel to the *c* axis. The central carbon atom of one molecule is located at (0, 0, 0) and that of the other is present at $(\frac{1}{2}, \frac{1}{2}, \frac{1}{2})$.

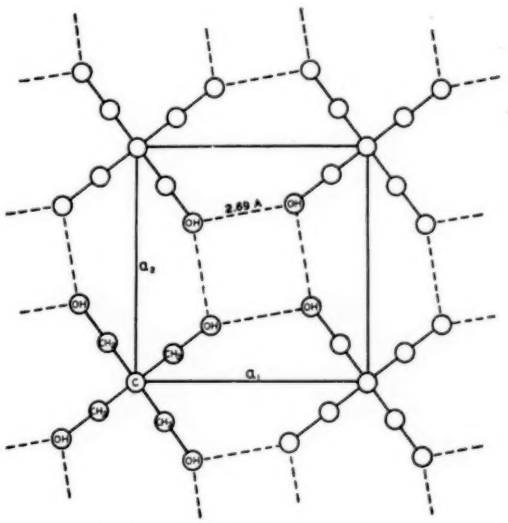

Fig. 1. Projection of four $C(CH_2OH)_4$ molecular units of pentaerythritol onto the (0 0 1) plane.

As shown in Fig. 1, which has been redrawn from the paper of Llewellyn and his co-workers, the molecular units are then arranged so as to place the oxygen atoms into planes parallel to the (0 0 1), i.e., perpendicular to the *c* axis. Oxygen atoms of four neighboring molecules form squares, shown by broken lines, whose sides are 2.69A long and inclined 10° to the a_1 and a_2 axes. The close approach, 2.69A, of two oxygen atoms to each other is regarded by Llewellyn, Cox and Goodwin as indicating the existence of hydrogen bonds, or "hydroxyl bonds" as they prefer to designate them. Moreover, they made the simplifying assumption that the H atoms all lie in the sides of the oxygen squares. From steric considerations alone there seems to be no clear-cut reason for con-

[1] Llewellyn, Cox and Goodwin, J. Chem. Soc., p. 883 (1937).
[2] R. B. Corey, J. Am. Chem. Soc. **60**, 1598 (1938).

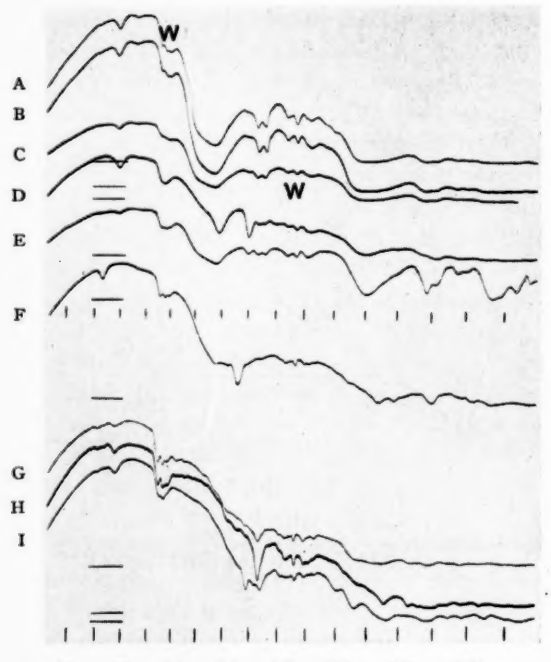

FIG. 2. Infra-red absorption spectra of pentaerythritol (*A–E*), resorcinol (*F*) and diketopiperazine (*G–I*). Bands *W* are caused by atmospheric water vapor.

sidering these atoms to be drawn into the oxygen planes.

X-ray diffraction is unable to locate the position of any H atoms. On the other hand it is just these light atoms whose oscillations give rise to absorption bands in the 1–3μ region. Consequently, Dr. Cox, after reading our note[3] on the near infra-red absorption of sucrose crystals in polarized light, suggested that we investigate pentaerythritol in order to obtain if possible further information about the OH arrangements.

Five spectra of this material, taken under varying conditions, are reproduced in Fig. 2, A–E. The curves have different maximum displacements, as shown by the sections of base lines drawn in near 1.1μ. The absence in all of these of a sharp band near 1.44μ, such as is found in sucrose[3] and elsewhere, shows clearly the absence of unperturbed OH groups, in this respect supporting the assumed model. There appears the usual broad absorption region around 1.55μ characteristic of highly perturbed hydroxyl groups. To obtain records *A* and *B* a single crystal was ground to yield a section 0.78 mm thick perpendicular to the *c* axis. In *A* and *B* the light was originally plane polarized with the electric vector making a 10° angle to a_2 and a_1, respectively, thus paralleling sides of the oxygen squares. The similarity of these records cannot be construed as indicating OH symmetry in the a_1a_2 plane, because the beam became partly depolarized owing to the "rings and brushes phenomenon" arising from the wide cone of light sent through the small crystal. In this instance, as in the other instances, we tested for the presence of depolarization by observing the visible radiation of the beam with a Polaroid plate inside of the spectrograph. Complications from rotatory dispersion need not be expected because of the absence of asymmetric carbon atoms.

The rings and brushes phenomenon will always limit the usefulness of polarized light in such studies whenever the beam travels along the optic axis. It should be recorded here that pentaerythritol is a slightly biaxial crystal, as shown by Ernst,[4] in spite of its tetragonal classification. Ernst points out that this probably results from strains associated with a tendency toward twinning. The angle between the optic axes varies from 8° to 0°, depending upon the specimen, but the bisector is always parallel to the *c* axis.

From the assumed OH arrangements a single OH band was anticipated in the region 1.6–1.7μ rather than the twofold band observed with maxima at 1.51μ and 1.58μ. From the model, all OH groups should be perturbed equally, and the displacement from a "free" OH position near 1.44μ should be large because each OH group is perturbed by two others. In the language of hydrogen bonds, each OH group is the donor and the acceptor of H atoms. We believe that the concept of perturbation is in general more useful, however. We digress to enlarge upon this point.

That H atoms bonded to such electronegative atoms as O and N play a unique role in association processes has been realized for at least twenty years. That it also has a unique behavior

[3] Ellis and Bath, J. Chem. Phys. **6**, 221 (1938).

[4] E. Ernst, Zeits. f. Krist. **68**, 139 (1928).

when it exists as a part of two neighboring polar groups within a single molecule is also well known. The term "hydrogen bond" or "hydrogen bridge" has been used in connection with these various phenomena. The actual picture of what happens has varied from that of proton resonance between two states of pure valence to simple electrostatic perturbation. Bauer and Magat[5] have advanced arguments and carried out calculations supporting the latter point of view. In attempting to explain our spectroscopic phenomena we have found it advisable to adopt it also.

In our study of sucrose[3] we pointed out that not more than two OH groups can approach one another in that crystal. We have associated the broad doublet at 1.51, 1.58μ with the first overtone valence vibrations of OH groups in which the OH acts as the acceptor and the donor, respectively, in the hydrogen bonds. Or, from the perturbation viewpoint, following somewhat the ideas advanced by Cross, Burnham and Leighton[6] in their Raman analysis of liquid water and ice, we say that these two components originate, respectively, in OH groups perturbed by amounts Δ_1 and Δ_2. By measuring the displacements of 1.51μ and 1.58μ from the sharp 1.44μ band of unperturbed OH groups we obtain $\Delta_1 = 320$ cm^{-1} and $\Delta_2 = 620$ cm^{-1}. The Δ_2/Δ_1 ratio is approximately 2/1, in good agreement with the ratio of analogous perturbations found by Cross, Burnham and Leighton. Moreover, Δ_1 and Δ_2 are approximately 2.6 times as large as the values found by those investigators for fundamental OH oscillations in water and ice. This also is the magnitude of the ratio of first overtone to fundamental band perturbation obtained by substituting $v=2$ and $v=1$ into the wave mechanics perturbation expression:

$$\Delta \propto (2v^2+2v+1).$$

Returning to pentaerythritol, the model of Llewellyn, Cox and Goodwin led us to expect a single band in the vicinity of 1.6μ, which represents a perturbation displacement of the order of magnitude of $(\Delta_1+\Delta_2)$ from 1.44μ. The 1.44μ position given by sucrose can be assumed to be reasonably near to the location of an unperturbed band in pentaerythritol, if such existed. The magnitudes Δ_1 and Δ_2 have been deduced from examples, ice[6] and sucrose,[3] in which tetrahedral directions have been satisfied by the perturbing OH groups. Such directions could not be involved in the assumed square arrangement of OH groups in pentaerythritol. Some strain would have to be assumed. Therefore, no exactness can be attached to the amount $(\Delta_1+\Delta_2)$ in this instance.

The presence of two perturbed components, as in sucrose, indicates that there is a differentiation among the OH groups. This assumption is further supported by the appearance of absorption in this region when E_0 is parallel to c and the beam parallel to a_2, as in record D. The crystal for this spectrum was an 0.88-mm specimen cut at right angles from the section used in A and B. The 1.51μ component is greatly reduced and the 1.58μ component is shifted to 1.59μ. It is not safe to conclude that the OH groups whose directions deviate least from the oxygen planes and hence are predominantly excited by electrical oscillations perpendicular to c are the least highly perturbed ones; for owing to strains, there may be a large alteration in the frequency of an unperturbed OH group in which the H atom does not occupy one of the tetrahedral valence positions of the O atom. That is to say, it does not follow that greater perturbation is represented by the 1.59μ band than by the 1.51μ one.

Record C was taken under the conditions of record D with the exception that E_0 was parallel to a_1. That it should be similar to A and B is expected. Our tests with the Polaroid plate showed that the amount of depolarization of the light was small in all records except those of A and B. This slight amount arises from small rotations of the azimuths of vibration of the nonaxial rays of the cone.

In E the specimen was powdered pentaerythritol immersed in a mixture of CCl_4 and CS_2 designed to match refractive indices so far as possible. Unpolarized light was used. The distribution in the 1.51–1.58μ band is intermediate between those of (A, B or C) and D. This is reasonable. We return to the consideration of record E later.

[5] Bauer and Magat, J. de phys. et rad. **9**, 319 (1938).
[6] Cross, Burnham and Leighton, J. Am. Chem. Soc. **59**, 1134 (1937).

Resorcinol, $C_6H_4(OH)_2$, according to the x-ray analysis of Robertson,[7] seemed to be sufficiently similar to pentaerythritol in regard to the degree of perturbation of the OH groups as to make it desirable to investigate it. The only record taken, F, was with unpolarized light and powdered crystals in the CCl_4 and CS_2 mixture. Only a trace of the 1.51μ band occurs, and the longer wave maximum appears near 1.59μ. The strong aromatic CH band, 1.67μ, and its weaker companion, 1.63μ, characteristic of the benzene ring are not to be confused with the OH band. The x-ray model directs four oxygen atoms towards one another. But, unlike their arrangement in pentaerythritol, they exist at different levels along the c axis so as to form spirals rather than squares.

The OH absorption in resorcinol more nearly fulfills the expectation of a single type of perturbation than does that of pentaerythritol. We are inclined to associate this fact with the spiral arrangement of the hydrogen bonds, each OH group being more nearly aligned in conformity with steric requirements. All OH groups are thus equally perturbed and this perturbation should more nearly approach the value of $\Delta_1+\Delta_2$. Of all the materials which we have studied involving perturbed OH groups, the results of which we shall publish later, resorcinol shows the greatest displacement of the OH absorption band. The value $\Delta=760$ cm^{-1}, determined from the 1.42–1.59μ displacement, is however somewhat less than $\Delta_1+\Delta_2=940$ cm^{-1}. There is, however, no good reason for expecting exactly this amount, as we have already pointed out.

2.11μ and 1.27μ OH Absorption of Pentaerythritol

Nayar[8] in a Raman study of pentaerythritol has identified the displacements 3252 and 3335 cm^{-1} with the fundamental OH absorption bands. His data also show two broad lines indicating molecular frequencies in the neighborhood of 1435 cm^{-1}. At least one of these doubtless arises from fundamental bending vibrations of the OH groups. Our broad intense band at 2.11μ (4750 cm^{-1}) is the combination of the 3300 and 1400 cm^{-1} bands. The weak band at 1.27μ (7880 cm^{-1}) is probably the combination of [1.51, 1.58μ] (6450 cm^{-1}) and 1435 cm^{-1}.

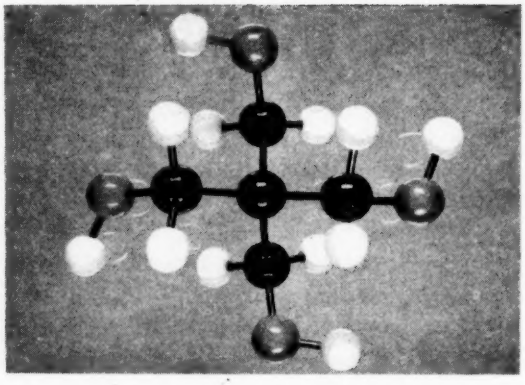

FIG. 3. Model of a pentaerythritol molecule, $C(CH_2OH)_4$.

1.7μ CH_2 Absorption of Pentaerythritol

The pleochroism, that is, the dependence of absorption upon the azimuth of vibration of the electric vector, E_0, is more strikingly displayed near 1.7μ than near 1.55μ. 1.7μ is a region of hydrocarbon absorption, which in the present instances must be interpreted in terms of valence and deformation frequencies of methylene groups, CH_2. The study by Llewellyn, Cox and Goodwin[1] leaves little doubt that the four CH_2 groups per molecule in pentaerythritol are aligned, with the bisectors of the HCH angles all parallel to the c axis. Two of these groups point upward and two downward as shown in the molecular model of Fig. 3. Any absorption bands which appear near 1.7μ when E_0 vibrates parallel to c must be wholly or in part π-type bands, that is, have an electric moment change parallel to the bisector of the CH_2 group. The strong 1.703μ band of Fig. 2, D we identify as $2\nu_\tau$, the first overtone of the symmetrical CH_2 vibration. This interpretation is supported by the almost complete disappearance of this band in A, B and C, in which E_0 was perpendicular to the c axis. The small residual was probably introduced by the nonaxial rays in the light cone, whose vibrations had small components parallel to c.

The doublet 1.735, 1.763μ is excited by vibrations both perpendicular and parallel to the CH_2 bisector, but with the greater intensity

[7] J. M. Robertson, Proc. Roy. Soc. **A157**, 79 (1936).
[8] P. G. N. Nayar, Proc. Ind. Acad. Sci. **7**, 251 (1938).

when these are perpendicular. The two components of the double band are about equal under all circumstances. Because of these facts the components must involve Fermi resonance between $2\nu_\sigma$ and $4\delta_\pi$, i.e., the first asymmetric valence overtone and the third deformation overtone. Equality of intensities indicates perfect superposition of $2\nu_\sigma$ and $4\delta_\pi$. Record *F*, taken with unpolarized light and randomly arranged small crystals, shows that the total absorption in *B* and *C* is greater than in *A*. This is reasonable because, although *B* and *C* were excited primarily through $2\nu_\sigma$-type vibration, the σ-type electric moment change should be greater than the valence π-type. Indeed, it is surprising that the 1.703μ $2\nu_\pi$ band should be as intense as it is. The corresponding water vapor band is not observable even in the fundamental, and its first overtone is ruled out by the selection rules deduced by Mecke.[9] According to these selection rules only $(\nu_\sigma+\nu_\pi)$ and $4\delta_\pi$ should be expected in this region. But it is impossible for us to correlate the bands at 1.7μ on the basis of the rules and so we conclude that they do not hold in such a CH_2 unit which forms part of a larger structure. Furthermore, the conclusion of Fox and Martin[10] that ν_σ is greater than ν_π, deduced from a consideration of ethylene, C_2H_4, as two coupled CH_2 oscillators, does not seem to hold in this instance. The one other assignment to the bands near 1.7μ which is consistent with the polarizations is: $1.703\mu=4\delta_\pi$; $[1.735,\ 1.763\mu]=[2\nu_\sigma,\ 2\nu_\pi]$. This would still violate Mecke's selection rules but would not depart as much from the conclusions of Fox and Martin as our former assignment does. However, we shall see that only the former is consistent with the observations at 2.3μ.

1.7μ CH_2 Absorption of Diketopiperazine

Diketopiperazine,[2] $(CH_2NHCO)_2$, forms a monoclinic crystal with the planes of the flat ring molecules as well as the symmetry axes of the two CH_2 groups per molecule parallel to the *b* axis and lying approximately in the (1 0 1) plane. Fig. 2, *I* was obtained with the beam and E_0 parallel, respectively, to the *c* and *b* axes in a 0.60-mm specimen. *H* and *G* were secured with the beam parallel to *b* and with E_0 vibrating, respectively, perpendicular and parallel to the (1 0 1) plane in a 0.78-mm section. Since the planes of the two CH_2 groups are parallel to each other and perpendicular to the (1 0 1) plane, greater σ-type excitation should occur in *H* than in *G*. In fact, it should be absent in *G*. We associate the residual 1.745μ band in *G* with imperfect alignment of the crystal and to the nonparallelism of rays in the beam.

Our interpretation of the 1.703, 1.745 and 1.754μ bands is similar to that for pentaerythritol. 1.703μ represents $2\nu_\pi$. 1.745μ and 1.754μ are essentially $2\nu_\sigma$ and $4\delta_\pi$. There is probably some Fermi resonance between these two states, since there seems to be evidence of 1.754μ absorption on the long wave side of 1.745μ in *H*. But the great intensity dependence upon polarization, as shown by *G* and *H*, indicates that this is slight. The small band between 1.703μ and 1.745μ, showing most plainly in *I*, we believe does not belong to the CH_2 groups. We shall discuss this band later.

The Anharmonicity Constants of the CH_2 Vibrators

We can make use of the double absorption band at 2.3μ in pentaerythritol, long known[11] as an absorption region common to all hydrocarbons, to strengthen our identification of σ- and π-type vibrations in CH_2. This band shows particularly well in Fig. 2, *E*, obtained with unpolarized light and powdered crystals. To offset the great loss of transmitted intensity in the short wave region resulting from Rayleigh ν^4 scattering, the slit widths were greatly increased. Since unpolarized light was used there has been no distortion of relative intensities. Thus, the absorption in 2.285μ is greater than in 2.313μ. When E_0 vibrates along the CH_2 symmetry axis, as in 2, *D*, relative intensities are reversed. We thus identify 2.313μ with $3\delta_\pi$ and 2.285μ with $\nu_\sigma+\delta_\pi$. To account for the appearances of both components in 2, *A*–*C*, with E_0 perpendicular to the symmetry axis, it is necessary to assume a considerable amount of Fermi resonance, although not as much as in the 1.75μ bands.

[9] R. Mecke, Zeits. f. Physik **81**, 313 (1933).
[10] Fox and Martin, Proc. Roy. Soc. **167A**, 257 (1938).
[11] J. W. Ellis, Phys. Rev. **23**, 48 (1924).

By assuming that 5720 cm^{-1}, i.e., the average wave number of the 1.735 and 1.763μ bands, represents the first overtone of ν_σ as well as the third overtone of δ_π and that 4320 cm^{-1} (2.313μ) and 4375 cm^{-1} (2.285μ) represent the second overtone of δ_π and $\delta_\pi+\nu_\sigma$, respectively, it is possible to calculate approximately the fundamental values of ν_σ and δ_π as well as the magnitudes of the anharmonicity constants. The reasonableness of these latter values serves as a further check on our identifications. To make these calculations the wave mechanics energy expression is used:

$$E=(v+\tfrac{1}{2})\omega_0-(v+\tfrac{1}{2})^2\omega_0 x=(v+\tfrac{1}{2})\omega_0-(v+\tfrac{1}{2})^2\epsilon.$$

From this there is obtained for the wave numbers:

$$\nu=(v_2-v_1)(\omega_0-\epsilon)-(v_2^2-v_1^2)\epsilon$$

or since v_1 equals 0 in each instance involved,

$$\nu=v(\omega_0-\epsilon)-v^2\epsilon=v\omega'-v^2\epsilon.$$

By substitution of the appropriate data there are obtained:

$$\nu_\sigma=\omega_\sigma'-\epsilon_\sigma=2915\ cm^{-1}$$
$$\delta_\pi=\omega_\delta'-\epsilon_\delta=1460\ cm^{-1}$$
$$\epsilon_\sigma=55\ cm^{-1};\qquad \epsilon_\delta=10\ cm^{-1}.$$

Assuming that $\epsilon=55$ is also approximately correct for ν_π, we obtain:

$$\nu_\pi=2985\ cm^{-1}.$$

To compare with δ_π, ν_σ and ν_π these are the values from Nayar's[8] Raman spectrum data: 1474, 2923 and 2961 cm^{-1}. The 2961 cm^{-1} line is stronger than the 2923 cm^{-1} one, as is expected for a ν_π vibration in the Raman spectrum. $\epsilon_\sigma=55$ cm^{-1} may be compared with the value $\epsilon=62$ found, for example, for cyclohexane and hexane.[12] $\epsilon_\delta=10$ cm^{-1} may be compared with 17 cm^{-1} obtained from Mecke's[10] values for δ_π and $2\delta_\pi$ in the similar molecule, water vapor.

Other CH_2 Bands of Pentaerythritol

Bands at 1.19μ and 1.38μ are well-known hydrocarbon bands, but lack of resolution prevents them from revealing any information of value.

Two interesting doublets are found with centers at 4190 cm^{-1} (2.372, 2.397μ) and at 4030 cm^{-1} (2.467, 2.490μ). These have displacements of 1285 and 1125 cm^{-1}, respectively, from the center of ν_σ and $2\delta_\pi$. They are assumed to represent combinations of $(\nu_\sigma, 2\delta_\pi)$ with two active frequencies of the $C(CH_2OH)_4$ structure. In Nayar's data 1281 and 1130 cm^{-1} may be identified as these fundamental frequencies.

Twinning in Pentaerythritol Crystals

It should be pointed out that two records, not shown in Fig. 2, obtained with a needle-like crystal of pentaerythritol, gave results apparently quite contradictory to all the others. Ernst[4] makes it quite clear that the crystals of this shape are far from single crystals. Twinning has resulted in a long skeleton pile of smaller crystals with their c axes perpendicular to the length of the needle. The deception is introduced by the fact that a final single crystal, with its c axis at right angles to all the others, caps the pile.

"NH" Absorption of Diketopiperazine

The study of diketopiperazine originated in an examination of the spectra of proteins.[13] There is a remarkable display of pleochroism in the region 1.9–2.6μ, but we make no attempt to analyze this complex region. We do wish to point out, however, that the absence of a clear-cut strong NH absorption band at 1.5μ strongly supports Corey's[2] assumption that there is electron resonance among four different structures in the $(CH_2NHCO)_2$ molecule. So far as the NH groups are concerned there is resonance between a normal NH state and an ionized NH state. We associate the broad structured absorption running from 1.55μ into the 1.7μ CH_2 bands with this resonating NH condition. This great departure from normal NH absorption represents more than a hydrogen bond perturbation, as our study[13] of water bound to protein shows.

[12] J. W. Ellis, Phys. Rev. **33**, 27 (1929).

[13] Ellis and Bath, J. Chem. Phys. **6**, 723 (1938).

The Variation in the Structure of Water in Ionic Solutions

G. W. STEWART
University of Iowa, Iowa City, Iowa

(Received July 3, 1939)

It has been long thought that the presence of ions in an aqueous solution produces a contraction of the water. Here it is shown by x-ray diffraction curves (1) that with concentration of ions there is a lessening of the amount of the 4-coordinated water structure, increasing the density, (2) that the alteration in structure is apparently similar to that produced by increasing the temperature of the water, and (3) that the effect on the water structure is not confined to the shell immediately adjacent to an ion. Further, by the use of fifteen strong electrolytes, selected because of their wide variation in type and also in apparent molal ionic volume, it is shown by measurements on the alteration in the minor diffraction peak (4) that the rate of variation of the liquid structure of the water with ionic concentration has a striking correspondence with the rate of variation of the apparent molal ionic volume. In fact, the alteration in liquid structure seems to have a much more important effect in the apparent molal ionic volume than has an electrostatic theory based on the Debye-Hückel theory.

INTRODUCTION

THIS paper presents certain observed variations in the liquid diffraction curves of water in various ionic aqueous solutions, and discusses the bearing of the experimental results upon the causes of the variations of the apparent molal volume of the ions. It will be shown that this influence of the ions upon the water structure, which is probably not local, is more important than the influence of the ionic charges as expressed by the simple Debye-Hückel theory, without any consideration of liquid structure.

For the purpose of this contribution it may be assumed that the x-ray coherent scattering from a liquid can be obtained by the use of a spherically symmetric density distribution of scattering centers about any one center. The approximation to be made is twofold; first, that the scattering from each ion and each molecule of water occurs as from a point, and that there is spherical symmetry.

As has been suggested,[1] this theory, ordinarily referring to only one kind of scattering centers, may be extended to any number of different kind of scattering centers. Let there be N particles each of scattering power A, n particles of a, and ν particles of b. The theory for atoms of one kind, gives as the coherent scattering at an angle θ from the incident x-ray beam.

$$NA^2\left[1+\int_0^\infty 4\pi r^2 g(r)\frac{\sin sr}{sr}dr\right],$$

wherein $g(r)$ is the radial density distribution function, using really excess-over-mean values, r is the distance from a selected scattering center and $s=(4\pi \sin\theta/2)/\lambda$ with λ the wave-length of the incident ray. With the three kinds of scattering centers it can be shown in a straightforward manner that the coherent scattering may be approximately expressed in three parts, (A), (B), (C) expressed as follows:

$$NA^2+(NA^2+2nAa+2\nu Ab)\times\int_0^\infty 4\pi r^2 g(r)\frac{\sin sr}{sr}dr, \quad \text{(A)}$$

wherein $g(r)$ will be taken as the radial distribution function of the water scattering centers about any scattering center, a molecule of water, a positive or a negative ion.

$$2nab\int_0^\infty 4\pi r^2 g_a(r)\frac{\sin sr}{sr}dr, \quad \text{(B)}$$

wherein $g_a(r)$ is the radial density distribution of the n ions about a b ion. It might as well be written $g_b(r)$ with the distribution of the ν ions, instead of n, about an a ion.

$$na^2\left[1+\int_0^\infty 4\pi r^2 g_a(r)\frac{\sin sr}{sr}dr\right]+\nu b^2\left[1+\int_0^\infty 4\pi r^2 g_b(r)\frac{\sin sr}{sr}dr\right], \quad \text{(C)}$$

wherein $g_b(r)$ refers to the distribution of the ν ions.

[1] E.g., J. Prins, J. Chem. Phys. **3**, 72 (1935).

In the above it has been assumed that, with any concentration, there is a distribution of water, $g(r)$, over the entire volume outside the central scattering center. Upon this distribution is superimposed an excess distribution representing the ions. Thus a and b will be the *excess* scattering factors, or the excess of scattering of the ions over that in an equal volume of water. It should be made clear that the approximations involve the following assumptions: (1) radial symmetry in the distribution functions; (2) only one $g(r)$ function, applicable about a water molecule and an ion alike; (3) only one $g_a(r)$ and only one $g_b(r)$ function; and (4) the assumption of mean density distribution of water in computing a and b, but actually using the $g(r)$ function there. The errors in these approximations increase with increasing concentration.

The expression (A) may be considered as a gas distribution term, NA^2, plus a coherent scattering term. In (A), the quantities n and ν are small in comparison with N and a and b are smaller or of the same order of magnitude as that of A. Writing the term in parenthesis as $1.1\times NA^2$, for example, adding and subtracting $0.1NA^2$, it is observed that (A) is approximately equivalent to 1.1 times the mere water value, less a gas curve $0.1NA^2$. Thus (A) is practically that of water alone except that there is a fairly uniform percentage increase over the angular range of immediate interest, 11° to 24° on the spectrometer. (B) and (C) are much smaller than (A) not only because of the small values of n and ν in comparison with N, but also because the density functions $g_a(r)$ and $g_b(r)$ are much smaller than $g(r)$. Under these circumstances any relative variation in the experimental curve of a dilute solution at diffraction angles herein considered, may be regarded as approximately a relative variation in the scattering curve from the solvent water, these changes being caused chiefly by a variation in $g(r)$. Undoubtedly this statement is more accurate the greater the dilution of the solution.

In Part I will be discussed the effect of a variation in concentration on the x-ray diffraction curves of the solutions, and in Part II the relatively greater importance of the variation of the water structure in comparison with a more direct electrostatic effect, upon the apparent molal ionic volume.

Experimental Method

The apparatus consisted of a spectrometer, methyl bromide ionization chamber, balanced zirconium and strontium filters for Mo $K\alpha$ radiation, Soller slits and a vacuum tube amplifying circuit with galvanometer.[2] The Coolidge tube was operated by a transformer whose applied voltage did not vary as much as one percent. The samples of liquids were placed in thin-walled, soft glass, cylindrical, blown tubes, having a transmission of Mo $K\alpha$ radiation of approximately 80 percent. The diameter of each tube was approximately 5 mm which with the samples used is nearly the mean of the "optimum thickness," or the reciprocal of the absorption coefficient of the liquid. The tube containing the liquid was placed at the axis of the spectrometer and rotated five to six times a second throughout the observations. An auxiliary slit was used to confine the x-ray beam to a width not greater than two-thirds the diameter of the sample tube. Observations at a given spectrometer setting for each filter were made over a three-minute interval, readings taken every five to eight seconds, but varying widely. The mean of the reading was obtained graphically, thus avoiding as much as possible the effect of alpha-particle ionization. For a gain in accuracy in averaging, the zirconium and strontium readings were plotted separately and smooth curves drawn. Differences were then taken between the smoothed out curves. By repetition several such sets of differences, usually three, were obtained and averaged.

There are a number of possible corrections which could be made to these data. (1) The cylindrical tube does not give a uniform thickness of transmission for either the incident or the scattered rays. (2) A finite slit width certainly affects the relative intensities wherever the change in the slope of the diffraction curve is rapid. (3) There is stray radiation. (4) Scattering occurs of both the incident beam and the stray

[2] The spectrometer was the same as used in previous work, and FP-54 (G. E. Co.) tube circuit was that of DuBridge and Brown, Rev. Sci. Inst. **4**, 532 (1935). One set of Soller slits was $10\times1.5\times0.7$ cm and the other $20\times1.5\times0.7$ cm. Each set consisted of seven channels.

radiation from the glass. (5) Incoherent scattering is present. (6) Absorption occurs in the air, as well as in the specimen and the container. In the procedure, the diffraction curve for water is compared with the curve obtained in the same cylindrical tube with a dilute solution. The difference in the peak positions and shapes of the two were desired. Hence, (1) is not important since one part of the curve is not compared with that at a widely different angle. The diffraction peaks remain so nearly in the same position that the slit width (2) does not interfere with the comparisons herein made. The error due to stray radiation, (3), and the scattering of both the incident beam and the stray radiation from the glass tube, (4), are ascertained by taking a diffraction curve with the tube empty, and multiplying these values by the transmission of the liquid. Subtraction from the observations of corresponding angles corrects for both (3) and (4). The correction for incoherent radiation (5), would move the diffraction peaks so slightly that it is not applied. By the differential use of filters, only Mo $K\alpha$ is concerned. Hence the correction for absorption, (6), would change similarly over the entire diffraction curve, without any alteration in shape. For the purposes of these experiments, it therefore seemed advisable to make but the one correction mentioned, that for stray radiation and the scattering from the glass tube.

There was always complete absorption of the Mo $K\alpha$ in the ionization chamber. This was constantly checked by the comparison of the two filter curves.

Tests of the zero of the spectrometer were usually made by locating the chief peak of triphenylmethane on both sides. The correct balance of the filters was checked by using a thin-walled cylinder of aluminum. The sensitivity of the galvanometer and amplifier was approximately 50,000 mm/volt and $\frac{1}{3}$ mm/10^{-16} amp. The drift was usually kept within 2–3 mm/min. Even with the most favorable manipulation the final accuracy was not reliable to within less than several percent.

Part I. The Variation in Water Structure with the Concentration of the Electrolyte

X-ray diffraction studies have been made of numerous aqueous solutions of strong electrolytes and it is well known[3] that the presence of ions modifies the diffraction curves plotted with intensity and angle of diffraction. For light ions the general results are that the chief diffraction maximum of pure H_2O is displaced by increasing concentration of ions toward greater angles, and that the second or minor maximum decreases in relative magnitude. Similar displacements occur with increasing temperature of pure water.[4] At least one observer[5] has reported that with KCl, at least, the chief water diffraction peak was sharpened, but the observation of Meyer[6] with LiCl and NaCl did not show this increased sharpness. Dainlow and Neumark[3] have found that LiOH and NaOH solutions have sharper first diffraction peaks than do LiCl and NaCl solutions of the same concentration, respectively. They have also shown that H^+ and OH^- ions disturb the water structure less than the other ions, and conclude from low temperature experiments that near the crystallization point NaCl and LiCl aqueous solutions have regions of inhomogeneous concentration.

Prins and Fontayne[7] and Prins[8] have studied more especially the heavier ions and have concluded that super-arrangement exists.

The rearrangements of the liquid structure of water by ions was first suggested by Bernal and Fowler.[9] These authors mention evidence for the generalization that if the ions are permanently hydrated, such as with Li^+, Na^+ (K^+, F^-), there is an increase in the regularity of the water structure, which is four-coordinated, and if unhydrated, there is a decrease, accompanied by a closer packing.

Prins and Petersen[10] have given a preliminary discussion of a "smearing out" process on a crystal lattice structure, using a one-dimensional model, and have shown that there is a peculiarity of structure with the coordination number 4. They discussed a cubic close-packed, a hexagonal

---

[3] See references in papers by: Dainlow and Neumark, Physik. Zeits. d. Sowjetunion [10] **5**, 673 (1936); J. Prins, J. Chem. Phys. **3**, 72 (1935); G. W. Stewart, J. Chem. Phys. **2**, 147 (1934).

[4] Shown originally by G. W. Stewart, Phys. Rev. **37**, 9 (1931), but most accurate and recently by Morgan and Warren, J. Chem. Phys. **6**, 666 (1938).

[5] Good, Hel. Phys. Acta **5**, 205 (1930).

[6] Meyer, Ann. d. Physik **5**, 701 (1930).

[7] Prins and Fontayne, Physica **2**, 570 and 1016 (1935).

[8] J. Prins, J. Chem. Phys. **3**, 72 (1935).

[9] Bernal and Fowler, J. Chem. Phys. **1**, 515 (1933).

[10] Prins and Petersen, Physica **3**, 147 (1936).

close-packed, a body-centered cubic, a simple cubic and a diamond structure. In one case, the diamond, coordination number 4, is there a relatively close second x-ray diffraction peak, caused chiefly by the nearest neighbors. Morgan and Warren[4] show that the corresponding coordination number in water changes from 4.4 at 1.3°C to 4.9 at 83°C and that this minor peak becomes relatively less with increase in temperature. The relative magnitude of the minor peak seems to vary rather sensitively with change in liquid structure. It is scarcely possible that the errors in the assumptions already noted concerning $g(r)$, $g_a(r)$ and $g_b(r)$ would account for the alteration in the minor peak for the effect is similar with all the electrolytes. One concludes, therefore, that the chief alteration by the ions is a change in $g(r)$. One need not say what the nature of that change is. It may be interpreted as usually but not necessarily indicative of an increase in the coordination number. It is the fact of a change in $g(r)$ that the experiments with electrolytes seem to establish and not any details concerning the nature of a liquid structure or its alteration. Subsequently, however, it seems simpler to refer to the increase in the coordination number as the effect produced by the presence of ions.

Results

The strong electrolytes selected were NH_4Cl, LiCl, NaCl, KCl and $MgCl_2$. These are readily obtained and are diversified both as to hydration and valency. Fig. 1 gives the diffraction curve of water at a temperature of 15°C, the angular range being that involved in this study. Fig. 2 presents the angular variation, with concentration of the electrolyte, of the major peak, marked M_1 in Fig. 1, and Fig. 3, the same information concerning the minor peak, M_2. For the reasons already stated, the diffraction curves of the solutions, all plotted to the same height at the major peak, are assumed to be approximately that of the solvent. Fig. 4 presents the variation in relative height of the minor peak with increasing concentration. The height h was obtained in the usual manner by drawing first a smooth curve connecting the observed values on both sides of the minor peak. All the variations indicated are approximately linear. At least the accuracy of the experiments does not permit of any more exact description.

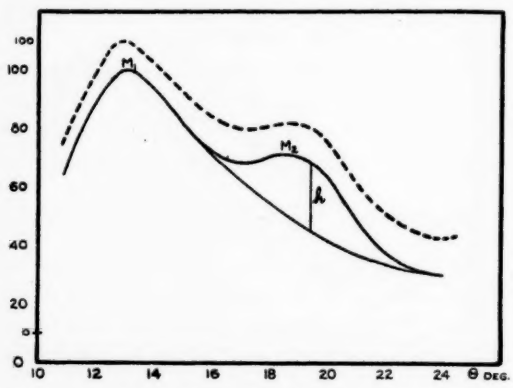

FIG. 1. Relative intensities at spectrometer diffraction angles O of H_2O at 15°C. Dotted curve the results of Morgan and Warren at 13°C.

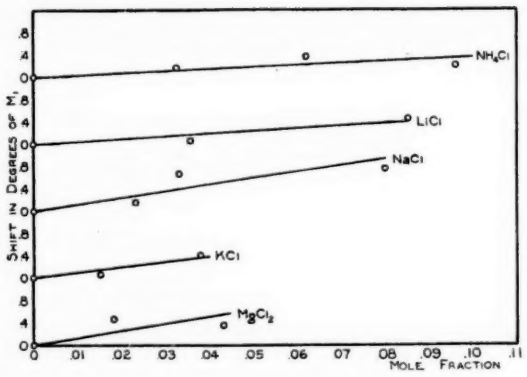

FIG. 2. Increase in angle of the major diffraction peak, M_1 in Fig. 1, with increasing concentration.

It might be anticipated that the changes of the width of the major diffraction peak are significant in magnitude. But this is not the case. The accuracy of the results, less than 10 percent of the width, does not permit any conclusions concerning the variation in peak width at the concentrations used.

In Table I are the numerical results per mole fraction of the peak positions and of the relative height of the minor peak.

The direct conclusions that can be drawn from these observations are:

(1) The alteration in the water diffraction curve, a movement of the major and minor peaks toward each other, is similar to that caused merely by an increase of temperature.[4, 6]

(2) The movement of peak M_1 to larger angles

is consistent with the view that $g(r)$ of the solvent is altered. This needs an explanatory statement. Referring to the foregoing theory it is evident that term (A) is the sum of a gas curve and a liquid diffraction curve. The gas curve may be regarded as that of water molecules and the diffraction curve as also one of water but increased relatively in magnitude. This increase would shift peak M_1 to smaller angles, provided $g(r)$ was the same in the solution as in pure water. But the actual movement of (A) is toward larger angles. It will be seen that terms (B) and (C) could not account for this movement. Term (B) is the "diffraction portion" of a liquid diffraction curves, but with relatively widely separated scattering units, which would give a peak at smaller angles than that of water. Its addition to term (A) would move the major peak to smaller angles. Term (C) is the sum of two liquid diffraction curves with the scattering units widely separated. Their addition would also move the major peak toward smaller angles. Qualitatively, then, one may see that $g(r)$ in the solvent must be different than in pure water.

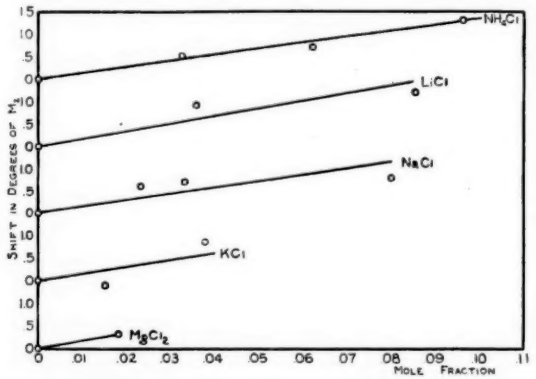

FIG. 3. Decrease in angle of the minor diffraction peak, M_2 in Fig. 1, with increasing concentration.

(3) The relative decrease in height of the minor peak with increasing concentration may be taken usually to indicate, as previously explained, that there is a lessening of the amount of the 4-coordinated structure of water, resulting in a more closely packed arrangement.

(4) In Table I, in general, the greater the modification of the 4-coordination of water, as indicated by column 4, the more the movement of the major peak which is produced chiefly by the non-immediate neighbors. Naturally, if the coordination changes, the major peak would alter, but there is no basis here considered for anticipating the magnitude and direction.

(5) The positive values in column 2 and negative values in column 3 of Table I do very definitely correspond to the effect of raising the temperature of water. That is, following Bernal and Fowler, the structure of the water in the solution is similar to that of pure water at a higher temperature. Consequently, maximum density will occur at a temperature lower than that of pure water, which is the case experimentally. These results do not fully agree with those of Meyer[4, 6] who found for LiCl and NaCl no change with temperature of the position of the minor peak, and a positive displacement of this peak with concentration of NaCl. But this disagreement is not regarded as a significant one.

(6) A less direct and perhaps less certain conclusion may be drawn from the measurements on the width of peaks. It is obvious that the two ions would not alter the water structure in precisely the same manner. If the effect on the water structure were distinctly local, then we might expect in dilute solutions three different structures, one in the immediate neighborhood of each ion and the third that of pure water. One should then obtain a major peak from each of the three, which thus might be expected, through overlapping, to make the first peak broader. This broadening, in the very nature of the case, could not be easily detected. Thus its apparent absence does not prove that the $g(r)$

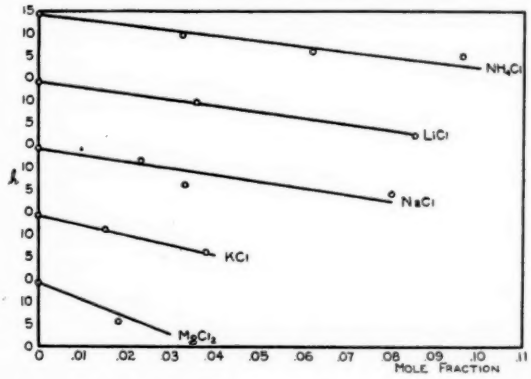

FIG. 4. Decrease in height or minor peak, M_2 in Fig. 1, with increasing concentration, the height of M_1 being kept constant.

TABLE I. *Variations in angular peak positions and in minor peak height per 0.01 mole fraction.*

SUBSTANCE	VARIATION IN M_1	VARIATION IN M_2	VARIATION IN HEIGHT OF M_2
NH_4Cl	0.042	−0.115	1.2
LiCl	.042	− .164	1.4
NaCl	.112	− .150	1.5
Kcl	.079	− .093	2.3
$MgCl_2$	.132	− .151	3.8

can rightly be regarded as applicable throughout. But one is led to lean toward that interpretation, especially in view of evidence presented in Part II.

(7) The NH_4^+ ions are not hydrated, as are the other positive ions in Table I. But in all cases there are similar effects, increasing the coordination number and the density.

PART II. THE INFLUENCE OF WATER STRUCTURE ON THE APPARENT MOLAL IONIC VOLUME

The change in the apparent molal volume of the ions of a strong electrolyte can be studied by assuming that the only electric forces involved are those of free ions. Then the variation between the conclusions of this theory and the experimental facts, if there is such, can be attributed to forces not considered in the free ion theory, to forces that participate in the formation of liquid structure. The simple form of the Debye-Hückel theory leads to definite conclusions in regard to the apparent molal volume of the solute of a strong electrolyte in a dilute solution. Redlich and Rosenfeld[11] used the theory to obtain the partial molal free energy of the electrolyte in solutions at any concentration, c, and that at infinite dilution, proceeding as follows:

From the theory, the difference between these free energies is,

$$\bar{F}_2-\bar{F}_2^0=(\Sigma\nu_i)RT\ln c-\frac{A}{D^{\frac{3}{2}}T^{\frac{1}{2}}}(\Sigma\nu_i z_i^2)^{\frac{1}{2}}\cdot c^{\frac{1}{2}}, \quad (1)$$

where $A=(\pi e^6N^3/1000k)^{\frac{1}{2}}$.

ν_i is the number of ions per molecule of charge z_i, N is Avogadro's number, e the electronic charge, k Boltzmann's constant and D the dielectric constant of the medium.[12]

[11] Zeits. f. physik. Chemie **A555**, 65 (1931).

[12] The expressions here are as in Gucker, Chem. Rev. **13**, 111 (1933), whose numerical values of the physical variables are also adopted.

If, now, the partial differentiation with pressure be performed, the difference of the partial molal volumes is obtained. The apparent molal volume differences are approximately two-thirds of this or

$$\varphi-\varphi_0=\tfrac{1}{3}A\frac{(\Sigma\nu_i z_i^2)^{\frac{1}{2}}}{D^{\frac{3}{2}}T^{\frac{1}{2}}}\left(\frac{3}{D}\frac{\partial D}{\partial P}-\beta\right)c^{\frac{1}{2}}, \quad (2)$$

where β is the compressibility.

This direct result of the Debye-Hückel free ion theory can be interpreted as follows. If water is compressed the dielectric constant rises. This means weaker electrostatic forces between the ions and therefore a change in the direction of higher potential energy. Again if the solution is compressed, the ions approach more closely and from the Coulomb forces there is a decrease in potential energy. It is thus reasonable to expect that with a change in pressure the energy would be affected in opposite directions. The dielectric term is about three times that of the other in the case of water. So this theory would throw practically the entire responsibility of the change of apparent molal volume on the variation in $(\Sigma\nu_i z_i^2)^{\frac{1}{2}}$ and on the electrostatic term $3\partial D/D\partial P$. It thus becomes desirable to see how far the results computed from the foregoing equations differ from the results actually obtained by measurement. From the foregoing there follows directly, with Gucker's values:

$$\partial\varphi/\partial c^{\frac{1}{2}}=0.89(\Sigma\nu_i z_i^2)^{\frac{1}{2}}. \quad (3)$$

That (3) is not correct for strong electrolytes in general was shown[13] by computation of the exponent of c in Eq. (2), above for 191 electrolytes. This exponent varies widely. Less than about thirty percent have the value $\frac{1}{2}$, about twenty-five percent the value 1, and about fifteen percent the value 0.2 or less. But it is interesting to assume Eq. (3) and compare Eq. (3) with experimental determinations of $\partial\varphi/\partial c^{\frac{1}{2}}$ while at the same time considering the correlation with the x-ray diffraction indications.

That there might be such a correlation is readily seen from the following. With the exception of two percent, all of the 191 strong electrolytes show an increasing apparent molal volume with increasing concentration. This is directly interpretable as a change in the solvent,

[13] G. W. Stewart, J. Chem. Phys. **7**, 381 (1939).

water. The "coordination number" of the water increases, with a corresponding increase in density. The effect per ion is greatest at the least concentration, and decreases with increasing concentration. This produces the same kind of variation in density measurements as would an increasing ionic molal volume. It is therefore proposed to assume that the increased packing of the water molecules is the chief cause of the variation in φ in Eq. (2) and to compare the electrolytes on that basis. A very crude indicator or basis of comparison is necessary. It will be assumed that $\partial\varphi/\partial c^{\frac{1}{2}}$ will be large when the structural change in water per mole fraction of solute is relatively large, the one-half power being used for convenience in computation.

Comparison with X-Ray Diffraction Measurements

Also from the foregoing discussion of the x-ray peaks, it was noticed that one can get a crude comparison of the magnitude of the structural change by determining the relative diminution of the minor peak per mole fraction. This is accomplished by adopting the same height of major peak for all the samples tried, and then computing the $\partial h/\partial m$, or the rate of change of height of minor peak per mole fraction. This indicator is justified in view of the approximately linear variation with concentration ascertained in Part I. For the sake of comparison, then, the assumptions will be made, that $\partial\varphi/\partial c^{\frac{1}{2}}$ is large when the structural change is relatively large, and that $\partial h/\partial m$ varies similarly. In view of the nature of these assumptions one can anticipate only a qualitative result, even though the view of the changing water structure be correct. It is clearly even more appropriate to use for comparison, instead of $\partial\varphi/\partial c^{\frac{1}{2}}$, the value $\partial\varphi/\partial c^{n}$, where φ seems to be experimentally proportional to c^n at the dilutions considered.

Table II. *Correspondence of the variation of the apparent molal ionic volume with the indicated change in the liquid structure of the solvent, water.*

Electrolyte	Temperature	Concentration (Mole Fraction)	$\frac{\partial h}{\partial m}\div 100$	$\frac{\partial\varphi}{\partial c^{\frac{1}{2}}}$	$\frac{\partial\varphi}{\partial c^{\frac{1}{2}}}$ Eq. (3)	$\frac{\partial\varphi}{\partial c^{n}}(n)$
$NH_4C_2H_3O_2$	17°	0.0908	1.0	0.84	2.5	0.58(1)
$LiNO_3$	17°	.0557	1.6	1.0	2.5	1.0 (.5)
		.0325				
NH_4Cl	25°	.0619	1.2	1.3	2.5	1.3 (.5)
		.0960				
LiCl	25°	.0357	1.4	1.7	2.5	1.7 (.5)
		.0853				
		.0231				
		.0331				
NaCl	25°	.0799	1.5	2.1	2.5	2.1 (.5)
		.0152				
KCl	25°	.0378	2.2	2.7	2.5	2.7 (.5)
		.0182				
$MgCl_2$	25°	.0431	3.8	5.5	13.1	3.8 (1)
$MgCl_2$	15°	.018	3.6	5.5	13.1	3.8 (1)
$Mg(NO_3)_2$	15°	.00848	4.6	5.9	13.1	4.0 (1)
$Al(NO_3)_3$	15°	.00935	6.2	8.5	37.0	8.5 (.5)
$AlCl_3$	15°	.0090	7.9	9.4	37.0	14. (.3)
$CoCl_2$	15°	.0065	8.1	16.	13.1	16. (.5)
$NiCl_2$	17°	.0048	14.	17.	13.1	17. (.5)
$K_2Cr_2O_7$	17°	.00491	16.	21.	13.1	16. (1)
$Co(NO_3)_2$	15°	.00175	36.	39.	13.1	39. (.5)
$Co(C_2H_3O_2)_2$	15°	.0010	60.	230.	13.1	106. (1)

Readings taken at 15° and 17° are corrected to the equivalent of 25°.

In Table II are presented the results of the comparison of fifteen strong electrolytes. For column four the values of the height of the peak were ascertained in the manner previously described. $\partial\varphi/\partial c^{\frac{1}{2}}$ in column five are for the concentration 0.55 mole/liter, this being selected merely as a convenient value. The density measurements from which $\partial\varphi/\partial c^{\frac{1}{2}}$ values were computed were those in the *International Critical Tables*, Vols. 4 and 6, and Landolt and Bornstein, fifth edition.

In using these data one is well aware of two inaccuracies. One is that the slope, $\partial\varphi/\partial c^{\frac{1}{2}}$, computed from them at $c=0.55$ may not be accurate, for errors in density measurements are accentuated in computing the φ's. The other is that this slope may vary quite a little from the slope at $c=0$, which is the value obtained from Eq. (3) and given in column six. In the comparison to be made it is desirable to know whether or not these inaccuracies vitiate the conclusions presently to be made. As to the exact accuracy of the data, only future measurements can determine. But with each of the fifteen electrolytes the data can be represented by fairly smooth curves and seem to be in good order. However, the tables do not indicate how the data were treated for presentation. It is not likely that the values of the slope $\partial\varphi/\partial c^{\frac{1}{2}}$ in column five for $c=0.55$ are in error by more than a few percent, wholly unimportant in our discussion. How far they vary from the values of $\partial\varphi/\partial c^{\frac{1}{2}}$ at $c=0$ might be important if the experimental curves were strikingly nonlinear. But for nine of the fifteen the curves are linear with φ and $c^{\frac{1}{2}}$ as shown by the values of n in the last column. With these the experimental value

for the slope at $c=0.55$ cannot differ by more than a few percent from the correct slope at $c=0$. An examination of the curves for the other six shows that the variation of the slope at $c=0.55$ from that at $c=0$ might be from ten to fifty percent in error. These errors are not large enough to disturb the conclusions of this paper. O. Redlich has recently made a careful study[14] of existing data for the electrolytes KBr, KCl, NaCl, NaBr, K_2SO_4, Na_2SO_4 and $SrCl_2$. With the first six the slope, $\partial\varphi/\partial c^{\frac{1}{2}}$, at $c=0.55$ differs less than ten percent from the slope at $c=0$. With the seventh the variation is less than twenty percent. With all of the above in view it will be recognized that the conclusions of this paper are not at all weakened by the uncertainties involved.

It is also recognized that one is not justified in using the value of $\partial\varphi/\partial c^{\frac{1}{2}}$ from Eq. (3), which refer to $c=0$, unless the correct value of the constant in the equation is known. Future changes in the constant in Eq. (3) will multiply the entire column six by a factor and will not alter the conclusions concerning the correspondence and noncorrespondence in Table II.

In columns four, five and seven there is a general increase in magnitudes downward. But not so in column six. But according to the simple electrostatic theory, columns five and six should have a correspondence. In accord with the preceding, column four, $\partial h/\partial m$, may be regarded as an indicator of the magnitude of the structural change in the water. The similar progressive change in magnitudes in column four and five leads to the following conclusion. The volume effect of the change in water structure by the ions is of greater importance than the volume effect produced directly by the charges of the ions and their direct effect on the dielectric constant and density of the solvent. It will be observed that there is even a greater correspondence between $\partial h/\partial m$ and $\partial\varphi/\partial c^n$, which is as one might expect for in each case the curve is a straight line with slope independent of concentration in the region considered. This correspondence is shown graphically in Fig. 5.

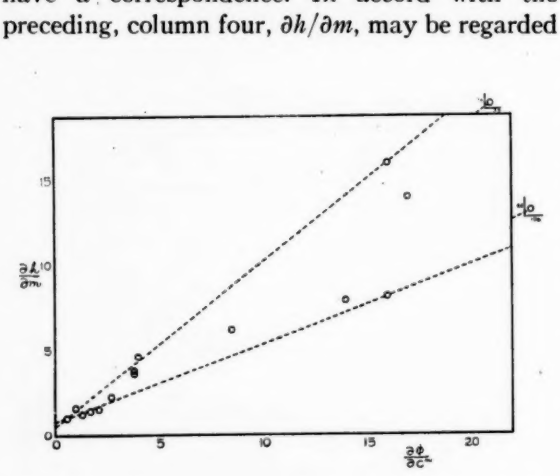

FIG. 5. The values of rate of change of minor peak height (major peak 100) with mole fraction, divided by 100, compared with values of $\partial\varphi/\partial c^n$.

If the change in apparent molal ionic volume rests chiefly in the decrease of volume in the changed water structure, as the above seems to indicate, there is an additional conclusion. The most rapid change in φ with concentration is at the greatest dilution. This can scarcely be accounted for by an effect of an ion only upon its immediate water neighbors. For then the effect on the water volume per ion would remain constant as the concentration increases, at least in fairly dilute solutions. On the other hand, if the effect on the structure were yet appreciable at a distance of perhaps a dozen molecules, then one would expect the volume decrease per ion to become less with increasing concentration, as it actually does. It therefore seems probable that the alteration in water structure is fairly extensive, although, of course, the water is by no means fully homogeneous at any instant. If this be true, the effect of the ion on the 4-coordination of water does not extend merely to its immediate neighbors. The extended change in the structure is thus not caused by a direct electrostatic effect of the ion.[15]

Table II contains electrolytes of different types, selected chiefly because they had a practicable optimum thickness in the apparatus. At the same time wide values of the exponent n

[14] Information kindly supplied by Dr. O. Redlich in correspondence.

[15] *Note added in proof.*—Beck (Physik. Zeits. **40**, 474 (1939)), concludes from experiments that at low concentrations the water builds the ions into its structure, as in an alloy, and that at high concentrations the salts begin to build their own structures. Hildebrand (Science **90**, 1 (1939)), calls attention to Latimer's study of the entropy of solutions of ions and to the basis adopted in the explanation; namely, alterations in the structure of the water.

were avoided. These selections were made in advance of the experimental test and not subsequently. Moreover, none tried has been thrown out because of disagreement. One, $Co(C_2H_3O_2)_2$, with such a high value of $\partial\varphi/\partial c^{\frac{1}{2}}$, was used because it was an extreme case. The approximately similar progression of values in columns four and seven seem, therefore, to have a definite significance, quite beyond the possibility of accident. It is thus difficult to escape the first conclusion, that the ions alter the structure of the water by producing closer packing and greater density.

On the other hand it is equally clear that one may not anticipate that the manner in which all ions affect the density will be precisely the same. Indeed, the similarity of columns four and seven cannot be expected to exist for all strong electrolytes, even those with positive values. In other words, $\partial h/\partial m$ is not at all a good or reliable indicator. One cannot anticipate that the influence of ions on the structure is additive, since, in the above view, the effect is not strictly local and would depend upon the ion combination. As a consequence of these limitations, one is prepared for a complexity difficult and quite impossible to unravel in any simple statement.

An examination[13] of 197 strong electrolytes shows not only a considerable variation in n, but six of them are anomalous. Also six electrolytes have a φ decreasing with increasing c in dilute solutions. Whether or not this variation of φ is explicable by a decrease in the coordination number of the water, remains to be determined. There are seven strong electrolytes that have negative values of φ, but at the same time φ increasing with c. These appear to be only exceptionally potent in altering the water structure.[16]

From the foregoing use of Table II it is evident that the possible errors in column five when the values are considered to apply at $c=0$ are not sufficient to negate the conclusions. The comparisons made are justified.

The picture of the solvent and its alteration in density by the ion solute, that is in agreement with the above, with the preliminary suggestion of Bernal and Fowler[10] and with the analysis of Morgan and Warren,[4] is as follows. The water at temperatures near freezing point has, instead of the coordination number in ice, a greater value with a corresponding closer packing and increased density. This change at freezing is the chief explanation of the latent heat of fusion and the increase in density. The structure in the water is not like that in a crystal, and the relation of any molecule to its neighbors is constantly changing. Coordination bonds are constantly being broken and re-formed. The water is homogeneous in density and structure only if a large enough group of molecules, say of the order of one hundred, are considered. The effect of the ions is not to contract a structure, but to increase the coordination number and thus change the closeness of packing, this increase referring to a mean result, and obviously not to each molecule.

I wish to express by indebtedness to Mr. B. J. Miller and Mr. James Jacobs, research assistants, the former for the data of Part I and the latter for that of Part II.

[16] The anomalous six are: $K_3Fe(CN)_6$, $LiCHO_2$, $Pb(ClO_3)_2$, $Sr(ClO_3)_2$, TlF, $UO_2(NO_3)_2$. The six with φ decreasing are: $Th(NO_3)_4$, $UO_2(NO_3)_2$, $Ba(OH)_2$, Cs_2SO_4, $KClO_3$, $(NH_4)_2C_2O_7$. The seven with negative values of φ are: $CoSO_4$, $CuSO_4$, LiOH, NaF, NaOH, Na_3AsO_4, $ZnSO_4$.

X-Ray Diffraction in Liquid Ethyl Alcohol

G. G. HARVEY
Eastman Laboratory, Massachusetts Institute of Technology, Cambridge, Massachusetts
(Received June 10, 1939)

X-ray diffraction patterns of liquid ethyl alcohol have been taken at temperatures of 25°C and −75°C with monochromatic Mo $K\alpha$ radiation out to values of $(\sin\theta)/\lambda = 1.2$ and Fourier analyses of these curves carried out. The weighted radial atom distribution function shows a number of well-defined peaks. The first of these, at about 1.5A, corresponds to the C−C (1.54A) and C−O (1.43A) distances in the molecule, the two being superposed. This composite peak is completely resolved from the remainder. A peak at about 2.4A may be interpreted as due to the other C−O distance in the molecule. These are the only definite distances, corresponding to permanent neighbors, that would be expected. A most interesting feature is the existence of a peak at about 2.9A corresponding to intermolecular linkage of hydroxyl groups, similar to the situation found in liquid methyl alcohol. The area under this peak shows that each hydroxyl is linked to, roughly, two others, as was also found to be the case for methyl alcohol. Beyond this there are no very definite distances, the density curve rapidly approaching the average density.

AMONG liquids studied by means of x-ray diffraction, the primary normal alcohols have always had a particular interest. Stewart and Morrow[1] in their investigation of these liquids found a number of interesting features. However, since they were principally concerned with the position of the main diffraction peak and the scattering at small angles they did not measure the scattering out to very large values of $(\sin\theta)/\lambda$. They did suggest the possibility of aggregation of OH groups in the liquid and this notion has been further extended by Zachariasen.[2] Further evidence in support of Zachariasen's ideas is to be found in a study of liquid methyl alcohol.[3] In view of these results it is of interest to study in more detail the x-ray diffraction pattern of liquid ethyl alcohol.

EXPERIMENTAL

The experimental arrangement and source of radiation was similar to that used for methyl alcohol.[3] A monochromatic beam of Mo $K\alpha$ radiation was obtained by reflection from a rocksalt crystal mounted on the camera at the entrance to the collimating system. The sample consisted of a free stream of ethyl alcohol which was circulated by means of a small "Fountainnette" pump. The alcohol used was about 97 percent C_2H_5OH, the remainder being mostly water. Hydrogen or helium was circulated through the camera during all exposures so as greatly to reduce any small angle scattering from the medium surrounding the sample. At the lower temperature used, −75°C, the vapor pressure of the alcohol is a very small fraction of a millimeter of mercury and its effect can be neglected. Exposures of about fifteen hours usually sufficed. Care was taken to see that the alcohol stream (about 0.2 cm in diameter) was accurately centered in the camera. The rate of flow was adjusted so that no turbulence occurred and the flowing stream appeared to be a smooth, stationary cylinder when viewed with a low powered microscope. At the temperature of −75°C the viscosity of the alcohol had increased considerably and a larger nozzle was necessary in order to give the requisite flow. The low temperature was attained by surrounding a reservoir of alcohol, just above the nozzle, with a mixture of solid carbon dioxide and alcohol. As the rate of flow was small the temperature was practically that of the bath, roughly −75°C.

In the case of methyl alcohol[3] it was found that reducing the temperature from 25°C to −75°C resulted in a large increase in the detail of the diffraction pattern and the resulting atomic distribution curve, and it was hoped that a similar situation might occur with ethyl alcohol. Since ethyl alcohol freezes at about −117°C, however, a temperature of −75°C is

[1] G. W. Stewart and R. M. Morrow, Phys. Rev. **30**, 232 (1927).
[2] W. H. Zachariasen, J. Chem. Phys. **3**, 158 (1935).
[3] G. G. Harvey, J. Chem. Phys. **6**, 111 (1938).

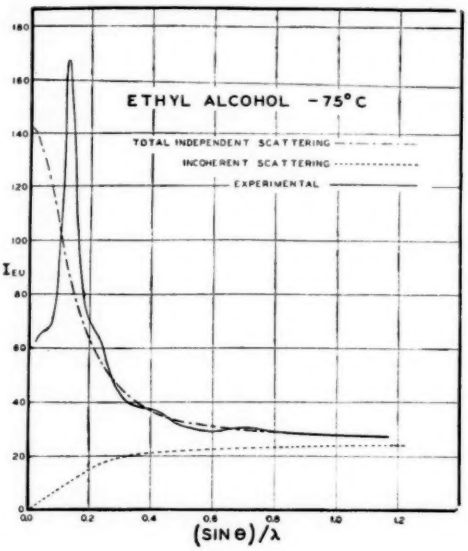

FIG. 1.

still quite far from the freezing point; on the other hand, methyl alcohol freezes at about −98°C. While some difference in the expected direction was found, the diffraction pattern of liquid ethyl alcohol at room temperature (about 25°C) was not appreciably different from that obtained at −75°C and in the following only the low temperature results will be considered.

RESULTS

The exposed films were microphotometered and converted to intensities in the usual way. When corrected for polarization and reduced to electron units they give the scattering per molecule as a function of $(\sin\theta)/\lambda$. The absorption correction was negligible. The resulting average intensity curve, computed from a number of films, is shown in Fig. 1. It will be observed that beyond $(\sin\theta)/\lambda=0.8$ the measured intensity differs inappreciably from the independent scattering curve. This means that both inter- and intramolecular interference is negligible at angles beyond this value.

This intensity distribution was then subjected to a Fourier analysis in order to obtain the radial atom distribution curve. The theory of the general method gives:[4]

$$\sum 4\pi r^2 K_m \rho_m(r) = 4\pi r^2 \rho_0 \sum Z_m + \frac{2r}{\pi}\int_0^\infty si(s)\sin rs\,ds, \quad (1)$$

where

$\sum$ = summation over the atoms in a molecule,
$4\pi r^2\rho_m(r)dr$ number of atoms, each multiplied by its effective number of electrons, between r and $r+dr$ from atom m,
ρ_0 = mean electron density of scattering matter,
Z_m = atomic number of atom of type m,
$K_m = (f_m/f_e)_{\text{average}}$,
f_m = scattering factor of atom of type m,
$f_e = (\sum f_m)/(\sum Z_m)$ = average f per electron,
$s = (4\pi \sin\theta)/\lambda$; 2θ = angle of scattering,
$i(s) = (I_{\text{e.u.}} - \sum f_m^2)/f_e^2$, and
$I_{\text{e.u.}}$ = experimental coherent scattering per molecule in absolute electron units.

A curve giving $si(s)$ is computed from the experimental scattering curve and the integration in Eq. (1) is carried out with an harmonic analyzer for a series of values of r. The result is a weighted atom distribution curve, the quantity $\sum 4\pi r^2 K_m \rho_m(r)$ being the number of atoms at a distance r from a given atom, each atom being weighted by its effective number of electrons and the summation being taken over all the atoms in a molecule. The resulting distribution curve is shown in Fig. 2. The first peak at about 1.5A is due to the intramolecular distances C−C and C−O. These correspond to perfectly definite numbers of neighbors at definite distances.

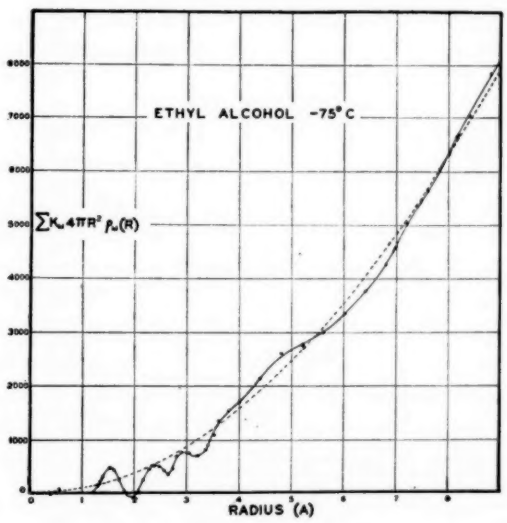

FIG. 2.

[4] E.g., B. E. Warren, H. M. Krutter and O. Morningstar, J. Am. Ceramics Soc. **19**, 202 (1936). Also, B. E. Warren, J. App. Phys. **8**, 645 (1937).

Each of the carbon atoms in the C_2H_5OH molecule has another carbon atom in the same molecule at a distance of 1.54A and one of these carbons has an oxygen atom at 1.43A. The oxygen atom also has a carbon atom at 1.43A. Thus the area under the first peak should be $2\times K_C\times K_C+2\times K_C\times K_O$. In a molecule such as C_2H_5OH it is a little difficult to know just how to distribute the hydrogen electrons among the atoms but as far as x-ray scattering is concerned we shall probably not be far wrong if we assign about seven electrons to each carbon atom and eight or nine electrons to oxygen. This would give an area of about 210 electrons[2] for the first peak. The experimental value is about 180 electrons.[2] The next two peaks in the distribution curve overlap somewhat but the separate peaks can probably be estimated fairly accurately. The first of these, at about 2.4A, is due to the other C−O distance in the molecule. If we assume the C−C bond to make a tetrahedral angle with the C−O bond and use distances of 1.54A for C−C and 1.43A for C−O then the second C−O distance is about 2.42A. This is also an intramolecular distance and thus corresponds to a known number of neighbors. As before, we may compute its value to be about 125 electrons.[2] The observed value is about 200 electrons.[2] The remaining peak at about 2.9A is of especial interest. It is undoubtedly due to hydroxyl bonding between molecules, similar to the situation in methyl alcohol.[2,3] From the observed area of this peak we may compute the number of hydroxyls surrounding any given hydroxyl group: Area$=n\times 9^2$. As usual, it is difficult to know just how much area to include in this peak, but it certainly is of the order of 200 units. Thus, as is also found to be the case in methyl alcohol, we may conclude that each hydroxyl is linked, temporarily of course, to about two other hydroxyls.

Beyond this distance the peaks rapidly decrease in prominence and not much more can be said with any degree of certainty; this is unfortunately true for most organic liquids, due to the small scattering power of the atoms and the fact that a large number of comparable distances serve to smear out the distribution curve, making it rapidly approach the average density distribution.

OCTOBER, 1939 JOURNAL OF CHEMICAL PHYSICS VOLUME 7

The Raman Spectra of Gaseous Substances

1. Apparatus and the Spectrum of Methylamine

J. S. KIRBY-SMITH* AND L. G. BONNER
Physics Department, Duke University, Durham, North Carolina

(Received July 11, 1939)

An apparatus is described by means of which the Raman spectra of gases may be obtained at pressures as low as 2–3 atmospheres and with exposure times of 3–6 hours. The fundamentals of this apparatus are a high intensity light source, a large scattering volume and a large aperture spectrograph camera. Nine lines in the spectrum of methylamine have been measured and are compared with previous measurements on the liquid. An interesting feature of this spectrum is the existence of four lines in the region of C−H valence vibrations, where but two are expected. This anomaly is interpreted in terms of a double resonance interaction.

INTRODUCTION

FOR Raman spectroscopy to attain its maximum value in the determination of the structure of individual molecules, it is essential that measurements be made in the gas phase whenever possible. Gas measurements, however, have been few and sporadic due to the great experimental difficulties involved in such determinations. The present work represents a successful attempt to obtain Raman spectra of gases at comparatively low pressures in reason-

* Part of a thesis submitted to the Graduate School of Arts and Sciences of Duke University in partial fulfillment of the requirements for the degree of Doctor of Philosophy.

able exposure times. This has been accomplished by the use of large scattering volumes, a powerful light source, and a fast spectrograph.

Apparatus

The light source consists of 16 high intensity mercury arcs, operating in a vertical position, and mounted about the central Raman tube. The lamps are constructed of standard Pyrex tubing 1.2 cm inside diameter with wall thickness 1.5 mm. A condensing chamber is included in each lamp in order to control the mercury vapor pressure in the discharge tube and hence the characteristics of the discharge itself. Total over-all length, including condensing chamber, is 90 cm. The effective arc length available for the illumination of the scattering tube is 55 cm. Mercury pool electrodes are used, with tungsten leads sealed in through Nonex glass.

The lamps are operated on direct current at a line voltage of from 130 to 140 volts. The voltage drop across each lamp is roughly 80 volts under usual operating conditions. Normal power dissipation is approximately 500 watts per lamp. Each lamp is equipped with a separate circuit including ballast resistor and a small inductance.

The lamp housing consists essentially of three circular metal plates, mounted one above the other and supported by three steel rods. These plates are 30 cm in diameter and have circular holes cut in their centers. The resulting opening along the vertical axis of the housing serves to accommodate the Raman tube and such concentric filter jackets as may be necessary. Scattering tubes up to 6 cm diameter and filter jackets as large as 10 cm diameter may be used with the present arrangements. The top plate of the housing is slotted, permitting the arcs to be inserted in operating position. During operation cylindrical aluminum reflectors are placed around the lamp housing.

Since as much as 8 kw is dissipated in the lamp housing, cooling is of major importance, and is obtained primarily by means of compressed air blasts. Eight $\frac{5}{16}$-in. copper pipes are built into the lamp housing parallel to the vertical axis and 3 mm behind the arc positions. These tubes are connected directly to compressed air mains. Air is blown upon the arcs through numerous small holes drilled in the tubing. Also, a strong air blast is directed upward between the arcs

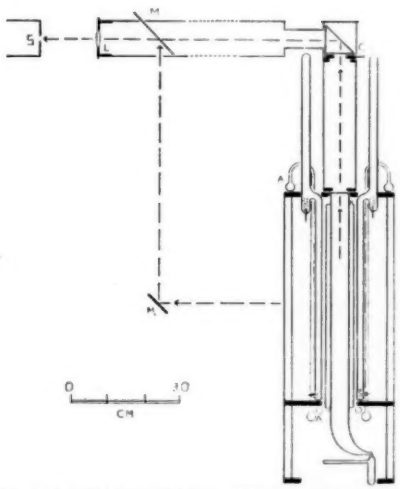

FIG. 1. Vertical section of Raman apparatus.

and scattering chamber. A large volume of cold air is thus available in the small space occupied by the source, which permits the lamps to be mounted very close to the Raman tube. Two fans directed upon the entire apparatus complete the air cooling arrangements.

Even with maximum air cooling, the temperature of the scattering chamber and filter jacket sometimes exceeds 100°C. In order to keep the filter solution from boiling, and to control the temperature of the scattering substance, the filter is continuously circulated and cooled by passing through two water-cooled condensors.

The optical system is represented in Fig. 1. Scattered light passes vertically upward from the end of the Raman tube, is totally reflected through 90° by a prism, collimated by means of a long brass tube with several diaphragms and focused on the slit of the spectrograph.

As all stray light must be eliminated when dealing with scattering by gases, some collimation of the scattered beam is necessary before it reaches the prism, in order to avoid scattering by the glass itself. This is accomplished by placing the prism 30 cm above the end of the Raman tube and inserting two diaphragms. The mirror M and the removable mirror M_1 serve to reflect direct light from the arcs into the spectrograph for comparison purposes.

The spectrograph employed is the Zeiss 3-prism instrument with collimator aperture $f:6$ and effective camera aperture $f:2.3$. Dispersion is only 60A per mm at 4500A, but resolution is extremely good.

Experimental

The methylamine used was obtained from Kahlbaum, distilled in vacuum, and introduced into the Raman tube by means of a second vacuum distillation. The tube was then sealed off and the substance allowed to reach equilibrium between the liquid and vapor phases at room temperature, resulting in a pressure of approximately 3 atmospheres. No Raman lines have been observed which might be attributed to the most probable impurities, i.e., NH_3 and H_2O.

Excitation was by Hg 4047 and Hg 4358. Plates were obtained with both lines present as exciting radiation, with Hg 4358 alone, and with Hg 4047 very intense and Hg 4358 considerably diminished. In some cases, the strong high frequency shifts from the Hg 3650 group were observed, but this did not introduce any ambiguity in the assignment of the frequencies.

The filters used for the two-line excitation were a ten-percent aqueous solution of $CoCl_2$ plus ten percent 6*N* HCl, or a dilute solution of methyl-violet in water (0.05 g per liter). A filter is desirable even in the case of two-line excitation in order to remove the continuous radiation and also to weaken the line Hg 4916 which frequently interferes with 3000 cm^{-1} shifts from Hg 4358. For excitation by Hg 4358 alone, the previous $CoCl_2$ solution plus 15 g quinine sulphate per liter was used. A stronger solution of methyl-violet was employed when it was desired to diminish Hg 4358 and obtain excitation primarily by Hg 4047.

All exposures were made on Ilford hypersensitive panchromatic plates. The slit width was varied from 0.20 mm for observing the weaker lines to 0.045 mm for the more precise measurements on the stronger lines. Exposure times of from 3 to 6 hours were sufficient to bring out all lines, although some exposures of 8 to 12 hours were made with the narrowest slit widths.

The wave-lengths of the Raman lines were obtained by direct interpolation from the position of the nearest iron lines in the comparison spectrum. A comparison spectrum of the direct radiation from the arcs was also photographed on each plate, in order to eliminate the possibility of any spurious Rayleigh scattered lines being mistaken for Raman lines. Measurements were made directly from the plates by means of a comparator and also from photographic enlargements of each plate. The plates were microphotometered, and the estimated relative intensities obtained from these results.

Table I.

Gas Frequency in cm^{-1}	Intensity	Liquid Frequency in cm^{-1}
781	1*s*	
1044	7*s*	1039 (6)
1460	3*vb*	1466 (3*b*)
2820	8*s*	2808 ($\frac{1}{2}$)
2883	3*s*	2879 (5*b*)
2900	4*b*	
2960	10*s*	2955 (2)
3360	10*s*	3312 (4)
3470	2*s*	3372 (2)

Results

Table I gives the results obtained from 12 plates, together with estimated intensities. For comparison the latest results obtained by Kohlrausch[1] in the liquid are included with intensities.

Discussion

As is to be expected, the measurements in the gas phase differ considerably from previous liquid measurements in intensity and in many cases in frequency. This is particularly true in the case of the N−H valence vibrations in the neighborhood of 3400 cm^{-1}, where the shifts are 50 cm^{-1} and 100 cm^{-1}, respectively. The largest difference between gas and liquid in the C−H vibrations is only 12 cm^{-1}. The magnitude of the N−H shifts is undoubtedly due to hydrogen bonding between adjacent NH_2 groups in the liquid. This cannot occur to any appreciable extent in the gas at the comparatively low pressures used in the present investigation.

In the case of the C−H bending frequency at 1460 cm^{-1} it is interesting to note that although its value is very close to the result obtained in the liquid state, this line is extremely broad and diffuse in the gas. Attempts to resolve any structure in this band were not successful.

The weak line at 781 cm^{-1} which is not observed in the liquid is undoubtedly to be associated with an N−H bending vibration.[2] One would expect the N−H bending frequencies to

[1] K. W. F. Kohlrausch, Monatsh. f. Chemie **68**, 349 (1936).

[2] This assignment is based in part on results of infra-red absorption measurements on methylamine vapor. (A. P. Cleaves and E. K. Plyler, J. Chem. Phys. **7**, 563 (1939)).

be quite sensitive to hydrogen bonding and association in the liquid, and it is not surprising that this line appears only in the gas.

The C−H valence vibrations are particularly interesting. It is well known that any methyl compound should possess only two vibrations characteristic of stretching of the C−H bonds. However, it is also well known that the methyl halides exhibit three Raman lines in the C−H valence region, and, in the present case of methylamine, four have been observed. This anomaly has been explained in the methyl halides[3] as due to an interaction of a type first described by Fermi,[4] consisting essentially of a resonance interaction between one of the C−H valence fundamentals and the first harmonic of a lower frequency. The four Raman lines observed in the present investigation may be tentatively explained by either one of two similar mechanisms involving multiple interactions with the harmonics of two lower frequencies.

The infra-red measurements of Cleaves and Plyler[2] show, in addition to the band at 1460 cm^{-1}, a $||$ C−H band at 1426 cm^{-1}. The 1460 cm^{-1} vibration must, therefore, be of the $\perp$ type. These measurements also indicate that the 2960 cm^{-1} C−H valence frequency is $\perp$.

Since the first harmonic of 1460 cm^{-1} will have both $||$ and $\perp$ components there is the possibility of resonance either with the $||$ or with the $\perp$ C−H valence vibration. This gives rise to two possible mechanisms for the double interaction responsible for the appearance of four lines in the 3000 cm^{-1} region. In the first the harmonic of 1426 cm^{-1} interacts with a fundamental near 2840 cm^{-1}. The upper member of the resulting pair of levels then interacts with the $||$ component of the harmonic of 1460 cm^{-1}. The alternate mechanism involves simply interaction between 2×1426 and the $||$ fundamental, giving rise to the 2820 and 2883 cm^{-1} lines and between the $\perp$ component of 2×1460 and the $\perp$ fundamental, giving rise to 2900 and 2960 cm^{-1}. On the basis of observed intensities we are rather inclined to favor the first mechanism over the second.

So far as we are aware, a double resonance interaction of this type has not previously been observed. However, the only other possible interpretation of our results seems to be that a partial resolution of rotational structure has been attained. This is highly improbable.

The line at 1044 cm^{-1}, in very good agreement with measurements in the liquid and with infra-red measurements, is undoubtedly to be associated with the valence vibration of the C−N bond.

Further work is now in progress extending these investigations to measurements of higher amines.

[3] A. Adel and E. F. Barker, J. Chem. Phys. **2**, 627 (1934).
[4] E. Fermi, Zeits. f. Physik **71**, 250 (1931).

OCTOBER, 1939 JOURNAL OF CHEMICAL PHYSICS VOLUME 7

The Nature of the Fusion Process in Argon*

O. K. Rice
University of North Carolina, Chapel Hill, North Carolina

(Received June 29, 1939)

A brief review is presented of the method previously used of treating the phenomenon of fusion by means of curves for the thermodynamic functions $(\partial E/\partial V)_T$ and $(\partial S/\partial V)_T$ as functions of the molal volume. The curves used by the writer in previous work are shown to be consistent with Bridgman's P-V-T data. The characteristics of these curves are discussed, and the evidence is considered which tends to indicate that fusion involves an order-disorder phenomenon. The applicability of various types of order-disorder theory is critically considered in the light of the available experimental data.

IT has recently been suggested from several sources that the process of fusion involves an order-disorder phenomenon of one kind or another. Frank[1] set forth the idea that when a

* Presented at the Symposium on the Liquid State and Polyatomic Molecules, University of Chicago, June 23–27, 1939.

[1] F. C. Frank and K. Wirtz, Naturwiss. **26**, 687, 697 (1938); F. C. Frank, Proc. Roy. Soc. (London) **A170**, 182 (1939).

crystal melts the transition is of the same type that occurs in alloys. This idea was also suggested independently and considerably elaborated by Lennard-Jones and Devonshire.[2] Earlier Hirschfelder, Stevenson and Eyring[3] expressed the belief that the entropy of fusion of a monatomic substance was to be traced to the communal entropy, which, according to their ideas, was excited only when the atoms or molecules in the condensed phase were able to exchange places freely; this, therefore, also implied an order-disorder phenomenon, and, indeed, Lennard-Jones and Devonshire have suggested that it is not inconsistent with their theory, though, superficially, there seems to be but little resemblance between the two hypotheses. A few months ago I suggested that the phenomenon of fusion was intimately connected with an order-disorder transition of a different type; namely, it was supposed that the melting was associated with a change of coordination number from 12, let us say, which permits a regular arrangement of atoms, to such a coordination number as 11, with which a regular arrangement is not possible.[4]

Though a number of investigators who have written on the subject are thus agreed that some type of order-disorder phenomenon is involved, it would not appear offhand that this is necessary, as it is quite possible to have transitions which are apparently not connected with any change in the order of system. Evaporation of a liquid phase is such a transition. The fact that van der Waals' theory gives a sharp transition, even though it does not reproduce all the details, may be taken as evidence that the entropy in this case is largely controlled by the free volume rather than by a change in the degree of order or disorder of the system.

It seems, therefore, worth while to consider the evidence that there actually is an order-disorder change involved in the process of fusion, to attempt to evaluate the various theories which have been proposed, and to consider the difficulties which have yet to be overcome. I shall confine my attention to the case of argon, and base the discussion upon the simple thermodynamic diagrams which I have recently used in attempting to correlate the melting phenomena.[5] I now propose to determine how these diagrams fit in with the other thermodynamic properties of liquid and solid phase. In this way it will be possible to learn just what any proposed theory of fusion must explain, and it will also be possible to get some idea of the general type of theory required.

The method is based upon the thermodynamic equation[6]

$$T(\partial S/\partial V)_T=(\partial E/\partial V)_T+P. \qquad (1)$$

If the quantities $T(\partial S/\partial V)_T$ and $(\partial E/\partial V)_T+P$ are plotted separately as functions of the volume, the points of intersection of these curves determine the volumes of phases which are in internal equilibrium at the given temperature and pressure. Such an equilibrium is a stable rather than an unstable one (i.e., corresponds to a minimum rather than a maximum of free energy) if $(\partial E/\partial V)_T+P$ is increasing more rapidly with V (or decreasing more slowly) than $T(\partial S/\partial V)_T$. If there are two or more stable equilibria indicated in this way, in general one of them is the most stable; the condition under which two phases are equally stable and, hence, capable of coexistence

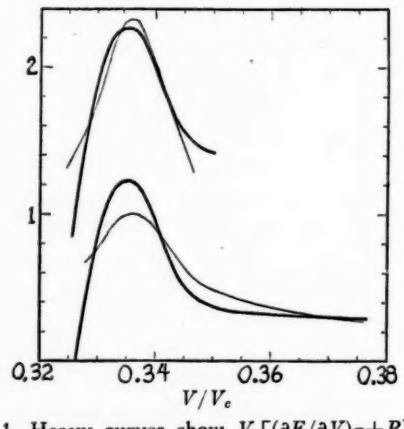

FIG. 1. Heavy curves show $V_c[(\partial E/\partial V)_T+P]$. Light curves show $V_cT(\partial S/\partial V)_T$. Lower pair of curves for 83.9°K; upper pair for 193.1°K. Ordinates should be multiplied by 10^4 to give energies in calories.

[2] J. E. Lennard-Jones and A. F. Devonshire, Proc. Roy. Soc. (London) **A169**, 317 (1939); **A170**, 464 (1939).

[3] J. O. Hirschfelder, D. Stevenson and H. Eyring, J. Chem. Phys. **5**, 896 (1937).

[4] O. K. Rice, J. Chem. Phys. **7**, 136 (1939); and see J. D. Bernal, Trans. Faraday Soc. **33**, 27 (1937).

[5] O. K. Rice, J. Chem. Phys. **6**, 472 (1938).

[6] We use the standard notation of Lewis and Randall, *Thermodynamics* (McGraw-Hill Book Co., 1923). E, S, and V are always *molal* quantities. In reference 4, V was expressed in terms of the critical volume, but here it is more convenient to always let V be equal to the molal volume in cc and bring in the critical volume explicitly when needed.

at a transition point, is that the area under the $(\partial E/\partial V)_T+P$ curve between the volumes corresponding to the two phases be equal to the similar area under the $T(\partial S/\partial V)_T$ curve.

In the case of argon I was able, by a method of trial and error, assuming $(\partial E/\partial V)_T$ and $(\partial S/\partial V)_T$ to be independent of temperature, to determine these quantities as functions of V in such a way that application of Eq. (1) in the manner indicated above reproduced Bridgman's data on the melting parameters with fair accuracy.

This procedure is illustrated by Fig. 1. Here $(\partial E/\partial V)_T+P$ and $T(\partial S/\partial V)_T$ (both multiplied by the critical volume, V_c) have been plotted against V/V_c for two cases: the first case is $T=83.9°$K, the normal melting point, and $P=0$; the second case is $T=193.1°$K with the proper P added to $(\partial E/\partial V)_T$, so that the condition for having two phases in equilibrium is fulfilled—this value of P is thus the pressure at which liquid argon (i.e., amorphous or "molten" argon —we use the term "liquid" even though the critical temperature be exceeded) at 193.1° freezes. The same functions for $(\partial E/\partial V)_T$ and $(\partial S/\partial V)_T$ have been used for both temperatures.

As stated, these particular functions gave a good account of the melting parameters, for by their use it was possible to reproduce fairly well the values of the pressure at which melting occurred, as well as the ΔV and ΔE of melting at various temperatures. However, if the curves for $(\partial E/\partial V)_T$ and $(\partial S/\partial V)_T$ were supposed to remain independent of temperature, it was found to be impossible to account for the slight experimentally observed decrease with increasing temperature of V_s, the molal volume of the solid which is in equilibrium with liquid at any temperature. It was pointed out that this decrease of V_s could be accounted for if it were supposed that the $(\partial E/\partial V)_T$ and $(\partial S/\partial V)_T$ curves moved bodily to the left as the temperature increased. Though such a shift was believed at the time to be improbable, later considerations, discussed in this paper, will show that it is really quite to be expected.

Experimental Check on the $(\partial E/\partial V)_T$ Curve

Before proceeding to any theoretical considerations, it seems desirable to see if any further check on the accuracy of the $(\partial E/\partial V)_T$ curve can be obtained. Use of the relationship

$$(\partial E/\partial V)_T=T(\partial P/\partial T)_V-P \qquad (2)$$

with available P-V-T data can provide some information regarding $(\partial E/\partial V)_T$. Unfortunately, however, the chief interest centers on the properties of the system when it has a volume between that of the solid and that of the liquid, which region is inaccessible because it corresponds to an unstable condition. The best that can be done, therefore, is to see whether extrapolation of the available data is consistent with the $(\partial E/\partial V)_T$ curve used. To this end I have interpolated in Bridgman's P-V-T data,[7] and have plotted P against T for various values of V (Fig. 2). By measuring the slope of the P *vs.* T curves $(\partial E/\partial V)_T$ can be found with the aid of Eq. (2), but to get $(\partial E/\partial V)_T$ for volumes in the range between solid and liquid considerable extrapolation is often needed. On this account, and since my purpose is only to check the consistency of the experimental data with Fig. 1, I have used Fig. 1 to get another point on the curve. This is done by calculating the pressure at which internal equi-

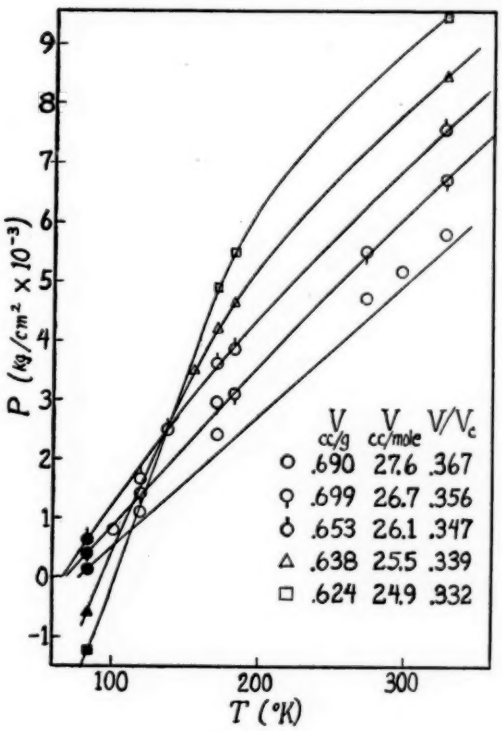

Fig. 2.

[7] P. W. Bridgman, Proc. Amer. Acad. 70, 1 (1935).

librium would occur at any given volume and with $T=83.9°$, using the curves of Fig. 1 and applying Eq. (1), which is the condition for internal equilibrium. The extra points (shown black) on the curves of Fig. 2 make them more definite in form, and $(\partial E/\partial V)_T$ may be calculated from their slope at $T=83.9°$ and compared with the value of $(\partial E/\partial V)_T$ from Fig. 1. Even with this procedure, however, it is hard to get unambiguous results. I have, therefore, merely constructed curves which are consistent with Fig. 1, and these are shown in Fig. 2. Since the curves go through the black points they are consistent with $(\partial S/\partial V)_T$ from Fig. 1 as well as $(\partial E/\partial V)_T$.

Some special remarks are required concerning the curve for $V=0.367\ V_c$. It will be observed that Bridgman's points show considerable deviation from this curve. The slope of the curve agrees with that indicated by the data, but a direct extrapolation from Bridgman's points leads to a pressure at $T=83.9°$, which is not in accord with the pressure read from Fig. 1. But the magnitudes and slopes of the curves of Fig. 1 for 83.9° were rather definitely determined at $V=0.379\ V_c$ (the volume of the liquid at its normal melting point) from other data. It seems quite unlikely that there were any great errors in these data, or that extrapolation of the curves to $V=0.367\ V_c$ could produce as much error as indicated by the difference between the curve of Fig. 2 for $V=0.367\ V_c$ and Bridgman's points, especially since good consistency is obtained at $V=0.356\ V_c$. It seems possible that there is some experimental error in Bridgman's points for $V=0.367\ V_c$. Bridgman remarks that a determination of the molal volume of the freezing liquid in equilibrium with solid at 750 kg/cm² pressure lies too high to fit in with the other experimental points for this quantity and the known value at atmospheric pressure. This determination which is out of line lies in the range of the points which seem to be in error in Fig. 2. We feel, therefore, that it is fair to conclude that, within the limits of experimental accuracy, and insofar as may be judged in view of the extrapolations required, Bridgman's data are consistent with the $(\partial E/\partial T)_T$ and $(\partial S/\partial V)_T$ curves of Fig. 1 for temperatures near the normal melting point.

It will be noted by careful observation of Fig. 2, that the curve for $V=0.332\ V_c$ has a slight inflection near the low temperature end. The curve is drawn this way because $V=0.332\ V_c$ is to the left of the maximum of $(\partial E/\partial V)_T$ at $T=83.9°$. If, when the temperature is increased, the maximum of the $(\partial E/\partial V)_T$ curve moves to the left, the result should be, first, an increase, then a decrease in $(\partial P/\partial T)_V$, thus producing an inflection in the P-T curve. The curve as shown in Fig. 2, does not, to be sure, follow exactly and quantitatively the course expected if there is a mere shift of the maximum in Fig. 1 to the left. The slope of the long straight portion of the P-T curve corresponds to a value of $(\partial E/\partial V)_T$ very slightly greater than the highest value shown in Fig. 1, and the value of $(\partial E/\partial V)_T$ falls off at the higher temperatures more rapidly than expected from Fig. 1. However, it is to be anticipated that the shape of the $(\partial E/\partial V)_T$ curve is not entirely independent of temperature, as we shall see later. The most interesting point is that the inflection in the curve of Fig. 2 does apparently exist, and without it it is impossible to get good correspondence with the $(\partial E/\partial V)_T$ value from Fig. 1 for 83.9°. Further discussion of the shift in the maximum of $(\partial E/\partial V)_T$ and phenomena connected therewith will be postponed to the theoretical part of the paper. It may be remarked that extension of Bridgman's suggestive work on the properties of argon would be extremely valuable. It would, of course, be interesting to penetrate as far as possible into the region of unstable volumes by super-compression or supercooling. But even outside this region, a more closely spaced set of experimental points would be helpful in determining the trend of the curves and in making possible a more precise evaluation of $(\partial E/\partial V)_T$.

As a final check on our $(\partial E/\partial V)_T$ curve, recourse may be had to some data on solid argon obtained by Simon and Kippert,[8] from which $(\partial E/\partial V)_T$ can be calculated for normal (i.e., practically zero) pressure at 73°; $V_c(\partial E/\partial V)_T$ turns out to be 5100 calories. From the curve of Fig. 1, we estimate 6200 at 73°, which seems to be reasonably good agreement.

Discussion of the $(\partial E/\partial V)_T$ Curve

In the light of the above considerations, it seems reasonable to accept the $(\partial E/\partial V)_T$ curve

[8] F. Simon and F. Kippert, Zeits. f. physik. Chemie **135**, 113 (1928). I am indebted to Professor J. H. Hildebrand for suggesting the use of these data.

of Fig. 1 as a basis for discussion. The most remarkable thing about this curve is the sudden rise to a steep and high maximum. I have already pointed out that this cannot be accounted for by any of the usual potential energy curves if the assumption be made that the expansion that occurs from the solid to the liquid is a simple swelling, without distortion, of a face-centered lattice. If we use the interatomic potential, U, suggested by Herzfeld and Goeppert-Mayer,[9] and calculate the energy, E, of the lattice by summation over the lattice points, it is readily seen that the slope of this curve for E does not reproduce the $(\partial E/\partial V)_T$ curve of Fig. 1. The same statement may be made regarding the interatomic potential recently proposed by Buckingham.[10]

It is possible to construct an interatomic potential curve which does reproduce this behavior of $(\partial E/\partial V)_T$ and is also consistent with data on the equation of state of the gas, but the shape of the required curve is rather queer.[11] This may, perhaps, be taken as evidence that the expansion from solid to liquid is more complicated than the mere swelling of a simple lattice, and suggests something in the nature of an order-disorder theory.

This suggestion is further corroborated by a consideration of the entropy of fusion. I have made a rough estimate of the entropy which would be due only to simple expansion of a lattice in the following, by no means novel, manner. First, let us consider an atom in the field due to two neighboring atoms, the centers of all three lying in a straight line. It is not unreasonable to suppose that the actual field in which an atom in the crystal is moving is very similar to this, but in three dimensions, and having nearly spherical symmetry. If we calculate the entropy of the atom in the field of but two neighbors, the entropy of an atom in the crystal will be obtained approximately by multiplying this one-dimensional entropy by three. However, since we are only interested in the *change* of entropy with volume, a sufficiently good estimate can be obtained by inspection of the potential curve for one atom in the field of two others. Using Buckingham's value of U, I have drawn such potential curves for positions of the outside atoms corresponding to different volumes of the face-centered lattice, and have assumed that the one-dimensional molal entropy is given to within an additive constant by

$$S = R \ln l$$

where l is the distance across the resultant potential curve at an energy above the minimum equal to RT, i.e., l is the free distance, whose cube gives the free volume. (See Fig. 3, which shows how l is found.) In this way I have calculated the entropy change due to the change of volume on fusion (normal pressure) as approximately 2.0 entropy units, while the entropy of fusion is 3.12 entropy units.[12] Further, the entropy increases very regularly with V, and $(\partial S/\partial V)_T$ shows no maximum. So by considering the entropy we are also led to the conclusion that the phenomenon of fusion involves more than a simple expansion of the lattice. It is true that this conclusion is based upon the interatomic potential curve of Buckingham, not on the interatomic potential curve which I used[11] in order to fix the $(\partial E/\partial V)_T$ function. However, the curves differ from each other in detail rather than in large outline. The entropy depends logarithmically on the free distance, and the latter cannot depend very

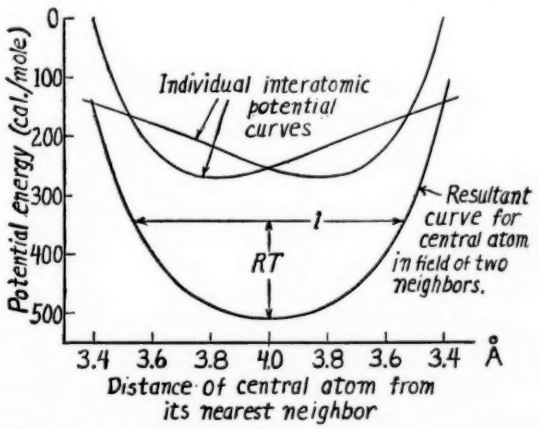

FIG. 3. Calculation of l for an atom in the lattice. The individual atomic potential curves are for the atom under consideration in the respective fields of its two neighbors, the latter assumed fixed in position. The resultant curve is the sum of the two individual curves. The figure shows the special case in which the distance between the two outside atoms is fixed at 8.0A.

[9] K. F. Herzfeld and M. Goeppert-Mayer, Phys. Rev. **46**, 995 (1934); K. F. Herzfeld, *ibid.* **52**, 374 (1937), Eq. (2).

[10] R. A. Buckingham, Proc. Roy. Soc. (London) **A168**, 264 (1938).

[11] O. K. Rice, Science **88**, 440 (1938).

[12] Similar results were obtained with the Herzfeld-Goeppert-Mayer potential. Lennard-Jones and Devonshire estimated that half the entropy of fusion was entropy of disorder.

strongly on the interatomic potential within reasonable limits. It, therefore, seems unlikely that the conclusions would be greatly altered by any reasonable change in the interatomic potential.

It is further to be emphasized that the maxima of $(\partial E/\partial V)_T$ and $(\partial S/\partial V)_T$ come at nearly the same value of V. This, as I have pointed out,[13] is necessary in order that the process of fusion should be a sharp transition. It is, perhaps, not an absolutely necessary condition for a given temperature, but seems necessary if the transition is to remain a sharp one over a considerable range of temperatures.

The fact that the maxima of $(\partial E/\partial V)_T$ and $(\partial S/\partial V)_T$ come at about the same value of V is another argument in favor of an order-disorder phenomenon, for it indicates that an abnormal increase of entropy is associated with an abnormal increase of energy. This is characteristic, for the state of disorder has both a high energy and a high entropy. In view of the importance of the positions of the maxima of $(\partial E/\partial V)_T$ and $(\partial S/\partial V)_T$, we may well assert that the order-disorder phenomenon is an essential feature of melting.

If this is accepted, it then becomes of importance to consider the evidence which may help to decide which of the proposed order-disorder processes is most nearly correct.

Critique of Order-Disorder Theories

As I have already discussed it at length,[14] I do not think it necessary to consider here the theory that the process is the excitation of communal entropy. My conclusion was that communal entropy probably does not play any decisive rôle in the fusion process.

The suggestion that the order-disorder transition is of the type observed in alloys seems to have had a considerable success in the hands of Lennard-Jones and Devonshire.[2] In this theory it is assumed that there are two interpenetrating sets of lattice points, designated by α and β, respectively. Each set is a face-centered cubic arrangement. The two together form a simple cubic arrangement, just as in the sodium chloride type crystal the face-centered lattice of positive ions and the similar lattice of negative ions together give a simple cubic arrangement. It is supposed that in the crystal (perfect order) only one of these sets of lattice points is occupied by atoms. As disorder sets in, points of the other set start to be occupied, and when the disorder is complete there is an equal change that any given lattice point of either α or β be occupied or not. Such a random arrangement is a state of relatively high energy, because it is difficult to put an atom in a β-position when there are already atoms in surrounding α-positions. This is the same thing as saying that a face-centered arrangement has a lower energy than a simple cubic arrangement. However, a random arrangement has a higher entropy, so under the proper circumstances it becomes stable.

The assumptions underlying this theory are quite arbitrary, and Lennard-Jones and Devonshire apparently did not intend that the physical picture should be taken too literally; it was meant rather as a schematic approach to be used as a basis for calculation. In making these calculations it was assumed that to the entropy of the crystal due to the free volume of the atoms, should be added directly the entropy of disorder, arising from the fact that in a state of complete disorder there are twice as many possible positions for the atoms as in a state of complete order. The transition from order to disorder should therefore give a contribution to the molal entropy of $R \ln 2 = 1.38$ entropy units. Since this is just about equal to the difference between the observed ΔS of fusion and the ΔS due to change in free volume alone, it is obvious, at least if it be assumed that at the normal melting point the solid is in a state of practically complete order and the liquid a state of practically complete disorder, that this theory should give a reasonable value for the ΔS of fusion provided the ΔV comes out right. When a parameter was introduced to get the right melting point, it was found that ΔV and ΔS of fusion came out about right. The coefficient of expansion of the liquid is also reproduced by the theory.

This is a very interesting result, but I believe that the hypothesis on which it rests may be justly criticized. It does not seem to be justifiable to assume that an entropy of disorder can be merely added to the volume entropy, because the

[13] O. K. Rice, J. Chem. Phys. **5**, 492 (1937).
[14] O. K. Rice, J. Chem. Phys. **6**, 476 (1938).

latter will also be changed when disorder occurs. A state of disorder is a state in which portions of the crystal are in a simple cubic lattice rather than a face-centered lattice. A simple cubic lattice is by no means as compact as a face-centered lattice. Therefore, at any given molal volume, the atoms of a crystal which is partly of a simple cubic structure must be much more tightly pressed together than in one which has throughout a face-centered lattice. This was recognized by Lennard-Jones and Devonshire, who allowed for its effect on the energy but did not try to take into account its effect on the free volume and hence on the entropy.[15] This same effect is very troublesome in my own theory, which I will discuss later.

The theory of Lennard-Jones and Devonshire apparently does not work well at high pressures. It gives a critical point for fusion of argon at a pressure of approximately 2400 atmospheres, whereas the experiments have been carried up to 6000 atmospheres and 193°K without any indication of a critical point. It may be remarked that there is possible evidence that there is a critical temperature below 328°K for at this temperature Bridgman compressed liquid argon to a volume of 0.573 cc/g at 15,000 kg/cm². A rough extrapolation of the volume of 1 g of liquid in equilibrium with solid suggests that it should not be less than 0.60 cc at 15,000 kg/cm², and an extrapolation of the volume of 1 g of solid in equilibrium with liquid gives a volume of 0.593 cc at 15,000 kg/cm². These are long extrapolations but they do show that the volume of 0.573 cc per gram under the conditions quoted is quite small, and suggest that no transition is going to occur at 328°K. Be this as it may, it is clear that the critical pressure, if one exists, is far higher than 2400 atmospheres. Just how serious an objection this constitutes to the theory of Lennard-Jones and Devonshire, it is a little difficult to say. The occurrence of a sharp transition depends upon a nicely balanced adjustment between two phases. Unfortunately, Lennard-Jones and Devonshire have not calculated other quantities which might be compared with experimental values at high pressure. It seems to me, however, that this essentially oversimplified picture should not be expected to give correct res !ts over any considerable range of pressures.

The theory which I proposed,[4] namely, that the phenomenon of fusion is intimately connected with a change in coordination number, has some points of resemblance to the theory of Lennard-Jones and Devonshire. The latter have treated a case in which the coordination number tends to change from 12 to 6, but, of course, some atoms would have a coordination number of 6, some of 12, and others would have values in between. In the liquid, the average would undoubtedly, according to their picture, lie somewhere between 6 and 12.

My proposal was to consider the coordination number as an additional parameter, which could be used to fix the properties of the system. Thus for any definite value of the molal volume, one could imagine a system in which the average coordination number of the atoms was 11, another in which it was 10.5, say, and so on. Of course, one such arrangement would have the least free energy, and, with fixed molal volume, the system would naturally revert to this most stable form. However, it is possible to imagine the coordination number instead to be fixed, and consider how the energy, entropy, etc., change with the molal volume under these circumstances even though the system is not in its most stable condition.

For example, we could use some standard form of interatomic potential and, assuming a face-centered lattice with coordination number, N, equal to 12, calculate the energy as a function of the molal volume by simple summing over the lattice. As already noted above, this assumes that when the volume increases the atoms remain, at least on the average, in the regular positions for a face-centered lattice. A similar calcu-

[15] Lennard-Jones and Devonshire believed that this was justified because the average volume occupied by an atom remains constant at fixed molal volume. It is my belief, however, that the rough kind of averaging of free volumes implied in this statement is not allowable. I believe (see below) that the essence of the problem is to find the change of free volume due to disorder, and that the change of entropy thereby introduced is the entropy of disorder. Lennard-Jones and Devonshire believe that the change of entropy due to disorder is really essentially equivalent to the excitation of communal entropy, the chief difference being that they are able to calculate the degree of excitation of this communal entropy in detail. This communal entropy, or entropy of disorder, is then merely superimposed upon the entropy due to free volume. But if the communal entropy is already excited in the solid state, as seems likely, this method of procedure must break down. On the other hand, even if communal entropy should play a rôle, the considerations involving free volume are sufficiently general so that they can be made to include it.

lation could be made for the body-centered cubic lattice. If we use the interatomic potential of Herzfeld and Goeppert-Mayer we obtain an energy curve for the body-centered lattice which is almost the same as (slightly higher than) the curve for the face-centered lattice.[16] This result depends greatly on the six *next* nearest neighbors of the body-centered lattice. These next nearest neighbors are relatively close in the case of the body-centered lattice, but they are still too distant to make possible the use of Buckingham's interatomic potential, which is defined only for a fairly narrow range of interatomic distances. It seems likely, however, that the result obtained from the Herzfeld Goeppert-Mayer-potential is correct in indicating that the energy curves for the face-centered and body-centered lattice are close together. It is difficult to make estimates of relative entropies—however, it is clear that the body-centered lattice cannot have an appreciably higher entropy than the face-centered, as there is no indication of a tendency for the crystal to go over to a body-centered form.

An attempt can be made to estimate the energy of states having varying coordination numbers, at least if the coordination number is not too far removed from 12. A system with $N=11$, say, could be imagined to be formed from a face-centered system in which every twelfth atom was removed, leaving a hole, the energy then being just 11/12 that of the original arrangement. Of course, further rearrangement migh occur, leaving, perhaps, more holes of smaller average size, but as long as the average coordination number remains 11, it seems reasonable to accept the estimate of the energy made in the way just indicated.* The energy is compared, however, for similar *interatomic distances* (exclusive of distances across holes); with the same interatomic distance, the density for $N=11$ is less than for $N=12$. If E be plotted against *molal volume*, V, the curves are displaced along the V axis. A set of such curves for various values of N, based on Buckingham's interatomic potential,[17] is shown in Fig. 4.

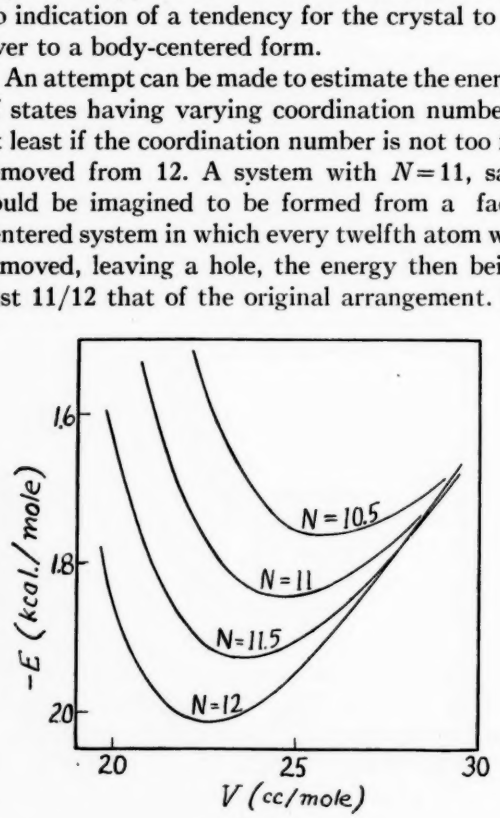

FIG. 4.

It is unfortunately not as easy to make an estimate of the entropy of the system with various coordination numbers. If a hole is formed in the lattice, all the atoms surrounding that hole will have increased freedom of motion, but it is difficult to estimate the magnitude of the increase. Further, the hole may be partially filled up, giving rise to various configurations, all of which contribute to the entropy. We are interested in the change of entropy in going from one coordination number to another, keeping the molal volume constant, for we desire to know what coordination number is stable at any fixed molal volume. This makes matters still more difficult, for in order to maintain a constant molal volume it is necessary, as noted above, to decrease the interatomic distance when holes are formed. This results in a decrease in free volume in regions where there are no holes. The concomitant decrease in entropy is of more or less the same order of magnitude as the increase of entropy due to the holes, so that it becomes doubly hard to estimate the net increase.

This lack of knowledge of the entropy to be associated with systems having different coordination numbers makes it difficult to decide how far the average coordination number is likely to deviate from 12. With smaller co-

[16] See Fig. 1 of reference 4, and compare F. London, Proc. Roy. Soc. (London) **A153**, 576 (1936).

* This breaks down of course, in the way indicated in the second paragraph below, if N is two much lower than 11 or thereabouts, on account of the penetration of next nearest neighbors into the holes in the lattice.

[17] We neglect the thermal and zero-point energy of the system. The curves, of course, give only potential energy, but our interest is in energy differences, and the differences in thermal energy which are involved in the transitions and changes of the system will not be sufficient to upset our considerations. At higher temperatures, however, the thermal energy will probably be of some importance in the quantitative working out of any theory.

ordination numbers, the holes in the lattice become larger and more numerous. This allows the next nearest neighbors of any atom to penetrate close enough to that atom to have an effect on the total potential energy appreciable compared to that of the nearest neighbors. With decreasing N it might be expected that the potential energy curves (Fig. 4) would reach a maximum displacement from the $N=12$ curve (occurring at $N\sim10$), after which they would again drop, approaching the position of the curve for $N=8$. On the other hand, it does seem possible that a condition in which the general face-centered structure remained, but in which there were many large holes, would have a sufficiently high entropy, at least under some circumstances, to render it stable. However, it must be remembered that the entropy is a logarithmic function of the free volume or of the number of possible configurations, so, once it has become sufficiently large, it does not increase as rapidly as the energy. Therefore, it seems likely that the curve for $N=10.5$, shown in Fig. 4, is a rough practical upper limit for the energy function. We take the curve for $N=10.5$ rather than the curve for $N=10$, because no allowance has been made for the effect on the energy of the filling in of the holes as the lattice starts to approach the body-centered condition. As we have noted, this filling in of the holes decreases both energy and entropy. Therefore, it seems reasonable to suppose that when N is equal to 10, the condition of the system is actually given better by the curve for a somewhat larger value, such as $N=10.5$, when the effect of the filling in of the holes is neglected.

It will be noted that the differences in energy between the curves of Fig. 4 decrease rapidly as V increases. The entropy differences for different values of N undoubtedly depend much less strongly on V, since the entropy is a logarithmic function of the free volume. The most stable coordination number at any value of V is that for which $TS-E$ is a maximum. At very small volumes the stable condition will be that for which $N=12$, for the gain in entropy on going to a smaller value of N will not be sufficient to counteract the large increase of energy. This is illustrated by Fig. 5. In this figure $\Delta S_N=S_N-S_{12}$ where S_N is the entropy when the coordination number is equal to N and S_{12} is the entropy when

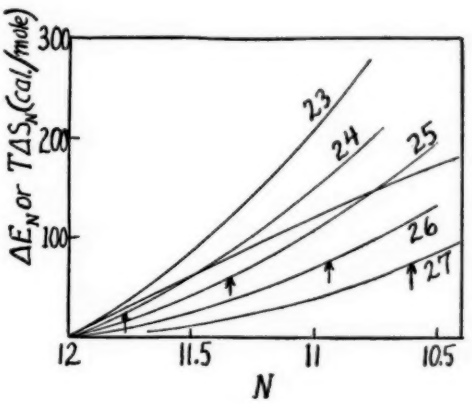

FIG. 5.

the coordination number is equal to 12. Similarly, $\Delta E_N=E_N-E_{12}$. ΔE_N and $T\Delta S_N$ are shown as functions of N. $T\Delta S_N$ is the unlabeled curve; it is purely schematic and is assumed, for purposes of illustration, to be independent of V. The values of ΔE_N, with a preassigned V, can be found from Fig. 4. The numbers on the curves for ΔE_N give the corresponding values of V in cc per mole. In each case, the value of N for which $TS-E$ (or better, conforming to the notation just introduced, TS_N-E_N) is a maximum is indicated by an arrow. It is seen from Fig. 5 how the stable value of N decreases as V increases.

It is this process of changing coordination number, which, according to this theory, produces the abnormally large values of $(\partial E/\partial V)_T$ and $(\partial E/\partial V)_T$ in the range of volumes between solid and liquid. Unfortunately, the theory is not sufficiently developed to allow us to follow the exact way in which the system goes from one potential energy curve to the next, so the exact shape of the $(\partial E/\partial V)_T$ and $(\partial S/\partial V)_T$ curves cannot be calculated.

It is obvious, however, that the higher the temperature, the lower will be the volume at which the entropy term overcomes the energy term and causes the transition to a lower coordination number.[17] This probably accounts for the shift of the maxima of $(\partial E/\partial V)_T$ and $(\partial S/\partial V)_T$ to lower volumes when the temperature is increased. It is important to note that these maxima will always shift together, so we can understand the persistence of the sharp transition over a long range of temperatures and pressures.

If we suppose that the change in entropy accompanying the transition from the state with $N=12$ to the state of maximum energy deviation, $N\sim10$, remains constant with temperature and does not vary very greatly with volume, examination of Fig. 4 leads to the expectation that the maximum of $(\partial E/\partial V)_T$ should shift to smaller volumes more rapidly with increasing temperature than it actually does. This suggests that the repulsive parts of the curves of Fig. 4 should increase more rapidly as V decreases, as this would increase the spread between the curves at the left-hand side of the diagram.[18]

At a high enough temperature the transition from $N=12$ should begin to occur at a low enough volume so that the highest curve of Fig. 4 would be reached at a point to the left of its minimum. If this curve really represents the maximum energy the system can attain it should be possible at a high enough temperature to reach a liquid volume where $(\partial E/\partial V)_T$ is negative. As a matter of fact, this is a common occurrence in liquids and argon, in particular, shows negative values of $(\partial E/\partial V)_T$. An estimate can be made of $(\partial E/\partial V)_T$ at various values of V and T from the curves of Fig. 2. Estimates for 190°K and 320°K are presented in Table I. Unfortunately these are subject to considerable uncertainty and further experimental data would be highly desirable. However, it will be seen that the experimental values for 320°K suggest a curve of somewhat the same type as that for $N=10.5$ of Fig. 4, though the minimum is shifted somewhat, and there is no exact quantitative correspondence.[18] And at larger molal volumes than 28 cc (the volume of liquid in equilibrium with the solid at the normal melting point) the experimental experience is that $(\partial E/\partial V)_T$ tends to decrease while the curves of Fig. 4 would have it increase further before decreasing.

[18] Table I also suggests that the repulsive part of the curves should be steeper.

TABLE I.

	$V_c(\partial E/\partial V)$		
	From Fig. 2		From curve for $N=10.5$, Fig. 4
V/V_c	$T=190°$	$T=320°$	
0.367	3070	3070	1800
.356	3060	1600	1020
.347	2240	50	150
.339	2900	−2430	−525
.332	4960		

In spite of this lack of quantitative correspondence, it seems reasonable to say that the proposed picture gives a fairly good qualitative correspondence with the facts. The values of $(\partial E/\partial V)_T$ as a function of volume have the expected qualitative behavior at both of the temperatures shown in Table I. Further refinements, however, as well as a reliable means of calculating entropy charges will be needed before the theory can be said to be complete. It may be that some entirely different formulation will prove better, but I believe the formulation in terms of changing coordination number has a considerable element of truth and has the advantage that the significance is readily visualized.

It should be noted that since negative values of $(\partial E/\partial V)_T$ occur for high temperatures and not for low, my original hypothesis that $(\partial E/\partial V)_T$ is independent of temperature cannot hold without modification. Even in addition to the shift of the maximum, some change in shape must take place. It may, however, be true that the shape of the curve near the maximum is not very strongly dependent on temperature, and since it is the region of the curves which chiefly determines the melting phenomena, especially at the higher temperatures, it seems not unlikely that my suggestion offers a good working hypothesis to use as basis for discussion.

Exchange Reactions of Nitrogen Isotopes on Iron and Tungsten Surfaces

GEORGE G. JORIS AND HUGH S. TAYLOR
Frick Chemical Laboratory, Princeton University, Princeton, New Jersey

(Received June 21, 1939)

The activities of iron synthetic ammonia catalysts and of tungsten filaments in promoting the reaction between N_2^{30} and N_2^{28} have been studied in the range from room temperature to 725°C with iron and to 900° on tungsten. In contrast to the exchange reaction of molecular hydrogen isotopes, the exchange reaction of nitrogen molecules is very slow, first measurable above 450°. The reaction is accelerated by the presence of hydrogen. The evidence indicates that the exchange involves, as the slow process, either the rupture of valence bonds of adsorbed molecular nitrogen on the surface or migration of nitrogen atoms over the surface, and that hydrogen accelerates such processes. The temperature coefficient of exchange in a $N_2 : 3H_2$ mixture is ~50 kcal. The data suggest that measurements of the velocity of nitrogen adsorption at *ca.* 400°C on synthetic ammonia catalysts are measurements of true activated adsorption.

THE exchange reactions between hydrogen and deuterium at the surfaces of hydrogenation catalysts[1] and the exchange occurring between ammonia and deuterium on catalytic iron surfaces even at room temperatures[2] served to indicate that the activations of the H−H and of the N−H bond readily occur at such surfaces at temperatures far below those at which the synthesis of ammonia from its elements occurs catalytically on such surfaces. These researches led to the conclusion that the activations of these bonds are not significant rate-determining steps in the synthesis or decomposition of ammonia. Such lines of reasoning lead, by processes of elimination, to the conclusion that it is the process $N_{2gas} \rightleftharpoons 2N_{ads}$ which is the rate determining step in both synthesis and decomposition on such iron catalysts; this conclusion from isotope chemistry is in best agreement with evidence accumulated by Emmett and Brunauer[3] from studies of the velocity of activated adsorption of nitrogen on the same catalysts.

The development of Urey and his collaborators[4] of methods for the concentration of the heavy nitrogen isotope permitted a direct experimental test of the correctness of these deductions, by observation of the velocity with which the nitrogen isotopes would undergo the exchange reaction $N^{28}{}_2 + N^{30}{}_2 = 2N^{29}{}_2$, in the range of temperatures where synthesis and decomposition of ammonia occur. The exchange reactions involving deuterium have shown themselves to be a particularly effective tool for the indication of the interaction between gas and catalyst surface involved in activated adsorption. We record in the following sections our experimental results with a number of iron catalysts and with a tungsten filament as the activating surface for the nitrogen exchange reaction and also the influence of hydrogen on the velocity.

[1] (a) A. J. Gould, W. Bleakney and H. S. Taylor, J. Chem. Phys. **2**, 362 (1934); (b) A. Farkas, L. Farkas and E. K. Rideal, Proc. Roy. Soc. **A146**, 630 (1934).
[2] H. S. Taylor and J. C. Jungers, J. Am. Chem. Soc. **57**, 660 (1935).
[3] P. H. Emmett and S. Brunauer, J. Am. Chem. Soc. **55**, 1738 (1933); **56**, 35 (1934).
[4] H. C. Urey, J. R. Huffman, H. G. Thode and M. Fox, J. Chem. Phys. **5**, 856 (1937); H. G. Thode and H. C. Urey, *ibid.* **7**, 34 (1939).

Experimental Details

Catalysts

The majority of our experiments have been carried out with the catalyst No. 931 of the Fixed Nitrogen Research Laboratory, U. S. Bureau of Chemistry and Soils, kindly placed at our disposal by Doctor S. Brunauer to whom we wish to express indebtedness for his help and advice as to best methods of procedure. This catalyst is the so-called doubly-promoted iron, in which K_2O and Al_2O_3 are the promoters. Its characteristics are well known. In the majority of experiments here reported the catalyst was prepared by reduction of the oxide according to the following schedule, 4 hours at 350°, 4 hours at 400°, 48 hours at 450° and 24 hours at 500° with hydrogen at a flow rate of 6 liters per hour, using 2 grams of catalyst. A few experiments were

carried out with Catalyst No. 954 of the same origin, an Fe_3O_4 catalyst containing 10.2 percent Al_2O_3 as promoter, with the same reduction schedule. After each group of experiments at a given temperature the activity of the catalyst was normally tested by decomposition of ammonia at 410°C. In every case the ammonia decomposed at a rate which was immeasurably rapid and analysis of the product gas showed the normal $N_2 : H_2$ ratio of 1 : 3.

For the experiments on tungsten surfaces we employed a 150-watt Mazda tungsten filament lamp of 325 cc capacity employed by Jungers and Taylor[5] in studies of the decomposition of deutero-ammonias. The lamp was immersed in a cold water bath at a temperature of approximately 25°C and the tungsten wire could be maintained at constant temperatures between 700 and 900°C by maintaining a constant resistance of the wire with energy from a suitable d.c. source at 110 volts and adjustable external resistances.

Nitrogen isotope mixture

All our experiments have been carried out on a two-liter sample of nitrogen gas, containing approximately 10 percent N^{15}, kindly placed at our disposal by Professor H. C. Urey of Columbia University to whom we express our deep indebtedness. A mass-spectrographic analysis of the sample showed it to contain N^{28}_2, 1000; N^{29}_2, 103; and N^{30}_2, 59 parts. This mixture, which had been obtained by dilution with ordinary nitrogen of a sample much richer in heavy isotope was ideally suited to our needs since it was far removed from the equilibrium ratios of constituents. Assuming a statistical equilibrium constant of 4 for the reaction, $N^{28}_2+N^{30}_2=2N^{29}_2$, an equilibrium mixture of the several species obtained from the initial sample would show, per 1000 parts of N^{28}_2, approximately 200 parts of N^{29}_2 to 10.5 parts of N^{30}_2. The mass ratio $N^{29}_2 : N^{30}_2$ would therefore change from an initial value of 1.75 to an equilibrium value of 19. The course of reaction could therefore be followed, owing to the tenfold excess of N^{28}_2, with adequate accuracy by following this ratio mass-spectrographically.

In the initial sample the mass spectrograph revealed a constituent of mass 31 in amount equal to eight parts per 1000 of N^{28}_2. We learned subsequently from Professor Urey that this constituent was methylamine. Some of the experiments recorded were made with samples from which this constituent was not removed. In the mass analysis it was found possible to eliminate this constituent by a preliminary liquid-air trap and a similar elimination was effected in all of our decisive experiments. No oxygen was present in the sample according to mass analysis, but in all experiments the precaution was taken of eliminating traces by introducing the gas into the reaction zone through a tube maintained at 220°C of freshly reduced catalyst composed of Cu·4MgO, the latter constituent acting as support for a copper of high activity[6] readily reactive with oxygen. This copper was inactive, by test, in the exchange reaction of the nitrogen isotopes at this temperature (see Table I) and even at 410°C.

Reaction system

Two grams of catalyst were loosely disposed on the surface of a horizontally placed cylindrical quartz tube whose dimensions were 12 cm long by 2.2 cm diameter. This was connected through a quartz to Pyrex seal to a capillary U-tube immersed in solid carbon dioxide-acetone mixtures which served as guard tube against moisture and mercury vapor poisons. This guard tube was connected via a vacuum stopcock to the evacuation system and to the gas reservoir and the purification train of copper already discussed. This latter was protected before and after by two

TABLE I.

Catalyst	Temp. °C	Time in Hours	Parts per 1000 N^{28}_2 of		Ratio 29 : 30
			N^{29}_2	N^{30}_2	
Glass	25	—	103	59	1.75
Quartz	750	20	108	62	1.76
"	750	44	99	54	1.83
Fe (931)	220	2	115	50	2.3
"	220	12	106	54.5	1.94
"	410	3	116	55.3	2.10
Cu-MgO	220	2	100	52.5	1.90
"	220	12	114	60	1.90
"	220	30	106	55.7	1.90
"	410	3	105.5	54.3	1.94

[5] J. C. Jungers and H. S. Taylor, J. Am. Chem. Soc. **57**, 679 (1935).

[6] H. S. Taylor and G. G. Joris, Bull. Soc. Chim. Belg. **46**, 241 (1937).

other U-tubes immersed in liquid air. Hydrogen for reduction purposes also entered the reaction system through this copper purifier.

Experimental Results

In the following tables are set forth the definitive experiments performed subsequent to a considerable number of earlier trials designed to define the best operating conditions and method of analysis. Table I records experiments in the temperature range 220–410° with the iron catalyst No. 931 and with the reduced Cu-MgO used to remove any traces of oxygen which might be present. With neither catalyst in this range was exchange observed even with contact times extending to 30 hours. The same table records the absence of any exchange in a quartz tube without catalyst at temperatures as high as 750° and with contact times up to 44 hours.

Table II. *Nitrogen isotope exchange in* N_2-3H_2 *mixtures on iron catalyst No. 931.*

Temp. °C	Time in Hours	Parts per 1000 N^{28}_2 of N^{29}_2	Parts per 1000 N^{28}_2 of N^{30}_2	Mass Ratio 29 : 30
460	2	106	52.5	2.01
	5	121	45.6	2.60
	19	171.5	21.4	8.02
	27	174.5	15.1	11.65
	42	185	12.3	15.05
	50	194	12.75	15.25
	70	188	11.55	16.30
500	2	146	39.6	3.70
	6	191.8	19.1	10.03
	8.5	204	16.7	12.18
	20	203	15.1	13.50
		174.5*	17.1*	10.20*

* The analyses in the last line were taken of the gas residue from the experiment at 500° after the system had cooled to room temperature.

The first line shows an analysis on the original nitrogen used. The second line shows a test in quartz with a $N_2 : 3D_2$ mixture while in the remaining experiments the nitrogen containing a trace of methylamine (31) was the reactant. The analyses shown reveal the maximum divergencies obtained. Owing to the height of the N^{28}_2 peak in the mass-analysis the ratio of masses 29 : 30 is more significant than the actual numerical amounts of each. It is evident, however, that with neither catalyst in the range 200–400°C nor with quartz at 750°C does any marked exchange occur. The activity of the catalyst was controlled continuously between experiments by observing the rapid decomposition of ammonia gas at 400°C, nitrogen and hydrogen in the stoichiometric ratio being produced.

Table III. *Nitrogen isotope exchange on iron catalyst No. 931 with hydrogen from methylamine present.*

Temp. °C	Time in Hours	Parts per 1000 N^{28}_2 of N^{29}_2	Parts per 1000 N^{28}_2 of N^{30}_2	Mass Ratio 29 : 30
465	2	100.5	51.5	1.95
	17	125.8	39	3.23
	37	163	22.6	7.32
	60	194	14	13.52
500	2	108	48	2.24
	8	142	38	3.75
	21	184	20	9.30
	26	197.5	17.4	11.40
	35	202	13.4	15.07
	46	207	13.25	15.70

Table II records the results of mass analyses on mixtures of N_2+3H_2 maintained for increasing periods of time at 460° and at 510°C. Small samples withdrawn at the stated intervals reveal the progress of the exchange reaction by the increase in the mass ratio 29 : 30.

Table III records the results on the nitrogen isotope mixture without admixed hydrogen but probably containing some small amount of hydrogen from decomposition of methylamine (31) together with any traces of the gas left on the surface after the evacuation procedure.

It will be obvious from comparison of Tables II and III that reduction in the hydrogen content of the nitrogen has materially decreased the velocity of the exchange reaction. Still slower rates of exchange were obtained when special procedure was employed to remove, in a liquid-air trap, the methylamine (31) content of the nitrogen prior to passage over the hot copper catalyst and intro-

Table IV. *Nitrogen isotope exchange on iron catalyst No. 931 with gas specially purified from mass 31.*

Temp. °C	Time in Hours	Parts per 1000 N^{28}_2 of N^{29}_2	Parts per 1000 N^{28}_2 of N^{30}_2	Mass Ratio 29 : 30
500	2	91.9	49.7	1.85
	6	100.5	53.3	1.89
	27	109.3	49.6	2.20
	49	121	47.5	2.57

TABLE V. *Nitrogen isotope exchange on iron catalyst No. 931 reduced in hydrogen up to 550°C with gas specially purified from mass 31.*

Experiment No. and Temperature							
1 AT 500°		2 AT 550°		3 AT 545°		4 AT 500°	
TIME IN HOURS	MASS RATIO 29 : 30	TIME IN HOURS	MASS RATIO 29 : 30	TIME IN HOURS	MASS RATIO 29 : 30	TIME IN HOURS	MASS RATIO 29 : 30
0	1.84	0.5	1.85	2	2.29	0	1.85
2.25	1.91	2.25	2.40	5	3.0	5.75	1.91
9	2.59	0(a)	2.74	14	9.0	13	2.12
20	4.19	2.66(a)	3.96	17	10.12	23	2.33
30	6.40						

(a) An interruption in the heating prior to this reading is responsible for the times given. The final rate agrees with the initial rate within experimental error.

duction into the iron catalyst vessel. The data are recorded in Table IV and are evidence of the extreme slowness of the reaction when the procedure employed reduces the hydrogen present to minimal amounts. Evidence for the influence of traces of hydrogen was obtained in the experiments recorded in Table V which were carried out on a new sample of Catalyst No. 931 which, in addition to the normal reduction schedule, was treated for four days in hydrogen at 550°C and then evacuated as thoroughly as possible. The initial experiment at 500°C with nitrogen freed from methylamine (31) and in absence of hydrogen showed a velocity much greater than that recorded in Table IV. The mass analysis revealed traces of hydrogen in the sample analyzed which points to the difficulty of completely removing hydrogen by the evacuation technique. A second experiment at 550°C showed a change in mass ratio 29 : 30 from 1.85 to 3.96 in 6 hours, while a third experiment at 545°C showed a slower rate. In each case traces of hydrogen appeared in the product analyzed. The successive experiments, however, presumably diminished the hydrogen content since a fourth experiment at 500° showed a much slower velocity of exchange than in the initial run at the same temperature. These data in Table V must serve to emphasize the slowness of the exchange and the large influence of hydrogen. Special test after the sequence of the four experiments showed that the catalyst was still extremely active for the decomposition of ammonia at 400° to yield a $N_2 : 3H_2$ stoichiometric mixture.

A sample of doubly-promoted iron catalyst No. 931 when reduced on the schedule: 4 hours at 350°, 4 hours at 400°, 24 hours at 450° and 12 hours at 500°C, and showing marked activity for both synthesis and decomposition of ammonia in flow measurements at 400°C shows very low activity for exchange in a static system at 450° as shown in Table VI. On raising the temperature to 725°C the exchange reaction readily occurred, as shown in the same table, where three experiments at this temperature show also the marked acceleration of the exchange by hydrogen.

The slowness of reaction at 450° on the catalyst so reduced may possibly be ascribed to incomplete reduction with the schedule employed. Any water vapor formed by interaction of unreduced oxide with the hydrogen of the gas mixture would act as a poison and diminish reaction rate. In passing to the higher temperature, reduction would be completed and, hence, exchange could proceed.

With the singly promoted iron catalyst No. 954 on the normal reduction schedule, exchange occurs at approximately the rate found with catalyst No. 931, as the data in Table VII indicate.

A sample of this gas taken after more than 48 hours reaction at 455° showed a mass ratio of 12.9. After cooling to room temperatures, a sample of the gas after standing in contact with the catalyst gave a mass ratio of 9.8. This is another observation similar to that in the last line of Table II. It suggests a stronger adsorption of N^{29}_2 relative to N^{30}_2. Throughout the whole work the evidence has consistently indicated a strong preferential adsorption of the heavier over

TABLE VI. *Nitrogen isotope exchange on catalyst No. 931 at 725°C.*

TIME IN HOURS	TEMP. °C	GAS MIXTURE	MASS RATIO 29 : 30
60	450	N_2+3H_2	1.71
15	725	N_2+3H_2	12.7
22	725	$N_2+1\%\ H_2$	5.7
44	725	N_2+Trace of Hydrogen	3.35

TABLE VII. *Nitrogen isotope exchange on catalyst No. 954 at 450° with $N_2 : 3H_2$ mixture.*

Time in Hours	0	2	6	12	22
Mass Ratio 29 : 30	1.81	1.90	2.05	2.83	4.65

the lighter isotopes. We shall devote a separate communication to this matter.

Nitrogen exchange on tungsten filament

The experiments were performed after the filament was reduced in hydrogen. That the velocity of exchange was very much slower than on the iron catalyst is evident from the fact that, with nitrogen containing a trace of mass 31, and therefore with ~1 percent hydrogen as decomposition product, a period of 48 hours reaction at 900° only changed the mass ratio, 29 : 30 from 1.8 to 2.3. Even with a stoichiometric mixture $N_2 : 3H_2$ no exchange occurred in 5 hours at 720°C. Sixteen hours at 770° gave a mass ratio 29 : 30 of 2.06 while a further 16 hours at 900°C produced a mass ratio of 8.4.

General Discussion

The outstanding result of these investigations is the determination that the exchange reaction between isotopic nitrogen molecules is an extraordinarily slow process on synthetic ammonia catalysts, and that this is true even in comparison with the velocity of the ammonia synthesis process. In this it is conspicuously divergent from the exchange reactions between isotopic hydrogen molecules which occurs measurably on these catalysts even at ordinary temperatures.

The direct exchange reaction of nitrogen molecules requires adjacent adsorption of two isotope molecules $N^{28}{}_2$ and $N^{30}{}_2$ on the iron catalyst,

$$N^{28}{}_2 + N^{30}{}_2 \overset{Fe}{\rightleftarrows} 2N^{29}{}_2 \qquad (a)$$

or at least one isotopic atom adjacent to a molecule.

An indirect exchange involving hydrogen would require adsorption of nitrogen molecules, interaction of these with hydrogen to form NH, NH_2 and NH_3 which, in the limit, might be desorbed as ammonia gas, followed by the reverse of these reactions which, from equilibrium considerations, would be rapid processes

$$N_{2\ ads} + H_{2\ ads} \rightleftarrows NH_{ads} \rightleftarrows NH_{2\ ads} \rightleftarrows NH_{3\ ads} \rightleftarrows NH_{3\ gas}.$$

We have shown, by special test, that the decomposition of ammonia containing a concentration of N^{15} isotope greater than normal yields a molecular nitrogen whose isotopic composition approaches equilibrium. In presence of hydrogen it is evident that the exchange reaction must be determined by the slowest of the processes involved in the above reversible sequence. The experimental observations also indicate that even the slowest of these is faster than the steps which lead to exchange in nitrogen alone.

The rapid decomposition of ammonia, to yield the stoichiometric N_2+3H_2 gaseous product, on these surfaces where the exchange reaction is slow indicates that the slow process in the ammonia decomposition process, the evaporation of molecular nitrogen from the surface is rapid compared with the rate of exchange reaction in pure nitrogen. The desorption of molecular nitrogen is, of necessity, slower than the adsorption of molecular nitrogen since the heat of adsorption must be supplied, in addition to any activation energy of adsorption, for the desorption process. Adsorption and desorption are therefore more rapid than the over-all interchange process. From this we conclude that the slow, rate-determining process in the exchange reaction of molecular nitrogen isotopes on catalytic iron surfaces involves the actual interchange of the nitrogen atoms on the surface. This might arise in several ways. If the adsorbed nitrogen were still in the molecular form, with only a portion of its valence bonds involved in the attachment to the iron surface, the slow process might involve the rupturing of the residual valencies and a more rapid migration of nitrogen atoms to the equilibrium isotopic configurations, from which desorption would lead to the equilibrium isotopic gas mixture. If the nitrogen adsorbed in the high temperature range is already completely dissociated, during adsorption, into atoms then it is the migration of such atoms over the surface to the equilibrium configurations which is the slow process. Dr. S. Brunauer has informed us in a private communication that his own researches on the adsorption of the nitrogen compel him to the conclusion that the gas does dissociate into atoms and that the surface is covered with a surface layer in which the Fe : N ratio is 2 : 1. On this view, the rate-determining step would be the migration of these atoms over the surface

to positions adjacent to the isotopic species, from which positions desorption to give the exchange equilibrium could occur. Dr. Brunauer has pointed out to us that a symmetrical placing of adsorbed nitrogen atoms on an iron surface, yielding a Fe : N ratio of 2 : 1 would require a motion of nitrogen atoms across the surface before configurations favorable to exchange could be obtained.

It is evident that these two points of view with reference to the slow process on the surface represent the two extreme possibilities. It may well be that the surface of iron with its nitrogen covering would reveal all stages of an equilibrium condition between these two extremes which, together with one mean configuration, are representable thus:

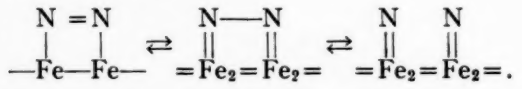

It would require other evidence and more refined tools to decide such questions.

On either hypothesis the role of the hydrogen in accelerating the exchange is readily understandable. The formation of NH linkages would quite definitely weaken the residual valence forces between the nitrogen atoms of an adsorbed molecule. With atomic adsorption the formation of NH bonds would decrease the Fe-N forces restraining migration on the surface. The low concentrations of hydrogen producing a marked acceleration of the exchange would indicate that it is the formation of imido or amido groups rather than actual ammonia formation and decomposition that is the important function of the hydrogen as accelerant. The temperature coefficient of the reaction as deduced from the rate data in Table II leads to an observed activation energy of about 50 kcal. Since hydrogen was present it is evident that this value is to be associated with the processes which hydrogen produces. The sensitivity of the velocity to traces of hydrogen makes a determination of temperature coefficient of direct molecular nitrogen exchange a virtual impossibility. It should, however, be higher than that for hydrogen-assisted exchange.

The high value of the activation energy of exchange revealed by this work does yield a conclusion of considerable importance in the general theory of adsorption. Emmett and Brunauer[3] measured the velocity of adsorption of nitrogen on these iron catalysts and derived a value of 15 kcal. for the energy of activation. Since this is so much less than the values indicated in the present experiments for the processes involved in migration over the surfaces it is probable that, in their particular case, Emmett and Brunauer were actually measuring a velocity of adsorption and not a velocity of diffusion or migration, and that, by reason of the high values of the activation energy of these latter processes these processes could not have been determining influences in the adsorption measurement. The adsorption of nitrogen on iron synthetic ammonia catalysts becomes, on this view, the best example of the concept of activated adsorption, involving the by-no-means negligible activation energy of 15 kcal., in contrast to the very small values for the energies of adsorption indicated by John K. Roberts[7] in his studies of hydrogen as the adsorbed gas on tungsten surfaces.

The data on tungsten surfaces indicate a similar slow velocity of direct exchange and a more rapid reaction path in presence of hydrogen. On both surfaces we have, therefore, the very interesting case of a gaseous "catalyst," hydrogen, for a reaction between gas molecules N^{28}_2 and N^{30}_2 at a solid surface.

Acknowledgments

One of us (G. G. J.) wishes to express his thanks to the Belgian-American Educational Foundation, Incorporated, for a fellowship which made possible this work. We renew our thanks to Professor H. C. Urey for the supplies of isotopic nitrogen and ammonia and to Dr. S. Brunauer for valuable advice and supplies of catalytic iron. To Dr. J. M. Delfosse and W. R. F. Guyer we are indebted for patient assistance in many analyses, by the mass-spectrographic method, of our gas samples. Professor W. Bleakney of Palmer Physics Laboratory, Princeton University, kindly placed at our disposal one of his mass spectrographs. We tender him our thanks for this generosity and kindness to us in our work.

[7] J. K. Roberts, Proc. Roy. Soc. **A152**, 445 (1935).

The Diffusion of Gases Through Metals from a Chemical Point of View

J. H. SIMONS AND W. R. HAM
School of Chemistry and Physics, The Pennsylvania State College
(Received June 5, 1939)

The diffusion of gases through metals is considered from the point of view of chemical compounds between the metal or a constituent of it and the gas, all at chemical equilibrium. Without reference to the surface conditions the usual laws of diffusion are derived, and Fick's linear diffusion law is shown to be a consequence of the hypothesis. Cases are treated where one compound between the gas and metal is formed, where two compounds are formed, where one compound is formed between the metal and gas and another formed between an alloying agent and the gas, and where the same compound is formed but the metal has a transition between two forms. The theory correlates the magnitude of the exponent of the gas pressure in the diffusion isotherms with the chemical reactions within the metal. It also leads to certain consequences in regard to the magnitude of the diffusion and the energy of activation.

NUMEROUS facts relative to the solubility of gases in metals indicate that at least the major portion of the gas must exist in the metal in the form of compounds between the gas and the metal or some constituent of the metal system, if this is a mixture. Among these facts is the high selectivity of metals for different gases such as that of members of the iron-platinum family for hydrogen and silver and copper for oxygen. An interesting fact is the solubility of oxygen in silver which is a minimum at constant pressure at about 400°C. This has been explained by Simons[1] on the basis of the solubility of silver oxide in silver, its increase with increasing temperature and the dissociation pressure of silver oxide which increases with increasing temperature.

The precise determinations of the diffusion of gases through metals as for example those of Ham and co-workers[2] also supply facts which support the contention that the gas exists in the metal in the form of chemical compounds with the constituents of the metal system. In these papers it has been shown that an adsorption isotherm applied to the surface of the metal would not explain the facts of diffusion as had been previously assumed. It is difficult to correlate the known fact that the rate of diffusion of a gas through a metal is inversely proportional to the thickness of the metal with the character of the adsorbed surface film. It has also been shown that the variation from the simple square root of pressure law of the rate of diffusion of hydrogen at constant temperature could be explained on the basis of chemical equilibria existing in the metal, and that this variation in all cases carefully investigated depends upon the presence of impurities in the metal, for example, carbon in nickel or iron and oxygen in copper.[2a, c, d, f]

For some years the authors of this paper have separately believed that the solution and diffusion of gases through metals may be considered as purely chemical phenomena.[3] We are now presenting the derivation of the diffusion laws from this point of view.

ONE COMPOUND FORMED

If the passage of gas G through metal M is considered and it is assumed that in the body of the metal a compound is formed of the formula NG_y where N is an atom of the metal, a group of such atoms, an atom or group of atoms of an alloying agent, A, or a combination of A and M, a chemical equation can then be written, where x is the number of atoms in a molecule of the gas.

$$(y/x)G_x+N=NG_y. \tag{1}$$

When close to the equilibrium condition, the rate of approach to equilibrium of this reaction is

$$R=K_f(G_x)^{y/x}(N)-K_r(NG_y), \tag{2}$$

[1] J. H. Simons, J. Phys. Chem. **36**, 652 (1932).
[2] (a) W. R. Ham, Am. Soc. Metals **25**, 536 (1937); (b) C. B. Post and W. R. Ham, J. Chem. Phys. **5**, 913 (1937); (c) W. R. Ham and W. Rast, Am. Soc. Metals **26**, 885 (1938); (d) C. B. Post and W. R. Ham, J. Chem. Phys. **6**, 598 (1938); (e) C. B. Post and W. R. Ham, Am. Soc. Metals, (1939); (f) W. R. Ham, Easter Meeting Am. Phys. Soc. (1939).
[3] See particularly the application of the Van't Hoff equation in 2e.

where parentheses represent thermodynamic activities of the different species and K_f and K_r represent the specific reaction velocity constants for the forward and reverse chemical reactions. The forward reaction is for the formation of the compound (NG_y) and the reverse reaction is for its decomposition.

For a steady state of flow of gas through the metal the activity of the gas at any point will remain constant, and the chemical reaction will reach approximate equilibrium in time.

That is,

$$R=0, \quad \text{and} \quad \frac{K_f}{K_r}=\frac{(NG_y)}{(N)(G_x)^{y/x}}=E, \qquad (3)$$

where E is the equilibrium constant of the reaction.

Let us consider a cross section area of the metal perpendicular to the direction of flow of G, and let (G_x') and (NG_y') be the activities of G_x and NG_y at this area. At a distance ds beyond in the direction of flow of G let these activities be (G_x'') and (NG_y''). The compound NG_y' is dissociating in all directions at the rate $K_r(NG_y')$ and a fraction, ϕ, of the gas so formed will cross an area halfway between NG_y' and NG_y'' in unit time, that is $\phi K_r(NG_y')$. The compound NG_y'' is also dissociating, and the rate at which the gas from this dissociation will cross this same area in the reverse direction is $\phi K_r(NG_y'')$. The difference between these two rates will be the rate of flow of the gas in the forward direction. This is the rate of diffusion, R_d, as only the gas moves.

$$R_d=\phi K_r(NG_y')-\phi K_r(NG_y'') =\phi K_r d(NG_y)/ds. \qquad (4)$$

At the same amount of the gas must pass each cross section in the metal in a unit of time,

$$R_d=\phi K_r\Delta(NG_y)/s, \qquad (5)$$

where, s, is the total thickness. This corresponds to Fick's linear diffusion law, which is usually given in the form $dm/dt=Ddc/ds$, where dm/dt is the rate of diffusion, D is the diffusion constant, c is the concentration, and s is the thickness.

As chemical equilibrium is reached at every point in the metal,

$$K_f(N)(G_x')^{y/x}=K_r(NG_y')$$

and

$$K_f(N)(G_x'')^{y/x}=K_r(NG_y''). \qquad (6)$$

Eq. (5) becomes

$$R_d=\frac{\phi K_f(N)\Delta(G_x)^{y/x}}{s}=\frac{K_f'\Delta(G_x)^{y/x}}{s}. \qquad (7)$$

As the metal is considered homogeneous, the concentration of N is nearly the same throughout the sample for small amounts of NG_y and (N) is constant; ϕ is also a constant. $\phi K_f(N)=K_f'$.

Now as K_f is the rate of formation of a chemical molecular species in its solution in the metal its change with temperature must follow the usual law,

$$\frac{d\ln K_f}{d(1/T)}=-\frac{A}{R}+f(T), \qquad (8)$$

where A is usually called the energy of activation of the reaction. $f(T)$ arises from terms related to heat capacities and their temperature variation. This can be put in the form,

$$\phi(N)K_f=Be^{-A/RT}T^z.$$

Then, as ϕ and (N) are constant and independent of temperature,

$$R_d=Be^{-A/RT}T^z\Delta(G_x)^{y/x}/s, \qquad (9)$$

where B is a constant and T^z is usually neglected and included in A and B.

This equation reduces to the equation for the diffusion of hydrogen through pure decarburized iron or nickel. $y=1$ and $x=2$. (G_x) can be defined as equal to the fugacity of hydrogen in equilibrium with the metal; and for pressures, where the perfect gas law may be used, $(G_x)=P_{H_2}$. Then,

$$R_d=\frac{B}{s}e^{-A/RT}T^z(P'^{\frac{1}{2}}_{H_2}-P''^{\frac{1}{2}}_{H_2}), \qquad (10)$$

where P' and P'' are the pressures of the gas on the two sides of the sample of metal.

Two Compounds Formed

Now let us consider the case where two species NG and NG_2 exist in the metal and the gas has the formula G_2,

$$\tfrac{1}{2}G_2+N=NG \qquad \text{and} \qquad (11)$$

$$G_2+N=NG_2. \qquad (12)$$

The equilibrium constants will be

$$E_1=(NG)/(N)(G_2)^{\frac{1}{2}} \quad \text{and}$$
$$E_2=(NG_2)/(N)(G_2). \quad (13)$$

If one mole of N is involved in the two reactions and a certain fraction of a mole (a) be used in the first equilibrium, then $(1-a)$ will be used in the second equilibrium.

$$aG_2/2+aN=aNG, \quad E_{1,1}=E_1^a, \quad (14)$$

$$(1-a)G_2+(1-a)N=(1-a)NG_2,$$
$$E_{2,2}=E_2^{(1-a)}. \quad (15)$$

Adding these two equations we obtain a new equilibrium equation between the different compound species.

$$(1-a/2)G_2+N=aNG+(1-a)NG_2, \quad (16)$$
$$E_3=E_{1,1}E_{2,2}. \quad (17)$$

There is also another equilibrium

$$NG_2+N=2NG$$
$$E_4=(NG)^2/(N)(NG_2)=E_1^2/(N)E_2, \quad (18)$$

which is independent of the gas activity or pressure.

The rate of approach to equilibrium of Eq. (16) is

$$R=K_f(N)(G_2)^{1-a/2}-K_r(NG)^a(NG_2)^{1-a} \quad (19)$$

and the rate of diffusion through a section can be given in the same way as obtained previously because of the previous argument and also Eq. (18)

$$R_d=K_f'((G_2')^{1-a/2}-(G_2'')^{1-a/2}). \quad (20)$$

For the case at constant temperature where the pressure is negligible on the exhaust side of the specimen and the pressure on the fore side is not so high that deviations of the gas law need be considered,

$$R_d=\frac{K_f'}{s}P_{H_2}{}^{1-a/2}. \quad (21)$$

It is to be noted that K_4 represents the rate of formation of chemical species expressed in terms of activity. Then,

$$\frac{d\ln K_f}{d(1/T)}=\frac{-A_t}{R}$$

approximately, where A_t is the energy of activation of the reaction. Now as Eq. (16) is the sum of Eqs. (14) and (15),

$$A_t=aA_1+(1-a)A_2, \quad K_f=K_{f_1}{}^aK_{f_2}{}^{(1-a)}, \quad (22)$$

where A_1 and A_2, K_{f_1} and K_{f_2} represent the energies of activation and rate constants of Eqs. (11) and (12).

$$\frac{d(a\ln K_{f_1}+(1-a)\ln K_{f_2})}{d(1/T)}=$$
$$-\frac{aA_1}{R}-\frac{(1-a)A_2}{R}. \quad (23)$$

As the equilibrium (18) will also change in temperature by the equation

$$\frac{d\ln E_4}{d(1/T)}=-\frac{\Delta H}{R},$$

the ratios of the activities of NG and NG_2 will change with temperature and the value of (a) change. As we may define these activities as approaching the mole fraction as this approaches zero we can replace activities with concentration when these are small, also if N represents the pure metal (N) is very nearly unity, for in the case of the major constituent, its activity is defined as equal the mole fraction as this approaches unity. At some high temperature where one species predominates, usually the NG, $a=1$, and K_{f_1} and A_1 are thereby determined. At some other temperature with these known K_{f_2}, a, and A_2 can be determined.

This method of analysis can be expanded to include 3 or more sets of compounds and used for gases in which the number of atoms in the molecule is different from two. As the ratio of the compounds is independent of the gas activity, the linear diffusion law can be shown to hold. The above case can be treated in a more general manner as was done for the case where one compound is formed. Other cases such as the simultaneous diffusion of two gases can also be treated in a similar manner. From this picture compounds must be formed for diffusion except where the gas can go through the voids in the crystal lattice. If the compounds formed are very stable, diffu-

sion will be slow as it will be difficult to have (G_x'') below the equilibrium value, because this will be very small until a large concentration of the compound is produced.

Small Amount of Impurity in the Metal

In the diffusion of hydrogen through iron or nickel containing small amounts of carbon or nitrogen[2a] and through copper containing a small amount of oxygen[2f] the chemical equations appear to be

$$\tfrac{1}{2}H_2 - M = MH, \tag{24}$$

$$H_2 - A = AH_2. \tag{25}$$

(A) represents a compound of the impurity with the metal.

$$sR_d = K_{f_1}{}^a P_{H_2}{}^{a/2}(M)^a K_{f_2}{}^{(1-a)} P_{H_2}{}^{(1-a)}(A)^{(1-a)}. \tag{26}$$

For very small concentrations of A the activity of M is very nearly unity and (A) can be considered equal to the concentration of A, that is, C_A.

$$sR_d = K_{f_1}{}^a K_{f_2}{}^{(1-a)} P_{H_2}{}^{1-a/2} C_A{}^{1-a}. \tag{27}$$

From an experiment with a sample of pure metal where $a=1$ and $sR_d = K_{f_1} P_{H_2}{}^{\frac{1}{2}}$, the quantity K_{f_1} can be determined. A diffusion experiment on a sample of known concentration of A will give K_{f_2} and on isotherm establish whether Eq. (25) is correct or not. Data from unknown samples can then be used to determine the concentration of A. This may also be determined approximately by considering $(1-a)$ the mole fraction of A, assuming Eq. (25) and evaluating a from the diffusion isotherms. This method was used[2a] for the determination of the carbon content in iron.

As the concentration of the impurity is here considered as constant throughout the metal, the linear diffusion law will hold. The carbon in iron or nickel is removed by treatment with hydrogen so that for such cases the carbon concentration will not be uniform and the equations should be modified to include this effect.

Investigation of Transitions

If a metal has a transition point and above the transition temperature exists chiefly in the higher temperature form and below it chiefly in the low temperature form, gas diffusion experiments should enable the energy of transition to be calculated.[4] The chemical equations may be represented by

$$\tfrac{1}{2}G_2 + M' = M'G, \tag{28}$$

$$\tfrac{1}{2}G_2 + M'' = M''G. \tag{29}$$

From the change of the rate of diffusion with temperature above and below the transition temperature, A' and A'' can be determined. These are the differences for the energy of activation for the two reactions. As it is highly unlikely that the compound MG would have, in its solution in the metal, a transition at the same temperature, $M'G$ is identical with $M''G$. If the chemical equations represent the true mechanism, the difference between A' and A'' should be the energy of transition of the metal.

Credit should be given Dr. Nelson W. Taylor, of the Ceramics Department in the School of Mineral Industries at The Pennsylvania State College, for helpful criticisms and constructive suggestions.

Conclusions

The assumption of chemical compounds existing in the metal can be used to derive the laws of diffusion of a gas through a metal. This is accomplished without considering the condition of the adsorbed surface. Upon this basis an explanation is found for the magnitude of the exponent of the pressure in the diffusion equations. The theory allows a number of important factors to be determined from diffusion experiments such as the amount of certain impurities in the metal, the energy of transition between different forms of the metal, etc.

[4] This phenomenon may be complicated by an order-disorder transformation that accompanies the transformation in the metal proper, provided there is a contamination present.

The Diffusion of Hydrogen Through Oxygen-Free Copper

W. R. HAM
Department of Physics, The Pennsylvania State College, State College, Pennsylvania
(Received June 5, 1939)

A precise determination has been made of the diffusion of hydrogen through copper that is spectroscopically oxygen-free. The range of temperatures is from 450°C to 1050°C. The copper appears perfectly homogeneous over the entire range, the equation followed being

$$\text{Rate} = Ap^{y}T^{z}e^{-b/T},$$

where p is pressure, T absolute temperature, A and b constants characteristics of copper. The value of z is about $+0.5\pm0.2$ as was found in pure nickel. The principle point to be noted is that $y=0.50\pm0.01$ even at 450°C. It is well known that copper containing any appreciable amount of oxygen shows isotherms in this region with a value of y as large as 0.8 in some instances, when $\log R$ is plotted against $\log p$. When this same copper diffusor is slightly charged with oxygen the value of y becomes greater than 0.5, except at high temperatures. However, when isotherms are plotted log rate against log pressure, the result is a perfectly straight line in all cases. It now appears that the removal of all traces of oxygen from copper has the same effect on low temperature hydrogen diffusion isotherms as the removal of all carbon from iron and nickel, *viz.*, these isotherms become perfectly normal, the rate varying exactly as the square root of the pressure.

INTRODUCTION

THIS experimental work was undertaken not with the expectation that hydrogen would show transitions such as are found in iron and nickel, but rather to ascertain whether the spectroscopically oxygen-free copper would show the isotherm abnormalities at low temperatures and pressures that are observed with copper not specially prepared so far as oxygen content is concerned. These abnormal isobars are shown by many observers, but the situation may be most easily grasped by consulting *Gases in Metals* by Smithells. An isotherm for hydrogen through copper at 450°C is found on p. 98. This isotherm is in every way similar to an isotherm for hydrogen through iron when the iron contains carbon (or nitrogen) in solution, and this also applies to nickel so far as carbon is concerned.

The writer and collaborators have shown that complete removal of carbon from iron and nickel furnishes normal hydrogen diffusion isobars where the rate varies exactly as the square root of pressure at any temperature.

However, in the case of copper, carbon is insoluble and about the only contamination that would be expected to cause abnormalities is oxygen. Hence, when spectroscopically oxygen-free copper became available in March, 1938, plans were made for a precise redetermination of hydrogen diffusion through this pure metal.

EXPERIMENTAL PROCEDURE

The schematic diagram of the diffusor system may be found in previous papers[1–5] and has not been materially changed.

Attention should be called again to the two methods used for measuring rates, (*a*) the trapping method which gives absolute values and has been used by nearly all observers, (*b*) the steady-state method which consists in building up a small pressure at the outgoing side, by means of a small aperture through which the gas diffuses (or flows) before being taken out by the pumping system, one side of this aperture having built up pressure that is constant up to the diffusor proper, the other side having a high vacuum maintained by good pumps. In the steady-state method the pressures on the gauge are directly proportional to the rates. One advantage of the steady-state method is that absolutely nothing is disturbed when taking a reading, the pressure on the outgoing side of the diffusor remains constant, but what is much more important, adsorption corrections for the outgoing section of the diffusion system are completely eliminated. Hence, at high temperature

[1] W. R. Ham, Am. Soc. Metals **25**, 536 (1937).
[2] C. B. Post and W. R. Ham, J. Chem. Phys. **5**, 913 (1937).
[3] W. R. Ham and W. Rast, Am. Soc. Metals **26**, 885 (1938).
[4] C. B. Post and W. R. Ham, J. Chem. Phys. **6**, 598 (1938).
[5] C. B. Post and W. R. Ham, Am. Soc. Metals (in process of printing) (1939).

particularly, a degree of consistency of results can be attained that is much greater than is generally possible in the trapping method. Without such a method of great flexibility (since the sensitivity of the apparatus can obviously be changed with ease) it is doubtful if data sufficiently consistent and over a wide enough range could be obtained to say whether the exponent of T is $+5$ or -5.

A much greater accuracy is possible than has ever been attained in any thermionic emission data, largely due to the great range of temperatures that may be used and measured accurately in diffusion processes.

The actual diffusor used in obtaining the following data is tubular. The writer prefers the disk type as far as avoidance of thermal gradients is concerned, but the tubular type could be constructed with less danger of oxygen contamination, which is of fundamental importance in this investigation.

The construction of the diffusor is shown in Fig. 1. Hydrogen is flowing as indicated, and burning at all cracks. A torch is then applied to the outside slightly above B and the upper part of the copper rod melted down so that copper extends across the diameter of the tube A. The quartz plate allows one to observe this process, which takes about five minutes to complete.

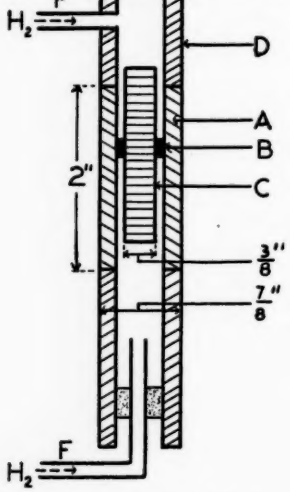

FIG. 1. Assembly for welding tubular copper diffusor A, nickel tube, B, steel disk or washer, C, solid rod o., oxygen-free copper, $D-D$, auxiliary nickel tubing, Ef quartz plate (clear) and $F-F$, hydrogen inlets.

FIG. 2. Appearance of copper diffusors after welding.

The central part now looks as in Fig. 2, the shaded portion being Cu. This is then put in a lathe and the closed end tube formed by boring along the axis with a high speed drill.

The copper was furnished by the American Smelting and Refining Company and spectroscopic analysis has been made by them of a finished diffusor. This showed no evidence of oxygen, nickel or iron. This analysis was carried out under the direction of the Superintendent, Dr. A. J. Phillips, who writes as follows: "We feel that you are quite safe in stating that you have tested the highest purity copper ever produced."

The central section (diffusor proper) then has ends welded on with an atmoic hydrogen torch, hydrogen again flowing on both sides of the diffusor, and is finally mounted in the assembly as shown in previous publications.[1-5]

The effective area of such a diffusor cannot be determined with the accuracy of the disk type, but for the purpose of this investigation that is unimportant.

It should be noted that the writer verified Smithell's observation that in hydrogen diffusion through copper, the exclusion of mercury vapor particularly at the ingoing surface is necessary. Three inches of close-packed gold leaf on the ingoing side and one inch on the exhaust was used and appeared sufficient inasmuch as the diffusion characteristics did not change over a period of two months.

Six hundred observations of rates were made during this time, the apparatus having been brought to temperature equilibrium each time. It required about eight hours for the hydrogen to come to flow equilibrium at 450°C, the diffusor being rather thick (0.067").

The photoelectric temperature control could be depended upon to hold the temperature to 1°C

at any setting over long periods of time, and could have been adjusted to hold to 0.1° if there was any point in so doing.

The thermocouple wire used has not been calibrated except at 960.5°C, the melting point of Ag, but again absolute values of the temperature are unimportant in this experiment. The values of the temperatures were taken as read from Leeds and Northrup "Standard Conversion Tables" for this type Chromel-Alumel. Any particular temperature should be correct to 2°, but the relative values of temperature in a range of 100° should be reliable to 0.5°C. At this point a note with regard to McLeod readings is appropriate. If a gauge has stood for some time at relatively high vacuum, the first few readings taken will progressively increase due to adsorption on the wall of the capillary. Hence, four or five readings at three-minute intervals were taken, until the maximum reading was reached.

The final isobar for copper as well as the previous similar isobar for pure nickel (above 360°C) shows that the calibration of the gauge used is linear within the accuracy of reading. This has also previously been demonstrated by trapping methods at low temperature (below 360°C) with pure nickel diffusors.

In discussing gauge errors the value of the steady-state method of measuring relative rates becomes marked. By changing the sensitivity (i.e., cracking the control stopcock more or less) the same section of the gauge may be used to measure rate in the region 500° to 600°C as in the range 900° to 1000°C. Hence, if errors in calibration of the gauge existed, they would have been easily noted.

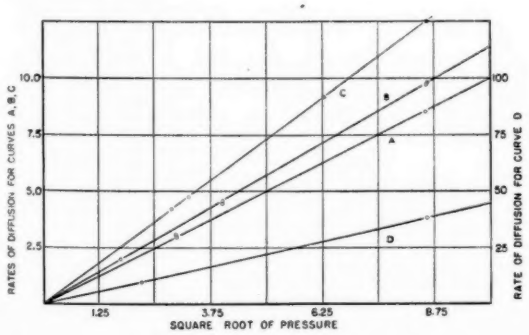

FIG. 3. Diffusion isotherms for hydrogen through spectroscopically oxygen-free copper. $R = CTP^{\frac{1}{2}}$. Temperatures: *A*, 451°C; *B*, 451°C; *C*, 541°C; *D*, 701°C.

Great care was taken with the isotherms at 450°, 540° and 700°, not so much in taking observations, but rather in making sure that true equilibrium had been obtained. It took about 30 minutes to come to equilibrium at 700°C and 8 hours at 450°C.

One particular diffusor was inserted in the apparatus on January 12, 1939, heated to 1055°C, with vacuum on both sides for four hours, the temperature lowered to 701°C and an isotherm taken from pressure of 73.8 cm to 1.8 cm. This took 5 days, the time consumed largely in investigating the time required to come to equilibrium, which was found to be about 30 minutes. The results are shown in Fig. 3 (*D*) which shows a perfectly simple isotherm with slope 0.5 within experimental error. The control stopcock had been closed to make the gauge reading 34.5 times that when fully open. This is referred to as a sensitivity of 34.5. The absolute value of the rate at 701° was determined by trapping and was 4μ-increase per minute with a trapped volume of 230 cu cm, the temperature of this volume being 26°C. The diffusor temperature was then reduced at 541°C and the isotherm of Fig. 3 (*C*) taken. The sensitivity was then increased to 200 on January 21, the temperature lowered to 450°C and isotherm (Fig. 3 (*B*)) taken, 12 hours being allowed for equilibrium to be obtained after each change of pressure. The procedure was to verify a few points with great accuracy rather than to take a large number. A further isotherm at 450, Fig. 3 (*A*), was taken at a lower sensitivity as a check.

These isotherms at 450°C also have a slope of 0.5 ± 0.01 and bear little resemblance to those by Smithell's. The only difference so far as one can see is that this particular copper diffusor is spectroscopically oxygen-free. All isotherms shown in Fig. 3 are plotted rates (in arbitrary units) against the square root of the pressure.

The remainder of the observations on this copper consisted in taking an isobar as carefully as possible from 450°C to 1000°C. There is one principle correction to make with this apparatus in taking such an isobar. Above 900°C there is a small but appreciable correction to make for oxygen diffusion through the outgoing side of the nickel holder. The correction obtained by running between 900° and 1050° first with

vacuum on ingoing side, then helium at atmospheric pressure. If the residual apparent leak rate is the same for both, it may be assumed that there is no imperfection in the diffusor proper and the leak is due to diffusion of some sort through the holder as well as residual degassing. If small, the cause of this correction is unimportant and the amount may readily be subtracted from the hydrogen readings.

This amount was checked at the start and end of the experiments, a month intervening, and was found substantially unchanged. No doubt this correction could be entirely eliminated by gold plating the central part of the holder, or by using a nitrogen or helium atmosphere inside the furnace, but it seems hardly worth the trouble, since the final results in the temperature range mentioned are comparable in every way with those taken in lower temperature intervals.

The interesting result shown in the isobar, Fig. 4, is the small upward curvature similar to that found in pure nickel.

It is necessary to plot $\log R - \log T$ against $1/T$ to remove this curvature as shown in dotted lines in Fig. 4 and the work function is changed from 4050 at high temperature and 3940 at low temperature to a constant value of about 3780. Multiplying by 2.3026 gives 8700°K for the value of b or 17,400 calories/g atom if one prefers to write $e^{-Q/RT}$ in the diffusion equation instead of $e^{-b/T}$.

Discussion of Results

The curvature of hydrogen isobars through copper (also iron and nickel) cannot be explained by the introduction of the Langmuir adsorption isotherm in the general diffusion equation as suggested by Smithell's, since in every case the curvature of the isotherm may be removed by the elimination of some contamination in the sample. The important contamination in copper seems to be oxygen, in iron and nickel it is usually carbon, though sometimes in impure iron it apparently may be nitrogen.

The general chemical theory applicable to diffusion isotherms will be found in another paper by Simons and Ham.[6]

Summary

Diffusion of hydrogen through copper and nickel is represented by

$$R = A p^{y} T^{\frac{1}{2}} e^{-b/T}.$$

The experimental value of the exponent of T necessarily has a large error. I suggest 0.5 ± 0.2

[6] J. H. Simons and W. R. Ham, J. Chem. Phys. **7**, 899 (1939).

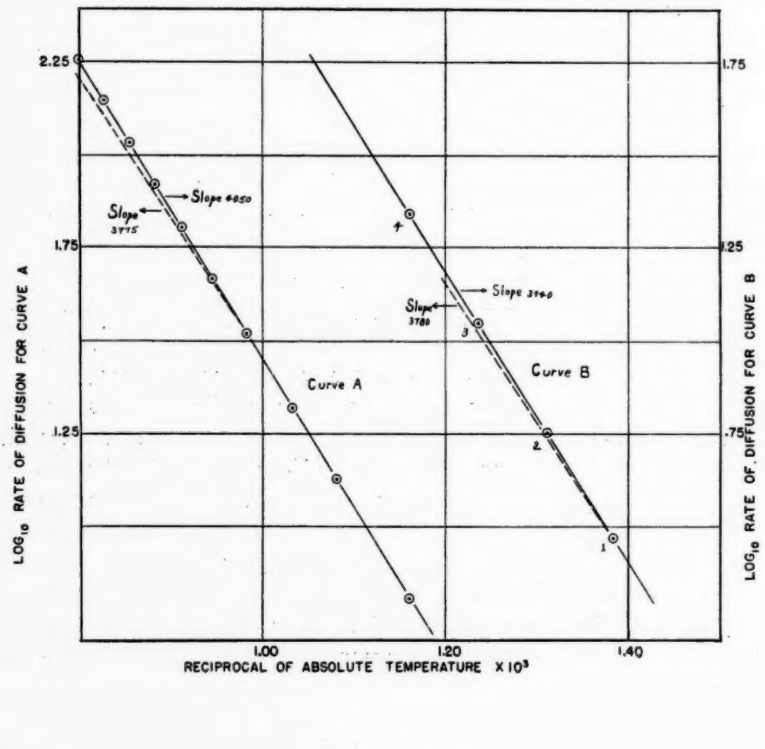

FIG. 4. Isobar for diffusion of hydrogen through spectroscopically oxygen-free copper. Curve A: Isotherms at 1, 2, 3 and 4 have a slope of 0.5 plotting $\log_{10}$ rate against $\log_{10}$ pressure. Of 50 points taken none deviates by as much as one percent. Curve B: Of 19 points taken none deviates by as much as one percent. In both cases the dotted lines give $\log_{10}$ rate $-\log_{10}$ temp. plotted against $1/T_k$. The equation for the rate is: $R = A p^{\frac{1}{2}} T' e^{-b/T}$ where $b = 3780 \times 2.3 = 8700$°K.

for the exponent of T; y, however, becomes exactly 0.5 at all temperatures and pressures with sufficiently pure iron, nickel, or copper. This has been shown to be the case with pure decarburized carbonyl iron above 250°C, with pure decarburized nickel above 150°C and with spectroscopically oxygen-free copper above 450°C.

PART II

This diffusor furnishing the data for Fig. 3 and 4 was assembled primarily to investigate the

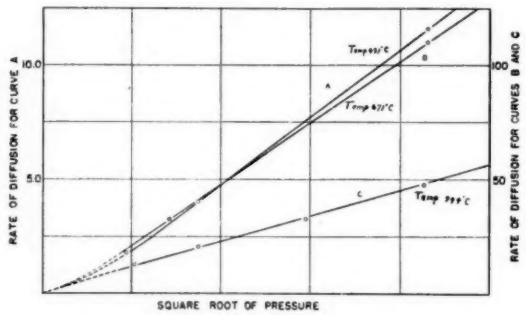

FIG. 5. Diffusion isotherms for hydrogen through copper slightly charged with oxygen showing deviations of low temperature isotherms from $P^{\frac{1}{2}}$ law. Curves A and B, high sensitivity, C, low sensitivity.

diffusion of oxygen through copper, but since it was in particularly good condition, the hydrogen diffusion was first run, then all traces of hydrogen removed by prolonged heating above 1000°C with vacuum on both sides of the diffusion tube.

On exposing the ingoing side to oxygen at a pressure of 3 mm at 906°C, gaseous diffusion started in a perfectly normal manner,

Helium was then put on at atmospheric pressure 74 cm and the temperature lowered in 1½ hours to 650°, whereupon hydrogen was substituted for the helium. The curve for the hydrogen coming to equilibrium (steady flow) was perfectly normal but somewhat surprisingly the rate was precisely the same as before the oxygen treatment.

The temperature was then raised in ½ hour to 792°C when the diffusor showed a much larger rate of hydrogen diffusion that originally at this temperature indicating opening up of grain boundaries (physical diffusion). On substituting helium for hydrogen this was found to be the case. In other words the diffusor now leaked although before oxygen treatment it would go nearly to

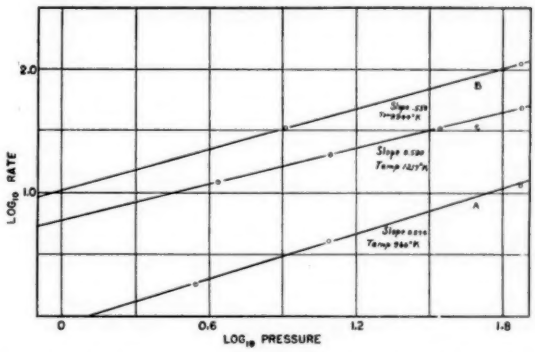

FIG. 6. Same data as in Fig. 5 but plotted logarithmically. $R = CTP^{y}$. A and B, high sensitivity, C, low sensitivity.

the melting point of copper without causing any difficulty whatever.

A vacuum was then put on the ingoing side and the temperature raised to 1060°C in an unsuccessful attempt to remove both the oxygen and hydrogen and heal the leak.

One may infer that pure oxygen diffusion is lattice diffusion with little concentration at grain boundaries, but that if hydrogen diffusion is attempted with oxygen in solution, at sufficiently high temperatures where the mobility of the oxygen becomes appreciable, that the oxygen migrates to the grain boundaries, unites with the hydrogen forming steam of sufficient pressure in some cases to open the grain boundaries.

Next a carefully degassed pure copper diffusor was exposed to nitrogen known to be slightly contaminated with oxygen, the temperature raised to 1050°C then cooled, and hydrogen substituted for the oxygen. The isobars shown in Fig. 5 were obtained. The value of y is no longer 0.5 or the isobars obtained by plotting rate against $p^{\frac{1}{2}}$ are not straight (Fig. 5).

Since pure nitrogen was originally used in annealing the copper at the laboratories of the American Smelting and Refining Company, we have a complete check on our previous conclusion that the curvature previously found in low temperature (450°C) diffusion isotherms of hydrogen through copper as found by Smithells and others was due to a small amount of oxygen in solution in the copper used by these experimenters.

Finally it should be noted in Fig. 6 that the same data of Fig. 5 when plotted logarithmically gives perfectly straight lines. The theory for this is presented in the paper by Simons and Ham.[6]

Remarks on the Hole Theory of Condensation

JOHN G. KIRKWOOD
Baker Laboratory, Cornell University, Ithaca, New York

(Received May 29, 1939)

The hole theory of condensation recently proposed by Cernuschi and Eyring is discussed from the standpoint of the order-disorder theory of critical solution phenomena. It is pointed out that the hole theory predicts critical temperatures which are several times larger than those observed for most nonpolar fluids. This is attributed to the failure of the theory to take adequate account of the lattice vibrational factor in the partition function.

I

IN a recent paper, Cernuschi and Eyring[1] have presented an ingenious theory of condensation based upon the order-disorder theory and a model fluid in which the liquid and vapor phases are treated as alloys of holes and molecules. It is perhaps not without interest to point out that the hole theory of condensation may be obtained as a special case of the writer's[2] theory of critical solution phenomena, in which holes constitute one of the components of a binary solution. At the same time, the theory of condensation has a serious defect. In a binary solution consisting of molecules of nearly equal size, the lattice vibrational factor in the partition function may be regarded as approximately independent of composition. However, if one of the components consists of holes, this is not even a moderately good approximation, and indeed leads to serious error. It is therefore not surprising that the theory of Cernuschi and Eyring predicts, as we shall show, critical temperatures about three times too high.

The following remarks will suffice to show the formal identity of the hole theory of condensation and the theory of critical solution phenomena. In a system consisting of N_1 molecules at temperature T and volume v, the chemical potential μ_1 of the molecules may be expressed as $(\partial A/\partial N_1)_{T,v}$ among alternative forms. The conditions for heterogeneous equilibrium between two phases of the one component system are, in addition to equality of temperature,

$$\mu_1=\mu_1', \qquad p=p', \tag{1}$$

where μ_1, μ_1', p, and p' are the chemical potentials and pressures in the respective phases. Eqs. (1) are, of course, equivalent to the condition of equality of pressures subject to the law of equal areas, the criterion employed by Cernuschi and Eyring. From another point of view, we may regard the fluid as a solution of two components, N_1 molecules, and N_2 holes, the holes being defined with reference to a virtual lattice composed of cells of volume Δ. The volume, v, equal to $(N_1+N_2)\Delta$ ceases to be an independent variable and is replaced by N_2. We can define chemical potentials μ_1^* and μ_2^* of molecules and holes as $(\partial A/\partial N_1)_{T,N_2}$ and $(\partial A/\partial N_2)_{T,N_1}$. If this is done, it is readily shown that the conditions

$$\mu_1^*=\mu_1^{*\prime}, \qquad \mu_2^*=\mu_2^{*\prime} \tag{2}$$

are equivalent to Eqs. (1). Since the addition of a hole is equivalent to increasing the volume of the system by Δ, μ_2 is merely $-p\Delta$, since $(\partial A/\partial v)_{T,N_1}$ is equal to $-p$. Thus the second of Eqs. (2) is equivalent to the second of Eqs. (1). The chemical potential μ_1 is evidently identical with $(\partial A/\partial N_1)_{T,N_1+N_2}$ or $\mu_1^*-\mu_2^*$ and the first of Eqs. (1) is equivalent to the difference of Eqs. (2).

If the writer's theory is applied to the problem of condensation, V_0 of Eq. ($K4$) becomes $-zV_{11}/2$, or $z\epsilon/2$ if $-\epsilon$ denotes the mutual potential energy V_{11} of a pair of neighboring molecules. Since the interaction between holes or between a molecule and a hole is zero, V_{22} and V_{12} vanish. The quantity α of Eq. ($K8$) is therefore given by

$$\alpha=z\epsilon/2kT. \tag{3}$$

The critical temperature is, according to Eq. ($K32$),

$$T_c=\frac{\epsilon}{2k}[1-(1-4/z)^{\frac{1}{2}}]^{-1}. \tag{4}$$

[1] Cernuschi and Eyring, J. Chem. Phys. **7**, 547 (1939).
[2] Kirkwood, J. Phys. Chem. **43**, 97 (1939). Equations of this paper are referred to as Eq. (K).

With a coordination number z, equal to 8, Eq. (4) yields for T_c a value of $1.71\epsilon/k$, which differs insignificantly from $1.74\epsilon/k$, the value of Cernuschi and Eyring. In the writer's theory, the mole fraction of molecules x_1 is evidently equal to the ratio ρ/ρ_0 of the density ρ to the density ρ_0 of a hole-free phase. The variable δ of Eqs. ($K30$) and ($K31$) therefore becomes

$$\delta=(\rho_l-\rho_v)/\rho_0, \tag{5}$$

where ρ_l and ρ_v are the densities of the coexistent liquid and vapor phases. The boundary of the evaporation field is determined by Eqs. ($K30$) and ($K31$).

$$\begin{gathered}\rho_l+\rho_v=\rho_0,\\ (\rho_l-\rho_v)/\rho_0=\tanh\,[B(\rho_l-\rho_v)/\rho_0],\\ B=\frac{1}{2}\left\{\alpha-\frac{\alpha^2}{2}[1-(\rho_l-\rho_v)^2/\rho_0^2]\right\}.\end{gathered} \tag{6}$$

We see, therefore, that except for minor differences the hole theory of condensation proposed by Cernuschi and Eyring may be regarded as a special case of the theory of critical solution phenomena.

The theory may easily be tested. The energy of vaporization, ΔE, of the liquid phase at its normal boiling point is to a close approximation given by

$$2\Delta E/RT_b=(1-\gamma_b)z\epsilon/kT_b, \tag{7}$$

where γ_b is the hole fraction of the liquid at its boiling point. Since $\Delta E/RT_b$ is approximately equal to $(K/2-1)$ where K is the Trouton constant, we may write

$$T_c=\frac{z(1-\gamma_b)}{K-2}\left(\frac{T_c}{T_b}\right)\frac{\epsilon}{k}. \tag{8}$$

For the bulk of nonpolar liquids, K is about 21 and T_b/T_c very close to 0.6. If the hole fraction is neglected in comparison with unity, and z is assigned the value 8, the empirical value of T_c from Eq. (8) is $0.7\epsilon/k$, as compared with the value $1.7\epsilon/k$ predicted by the hole theory of condensation. If the coordination number z is increased to 12, Eq. (8) yields for T_c a value ϵ/k whereas the hole theory predicts $2.8\epsilon/k$. The hole theory of condensation thus predicts critical temperatures which are between two and three times too high. As a quantitative theory, it therefore fails completely, although it does provide an interesting qualitative mechanism for condensation. The failure is probably due to the fact that the lattice vibrational factor in the partition function must be considered explicitly and cannot be treated as independent of composition. This complication is absent when the theory of critical solution phenomena is applied to systems composed of molecules of approximately equal size.

II

Although it is not yet possible to formulate a hole theory which is at the same time rigorous and explicit, the preliminary steps in such a theory may be outlined. It is easily shown that the Gibbs phase integral Z_{N_1} for a system of N_1 molecules confined in a volume v may be broken up into contributions from the cells of a virtual lattice spanning v. The size Δ of the cells is somewhat arbitrary, but it is convenient to choose Δ as $0.707a^3$ corresponding to close packing of molecules of diameter a. The number of cells N_0, contained in v is then v/Δ and no more than one molecule can occupy a specified cell at a time due to the excluding action of intermolecular repulsion. The phase integral $Z_{N_1}/N_1!$ may then be written in the form

$$\begin{gathered}Z_{N_1}/N_1!=\sum_{\eta_1,\cdots\eta_{N_0}=0}^{1}\exp\,(\alpha\sum_{a,\,b=1}^{N_0}\lambda_{ab}\eta_a\eta_b)\\ \sum_{a=1}^{N_0}\eta_a=N_1\\ \times g(\eta_1,\cdots\eta_{N_0})\\ g(\eta_1,\cdots\eta_{N_0})=\Delta^{N_1-N_0}\int^{\Delta_1}\cdots\int^{\Delta_{N_0}}\\ \times\exp\left(-\frac{1}{2kT}\sum_{a,\,b=1}^{N_0}\lambda_{ab}\eta_a\eta_b[V(r_{ab})-V_0]\right)\\ \times dv_1\cdots dv_{N_0},\\ \alpha=-V_0/2kT=\epsilon/2kT,\end{gathered} \tag{9}$$

where the sum extends over all distributions of the N_0 cells among the molecules, a distribution being specified by a set of numbers, $\eta_1,\cdots\eta_{N_0}$, each of which may take on one of two values, zero or unity, depending upon whether the specified cell is empty or occupied by a molecule.

V_0 is the mutual potential energy of a pair of molecules situated at the centers of neighboring cells and λ_{ab} is the ratio of the potential energy of a pair of molecules situated at the centers of cells a and b to V_0, unity for neighboring cells and small for non-neighboring cells. The integral $g(\eta_1, \cdots \eta_{N_0})$ extends over the volume Δ_a of each of the N_0 cells, $V(r_{ab})$ being the mutual potential energy of a pair of molecules a distance r_{ab} apart in neighboring cells a and b. The integrals g are the classical analogs of the lattice vibrational factors in the partition function of crystals, divided by $(2\pi mkT/h^2)^{3N_1/2}$. In a given configuration, the factor g makes a contribution $W(\eta_1, \cdots \eta_{N_0})$ to the free energy, in excess of $-N_1kT \log \Delta$, of the following magnitude

$$g(\eta_1, \cdots \eta_{N_0}) = [\exp(-W(\eta_1, \cdots \eta_{N_0})/kT)]\Delta^{N_1}. \quad (10)$$

If one desires, a free volume v_f may be formally defined in terms of g.

$$v_f(\eta_1, \cdots \eta_{N_0}) = [g(\eta_1, \cdots \eta_{N_0})]^{1/N}, \quad (11)$$

but it should be remembered that this is merely a change in notation which does not facilitate the calculation of the integral.

The partition function, $Z_{N_1}/N_1!$ may be expanded by the method of semi-invariants.[3] The resulting expression for the configurational free energy A is

$$A/N_1kT = \log\left[\frac{\gamma(1-\gamma)^{1-1/\gamma}}{\Delta}\right] + \frac{W_0(\gamma)}{N_1kT} - \sum_{n=1}^{\infty}\frac{\lambda_n\alpha^n}{n!N_1},$$

$$e^{-W_0(\gamma)/kT} = \binom{N_0}{N_1}^{-1} \sum_{\eta_1, \cdots \eta_{N_0}=0}^{1} e^{-W(\eta_1, \cdots \eta_{N_0})/kT}, \quad \sum_{a=1}^{N_0}\eta_a = N_1 \quad (12)$$

$$\sum_{m=1}^{n}\binom{n-1}{m-1}\lambda_m M_{n-m} = M_n; \quad n = 1, 2, \cdots,$$

$$M_n = \binom{N_0}{N_1}^{-1} \sum_{\eta_1, \cdots \eta_{N_0}=0}^{1} \left(\sum_{a,b=1}^{N_0}\lambda_{ab}\eta_a\eta_b\right) \sum_{a=1}^{N_0}\eta_a = N_1 \times e^{-[W(\eta_1, \cdots \eta_{N_0}) - W_0]/kT},$$

where γ is equal to N_1/N_0, the ratio of the density of the system, ρ, to its close-packed density ρ_0.

If $W(\eta_1, \cdots \eta_{N_0})$ is assumed independent of configuration, $W_0(\gamma)$ independent of γ, and the first two terms of the semi-invariant series are retained, the hole theory of condensation outlined in the previous section is obtained. Similar assumptions are evidently implicit in the theory of Cernuschi and Eyring, since their critical temperature differs insignificantly from our own. However, below the critical temperature, they make a step in right direction by treating the size of the basic cell Δ as a function of density, which is doubtless equivalent to taking partial account of the dependence of W_0 on density.

If we attempt to calculate W_0, we are led back to the problem of evaluating the phase integral in a somewhat modified form. The only precise method available for this purpose at the present is that of Mayer,[4] but his method is not yet capable of yielding explicit results for condensed phases. Fortunately, in his theory of condensation, which is to be considered superior to the hole theory, he is able to avoid direct consideration of the condensed phase. Since we know that $W_0(\gamma)$ must vanish when $\gamma = 0$, and must become infinite when $\gamma = 1$, it is possible to employ various empirical interpolation formulas in Eq. (12). It is possible to find a number of such formulas, for example, $W_0 = -\beta \log(1-\gamma)$ which with appropriate choice of constants lead to correct values of the critical temperature. However, this does not seem a desirable procedure, since it places the theory on an *ad hoc* basis, which obscures the underlying principles.

The possibility of a solid phase and a theory of fusion is implicit in $W_0(\gamma)$ and should follow from its exact calculation, since it appears that the series in α cannot lead to a third phase but only to one expanded and one condensed phase. Lennard-Jones and Devonshire[5] have proposed a theory of fusion based upon destruction of long range order of the Bragg and Williams type in

[3] Kirkwood, J. Chem. Phys. **6**, 70 (1938).

[4] Mayer and Harrison, J. Chem. Phys. **6**, 87 (1938).

[5] Lennard-Jones and Devonshire, Proc. Roy. Soc. London **A169**, 317 (1939).

the distribution of holes in the lattice.* The partition function, Eq. (9), may be easily set up for two interpenetrating lattices with fixed long range order. It is then found that the ordering contribution to the free energy must arise from $W_0(\gamma, s)$, since α is certainly positive, and its contribution to the free energy could only establish long range order if it were negative. It seems likely, therefore, that the ordering potential in the free energy of the Lennard-Jones-Devonshire theory is not a direct contribution from the binding energy of the lattice, but rather an indirect contribution from the lattice vibrational or "free volume" part of the free energy.

While the general formulations given in this section may not appear very useful due to our present inability to calculate $W_0(\gamma)$, they serve to bring into relief the central problem which must be solved before an exact "hole" theory of phase transitions based on the order-disorder theory can be achieved.

* Lennard-Jones and Devonshire refer their calculation to a different basic lattice than our own. They employ twice as many sites as there are molecules, one for each molecule on each of two interpenetrating lattices. One of the lattices consists of interstitial sites of high energy. The distribution of molecules between normal and interstitial sites corresponds to the lattice vibrational factor of the present formulation.

OCTOBER, 1939 JOURNAL OF CHEMICAL PHYSICS VOLUME 7

The Dielectric Polarization of Polar Liquids*

JOHN G. KIRKWOOD
Baker Laboratory, Cornell University, Ithaca, New York

(Received July 6, 1939)

An extension of the Onsager theory of dielectric polarization is presented. The local dielectric constant is approximated by the macroscopic dielectric constant of the fluid in a region outside a molecule and its first shell of neighbors rather than in the entire region exterior to the molecule. In addition to the molecular dipole moment, the average value $\langle\cos\gamma\rangle_{Av}$ of the cosine of the angle between neighbor dipoles is a determining factor. Hindered relative rotation of neighboring molecules produces a correlation between their orientations and prevents $\langle\cos\gamma\rangle_{Av}$ from vanishing. The theory is applied to liquid water under the assumption of tetrahedral coordination and directed bonds between neighboring molecules.

I

OF the inadequacy of the Lorentz field, $E+4\pi P/3$, as an approximation to the local field in polar dielectrics, there seems to be little doubt. It leads to the prediction of electric Curie points at rather high temperatures for polar liquids. Such fictitious Curie points can only be avoided by assuming molecules in the liquid to possess dipole moments of a magnitude entirely inconsistent with their structure, as exhibited in the vapor. Further evidence against the Lorentz field is provided by the experimental work of Wyman[1] on polar mixtures. He finds an entirely different dependence of the dielectric constant on composition than that predicted by the Clausius-Mosotti formula, based on the Lorentz field.

The original treatment of the local field by Lorentz[2] was, of course, formally free from objection. He pointed out the existence of a field F', in excess of $E+4\pi P/3$, due to the polarization of the content of the Lorentz cavity, a sphere large relative to molecular dimensions. Although he was unable to prescribe a general method for the calculation of F', an exact theory might be based upon its calculation. However, it is apparent from the work of Wyman and Onsager that the Lorentz formula-

* The present theory was outlined by the author at the Symposium on Dielectrics held by the New York Academy of Sciences, April 10, 1939.

[1] Wyman, J. Am. Chem. Soc. **58**, 1482 (1936).

[2] H. A. Lorentz, *Theory of Electrons* (Teubner, Leipzig. 1909), p. 303.

tion does not provide the most convenient point of departure, since in polar liquids the term $4\pi P/3$ is largely nullified by F'. The complete neglect of F' is equivalent to shrinking the macroscopic Lorentz cavity onto the surface of the molecule in which the local field is to be calculated. This involves the neglect of the deviation of the local polarization near a molecule from the average polarization of the medium in the large. The failure of the Lorentz approximation is principally due to this deviation.

Attempts have been made to salvage the Lorentz field by Debye[3] and Fowler,[4] who postulate hindered rotation of a molecule relative to its environment in a liquid or solid. While there is certainly a physical basis for such an assumption, the phenomenological character of the hindered rotation theories obscures the nature of the underlying molecular processes. It is fairly clear that hindered rotation does play a role in the dielectric polarization of polar liquids, but equally clear that it is responsible for large departures from the Lorentz field. It should therefore not be used to supplement the Lorentz field, with which it is really incompatible, but should be introduced as a means of correcting the Lorentz field. The deviation of the local polarization from the average polarization is of course due to hindered rotation of the neighbors of a molecule, relative to itself. The hindered relative rotation of a pair of neighboring molecules may be due in part to electrostatic dipole-dipole coupling, and, in part, to other intermolecular forces, for example, multipole forces of higher order, van der Waals forces, and the repulsive forces determining molecular shape. The relative importance of the several types of forces responsible for hindered relative rotation doubtless varies in individual cases.

An entirely rigorous formulation of the problem, in which hindered rotation and deviations from the Lorentz field are implicit, has been given by Van Vleck.[5] Unfortunately, the method of calculation which he proposes, becomes prohibitively difficult in condensed phases. However, he is able to show that the first of a series of corrections to the Lorentz field is in the right direction and eliminates the spurious electric Curie points predicted by the Lorentz theory.

The most successful calculation of the local field in polar liquids is due to Onsager.[6] He takes account of the deviation of the local polarization from the average by treating the molecule as a real cavity in a statistical continuum of uniform dielectric constant ϵ equal to that of the liquid in bulk. With this model and the macroscopic electrostatic theory of continuous media, the local field and average torque, effective in orienting a dipole molecule relative to an external field may be calculated in a very simple fashion. The Onsager cavity is a real cavity, which in the presence of an external field, produces a reaction field in its neighborhood with an accompanying disturbance of the local polarization. It differs from the Lorentz cavity, which is assumed to be filled with material of the macroscopic dielectric constant. Although the Onsager theory constitutes a brilliant advance, the oversimplified model, a molecular cavity in a continuum of uniform dielectric constant, prevents it from being exact. The most serious defect of the model lies in the assumption of a uniform local dielectric constant, identical with the macroscopic dielectric constant of the medium. Moreover, the hindered rotation of the neighbors of a molecule, relative to itself, which is implicit in the deviation of the local from the average polarization, is attributed entirely to the dipole field of the central molecule.

In the present article, we shall describe a generalization of the Onsager theory which is entirely rigorous within the limits of applicability of classical statistical mechanics. In this theory the dielectric constant is related to two electric moments, the moment μ a single molecule and and the total moment, $\bar{\mu}$, a molecule and its neighbors, in the absence of an external field. If a molecule is assumed to orient its neighbors solely by its dipole field and they are treated as part of a statistical continuum having the macroscopic dielectric constant, $\bar{\mu}$ reduces to μ and the Onsager theory is obtained. Although the calculation of $\bar{\mu}$ is not without its own difficulties and, in most cases, can be done only approximately, the present theory has the ad-

[3] Debye, Physik. Zeits. **36**, 100 (1935).
[4] Fowler, Proc. Roy. Soc. **A149**, 1 (1935).
[5] Van Vleck, J. Chem. Phys. **5**, 556 (1937).
[6] Onsager, J. Am. Chem. Soc. **58**, 1486 (1936).

vantage of reducing the complicated problem of dielectric polarization to a problem of considerably lower order of complexity. The theory has the further advantage of clarifying the role of hindered rotation. It will be shown the moment $\bar{\mu}$ can be simply related to the potential of the torque restricting the relative rotation of neighboring molecules.

II

The average electric moment, $\bar{\mathbf{p}}$, of an arbitrary molecule of an isotropic fluid dielectric under the influence of an applied electric field $\mathbf{E}$ may be expanded in a power series in the field strength E.

$$\bar{p}=p_1E+p_2E^2+\cdots. \tag{1}$$

If electrical saturation is neglected, only the linear term is to be retained. The dielectric constant ϵ of the fluid is related to the coefficient p_1 in the following manner,

$$\epsilon-1=4\pi Np_1/v, \tag{2}$$

where N is Avogadro's number and v is the molar volume. The average component of the permanent dipole moment of any molecule in the direction $\mathbf{e}$ of the applied field may also be expanded in powers of the field strength,

$$\langle\boldsymbol{\mu}\cdot\mathbf{e}\rangle_{Av}{}^{E}=\mu_1E+\mu_2E^2+\cdots. \tag{3}$$

The coefficient p_1 is related to μ_1 and the molecular polarizability as follows,

$$p_1=\mu_1+\alpha F/E, \tag{4}$$

where F is the average local field in the interior of the molecule.

In order to calculate μ_1, we imagine a specimen of the dielectric consisting of N molecules confined in a spherical region of volume v to be introduced into a region of free space in which an homogeneous field $\mathbf{E}_0$ is maintained by fixed external charge distributions. The specimen in a fixed configuration of its molecules with total electric moment $\mathbf{M}$, acquires a potential energy $-\mathbf{M}\cdot\mathbf{E}_0$ by virtue of the field, terms in E_0^2 associated with induced polarization being neglected. The average component $\langle\boldsymbol{\mu}_i\cdot\mathbf{e}\rangle_{Av}{}^{E}$ of any molecule i in the direction $\mathbf{e}$ of the field can be calculated on the basis of classical statistical mechanics by means of the formula

$$\langle\boldsymbol{\mu}_i\cdot\mathbf{e}\rangle_{Av}{}^{E}=\frac{\int\cdots\int\boldsymbol{\mu}_i\cdot\mathbf{e}\exp\left(-[V_N-\mathbf{M}\cdot\mathbf{E}_0]/kT\right)d\tau_1\cdots d\tau_N}{\int\cdots\int\exp\left(-[V_N-\mathbf{M}\cdot\mathbf{E}_0]/kT\right)d\tau_1\cdots d\tau_N}, \tag{5}$$

$$\mathbf{M}=\sum_{k=1}^{N}\boldsymbol{\mu}_k,$$

where V_N is the potential of intermolecular forces and $d\tau_k$ a differential element of the rotational and translational configuration space of molecule k. Expansion of the right-hand side of Eq. (5) in powers of E_0 yields

$$\langle\boldsymbol{\mu}_i\cdot\mathbf{e}\rangle_{Av}{}^{E}=(1/kT)\langle(\boldsymbol{\mu}_i\cdot\mathbf{e})(\mathbf{M}\cdot\mathbf{e})\rangle_{Av}E_0+O(E_0^2), \tag{6}$$

where the mean value $\langle(\boldsymbol{\mu}_i\cdot\mathbf{e})(\mathbf{M}\cdot\mathbf{e})\rangle_{Av}$ refers to the specimen in the absence of the external field. From macroscopic electrostatics we know that the field strength E in the interior of a spherical specimen is $3E_0/(\epsilon+2)$ if E_0 is the field existing in free space before the introduction of the specimen. Conversion of the power series, Eq. (6), into a power series in E and comparison with Eq. (3) yields

$$\mu_1=\left(\frac{\epsilon+2}{3}\right)\frac{\langle(\boldsymbol{\mu}_i\cdot\mathbf{e})(\mathbf{M}\cdot\mathbf{e})\rangle_{Av}}{kT}. \tag{7}$$

Moreover, since in an isotropic spherical specimen, the polarization must be independent of the direction $\mathbf{e}$ of the field, μ_1 is unchanged by an average over all directions of $\mathbf{e}$.

$$\mu_1=\left(\frac{\epsilon+2}{3}\right)\frac{\langle\boldsymbol{\mu}_i\cdot\mathbf{M}\rangle_{Av}}{3kT}. \tag{8}$$

The mean value operation on $\boldsymbol{\mu}_i\cdot\mathbf{M}$ may be carried out in two stages, first over all configurations of all molecules except i and finally over all positions and orientations of molecule i

$$\langle\boldsymbol{\mu}_i\cdot\mathbf{M}\rangle_{Av}=\langle\boldsymbol{\mu}_i\cdot\overline{\mathbf{M}}_i\rangle_{Av}, \tag{9}$$

where $\overline{\mathbf{M}}_i$ is mean total moment of the specimen produced by molecule i fixed at a specified position and in a specified orientation, in the absence of the external field. Although the

vectors $\boldsymbol{\mu}_i$ and $\overline{\mathbf{M}}_i$ vanish individually when averaged over all orientations of molecule i, this will not be true of their scalar product $\boldsymbol{\mu}_i \cdot \overline{\mathbf{M}}_i$. In fact, in a liquid, $\boldsymbol{\mu}_i \cdot \overline{\mathbf{M}}_i$ must be independent of the position and orientation of molecule i, except in a region of negligible volume near the boundary of the specimen. We may therefore omit the final average over configurations of i and write

$$\mu_1 = \left(\frac{\epsilon+2}{3}\right)\frac{\boldsymbol{\mu}\cdot\overline{\mathbf{M}}}{3kT}, \tag{10}$$

where the subscript i has been dropped, since $\boldsymbol{\mu}\cdot\overline{\mathbf{M}}$ has, of course, the same value for any molecule i of the specimen. If Eq. (10) were inserted in Eq. (2), an expression identical in form with the Clausius-Mosotti equation would result, $\boldsymbol{\mu}\cdot\overline{\mathbf{M}}$ replacing μ^2 in the Langevin-Debye formula. We shall not do this, since it is more convenient to introduce instead of $\overline{\mathbf{M}}$ an electric moment more closely related to the properties of a single molecule and its immediate environment. $\overline{\mathbf{M}}$ is the total moment induced in a spherical specimen by any one of its molecules maintained in a fixed position and orientation. It is easy to show that $\overline{\mathbf{M}}$ is, as it must be, independent of the radius of the specimen. However, $\overline{\mathbf{M}}$ is not concentrated in the neighborhood of the fixed molecule, but arises in part from a homogeneous polarization of the entire specimen by a reaction field produced by the external boundary of the specimen. (See Appendix.) By allowing the boundary to recede to infinity, this polarization may be reduced to zero in any finite region of the specimen, or in an infinite region, the volume of which is an infinity of lower order than that of the whole specimen. It is desirable to define a moment $\bar{\boldsymbol{\mu}}$ from which the polarization by the boundary field is absent,

$$\bar{\boldsymbol{\mu}} = \lim_{\substack{r_0\to\infty \\ R/r_0\to\infty}} \overline{\mathbf{M}}(R, r_0), \tag{11}$$

where $\overline{\mathbf{M}}(R, r_0)$ is average moment of a spherical region of radius r_0, referred to a reference system in a molecule at its center, in a spherical specimen of radius R. In the Appendix, it is shown that

$$\overline{\mathbf{M}} = \left(\frac{3}{\epsilon+2}\right)\left(\frac{3\epsilon}{2\epsilon+1}\right)\bar{\boldsymbol{\mu}}. \tag{12}$$

The moment $\bar{\boldsymbol{\mu}}$ (not to be confused with Onsager's external moment $\boldsymbol{\mu}^*$ to be discussed in the Appendix) is also the total moment of any finite macroscopic spherical specimen polarized by a fixed molecule, when immersed in a medium of its own dielectric constant. Although in the definition, Eq. (11) the radius r_0 of the sphere containing the moment $\bar{\boldsymbol{\mu}}$ is infinite, it is actually concentrated in a sphere of molecular dimensions around the fixed molecule, since, as we shall show, any spherical shell, in which the local dielectric constant is uniform and equal to the macroscopic dielectric constant of the specimen, makes no contribution to $\bar{\boldsymbol{\mu}}$. Thus a less rigorous, but adequate definition of μ is

$$\bar{\boldsymbol{\mu}} = \overline{\mathbf{M}}(r_0), \tag{12}$$

where r_0 is a distance of molecular magnitude beyond which the local dielectric constant in the neighborhood of an arbitrary molecule is effectively equal to the macroscopic dielectric constant, and $\overline{\mathbf{M}}(r_0)$ is the average total moment of a sphere of radius r_0 relative to a reference system fixed in a molecule at its center. The moment $\bar{\boldsymbol{\mu}}$ is not necessarily parallel to $\boldsymbol{\mu}$, but will be so if the molecule has an axis of threefold or greater symmetry parallel to its permanent moment $\boldsymbol{\mu}$.

Since the optical polarization makes a very small contribution to the dielectric constant, the local field F in the last term of Eq. (4) may be adequately approximated by the Onsager local field $3\epsilon E/(2\epsilon+1)$. With this minor approximation and the use of Eqs. (2), (4), (10) and (12), we obtain

$$\frac{\epsilon-1}{3} = \left(\frac{3\epsilon}{2\epsilon+1}\right)\frac{P_0}{v}, \qquad P_0 = \frac{4\pi N}{3}\left[\alpha + \boldsymbol{\mu}\cdot\bar{\boldsymbol{\mu}}/3kT\right]. \tag{13}$$

Solution of Eq. (13) for $\epsilon-1$ gives

$$\frac{\epsilon-1}{3} = \frac{3}{2}\frac{P_0}{v}\varphi(P_0/v), \qquad \varphi(x) = \frac{1}{2}\left\{1 - \frac{1}{3x} + \left[\left(1-\frac{1}{3x}\right)^2 + \frac{4}{9x}\right]^{\frac{1}{2}}\right\}. \tag{14}$$

When x is large relative to unity, we have the expansion

$$\varphi(x)=1-1/18x+2/81x^2+\cdots.$$

Since P_0/v is in general greater than unity in polar liquids, we might write to a very close approximation,

$$\epsilon-1=9P_0/2v. \tag{15}$$

This formula may be readily generalized for polar mixtures, with the result

$$\epsilon-1=\frac{9}{2}\sum_{K=1}^{\nu} c_k P_k,$$
$$P_k=\frac{4\pi N}{3}[\alpha_K+\boldsymbol{\mu}_k\cdot\bar{\boldsymbol{\mu}}_k/3kT], \tag{16}$$

where c_k is the concentration in moles per cubic centimeter of component k. The moment $\bar{\boldsymbol{\mu}}_k$ will of course depend on composition.

It should be pointed out that the molecular moment $\boldsymbol{\mu}$ is not necessarily equal to the moment $\boldsymbol{\mu}_0$ of a molecule in the gas phase. Although it is not possible to make an exact calculation at present, we may say that $\boldsymbol{\mu}$ is in general somewhat greater than $\boldsymbol{\mu}_0$ because of a polarization of the molecule by its neighbors in the liquid. An approximate relation between $\boldsymbol{\mu}$ and $\boldsymbol{\mu}_0$ may be obtained if the Onsager reaction field is assumed valid. The calculation may be made in two ways: (a) the induced polarization is assumed to be that of a sphere of the molecular radius b of dielectric constant n^2 where n is the extrapolated optical refractive index of the liquid; (b) the total moment of the molecule consists of a point dipole at the center of a sphere b of dielectric constant unity. The results in the two cases are

$$\text{(a)}\quad \mu=\frac{2\epsilon+1}{2\epsilon+n^2}\frac{n^2+2}{3}\mu_0,$$
$$\text{(b)}\quad \mu=\mu_0\Big/\left[1-\frac{2(\epsilon-1)}{2\epsilon+1}\frac{\alpha}{b^3}\right]. \tag{17}$$

A more accurate calculation of μ/μ_0 will be given later. It should also be remarked that Eq. (17) is restricted to molecules of spherical shape.

Equations (13) and (14) are exact except for the minor approximation embodied in the use of the Onsager local field for the small optical contribution to the dielectric constant. In order to use them, it is necessary to calculate $\bar{\boldsymbol{\mu}}$, the total moment of a molecule and its neighbors, in the region surrounding it, in which the local dielectric constant deviates effectively from the macroscopic dielectric constant. The moment $\bar{\boldsymbol{\mu}}$ reduces to the molecular moment $\boldsymbol{\mu}$ for spherical molecules if the region of macroscopic dielectric constant is assumed to extend to the molecular surface and if short range orienting forces in addition to dipole-dipole coupling are assumed absent. With these assumptions the present theory reduces to the Onsager theory. A formally exact expression for $\boldsymbol{\mu}\cdot\bar{\boldsymbol{\mu}}$ may be given in terms of W, the potential of average force and torque acting on an arbitrary pair of molecules.

$$\boldsymbol{\mu}\cdot\bar{\boldsymbol{\mu}}=\mu^2\left[1+\frac{N}{v}\int^{v_0}\cos\gamma e^{-W/kT}d\omega dv\right],$$
$$\int^{v} e^{-W/kT}d\omega dv=1, \tag{18}$$

where γ is the angle between the dipole moment of an arbitrary pair of molecules and the integration extends over all relative orientations and positions of centers of gravity of the pair within a sphere of volume v_0, outside of which the local dielectric constant is effectively equal to the macroscopic dielectric constant. The calculation of W is a difficult task in statistical mechanics, and has not yet been successfully dealt with for polar molecules in polar media. It is perhaps interesting to remark that the integral of $e^{-W/kT}$ over all relative coordinates of the pair except their distance of separation is the radial distribution function, which may be obtained from the x-ray scattering of liquids. One might attempt to approximate W by the potential energy of a dipole pair in a continuous medium of the macroscopic dielectric constant, used by Fuoss[7] in conjunction with the Lorentz field in his calculation of the polarization of dilute solutions of polar molecules in nonpolar solvents. However, because of the high macroscopic dielectric constants of polar liquids, this leads to a value of $\boldsymbol{\mu}\cdot\bar{\boldsymbol{\mu}}$ differing very little from μ^2. The result, therefore, differs but little from that of the

[7] Fuoss, J. Am. Chem. Soc. **56**, 1027, 1031 (1934).

Onsager theory, in which the approximation of the local dielectric constant by the macroscopic value is introduced at an earlier stage in the calculation.

We propose to use a simple approximation to Eq. (18), which is probably adequate in most cases. We assume that the local dielectric constant may be approximated by the macroscopic dielectric constant outside a region containing a molecule and its z nearest neighbors. We then have

$$\mathfrak{y}\cdot\bar{\mathfrak{y}}=\mu^2[1+z\langle\cos\gamma\rangle_{Av}], \tag{19}$$

where γ is the angle between the dipole moments of a pair of neighboring molecules, and $\langle\cos\gamma\rangle_{Av}$ is an average over all orientations of both molecules,

$$\langle\cos\gamma\rangle_{Av}=\int\int\cos\gamma e^{-W_0/kT}d\omega_1 d\omega_2, \tag{20}$$

where W_0 is the potential of average torque acting on a pair of nearest neighbors. It may arise from short range intermolecular forces as well as from dipole-dipole interaction. Small corrections to Eq. (19) will be necessary if the region containing a molecule and its first shell of neighbors is not approximately spherical, since otherwise the total polarization of the external continuum will not vanish and will make some contribution to $\bar{\mathfrak{y}}$.

The role of hindered rotation in dielectric polarization is now clear. The important quantity is $\langle\cos\gamma\rangle_{Av}$ which measures the correlation between the orientations of neighboring molecules resulting from hindered relative rotation. It is possible to make certain empirical assumptions concerning W_0, but we shall not discuss them here. For the purpose of emphasis, it is desirable to introduce the approximation (19) into Eq. (15) to obtain the following formula

$$\epsilon-1=6\pi\frac{N}{v}\left[\alpha+\frac{\mu^2}{3kT}(1+z\langle\cos\gamma\rangle_{Av})\right]. \tag{21}$$

The significant molecular quantities determining the dielectric constant of a polar liquid are, in addition to the molecular dipole moment $\mathfrak{y}$, the average coordination number z and $\langle\cos\gamma\rangle_{Av}$.

In certain liquids, for example, water, the hindering torques are so great that a molecule and its shell of neighbors may be regarded as a quasi-rigid structure. According to the model of Bernal and Fowler,[8] the coordination number in liquid water is four and the average configuration of a molecule and its first coordination shell is supposed to resemble that of the β-quartz structure. Since the Bernal-Fowler model can certainly provide no more than a qualitative description, we shall employ only its more general features, the coordination number, four, and the existence of directed bonds between pairs of neighboring molecules. The bond is assumed to be directed along an O−H bond of one molecule toward the oxygen atom of the other along a line passing through one of its concentrations of negative charge due to the nonbonding $2p$ electrons. We shall suppose that the charge distribution of the molecule has the symmetry of a trigonal pyramid with concentrations of negative charge on two of its vertices and concentrations of positive charge on the other two. The angle between the vectors from the center to the two positive concentrations is taken to be 100°, the H_2O bond angle. The same angle is assumed for the vectors to the negative concentrations, and the planes determined by the two pairs of vectors are assumed perpendicular. On this model the dipole moment of each molecule is to be directed along the bisector of its OH bonds and makes an angle of 50° with the bond joining it to each neighbor, a neighbor bond corresponding to the matching of a pair of positive and negative charge distributions of the two molecules and having the direction of the O−H bond of the molecule containing the participating proton. If free rotation around neighbor bonds is assumed, $\langle\cos\gamma\rangle_{Av}$ may be calculated at once as $\cos^2 50°$, equal to 0.41. With z equal to four, $\mathfrak{y}\cdot\bar{\mathfrak{y}}$ becomes $2.64\mu^2$. We assume that $\mathfrak{y}$ differs from $\mathfrak{y}_0$ the dipole moment of a free water molecule only by its polarization in the dipole field of its neighbors. With free rotation around neighbor bonds, the four neighbors produce an average field $(8\cos^2 50°)\mu/a^3$ having the direction of $\mathfrak{y}_0$, where a is the distance between neighbors, $\mathfrak{y}$ is the sum of $\mathfrak{y}_0$ and the product of the polarizability

[8] Bernal and Fowler, J. Chem. Phys. **1**, 515 (1933).

α and the dipole field, so that we have

$$\mu=\frac{\mu_0}{1-3.28\alpha/a^3},$$
$$\mathfrak{y}\cdot\bar{\mathfrak{y}}=\frac{2.64\mu_0^2}{(1-3.28\alpha/a^3)^2}. \tag{22}$$

Taking α as 1.5 cubic angstroms and a as 3.27A, we find that μ is equal to $1.16\mu_0$. The dipole moment of the water molecule is thus increased by 16 percent due to polarization by the dipole field of its neighbors in the liquid, and $\mathfrak{y}\cdot\bar{\mathfrak{y}}$ becomes $3.55\mu_0^2$. The calculation of the ratio of μ to μ_0 is of course rather rough. Optical anisotropy of the molecule is neglected, the polarizing field is not really homogeneous, and the effect of electric multipoles of higher order is ignored. With μ_0 equal to 1.88 Debye units, we obtain for P_0, Eq. (13)

$$P_0=3.8+7.74\times10^4/T. \tag{23}$$

At 25°C, Eqs. (14) and (23) yield a value of 67 for the dielectric constant of liquid water. This differs from the experimental value by about 14 percent. The agreement is all that could be expected from our somewhat idealized model of the water molecule and its first coordination shell and seems to confirm our basic theory. For example, if the ratio of μ to μ_0 is increased from 1.16 to 1.26 exact agreement with experiment is obtained. It is not at all unreasonable to suppose that the water molecule is more strongly polarized by its neighbors due multipole fields of higher order than the dipole. The theory predicts approximate proportionality between the dielectric constant of water and the reciprocal of the absolute temperature, which is confirmed by experiment in the range of ordinary temperatures. This fact supports our assumption of a combination of free and completely hindered relative rotation of neighboring molecules. Were the torque potentials associated with any of the degrees of rotational freedom of the magnitude of kT, $\langle\cos\gamma\rangle_{Av}$ would be sensitive to temperature, and the polarization would no longer be a linear function of $1/T$.

The exact value of the dielectric constant of water is rather sensitive to the bond angle of the water molecule. If this angle is assumed to be 90°, the dielectric constant becomes on our model 82 at 25°, differing only slightly from the experimental value 79. On the other hand, if the tetrahedral angle is assumed, the dielectric constant is reduced to 55. The calculations are summarized in Table I. Finally, in order to exhibit the need for the present theory, we may point out that the unmodified Onsager theory leads to a value of 31 for the dielectric constant of water at 25°.

TABLE I. *The dielectric constant of water at 25°.*

O(H)(H) BOND ANGLE	μ_0	$\langle\cos\gamma\rangle_{Av}$	z	$\mathfrak{y}\cdot\bar{\mathfrak{y}}/\mu_0^2$	ϵ (CALC.)	ϵ (EXP.)
90°	1.88	0.50	4	4.35	82	79
100°	1.88	.41	4	3.55	67	79
109° 28′	1.88	.33	4	2.91	55	79

III. APPENDIX

We shall be concerned here with the determination of $\overline{\mathbf{M}}$, the total moment of a macroscopic spherical specimen of dielectric of radius R, produced by a fixed molecule located at an arbitrary point in its interior. Due to the influence of the fixed molecule on the average distribution and orientations of its neighbors, the local dielectric constant of the statistical continuum surrounding it will deviate from the macroscopic dielectric constant, ϵ, of the fluid. We denote by $\bar{M}(R, r_0)$ the total moment of a spherical region of radius r_0 with the fixed molecule at its center. By making r_0 sufficiently large the local dielectric constant may be made to approach the macroscopic dielectric constant as closely as desired. For the total moment of the specimen, we may write

$$\overline{\mathbf{M}}=\overline{\mathbf{M}}(R, r_0)+\int_{v_0}^{v}\mathbf{P}dv, \tag{24}$$

where $\mathbf{P}$ is the polarization of the specimen exterior to the sphere r_0 of volume v_0. It is equal to $-(\epsilon-1)\nabla\psi_i/4\pi$ where ψ_i is the electrostatic potential in the interior of the specimen. Substitution in Eq. (24) and use of a generalized Green's theorem leads to

$$\overline{\mathbf{M}}=\overline{\mathbf{M}}(R, r_0)-\frac{\epsilon-1}{4\pi}\int^{S_e}\psi_i d\mathbf{S}+\frac{\epsilon-1}{4\pi}\int^{S_0}\psi_i d\mathbf{S}, \tag{25}$$

where S_e is a spherical surface just interior to the external boundary of the specimen, and S_0

is the surface of the spherical region v_0. The potential ψ_i, exterior to the region v_0 has the form

$$\psi_i = -\frac{\mathfrak{y}^*}{\epsilon}\cdot\nabla\left(\frac{1}{|\mathbf{r}-\mathbf{r}'|}\right)+\chi, \tag{26}$$

where $\mathfrak{y}^*$ is the external moment of the region v_0, the center of which is located at the point $\mathbf{r}'$, and χ is a solution of Laplace's equation with no point singularities in the interior of the specimen. Using an arbitrary polar coordinate system with origin at the center of the specimen, we may express χ in the form,

$$\chi=\sum_{n=1}^{\infty}\sum_{m=-n}^{+n} B_{nm}r^n P_n^m(\cos\vartheta)e^{im\varphi}. \tag{27}$$

The first term of (26) may be expanded in the form,

$$-\frac{\mathfrak{y}^*}{\epsilon}\cdot\nabla\left(\frac{1}{|\mathbf{r}-\mathbf{r}'|}\right)=\sum_{n=1}^{\infty}\sum_{m=-n}^{+n}\frac{(n-|m|)!}{(n+|m|)!}\times\frac{A_{nm}}{r^{n+1}}P_n^m(\cos\vartheta)e^{im\varphi}, \tag{28}$$

where the coefficients A_{1m} are μ_z^*, $\mu_x^*+i\mu_y^*$ and $\mu_x^*-i\mu_y^*$, respectively, and the multipole coefficients of higher order depend upon the position $\mathbf{r}'$ of the sphere v_0, but do not require detailed specification for our purposes. The potential, ψ_e, in free space exterior to the specimen is a solution of Laplace's equation vanishing at infinity.

$$\psi_e=\sum_{n=0}^{\infty}\sum_{m=-n}^{+n}\frac{(n-|m|)!}{(n+|m|)!}\frac{M_{nm}}{r^{n+1}}P_n^m(\cos\vartheta)e^{im\varphi}, \tag{29}$$

where the coefficients M_{nm} are the external multipole moments of the entire specimen. Since the external dielectric constant is unity the external moments M_{nm} are simply the total moments of the specimen, and M_{10}, $M_{1,1}$, $M_{1,-1}$ are the components $\bar{M}_z$, $\bar{M}_x+i\bar{M}_y$, $\bar{M}_x-i\bar{M}_y$ of the average dipole moment $\overline{\mathbf{M}}$ of the entire specimen. Applying the boundary conditions of electrostatics at the external boundary of the specimen, we obtain

$$\begin{aligned} M_{nm}&=\frac{2n+1}{n\epsilon+n+1}A_{nm},\\ B_{nm}&=\frac{n+1}{\epsilon R^{2n+1}}\frac{\epsilon-1}{n\epsilon+n+1}A_{nm}. \end{aligned} \tag{30}$$

For the dipole terms, $n=1$, Eq. (30) yields

$$\overline{\mathbf{M}}=\frac{3}{\epsilon+2}\mathfrak{y}^*, \quad B_{1m}=\frac{2}{\epsilon R^3}\frac{\epsilon-1}{\epsilon+2}\mu_m^*. \tag{31}$$

Returning to Eq. (25), we find that the first term of the potential, Eq. (26) makes a vanishing contribution to the sum of the surface integrals, so that

$$\overline{\mathbf{M}}=\overline{\mathbf{M}}(R,r_0)-\frac{\epsilon-1}{4\pi}\int^{S_e}\chi d\mathbf{S}+\frac{\epsilon-1}{4\pi}\int^{S_0}\chi d\mathbf{S}. \tag{32}$$

The integral on the exterior surface may be evaluated with the aid of Eq. (27) and the orthogonality properties of the Legendre functions. The integral on the interior surface is equal to $(4\pi/3)r_0^3\nabla\chi(\mathbf{r}')$, by virtue of the fact that χ is a harmonic function with no singularities in the interior of the specimen. Finally we obtain with the aid of the second of Eqs. (31)

$$\overline{\mathbf{M}}=\overline{\mathbf{M}}(R,r_0)-\frac{2}{3\epsilon}\frac{\epsilon-1}{\epsilon+2}\mathfrak{y}^*+O\left(\frac{r_0^3}{R^3}\right), \tag{33}$$

since by Eqs. (27) and (30) $\nabla\chi$ is of the order of magnitude $1/R^3$, and $(4\pi r_0^3/3)\nabla\chi(\mathbf{r}')$ is of the order r_0^3/R^3. Eliminating $\mathfrak{y}^*$ between Eq. (33) and the first of Eqs. (31), we have

$$\overline{\mathbf{M}}=\frac{3}{\epsilon+2}\frac{3\epsilon}{2\epsilon+1}\overline{\mathbf{M}}(R,r_0)+O\left(\frac{r_0^3}{R^3}\right). \tag{34}$$

If we pass to limit $R=\infty$, we have

$$\mathbf{M}_\infty=\frac{3}{\epsilon+2}\frac{3\epsilon}{2\epsilon+1}\bar{\mathfrak{y}}, \quad \bar{\mathfrak{y}}=\lim_{R\to\infty}\overline{\mathbf{M}}(R,r_0), \tag{35}$$

where $\bar{\mathfrak{y}}$ is the moment of any finite spherical region around the fixed molecule located at an arbitrary point in an infinite spherical specimen, in which the total moment is $\bar{M}_\infty$. Since, strictly speaking, r_0 must be infinite in order that the assumption of identity of the local and macroscopic dielectric constants in the region exterior to v_0, be valid, a double limiting process is necessary. Eq. (34) also leads to the result

$$\overline{\mathbf{M}}_\infty=\frac{3}{\epsilon+2}\frac{3\epsilon}{2\epsilon+1}\bar{\mathfrak{y}}, \quad \bar{\mathfrak{y}}=\lim_{\substack{r_0\to\infty\\ R/r_0\to\infty}}\overline{\mathbf{M}}(R,r_0). \tag{36}$$

Actually Eq. (35) is adequate for our purposes, since a finite r_0 of molecular magnitude, let us

say a thousand molecular diameters, certainly exists beyond which the error in approximating the local by the macroscopic dielectric constant is entirely negligible. Moreover, the total moment of any macroscopic spherical specimen, polarized by the microscopic region v_0 can differ from that of an infinite specimen only by terms of negligible order, according to Eq. (34). From Eq. (35) we remark that $\bar{\mu}$ is independent of radius of the sphere r_0. Thus the total polarization of any spherical shell, in which the dielectric constant has the uniform macroscopic value, vanishes. This permits another interpretation of the moment $\bar{\mu}$ as the moment of any macroscopic specimen of radius r_0 when immersed in an infinite medium of its own dielectric constant.

We emphasize the fact that our use of electrostatics of continuous media involves no approximation, as in the Onsager theory, since it is used only in the region in which the statistical continuum surrounding a molecule has attained the macroscopic dielectric constant. It might be objected that our model of a macroscopic specimen polarized by a molecule of fixed orientation in its interior is somewhat artificial, and that the polarization of the medium by a rotating molecule might be quite different due to relaxation effects. While this is possible, it is irrelevant, for we remark that our use of the fixed molecule is a rigorous mathematical artifice employed in the calculation of average values in a canonical ensemble. The moment $\mathbf{M}$ entering into that calculation is precisely the moment induced in the macroscopic specimen by a system of external forces equivalent to those which would be produced by a molecule of fixed position and orientation in its interior.

OCTOBER, 1939 JOURNAL OF CHEMICAL PHYSICS VOLUME 7

Molecular Distribution in Liquids

JOHN G. KIRKWOOD
Baker Laboratory, Cornell University, Ithaca, New York
(Received July 6, 1939)

A theory of the radial distribution function in nonpolar liquids composed of spherical molecules is developed. The characteristic features of experimentally determined radial distribution functions are reproduced by the theory. A single parameter, the work of formation of a cavity of of molecular size, determines the approximate form of the distribution.

IT is characteristic of the structure of liquids that, although the molecules are randomly distributed relative to an external reference system, each molecule establishes, in relation to itself, a partially ordered arrangement of its neighbors. The local structure of the environment of any molecule is characterized by the radial distribution function, $g(R)$, defined as the ratio of the average local density $\rho(R)$ at a distance R from an arbitrary molecule to the average density ρ_0 of the fluid in bulk.

$$\rho(R) = \rho_0 g(R). \tag{1}$$

If v is the volume occupied by the fluid, $g(R)dv/v$ evidently represents the probability that any specified molecule of the fluid lies with its center in the volume element dv at a distance R from another specified molecule.

The radial distribution function may be experimentally determined. By an elegant method involving the use of the Fourier integral theorem, Zernicke and Prins[1] and Debye and Mencke[2] have shown how $g(R)$ may be calculated from the angular distribution of intensity of x-rays scattered by a liquid. Another ingenious experimental approach to the determination of the radial distribution has been employed by Mencke[3] and by Morrell and Hildebrand,[4] based

[1] Zernicke and Prins, Zeits. f. Physik **41**, 184 (1927).
[2] Debye and Mencke, Physik. Zeits. **31**, 797 (1930).
[3] Mencke, Physik. Zeits. **33**, 593 (1932).
[4] Morrell and Hildebrand, J. Chem. Phys. **4**, 224 (1934).

upon direct observation in a model liquid consisting of a system of spherical balls maintained in a state of agitation to simulate thermal motion. The radial distribution function has been discussed from the theoretical standpoint by Prins[5] and by Bernal.[6] Both of these authors regard the radial distribution in liquids to arise from the blurring of a crystalline structure produced by random displacement of the molecules from the sites of an ordered lattice. In the present article, we shall present a somewhat different theory of the radial distribution function, in which the structure is not referred to a basic lattice.

As a consequence of its definition, the radial distribution function possesses certain general properties which it is desirable to state at once. The first of these properties is

$$\lim_{R\to\infty} g(R)=1. \tag{2}$$

Eq. (2) expresses the fact that a liquid possesses no long distance order as does a crystal. Thus the ordering influence of a specified molecule on its environment diminishes with increasing distance and the density $\rho(R)$ approaches ρ_0 as the distance from the molecule becomes large. A second property of $g(R)$ is associated with its normalization,

$$(1/v)\int^{v} g(R)dv=1. \tag{3}$$

Eq. (3) expresses the fact that an arbitrary neighbor of a molecule is certain to be somewhere in the region v occupied by the liquid. An alternative form of Eq. (3) is

$$\int_0^{\infty} R^2[g(R)-1]dR=0, \tag{4}$$

where all of space may be included in the integration if the additional condition,

$$\lim_{R\to\infty}[g(R)-1]R^n=0; \quad n>3$$

is imposed. This condition is somewhat more strong than Eq. (2), but is also demanded by the requirement of vanishing long range order at large distances. If intermolecular repulsive forces at short range are idealized by assigning a molecular diameter, a, determining a sphere ω around each molecule into which others cannot penetrate, we may write

$$g(R)=0; \qquad 0\leqslant R\leqslant a. \tag{5}$$

Subject to Eq. (5), the normalization condition (4) becomes

$$(1/a^3)\int_a^{\infty} R^2[g(R)-1]dR=\tfrac{1}{3}. \tag{6}$$

The radial distribution function $g(R)$ for an arbitrary pair of molecules 1 and 2 in a fluid consisting of N spherical molecules of diameter a, confined in a volume v is, according to statistical mechanics,[7] related to the local free energy of the configuration in which the two molecules are fixed at a distance R apart. Thus

$$g(R)=e^{-W(R)/kT}, \tag{7}$$

where $W(R)$ is the average work necessary to bring the two molecules from infinite separation in the fluid to the specified separation R. Since $g(R)$ is independent of the location of the molecules relative to an external reference system, we may, without loss of generality, regard molecule 1 of the pair as fixed at an arbitrary point. Molecule 2 can be located at a point $\mathbf{R}$ from 1 only if there is a spherical cavity ω of volume $4\pi a^3/3$ around this point, in the remainder of the fluid consisting of $N-2$ molecules. By a cavity, we mean a region from which the centers of all of the other $N-2$ molecules are excluded. If such a cavity did not exist at the point $\mathbf{R}$, molecule 2, if located there, would be at a distance less than the molecular diameter a from some other molecule, a configuration excluded by intermolecular repulsion. If $w(R)$ is the work required to create a cavity at the point R and w_0 the work required to create a cavity at infinity, $W(R)$ may be expressed in the following form

$$W(R)=w(R)-w_0+\chi(R), \tag{8}$$

where $\chi(R)$ is the work expended in transferring molecule 2 from a cavity at infinity to a cavity

[5] Prins, Physica III **3**, 147 (1936).

[6] Bernal, *Structure and Molecular Forces in Liquids*, The Faraday Society (Gurney and Jackson, London, 1936), p. 27.

[7] See for example Kirkwood, J. Chem. Phys. **3**, 300 (1935).

at R. If the fluid were merely a system of rigid spheres exerting no forces on each other except on contact, $\chi(R)$ would vanish. In actual fluids, $\chi(R)$ does not vanish, due to intermolecular attractive forces. However, there is good reason to believe that it plays a subordinate role in determining the molecular distribution in dense fluids.

If $p(R)$ is the probability that one or more of the $N-2$ molecules lies with its center in the sphere ω around the point R, $1-p(R)$ is the probability that no molecule of the set lies in the region, that is, the probability that a cavity ω exists around the point **R**. By a general theorem of statistical mechanics, this probability is proportional to $\exp(-w(R)/kT)$. Thus we may write

$$e^{-[w(R)-w_0]/kT}=(1-p(R))/(1-p_0), \tag{9}$$

where p_0 is the limiting value of $p(R)$ at infinity, that is, the probability that a region ω situated at an arbitrary point in fluid, not fixed relative to any molecule, is occupied by at least one molecule. By Eqs. (7), (8), and (9) we have

$$g(R)=e^{-\chi(R)/kT}[1-p(R)]/[1-p_0]. \tag{10}$$

By the definition of the radial distribution function, the average number of molecules $N_\omega(R)$ occupying a sphere ω around the point **R** is given by

$$N_\omega/N=(1/v)\int^{\omega(R)} g(r)dv, \tag{11}$$

where r is the distance of a point in ω from the fixed molecule 1 and the integration extends over this region. If only one individual of the set of $N-2$ molecules could occupy ω at a time, $p(R)$ would be equal to N_ω/N. This, however, is not the case, for a number of molecules ranging from zero to twelve can be simultaneously somewhere in ω (only if a molecule is located exactly at the center does it exclude all others from the region). Nevertheless, we may define a function $\eta(R)$ by the relation

$$\begin{gathered}p(R)/p_0=[1+\eta(R)]\omega_0^{-1}\int^{\omega(R)} g(r)dv \\ \omega_0=4\pi a^3/3; \quad \lim_{R\to\infty}\eta(R)=0.\end{gathered} \tag{12}$$

If now we introduce a new function $\varphi(x)$ related to $g(R)$ in the following manner

$$\begin{gathered}g(R)-1=\varphi(x)/x \\ x=R/a\end{gathered} \tag{13}$$

and employ dipolar coordinates in the integral of Eq. (12), we obtain from Eqs. (10), (12) and (13) the following integral equation*

$$\begin{aligned}\varphi(x)&=f(x)+(\lambda/4)(1+\eta)e^{-\chi/kT} \\ &\quad\times\int_{-\infty}^{+\infty}K(x-s)\varphi(s)ds; \quad x>1 \\ K(x-s)&=(x-s)^2-1; \quad -1\leqslant x-s\leqslant+1 \\ &=0 \qquad\quad ; \quad |x-s|>1 \\ f(x)&=x[e^{-\chi/kT}(1-\eta\lambda/3)-1] \\ \lambda&=3p_0/(1-p_0)=3(e^{w_0/kT}-1).\end{aligned} \tag{14}$$

The function $\varphi(x)$ must satisfy Eq. (14) for all values of x greater than unity, subject to the following auxiliary conditions, imposed by Eqs. (2) and (6),

$$\begin{gathered}\varphi(x)=-x; \quad 0\leqslant x\leqslant 1 \\ \int_1^\infty x\varphi(x)dx=\tfrac{1}{3}.\end{gathered} \tag{15}$$

Eq. (14) is exact, but of course contains two functions, $\eta(x)$ and $\chi(x)$ which we do not know. However, due to the fact that both η and χ must approach zero for large x, we obtain the following asymptotic form for Eq. (14), in which these functions appear only in the inhomogeneous part,

---

* The dipolar coordinates of a point in ω are r the distance from molecule 1 and r' the distance from the center of the sphere ω. The volume element is $(2\pi/R)r'rdr'dr$. The integral on the right-hand side of (12) becomes

$$(2\pi/R)\int_{R-a}^{R+a}\int_{R-r}^{a}g(r)rr'drdr'.$$

The integration over r' may be carried out at once with the result

$$-(\pi/R)\int_{R-a}^{R+a}[(R-r)^2-a^2]rg(r)dr.$$

If we introduce the new variables, $x=R/a$ and $s=r/a$ the integral may be written as

$$\begin{aligned}&+\omega_0-(\pi a^3/x)\int_{-\infty}^{+\infty}K(x-s)\varphi(s)ds \\ &K(x-s)=(x-s)^2-1; \quad -1\leqslant x-s\leqslant+1 \\ &\qquad\quad =0 \qquad\quad ; \quad |x-s|>1\end{aligned}$$

for all values of x.

$$\varphi(x)=f(x)+(\lambda/4)\int_{-\infty}^{+\infty}K(x-s)\varphi(s)ds$$

$$K(t)=t^2-1;\quad -1\leqslant t\leqslant +1 \qquad (16)$$
$$=0\quad ;\quad |t|>1$$
$$f(x)=-x[\lambda\eta(x)/3+\chi(x)/kT].$$

Under the tentative assumption that $\eta(x)$ and χ/kT remain small relative to unity for all values of x greater than unity, the asymptotic equation (16) may be substituted for the exact equation (14), and we may approximate $\varphi(x)$ by the solution of (16) satisfying the auxiliary conditions (15). In order to obtain the form of this approximate solution, an exact knowledge of the inhomogeneous part, $f(x)$, is fortunately unnecessary. It is only necessary to assume that $f(x)$ satisfies certain rather general conditions.

The function $\varphi(x)$ is defined by the physical problem only for $x\geqslant 0$ and $f(x)$ is defined only for $x>1$. Purely for mathematical purposes, it is convenient to extend the definitions of $\varphi(x)$ and $f(x)$ onto the entire real axis $-\infty<x<+\infty$. This may be done by defining $\varphi(-x)$ to be equal to $\varphi(x)$ and by choosing $f(x)$ in the interval $0\leqslant x\leqslant 1$ of such a form that $\varphi(x)$ satisfies simultaneously the integral equation (16) and the first of conditions (15). Assuming that it is possible to extend the definition of $f(x)$ in this manner, solutions of Eq. (16) for $x>1$ satisfying first of conditions (15) will also be solutions of Eq. (16) on the entire real axis.

$$\varphi(x)=f(x)+(\lambda/4)\int_{-\infty}^{+\infty}K(x-s)\varphi(s)ds;$$
$$-\infty<x<+\infty \qquad (17)$$
$$\varphi(-x)=\varphi(x);\quad f(-x)=f(x)$$
$$\varphi(x)=-x;\quad 0\leqslant x\leqslant 1.$$

Eq. (17) is not a standard type of integral equation, for example of the Volterra or Fredholm types. It is not equivalent to a differential equation with boundary conditions but rather to a complicated differential difference equation. However, if $f(x)$ and $K(t)$ are integrable, in the square, a formal solution may be obtained by the use of the theory of Fourier transforms.[8]

[8] See for example Titchmarsh, *Fourier Integrals and Transforms* (Oxford Press, 1936).

The Fourier transform $L(u)$ of $\varphi(x)$ may be obtained directly from the integral equation (17) by a simple change of variable.

$$L(u)=l(u)/F(iu)$$

$$L(u)=\frac{1}{(2\pi)^{\frac{1}{2}}}\int_{-\infty}^{+\infty}\varphi(x)e^{iux}dx;$$

$$l(u)=\frac{1}{(2\pi)^{\frac{1}{2}}}\int_{-\infty}^{+\infty}f(x)e^{iux}dx \qquad (18)$$

$$F(iu)=1-(\lambda/4)\int_{-\infty}^{+\infty}K(t)e^{iut}dt$$
$$=1+(\lambda/(iu)^3)[iu\cosh(iu)-\sinh(iu)].$$

The inverse of the transform $L(u)$ may be put in the form

$$\varphi(x)=\frac{1}{i(2\pi)^{\frac{1}{2}}}\int_{-i\infty}^{+i\infty}\frac{l(-iz)}{F(z)}e^{-zx}dz. \qquad (19)$$

If $l(iz)$ is an analytic function of z in the right half-plane and

$$\lim_{|z|\to\infty}\frac{zl(-iz)}{F(z)}e^{-z}=0, \qquad (20)$$

the integral (19) may be evaluated by the theory of residues in the form, for $x>1$

$$\varphi(x)=\sum_n A_n e^{-z_n x};\quad x>1$$
$$A_n=-(2\pi)^{\frac{1}{2}}l(-iz_n)/F'(z_n), \qquad (21)$$

where the sum extends over all zeros of $F(z)$ in the right half-plane. They satisfy the transcendental equation

$$1+(\lambda/z^3)[z\cosh z-\sinh z]=0. \qquad (22)$$

The form of (21) is slightly modified if there are multiple zeros, the constants A_n being replaced by polynomials in x of degree one less than the multiplicity. From Eqs. (13) and (21), we obtain the radial distribution function

$$g(x)-1=(1/x)\sum_n A_n e^{-z_n x}. \qquad (23)$$

The roots of Eq. (22) with positive real parts are all complex and of the form $\alpha_n\pm i\beta_n$. They may be ordered according to the magnitude of their real parts, α_n. Due to the rapid increase of

TABLE I.

$\lambda/10$	α	β
1.33	1.60	5.50
1.69	1.32	5.56
2.26	1.00	5.65
2.75	.72	5.70
3.48	.00	5.76

the real parts, the exponential damping of the terms in Eq. (23), relative to the first two corresponding to the roots $\alpha \pm i\beta$ with smallest real part, is very rapid. If the infinite series (23) is approximated by these two terms alone and written in real form, we have

$$g(x)-1=(A/x)e^{-\alpha x}\cos(\beta x+\delta), \qquad (24)$$

where the constants A and δ are related to the first two coefficients A_n in a simple manner. In Table I, the real and imaginary parts of the roots $\alpha \pm i\beta$ of Eq. (22) are tabulated for several values of λ. The calculation of the coefficients A_n in the Cauchy series (23) of course demands a knowledge of the inhomogeneous part $f(x)$ of Eq. (17). We do not have this knowledge, nor indeed, have we proved that an $f(x)$ exists with properties which we have ascribed to it and its transform. We shall not go into this question here but only remark that it involves some difficult mathematical points. Should our assumptions concerning $f(x)$ prove inconsistent with a solution of Eq. (17) exactly satisfying the first of conditions (15), the inconsistency could probably be removed by some modifications in the approximation of the exact equation (14) by the asymtotic equation (17).

If we approximate the complete Cauchy series (23) by Eq. (24), requiring it to satisfy the second of conditions (15) and the first condition (15) at the end point $x=1$ of the interval $0 \leqslant x \leqslant 1$ only, the constants A and δ are determined by the following equations and explicit knowledge of $f(x)$ can be dispensed with.

$$\begin{aligned} \tan\delta &= (1+3B)/3C \\ A &= -(1+\tan^2\delta)^{\frac{1}{2}} \\ B &= \frac{\alpha(\alpha^2+\beta^2)+\alpha^2-\beta^2}{(\alpha^2+\beta^2)^2}; \\ C &= \frac{\beta(\alpha^2+\beta^2)+2\alpha\beta}{(\alpha^2+\beta^2)^2}. \end{aligned} \qquad (25)$$

We remark that in approximating the radial distribution function by Eq. (24) subject to two conditions leading to Eq. (25), we are ignoring the direct influence of molecular attractive forces, since the temperature dependence of $f(x)$ of Eq. (16), is evidently neglected. However, the indirect effect of attractive forces on the work of formation of the cavity, w_0, is not neglected. Eqs. (24) and (25) thus provide us with an approximate solution of Eq. (16) which of course only incompletely satisfies the condition that $g(x)$ vanish for x less than or equal to unity. Eq. (25) does not of course determine $f(x)$ but fixes only two values of its Fourier transform. A single parameter, λ, enters into the radial distribution function. It is equal to $3(e^{w_0/kT}-1)$ where w_0 is the work required for the creation of a cavity at an arbitrary point in the fluid. We shall presently discuss an approximate method of relating w_0 to the density of the fluid. We remark here that w_0 is certainly a monotonic increasing function of the density and therefore λ is also a monotonic increasing function of the density. Radial distribution functions computed from Eqs. (24) and (25) for two values of λ are presented in Figs. 1 and 2. It will be seen that they have the characteristic form of distribution functions in actual liquids determined by x-ray scattering. The distribution is characterized by a series of peaks of rapidly diminishing height. The peaks occur at intervals of $2\pi/\beta$, corresponding to a distance slightly greater than the molecular diameter a. The calculations therefore provide at least a qualitative confirmation of our theory of a molecular distribution in liquids.

A rather peculiar thing occurs when λ exceeds the value 34.8. At this point the real part of the

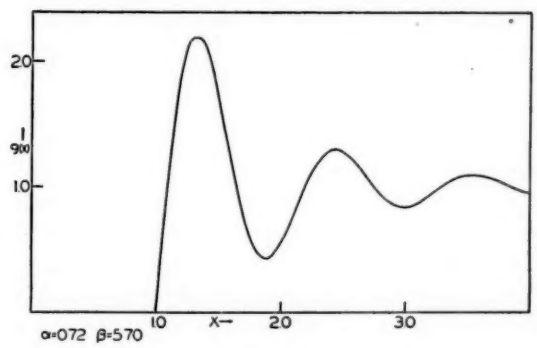

FIG. 1.

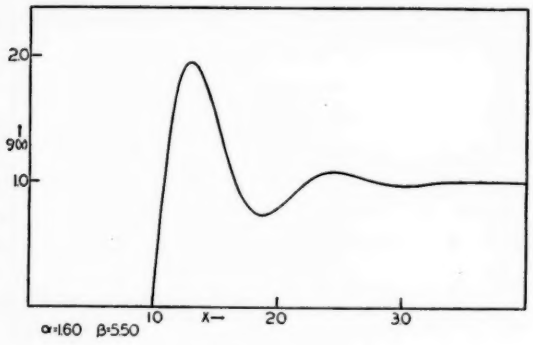

FIG. 2.

roots $\alpha \pm i\beta$ vanishes, the roots merge, and no solution of form (24) satisfying the normalization condition (6) exists. Since λ becomes infinite for a close-packed configuration of the molecules, this phenomenon occurs at a density less than the close-packed density. One would conclude, therefore, that a limiting density exists above which a liquid type of distribution and a liquid structure cannot exist. Above this density, only structures with crystalline long range order, would then be possible. This speculation should, however, be regarded as highly tentative, since the existence of a limiting value of λ may be a mathematical consequence of certain of our approximations and without physical significance.

At present no exact method is available for the calculation of the work, w_0, of creating a cavity ω in a liquid. We must therefore be content with a rather crude estimate of this quantity. If the cavity were of macroscopic size w_0 would be equal to the product of the surface tension γ and the area of the cavity. In the absence of a better method, we might try to estimate the work of formation of the molecular cavity in the same manner. However, we at once encounter a certain ambiguity in defining the size of the cavity from a macroscopic standpoint. The cavity ω is defined as a sphere of radius a from which the centers of all molecules are excluded. However, due to the finite size of the molecules, only a part of the cavity is empty, that is, contains no part of any molecule. The empty region is a smaller sphere of radius $a/2$. If we employ the macroscopic formula to calculate the work of formation, we must decide which sphere is to be regarded as the boundary of the cavity. Although it is somewhat arbitrary, the more reasonable choice seems to be the empty sphere of radius $a/2$. The work is then equal to $\pi a^2\gamma'$, where γ' is the effective surface tension of the molecular cavity. If ϑ is the ratio of γ' to γ, the macroscopic surface tension in a plane surface of the liquid, the formula for w_0 becomes

$$w_0 = \vartheta \pi a^2 \gamma. \tag{26}$$

At 85°K, the surface tension of liquid argon is about 13 dynes/cm. The diameter of the argon atom, obtained from the extrapolated density of the solid, is 3.72A. With ϑ equal to unity, Eq. (26) leads to a value of 4.8 for w_0/kT. Although this is of the right magnitude, it exceeds the critical value of w_0/kT of 2.53 above which solutions of the form (24) cease to exist. This is not particularly disturbing for the effective surface tension γ' is almost certainly less than γ. If ϑ is assigned a value of 0.485, w_0/kT reaches the critical value 2.53 at the freezing point. With this value of ϑ, we may use the following empirical formula for the calculation of the constant λ of Eq. (22)

$$\lambda = 3(e^{1.11\gamma a^2/T} - 1), \tag{27}$$

where the molecular diameter a is to be expressed in angstroms. For argon at its normal boiling point, Eq. (27) gives λ as 28.5. Thus, the radial distribution function of argon at its boiling point would, according to the present theory, be closely approximated by the curve of Fig. 1, which is calculated for a value of λ equal to 27.5.

Cavities play an important role in other theories of the liquid state, particularly in Eyring's theory of transport processes.[9] Eyring has shown that the energy of formation of a hole of molecular size is equal to the energy of vaporization of a molecule from the liquid. In the present theory we are interested in w_0, the work of formation of a hole, which is considerably less than the energy of formation due to an appreciable entropy term. On the basis of an approximate theory, in which fluctuations in

[9] Eyring, J. Chem. Phys. **4**, 283 (1936).

the energy of intermolecular attraction are neglected, it may be shown that,

$$w_0/kT=\Delta E_v/RT-\log\,(RT/pv_l), \qquad (28)$$

where ΔE_v is the molar energy of vaporization, v_l the molar volume, and p the vapor pressure of the liquid. The details of the basic theory will be given at a later time. The application of Eq. (28) to liquid argon at its normal boiling point gives for w_0/kT a value of 2.1 and for λ a value of 21.6. These values are of the same magnitude as those provided by the empirical equation (27). Since Eq. (28) is definitely of an approximate nature, it should not be disturbing if it occasionally predicts values of λ in excess of the critical value 34.8.

OCTOBER, 1939 JOURNAL OF CHEMICAL PHYSICS VOLUME 7

Specific Heat and Double Minimum Problem of NH_3

R. F. HAUPT* AND E. TELLER
George Washington University, Washington, D. C.

(Received June 3, 1939)

The specific heat of ammonia is calculated in the temperature range from 0°C to 150°C. The effect of the anharmonicity of the 948 cm^{-1} vibration on the specific heat is very noticeable. Small corrections due to the stretching of the molecule by centrifugal force and the interaction of vibration and rotation are taken into account. The results are in good agreement with measurements of Osborne, Stimson, Sligh and Cragoe.

THE specific heat of ammonia over the temperature range 0°C to 150°C has been observed at the National Bureau of Standards.[1] For a first comparison we have calculated values using the Planck-Einstein formula for the contribution of the vibrational degrees of freedom. The fundamental frequencies[2] used are (1) 3334 cm^{-1}, (2) 3219 cm^{-1}, (1) 948 cm^{-1} and (2) 1630 cm^{-1}; the numbers in parentheses give the degree of degeneracy.[3] Table I, column 2 gives these values, C_{vib}. The calculated values of C_p, column 3, were obtained from the relation

$$C_p=R+C_{tr}+C_{rot}+C_{vib}.$$

Assuming classical values for the contribution due to translation and rotation, the difference between columns 3 and 2 is, therefore, $4R$ which is 7.950 cal. $mole^{-1}$ deg^{-1}. The experimental values reduced to the ideal state, shown in column 4, have an average error estimated to be less than one-tenth of one percent. The differences between the experimental values and our calculated values, given in column 5, range from about 0.2 to 0.7 percent of the experimental values. A large deviation from the Planck-Einstein formula is not surprising because the 948 cm^{-1} vibration which takes place in a two-minima potential is known to have a large anharmonicity.

Dennison and Uhlenbeck[4] and others[5] have applied the two-minima problem to the ammonia molecule. This application is possible because the nitrogen atom has two equilibrium positions, one on each side of the plane formed by the hydrogen atoms. This causes a splitting of the zero and first energy levels into pairs having separations of 0.67 cm^{-1} and 32 cm^{-1}, respectively; the higher energy levels should also be double but their separation is so great that their grouping in pairs is no longer apparent.

Manning, using a double minimum potential function based on the observed separation of these first two pairs of this series, and other data

* This communication is based on a thesis submitted by R. F. Haupt in 1938 in partial fulfillment of requirements for the degree of Master of Arts in Physics at the George Washington University, Washington, D. C.

[1] N. S. Osborne, H. F. Stimson, T. S. Sligh, Jr. and C. S. Cragoe, Nat. Bur. Stand. Sci. Pap. **20**, 65 (1925), No. 501.

[2] H. Sponer, *Molekulspektren* (Berlin, 1935); N. Wright and H. M. Randall, Phys. Rev. **44**, 391 (1933).

[3] W. M. D. Bryant has also calculated values, Ind. and Eng. Chem. **25**, 22 (1933), using frequencies by Dennison, Phil. Mag. [7] **1**, 195 (1926).

[4] D. M. Dennison and G. E. Uhlenbeck, Phys. Rev. **41**, 313 (1932).

[5] M. F. Manning, J. Chem. Phys. **3**, 136 (1935); F. T. Wall and G. Glockler, J. Chem. Phys. **5**, 314 (1937).

TABLE I. *Specific heat of* NH_3 *in cal. mole*$^{-1}$ *deg.*$^{-1}$

1	2	3	4	5	6	7	8	9	10	11	12
TEMP. °C	C_{VIB}	C_1 C_p(CALC.)*	C_p(OBS.)†	$(O-C_1)$	ANHARMONIC TERM	C_2	$(O-C_2)$	CENTR. TERM	INT. TERM	C_3	$(O-C_3)$
0	0.403	8.353	8.374	+0.021	0.010	8.363	+0.011	0.016	−0.004	8.375	−0.001
35	.600	8.550	8.583	.033	.021	8.571	.012	.018	− .007	8.582	+ .001
55	.726	8.676	8.715	.039	.030	8.706	.009	.019	− .009	8.716	− .001
75	.859	8.809	8.854	.045	.038	8.847	.007	.020	− .011	8.856	− .002
115	1.140	9.090	9.149	.059	.057	9.147	+ .002	.022	− .018	9.151	− .002
150	1.400	9.350	9.421	+ .071	.071	9.421	.000	.024	− .025	9.420	+ .001

* The value of the gas constant, R, was taken as 1.9875 cal. mole^{-1} deg.$^{-1}$
† The fundamental unit of these measurements was the international joule. The observed values are based on the following constants: $T_0=273.1$, mole wt. of $NH_3=17.031$ g., and 4.183 int. $j.=1$ calorie.

of the spectra, calculated the following anharmonic energy levels: 1610 cm^{-1}, 1870 cm^{-1}, 2360 cm^{-1} and 2840 cm^{-1}. These energy levels lie above the potential hump so that the nitrogen atom may pass according to classical mechanics between its two equilibrium positions. We recalculated the contribution to the specific heat arising from this mode of vibration using the following series of anharmonic levels instead of a harmonic series with a spacing of 948 cm^{-1}: zero, the mean of the fundamental pair of levels; 948 cm^{-1}, the mean of the energy levels corresponding to the pair of levels in the first excited state; the energy levels calculated by Manning and an additional level, 3300 cm^{-1}. The latter assumed level affects the contribution to the specific heat only at the highest temperature, 150°C, and its exact placement is not important for these calculations. In the sum of energy states of this series,

$$Q=\sum_n p_n e^{-E_n/kT},$$

to the zero and the first energy levels weights of two have been assigned, $(p_0=p_1=2)$, and to the other energy levels weights of one, $(p_2=p_3=\cdots=1)$. The vibrational specific heat contribution is given by the relation

$$C_{\text{vib}}=RT^2\left[\frac{d^2Q/dT^2}{Q}-\left(\frac{dQ/dT}{Q}\right)^2\right].$$

Column 6 gives the increase in the calculated specific heat of this series due to the use of these anharmonic energy levels in place of the harmonic. Column 7 gives the calculated values of the specific heat and column 8 lists the differences between the observed values and these latter calculated values. These differences are within the experimental errors of the observations but they indicate a trend. It seemed reasonable to explain this trend by taking into account the effects of centrifugal force and interaction of vibration and rotation.

Correction terms to the specific heat due to the centrifugal distortion of the molecule have been calculated for ammonia by Wilson.[6] The centrifugal distortion increases the calculated values of the specific heat by the terms given in column 9.

In considering the interaction of vibration and rotation, the two normal vibrations of high frequencies can be disregarded for our present purpose because they are not sufficiently excited to have any appreciable effect. The 1630 cm^{-1} normal vibration can also be eliminated because it is a symmetrical vibration and, therefore, in first approximation, does not change the moments of inertia[7] of the molecule. The 948 cm^{-1} normal vibration will have an effect on the shape of the molecule, particularly in the 1610-cm^{-1} energy state. In this energy state the nitrogen atom is just passing over the potential hump between its two equilibrium positions. It is found with greatest probability in the region of the potential hump. Thus the molecule is flattened and A, the moment of inertia around an axis parallel to the plane of the H atoms, is changed. If we assume for sake of simplicity that all atoms move on straight lines, the moment of inertia, C, about the axis of symmetry remains unchanged. The rotational sum of states is, at high temperatures, proportional to $A\sqrt{C}$. The

[6] E. B. Wilson, J. Chem. Phys. **4**, 526 (1936).
[7] $A=2.782\times10^{-40}$ g cm^2, $C=4.33\times10^{-40}$ g cm^2, reference 2.

effect of interaction of vibration and rotation may be taken into account by multiplying the weight of each vibrational state with the rotational sum of states. Thus weight factors $\bar{A}\sqrt{\bar{C}}$ will appear in Q where $\bar{A}$ and $\bar{C}$ are values of the moments of inertia averaged over the vibration. The other members of the series will also have moments of inertia different from the moment of inertia in the equilibrium position. Again assuming motion on straight lines for all atoms we find that in the 948-cm^{-1} level the moments of inertia are somewhat smaller, in the levels higher than 1610 cm^{-1} they may be greater than in equilibrium. As a rough approximation we shall multiply by the factor $A\sqrt{C}$ for all levels of the 948 cm^{-1} vibration, where A and C are the values in the equilibrium position. For the 1610-cm^{-1} level we still assume $\bar{C}=C$, but for $\bar{A}$ we shall substitute the value $\frac{1}{2}C$ as would be obtained for a flat molecule. Thus the weight factor for the 1610-cm^{-1} level will be $\frac{1}{2}C\sqrt{C}=0.78A\sqrt{C}$. The terms showing the effect of interaction of vibration and rotation are listed in column 10. The calculated values, given in column 11, include both the terms for centrifugal force and interaction of vibration and rotation. The differences between the observed and these final calculated values are given in column 12.

The remaining differences between experimental and calculated values fall far within experimental error. In fact the agreement is better than could have been expected from the approximate nature of our calculation. In particular the term arising from the interaction of vibration and rotation has been estimated in a very rough way. Its magnitude and perhaps even its sign is open to question. Comparison of experiment and theory shows, however, clearly that the presence of two minima in NH_3 has a considerable effect on specific heats. Measurements of the specific heats of ND_3 would be highly desirable since such measurements would furnish a further check on the theory of vibrations of the ammonia molecule.

OCTOBER, 1939 JOURNAL OF CHEMICAL PHYSICS VOLUME 7

Dissociation Treatment of Condensing Systems. II*

WILLIAM BAND
Yenching University, Peiping, China

(Received June 6, 1939)

In a previous paper under the above title, in future referred to as Part I, it was shown how the theory of dissociating assemblies could be applied to an example containing only one component type of molecule which can form clusters of any size. The results were claimed as equivalent with those of Mayer (see reference 3, *a* and *b*). In a private communication Dr. Mayer has pointed out to the writer that this claim is only approximately correct, because the clusters were treated as of negligible size, excluded volumes being ignored. It is therefore necessary to regard Part I as giving a "perfect gas analogy" for the theory of the saturated vapor pressure curves at temperatures well below the critical value.

The present paper develops the more accurate theory by taking into account the excluded volumes and, besides the *s-v-p* curves, also presents a complete set of equations for the isothermals of the gas and vapor right through the critical temperature.

ASSUMPTIONS

As in Part I,[1] it will be assumed that the interaction energy between any pair of molecules drops off discontinuously at a definite distance between centers. Each cluster will be assumed approximately spherical in form. With a cluster of type s and a cluster of type r will be associated a similar distance σ_{rs} such that when their centers are separated by more than σ_{rs}, they are counted as separate clusters. This distance is assumed to depend only upon the numbers r and s in the following manner:

$$\sigma_{rs}=\tfrac{1}{2}(\sigma r^{\frac{1}{3}}+\sigma s^{\frac{1}{3}}). \quad (1)$$

* Contribution from the Physics Department, Yenching University.

[1] W. Band, "Dissociation Treatment of Condensing Systems," J. Chem. Phys. **7**, 324 (1939).

The assumption that σ is independent of r and s is equivalent with the assumption that all clusters are packed with equal closeness.

The results given by Fowler,[2] §8.6, for a dissociating assembly whose molecules have finite size, which will be used here, are as follows: The partition function for a cluster of type s will be

$$f_s(T)=V(1-\beta_s) \times(2\pi mskT)^{\frac{3}{2}}h^{-3}\exp(-W_s/kT), \quad (2)$$

where W_s is the mean energy per cluster to be treated in the same way as in Part I, Eq. (10); and where

$$\beta_s=(4\pi/3V)\sum_r N_r\sigma_{rs}^3 \quad (3)$$

with N_r as the number of clusters of type r. The law of mass action remains in the form

$$N_s/(N_1)^s=f_s(T)/\{f_1(T)\}^s. \quad (4)$$

The pressure exerted by the assembly is now, Fowler, Eq. (775),

$$PV=kT\sum_s N_s/(1-\beta_s), \quad (5)$$

which equation is true only so long as all β_s are less than unity.

Saturated Vapor Pressure Curves

In terms of the previous notation:

$$\mu_s=N_s/N, \quad \text{and} \quad \lambda=\sum_s{}'s\mu_s, \quad (6)$$

the law of mass action (4), using (2), becomes

$$\frac{\mu_s}{1-\lambda}=s^{\frac{3}{2}}e^{-\chi/kT}\left\{\frac{1-\beta_s}{1-\beta_1}\right\} \times\left[\frac{h^3e^{-W/kT}(1-\lambda)}{(2\pi mkT)^{\frac{3}{2}}V(1-\beta_1)/N}\right]^{(s-1)}. \quad (7)$$

The condition for saturation is that the square bracket shall become unity:

$$V^*(1-\beta_1^*)/N=\rho(1-\lambda^*), \quad (8)$$

where

$$\rho=(2\pi mkT)^{-\frac{3}{2}}h^3e^{-W/kT}. \quad (9)$$

Under this condition Eq. (7) gives

$$\mu_s^*/(1-\lambda^*)=s^{\frac{3}{2}}e^{-\chi/kT}(1-\beta_s^*)/(1-\beta_1^*). \quad (10)$$

[2] Fowler, *Statistical Mechanics*, 2nd edition (Camb. Univ. Press, 1936).

From (6) and (10) we have

$$(1-\lambda^*)=1/(1+\sigma^*), \quad (11)$$

where

$$\sigma^*=\sum_s{}'s^{5/2}e^{-\chi/kT}(1-\beta_s^*)/(1-\beta_1^*). \quad (12)$$

Then from (10) we derive

$$\mu_s^*/(1-\beta_s^*)=s^{\frac{3}{2}}e^{-\chi/kT}/(1+\sigma^*)(1-\beta_1^*). \quad (13)$$

Since $\chi(1, T)=0$, [see Part I, Eq. (12)], Eq. (5) now gives for the saturated vapor:

$$P^*V^*/NkT=(1+\phi_0)/(1+\sigma^*)(1-\beta_1^*), \quad (14)$$

where

$$\phi_0=\sum_s{}'s^{\frac{3}{2}}e^{-\chi/kT}. \quad (15)$$

The process of condensation will be complete when $\lambda=1$, which, in (8), requires that $\beta_1=1$. The value of V for which this is true will be written as V_l, so that Eqs. (3) and (1) lead to

$$V_l=\beta_0(8+\phi_3+3\phi_2+3\phi_1+\phi_0)/(1+\phi_3). \quad (16)$$

Here we have written

$$\phi_r=\sum_s{}'s^{(2r+9)/6}e^{-\chi/kT}, \quad (17)$$

$$\beta_0=(2/3)\pi N\sigma^3 \quad (18)$$

and neglected the presence of the β_s in the expression (13) for $\mu_s=N_s/N$. This neglect is justifiable because V_l is of the nature of a small correction term itself. From (8) it now follows that

$$V^*-V_l=N\rho/(1+\sigma^*).$$

When $\beta_s\ll 1$, all values of s, $\sigma^*\to\phi_3$, so that

$$V^*\to N\rho/(1+\phi_3). \quad (19)$$

Writing

$$\phi=8+\phi_3+3\phi_2+3\phi_1+\phi_0, \quad (20)$$

Eqs. (19) and (16) give

$$V^*-V_l=(N\rho-\beta_0\phi)/(1+\phi_3). \quad (21)$$

This equation is strictly true only so long as $V^*\gg V_l$, but it is possible to extend it formally right up to the point where $V^*=V_l$, giving, formally, a critical temperature where

$$N\rho=\beta_0\phi. \quad (22)$$

Putting (21) into (14), the latter becomes

$$P^*(V^*-V_l)/NkT =(1-\beta_0\phi/N\rho)(1+\phi_0)/(1+\phi_3) \quad (23)$$

which, again formally, can be used right up to the critical temperature given by (22).

The Eq. (22) determines a critical temperature in terms of the three physical parameters: the range of the molecular field, σ, the surface energy per molecule in a cluster, and the volume energy per molecule in a cluster. The volume V_l corresponds with the volume of the liquid phase, but does not pretend to be an accurate expression for it. Presumably the best way to apply the equations is to use (V^*-V_l) as the observed volume change upon condensation, substitute it as such into (21) or (23), and adjust the parameters to give the best fit with the recorded variations with T and P.

Equations for Imperfect Gas

Write

$$\phi_{sr}^* = s^{(2r+9)/6}e^{-\chi/kT}(1-\beta_s), \tag{24}$$

$$v = V/N, \tag{25}$$

$$Z = (\rho/v)(1-\lambda)/(1-\beta_1). \tag{26}$$

Eq. (7) becomes

$$\mu_s = \phi_{s0}^*(v/\rho)Z^s \tag{27}$$

and the first of conditions (6)† leads from this to

$$1 = (v/\rho)(1-\beta_1)Z + \sum_s{}'\phi_{s3}^* Z^s (v/\rho) \tag{28}$$

or

$$(\rho/v) = Z(1-\beta/v) + \sum_s{}'\phi_{s3}^* Z^s, \tag{29}$$

where

$$\beta = V_l/N. \tag{30}$$

Neglecting the factors $(1-\beta_s)$ in the ϕ_{s3}^* terms beyond $s=1$, the quantity Z can be expanded in a power series:

$$Z = a_1/v + a_2/v^2 + a_3/v^3 + \cdots, \tag{31}$$

whose coefficients are determined by substitution in (29):

$$a_1 = \rho, \quad a_2 = \beta\rho - \phi_{23}\rho^2$$

$$a_3 = \rho\{\beta^2 - 3\rho\beta\phi_{23} + \rho^2(2\phi_{23}^2 - \phi_{33})\}.‡ \tag{32}$$

Putting this approximation for Z into (27), and remembering the factor $(1-\beta_s)$ in φ_{s0}^*, we obtain:

$$\sum_s{}'\mu_s/(1-\beta_s) = (\rho\phi_{20})/v + \rho^2\phi_{20}\{2(\beta/\rho - \phi_{23}) + \phi_{30}\}/v^2 + \cdots. \tag{33}$$

Also, from (26),

$$\mu_1 = 1-\lambda = (v/\rho)(1-\beta/v)Z = 1-(\rho\phi_{23})/v - \rho^2\{2\phi_{23}(\beta/\rho - \phi_{23}) + \phi_{33}\}/v^2 - \cdots. \tag{34}$$

Finally, the pressure equation (5) can be written as

$$P(v-\beta) = kT\{1-\lambda+\mu(1-\beta/v)\} = kT(1-A/v-B/v^2\cdots), \tag{35}$$

where, by comparison with (33) and (34), the coefficients are:

$$A = \rho(\phi_{23}-\phi_{20}), \tag{36}$$

$$B = 2A(\beta-\rho\phi_{23}) + \rho\beta\phi_{20} + \rho^2(\phi_{33}-\phi_{30}). \tag{37}$$

etc. etc.

For comparison with classical equations, it is sufficient to retain only the term in $1/v$, and write

$$P(V-V_l) = NkT - a/V, \tag{38}$$

where, referring to (24) and (9), (36) leads to

$$a = N^2h^3(\pi^3m^3k)^{-\frac{1}{2}}T^{-\frac{1}{2}}e^{-(W+\chi_2)/kT}. \tag{39}$$

The equation of Dieterici is equivalent to the form (38) with the value $a = a'T^{-\frac{1}{2}}$ (see Fowler, Eq. (825)) which makes an interesting comparison with (39). The order of magnitude of (39) is correct, and it depends upon T in a promising manner. Its extension down to temperatures below the critical value into the true vapor states is theoretically justifiable, because all orders of clustering have been accounted for. The only theoretical limitation is that the condensed phase shall not be present; the onset of this restriction is determined by the equations of the previous section.

Phenomena at the Critical Point

The presence of considerable proportions of very large clusters in the assembly under conditions close to the critical point, gives rise to a dependence upon gravitational potential which

† $\Sigma_s s\mu_s = 1$.

‡ The asterisk omitted to indicate omission of $(1-\beta_s)$ from ϕ_{sr}^*.

up to now has been entirely neglected, both in the present work and in that of Mayer.[3]

At a point where the gravitational potential is gz, the partition function for a cluster of type s will have an extra factor $\exp(-msgz/kT)$. This factor will, through Eq. (7) affect the concentration of clusters of this type in the same ratio:

$$\mu_s(z)=\mu_s(0)\cdot\exp(-msgz/kT)$$

and
$$\partial\mu_s(z)/\partial z=-(msg/kT)\mu_s(z). \tag{40}$$

With m of order 10^{-23} there will be appreciable gradient of concentration per unit concentration only for clusters of type s of order 10^7 or larger. In an assembly containing a condensed phase, at a temperature well below the critical value, the mean concentrations are all very small except for small s, because even the liquid phase counts only for a single cluster. The transition from vapor to liquid is exceedingly sharp, and at no time are the concentrations of intermediate clusters appreciable. However as the temperature approaches the critical value, the transition becomes less sharp. At temperatures slightly below the critical value, under conditions which include the condensed phase, large clusters of type 10^7 or larger can be expected to occur in appreciable proportions. According to (40) there will then be an appreciable gradient of concentration among these clusters, physically observable as a blurring of the meniscus between the two phases.

This blurring of the meniscus while there still remains a difference in density between the two phases is well known, and has previously been interpreted by Harrison and Mayer[4] in an essentially different manner from that suggested above. While ignoring the above affect of gravity in causing a "settling down" of larger clusters into the lower part of the container, Harrison and Mayer projected their saturated vapor equations up towards the critical temperature. They found that surface tension should disappear at a temperature somewhat below the critical temperature derived by projecting the gas equations down to the latter point. Below the upper critical temperature the gas isotherms are parallel to the V axis for finite ranges.

However it should be pointed out that their partition functions were constructed on the assumption that all clusters are uniformly free to move about throughout the volume V of the whole assembly, when in fact the condensed phase, and all fairly large clusters, are effectively confined by the gravitational field to a comparatively small part of V. The equations developed on this assumption can therefore apply with precision only when there exists a negligible proportion of molecules in large clusters; their projection up to the critical point is not justified, and the results regarding the disappearance of surface tension would appear to be of doubtful validity.[5]

According to our present argument the usually observed critical temperature, at which the meniscus appears to vanish, is somewhat too low; the true critical point will be where the difference in density vanishes. The blurring of the meniscus could theoretically be made to occur simultaneously with the true critical conditions only by making the observations in an arrangement which neutralized the gravitational field.

Conclusions

The present work does not attempt to give an exact theory of the behavior of condensing systems, but claims only to reach similar precision, in the saturated vapor range, as did the Ursell theory in the imperfect gas range. It does, however, claim to give a more exact theory of the imperfect gas and the unsaturated vapor than the Ursell theory.

The theory of Ursell, considered as the basis for a van der Waals or Dieterici equation, has been extended down to critical temperature isothermals. This extension is merely formal in essence, because, as we now know, at these temperatures large clusters play a significant part, but were entirely omitted by the Ursell argument.

[3] "Statistical Mechanics of Condensing Systems," (a) Part I, J. E. Mayer, J. Chem. Phys. **5**, 67 (1937); (b) Part II, J. E. Mayer and P. G. Ackermann, *ibid.* **5**, 74 (1937); (c) Part III, J. E. Mayer and S. F. Harrison, *ibid.* **6**, 87 (1938).

[4] S. F. Harrison and J. E. Mayer, "Statistical Mechanics of Condensing Systems, IV," J. Chem. Phys. **6**, 100–104 (1938).

[5] See also some remarks by Born and Fuchs, "Statistical Mechanics of Condensing Systems," Proc. Roy. Soc. **166A**, 391–414 (1938).

The present equations permit a theoretically sound extension down below the critical temperature into the unsaturated vapor isothermals, so long as the volume is large compared with that of the liquid phase of the given assembly. It also permits an extension up to the critical temperature of the saturated vapor pressure curves, which is, however, merely a formal extension of equations which have been proved only under the limitation that the condensed phase shall contain a negligible proportion of the molecules of the assembly.

These restrictions are inherent in the assumptions made at the beginning of the work, and there seems no way of removing them if the dissociation method is to retain its advantage of simplicity over that of the more completely rigorous treatment of Mayer.[3a, b]

OCTOBER, 1939 JOURNAL OF CHEMICAL PHYSICS VOLUME 7

Changes of Phase and Transformations of Higher Order in Monolayers

D. G. DERVICHIAN*
Department of Colloid Science, The University, Cambridge, England
(Received June 7, 1939)

The gaseous, liquid, mesomorphous and solid states in monolayers are defined and their close connection with the corresponding states in three dimensions rigorously established. This involves a new treatment of the two-dimensional liquid and of its transformation to the mesomorphous state. The properties of the three-dimensional vitreous state of fatty substances are shown to be particularly important in connection with the behavior of monolayers. The different critical and transformation temperatures are also defined and their significance explained. From this is derived a systematic classification of the different types of isotherms observed. By determining the variations of the compressibility, viscosity and apparent dipole moment with change of area, higher order transformations are detected in monolayers. These transformations occur at the same areas as those at which ordinary phase transformations occur at lower temperatures.

THE aim of this paper is to establish a general correlation between all the transformation phenomena observed in surface films and to show that they correspond closely to the transformations found with the same substances in bulk. This enables us to set up a rigorously defined nomenclature without the implication of any vaguely justified assumption. *Critical temperatures* and a *triple point* will be defined thus permitting us to arrange the different states in which a film can exist, when its temperature and pressure are fixed, in a systematic classification. For this purpose some new experimental data are included together with a new interpretation of some of the published experiments.†

Both from the theoretical and experimental point of view, transformations in two dimensions are more readily studied than in three dimensions. In two dimensions, by relatively simple means, pressures which in three dimensions would correspond to some hundreds of atmospheres or alternatively to a few tenths of a millimeter of mercury can be attained. Likewise, molecular packing, molecular interaction, questions of order and disorder, are much simpler in a two-dimensional system than in a three-dimensional.

Besides the ordinary phase changes, transformations of a higher order are found in monolayers. These are detected by sharp discontinuities occurring simultaneously in three different physical properties: compressibility, apparent dipole moment and especially the surface viscosity. Accurate determination of variations in the compressibility and in the apparent dipole moment was made possible by the use of a method of automatic and continuous registration of both pressure and potential isotherms. A considerable improvement could thus be obtained

* Rockefeller Foundation Fellow 1938–39.

† References will be given only for typical experiments. For a general survey and bibliography see: E. K. Rideal, *Surface Chemistry* and N. K. Adam, *The Physics and Chemistry of Surfaces.*

in establishing the usual phase change discontinuities. The automatic registering apparatus has been previously described.[1] Contrary to what might be thought at first sight, there is less danger of recording metastable states by this method than by the ordinary methods. In the ordinary method, when the barrier is moved from one point to another, the film is compressed relatively quickly; while in the recording apparatus, the movement is continuous but slow enough to maintain the film continuously in equilibrium. On the other hand, the determination of the pressure at each point does not involve appreciable periods of time during which the film may dissolve or collapse. Records have been made at different speeds and it has been found that, provided the speed be not too great, the curves are identical.

Compressibility

Since every isotherm is recorded with the same film, the relative error in the surface concentration is kept constant all along the curve. This gives a much sharper determination of the shape of the curve (i.e., the slope at every point) and shows up any singularities. To plot the variations of the compressibility against the area per molecule A, values of $dA/d\pi$ are determined[2] and inserted in the expression:

$$K = -dA/Ad\pi.$$

The sharpness of the registered line permits us to make a graphical evaluation of the tangent at different points to within less than one degree. For angles between 30° and 60°, this gives an error of less than 5 percent. To keep between these limits the sensitivity of the recording instrument is adjusted to the part of the isotherm under examination and different initial concentrations are employed so that the curve is more or less tilted on the axis.

Apparent Dipole Moment

The same remarks about the sharpness of the curve are also applicable to registered isotherm of the surface potentials: singularities can be detected on the ΔV curve. It is well known[3] that values of the dipole moment $\mu = 4\pi n$, calculated from the potential fall ΔV, are very different from those found by other methods. We consider it here as an *apparent* moment corresponding to a *fictive* Helmholtz double layer which is not formed solely by the whole of the dipole moments of the film.

While ΔV increases generally with the surface concentration, μ is not necessarily constant and its variation shows transition points. The detection of these transition points is one of the aims of the present work.

Surface Viscosity

It has been previously shown[4] that the flow of a monolayer through a narrow canal reveals a true viscosity of the film which varies with its nature and state. In this paper variations of this viscosity at different surface concentrations (i.e., different pressures) of the same film are described. The film flows under a constant and accurately measured difference of pressure of less than 0.5 dyne/cm and the apparatus is so devised that both the high and low pressures are kept constant during the flow.[5] The determination of the viscosity in the layer, from the rate of flow implies some assumptions which are far from being unquestionable. We are here more interested in singularities in variations than in absolute values, so only the actually measured *rates of flow* are quoted. Moreover, for all determinations, the same canal has been used, thus making all the results comparable. The results are reproducible to within 2 to 3 percent.

Thermodynamical Definition of Transformations of Different Order

The conception of transformations of different orders, emphasized by P. Ehrenfest,[6] generalizes

[1] D. G. Dervichian, J. de phys. et rad. [7] **6**, 221 and 427 (1935); Ann. de physique [11] **8**, 361 (1937).

[2] The notation π for surface pressure will be used following E. A. Guggenheim (*Thermodynamics*, p. 179). The ordinarily used F notation may bring confusion with that of the free energy. Moreover, it stands as an abbreviation of "force," when actually, as is well known, it represents a two-dimensional pressure.

[3] See remarks by Schulman and Rideal, Proc. Roy. Soc. **A130**, 259 (1931) and by A. Frumkin, Zeits. f. physik. Chemie **109**, 34 (1924).

[4] Dervichian and Joly, Comptes rendus **204**, 1318 (1937); M. Joly, J. de phys. [7] **8**, 471 (1937); Derivichian and Joly, in press and Nature **141**, 975 (1938).

[5] All the viscosity work was carried out by M. Joly. For full details see an article to be published in this journal.

[6] P. Ehrenfest, Proc. K. Akad. Amsterdam **36**, 115 (1933).

the definition of such points as λ or Curie points. The various transformation points are considered as corresponding to discontinuities of the derivatives of different order of a thermodynamical function. For the surface phenomena, here considered, we have to introduce, in the definition of this function, a term corresponding to the surface energy. If γ is the surface tension of the surface covered by a film and γ_0 that of the clean surface, the work done by an infinitesimal displacement of the barrier, which changes each of the two areas by dA and $-dA$, respectively, is

$$dw^s = (\gamma - \gamma_0)dA. \tag{1}$$

Introducing the surface pressure, $\pi = \gamma_0 - \gamma$, the relation (1) takes the form

$$dw^s = -\pi dA \tag{1'}$$

similar to the work in the bulk

$$dw^v = -PdV. \tag{2}$$

If S represents the total entropy (surface and bulk) of the system, the variation of the total energy is defined by:

$$dE = TdS - PdV - \pi dA. \tag{3}$$

When T, P and π are considered as the independent variables, we adopt, as thermodynamical function, the thermodynamic potential G of Gibbs, in which we introduce a term corresponding to the surface energy, analogous to the term PV:

$$G = F + PV + \pi A,$$

where F is the free energy, $F = E - TS$. This gives with (3):

$$G = E - TS + PV + \pi A$$

and

$$dG = -SdT + VdP + Ad\pi, \tag{4}$$

which enables us to calculate the successive partial derivatives:

$$(\partial G/\partial \pi)_{P,T} = A, \tag{5}$$

$$(\partial^2 G/\partial \pi^2)_{P,T} = \partial A/\partial \pi. \tag{6}$$

An ordinary change of state will be called a *transformation of the first order*, since it is characterized by a discontinuity in the area A and consequently corresponds to a discontinuity in the first derivative of G. Likewise a transformation in which A does not undergo any sudden variation, but in which the compressibility

$$K = -\partial A/A\partial \pi \tag{7}$$

shows a discontinuity, will be a *transformation of the second order*, since according to (7) and (6) it corresponds to a discontinuity in the second derivative of G. In the same way, a transformation of the third order will be characterized by a discontinuity in the third derivative of G (with the exclusion of the two preceding derivatives), that is in $\partial K/\partial \pi$.[7]

Experimental material

Typical substances studied in monolayers are the long chain acids and alcohols or their derivatives: esters, triglycerides, amines, amides, etc. It is well known that for members of a homologous series, the melting point (and, in general, the various other transformation temperatures) increase with the chain length. As will be seen, the same variation is found in the changes of state of the same substances spread in monolayers. Hence, to study the different states in monolayers, we may either examine the same substance over a large range of temperature, or else examine the different members of the series at the same temperature. But the available temperature range is limited both by the freezing point of the substrate and by the fact that with present technique it is impossible to make precise measurements above 45–50°. So, by examining the various members of the series throughout that range, we obtain overlapping results which enable us to follow all the successive changes of state that a substance in monolayer form can undergo: from melting of the solid up to and beyond the critical temperature of liquefaction. We gain supplementary information by examining at a given temperature the changes of state that are produced by changes of the surface pressure.

The different states in films

H. Devaux was one of the first to point out that, even when they are one molecule thick,

[7] Likewise, discontinuities in one or other of the successive partial derivatives:

$(\partial G/\partial T)_{P,\pi} = -S = -q/T$ and $(\partial^2 G/\partial T^2)_{P,\pi} = C_P/T$

correspond, the first, to an ordinary transformation by change of temperature and the second, to a real Curie point.

solids and liquids maintain their mechanical properties. He thought that by varying the temperature over sufficient range, a given substance, spread in a monolayer, would show all the different states of matter. This is now well established. Monolayers may exist in the solid, mesomorphous, liquid and gaseous states.

The existence of gaseous films was predicted by I. Langmuir and the first systematic investigation on this state made by Adam and Jessop.[8] Different suggestions have been given[9] to explain the phase which is generally known as "liquid expanded." It will be shown that this is the corresponding state of the ordinary three-dimensional liquid. An intermediate state between the liquid and the solid, has been called "liquid condensed" by Adam. It was pointed out by Lyons and Rideal,[10] that this was the two-dimensional analog of the liquid crystal or smectic state of bulk matter. New evidence will be given to confirm this point of view. The word "mesomorphous," which implies no definite structure, will be used to designated this state of films. Before reaching the liquid state, the mesomorphous film undergoes a transformation which was first investigated by H. Labrouste.[11] It will be shown that this behavior is similar to that in three dimensions in the transition from anisotropic liquid crystal to the isotropic liquid state. The state of the film during this "Labrouste's transformation" will be termed "expanded mesomorphous." In the solid state, the *A*, *B*, *C*, crystalline varieties of the fatty acids, and the stable and unstable forms of triglycerides —known in three dimensions—are found in monolayers.[12] They give us some information on the probable arrangement of the molecules on the surface.

Existence of different points of transformation of higher order

It will be seen that *areas corresponding to ordinary phase changes, are found as points of discontinuity of higher order in those phases which exist at higher temperatures*. Thus 20.5A² being the sublimation point in the solid state is found as a point of second order in the mesomorphous state. It is interesting to note that the triple point 38–39A² persists in all liquid and highly compressed gaseous films in the form of discontinuities in the compressibility, viscosity and moment when that area per chain is reached. A list of these characteristic areas is given at the end of the paper.

The different critical and transformation temperatures

T_{cl}.—In their study of the transition from the gaseous to the condensed states, Adam and Jessop[8] considered critical phenomena analogous to the three dimensional. We shall define for every substance a *critical temperature of liquefaction* T_{cl} above which the film does not undergo liquefaction by compression.

T_{cc}.—Adam and Jessop[9] have established a whole series of isotherms for the transition by compression from the liquid to the condensed (expanded mesomorphous) state. Above a certain temperature, this transition does not occur and the film remains liquid up to the collapse pressure. We shall term this point the *critical temperature of crystallization*: T_{cc}.

T_s.—The solid state is well defined. The area per chain, under the pressure of the saturated vapor, remains constant and equal to *ca.* 20.5A² up to a temperature T_s. Then the mesomorphous state appears with an area of *ca.* 23.5A² per chain. This is invariable up to another temperature.

T_m.—Where the expansion of the mesomor-

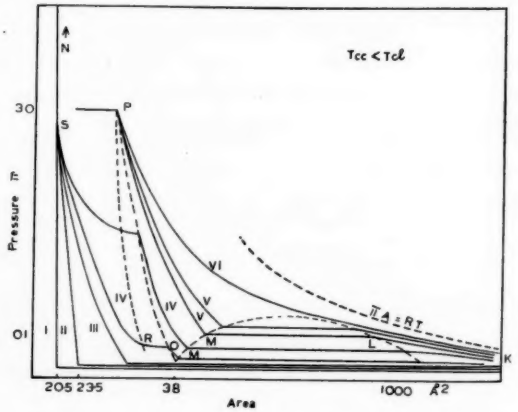

FIG. 1. Possible forms of isotherms when $T_{cc} < T_{cl}$.

[8] Adam and Jessop, Proc. Roy. Soc. **A110**, 423 (1926).
[9] Adam and Jessop, Proc. Roy. Soc. **A112**, 364 (1926); D. G. Dervichian, Comptes rendus **194**, 2129 (1932); I. Langmuir, J. Chem. Phys. **1**, 756 (1933).
[10] Lyons and Rideal, Proc. Camb. Phil. Soc. **26**, 419 (1930).
[11] H. Labrouste, Ann. de Phys. [9] **14**, 164 (1920).
[12] D. G. Dervichian, Comptes rendus **199**, 347 (1934) and Ann. de physique [11] **8**, 361 (1937).

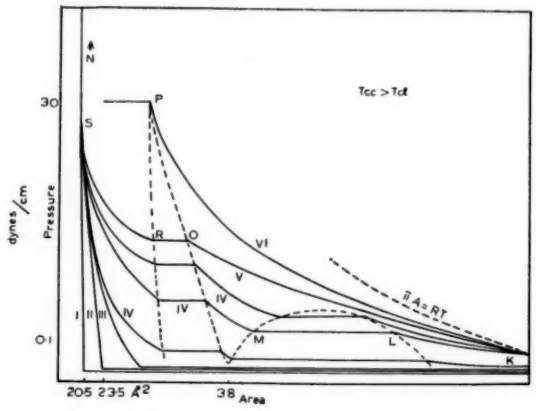

FIG. 2. Possible forms of isotherms when $T_{cc} > T_{cl}$.

phous state (Labrouste's transformation) commences.

T_l.—This transformation terminates at T_l, which is the real *melting point*, or temperature of appearance of the liquid state under the pressure of the saturated vapor. This will be defined as a *triple point* and the corresponding area (under the pressure of the vapor) is 38–39A² per chain. This plays an important rôle in the transformations of higher order.

We shall refer later to the three-dimensional correspondence and meaning of T_l and T_{cc}. The "half expansion temperature"[13] introduced by Adam, has an arbitrary definition and has no physical significance.

Classification of the different types of isotherms

For a given substance, the critical liquefaction temperature is not necessarily higher than the critical crystallization temperature. We shall consider the two cases in a general classification of the different types of isotherms. In Figs. 1 and 2 are depicted schematically all the possible forms of isotherms and their derivation according as T_{cc} is below or above T_{cl}. In order to represent on the same graph the complete development of the films, the pressure scale is larger at the bottom than at the top of the figure. Likewise, the area scale is extended on the right side. On the abscissae are indicated the characteristic areas per chain (under the pressure of the saturated vapor) of the different states and crystalline forms.

[13] It is defined as the temperature for which the area, under a pressure of 1.5 dynes/cm, is half-way between the condensed and the expanded states.

1°. $-T_{cc} < T_{cl}$.—Fig. 1 is applicable to substances in which the film always begins to liquefy before undergoing solidification by compression.

2.° $T_{cc} > T_{cl}$.—Fig. 2 is applicable to films which may still solidify by compression even when it can no longer liquefy.

We note that both types of isotherms have the same form at low temperature and even after the appearance of the liquid state; but they differ markedly at relatively higher temperatures. For the second type (Fig. 2), direct transition from the solid or mesomorphous phase to the gaseous may occur. This case must not be confused with the one where there is sublimation (lowest isotherms of both Fig. 1 and 2). In the later case, condensation takes place from a very dilute gas, while in the case under consideration the transition begins from a very concentrated gas occupying an area smaller than its "critical area."[14] Films in this state have been called by Adam "vapor expanded films" by analogy to the liquid films which he calls "liquid expanded films."

We shall now define successively the gaseous, solid, liquid and mesomorphous states, and particularly their transformation points (ordinary and higher order). An attempt will be made to explain their significance.

The two-dimensional gaseous state and condensation

From the outset of the work on surface films, a comparison was made between two- and three-dimensional gases, but we shall not dwell on the historical aspects.

Adam and Jessop established a series of isotherms, now classical, of a homologous series of acids. The general form of these curves (Fig. 1, *V*) recall the ordinary gas isotherms. The point *M* (molecular area of 20 to 100A²) is the beginning of a transition horizontal part, at relatively low but constant pressure (0.2 dyne/cm for

[14] Adam and Jessop [Proc. Roy. Soc. **A112**, 362 (1936)] have established the isotherm at 17° of ethyl palmitate up to about 2000A². This reveals, instead of a transition to liquefaction, a strong inflection around 150–200A², as if the film was near its critical temperature of liquefaction. While at 55A² and at a pressure of only 3.5 dynes/cm there appears a transition to crystallization. Films of methyl-11-ceto-stearate are gaseous up to a molecular area of 120A², then condense into a solid phase, along a horizontal transition flat, at a pressure of 5 dynes/cm. This is another example for the case illustrated by Fig. 2. (See D. G. Dervichian, Ann. de physique, reference 1.

myristic acid), which extends to some hundreds or thousands A² (*ca.* 900 for myristic acid). Then, beginning from L, the pressure π decreases gradually along LK tending asymptotically towards the $\pi A = RT$ hyperbola. If the areas and pressures are expressed in c.g.s. units, the constant R is the same as the three-dimensional perfect-gas constant; T is the absolute temperature.[15]

Adam and Jessop extended their measurements to about 5000A² per molecule. J. Guastalla[16] using oleic acid was able to reach extensions up to 30,000A² (area at $L=5000$) and found that the isotherm appeared to coincide with the ideal gas hyperbola. More recently Guastalla[17] has again taken up the question of measurements at very low surface concentrations with an apparatus based on a new principle, which enables him to measure easily surface pressures of the order of 1/1000 of a dyne/cm.[18] He has thus been able to reach areas of more than 100,000A². At this concentration, the mean intermolecular distance corresponds to that in a solution of 10^{-4} or 10^{-5} normal, or to a gas under the pressure of $\frac{1}{2}$-mm of mercury. Before reaching this value, the isotherm practically follows the $\pi A = RT$ hyperbola.

With a film of methyl-11-ceto-stearate, an isotherm was found[19] which follows the hyperbola from 1500A².

It is generally accepted that the LK part of the isotherm corresponds to the gaseous state. According to the case, this gas, or vapor, gives by condensation a liquid phase ($T>T_l$, oleic acid and tricaprin at room temperature, myristic acid above 5°, trimyristin above 30°, Fig. 1 or 2, IV and V) a mesomorphous phase ($T_s<T<T_m$, palmitic or stearic acid on dilute HCl at room temperature, Fig. 1 or 2, II and III), or a solid phase ($T<T_s$, tripalmitin or stearic acid on distilled water at room temperature, trimyristin

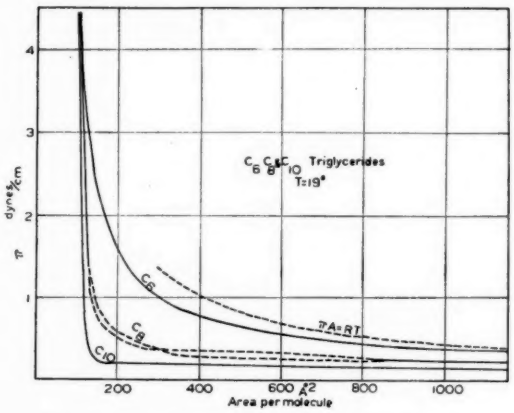

FIG. 3. Isotherms (π–A) of the C_6, C_8 and C_{10} triglycerides.

below 21°, Fig. 1 or 2, I). In other words, the reverse transformation would be a *vaporization* or a *sublimation*. Whatever be the assumption as to the orientation of the molecules, we must have, all along the LM flat part of the curve, two phases in coexistence, one growing at the expense of the other. Surface potential measurements show that the film is inhomogeneous in this region, and it has been proved that the condensed phase (liquid or solid) forms flat aggregates whose dimensions may attain some centimeters.[20]

Films not liquefying by compression ($T>T_{c1}$).—Films may give isotherms without a transition from the vapor (Fig. 1, VI, Fig. 2, V and VI). A typical case is given by the C_6 triglyceride: tricaproin. This is shown in Fig. 3, upper isotherm. There is no discontinuity in the isotherm. Likewise the surface potential curve decreases quite regularly. The two other curves refer to the two higher terms of the series: C_8 (tricaprylin) and C_{10} (tricaprin). C_{10} gives a transition flat between 120 and 4000A²; as for C_8, the results are quite variable in the middle range of concentration, presenting all the characters of an unstable region of transition. The variations of temperature which have been used were not sufficient to produce any state of equilibrium. It is to be noted that such large molecules can easily form metastable films; this is also noticed in solidification from the liquid.[21]

[15] This was observed by Langmuir for the adsorbed soluble substances and foreseen by him for the insoluble very dilute films. The kinetic interpretation may be found in Adam and Jessop's original paper, reference 8. We are not concerned here with the actual position of the molecules in the gaseous state (lying flat or not). See the discussion in Adam's *The Physics and Chemistry of Surfaces.*

[16] J. Guastalla, Comptes rendus **189**, 241 (1929).

[17] J. Guastalla, Comptes rendus **206**, 993 (1938) and J. de phys. et rad. (1939).

[18] The chief feature of the technique is the great care taken to clean the surface. This is always incomplete in the ordinary method of scraping the surface with movable barriers.

[19] D. G. Dervichian, Ann. de physique [11] **8**, 405 (1937).

[20] Adam and Harding, Proc. Roy. Soc. **A138**, 411 (1932); Schulman and Rideal, Proc. Roy. Soc. **A138**, 430 (1932); D. G. Dervichian, reference 1.

[21] According to Adam and Jessop's isotherms, lauric acid (C_{12}) seems to be in the neighborhood of its critical tem-

Critical temperature of liquefaction

As will be seen, the range of temperature, limited by experimental conditions, often includes different points of transformation of the condensed phase *of the same substance;* but to pass the critical point of liquefaction requires a much wider range, and it has not yet been possible to plot, for the same substance, isotherms situated on each side of the critical point. But in consequence of the fact that the temperatures of the different points of transformation increase with the length of the chain we can consider the different isotherms of Fig. 3 as if belonging to the same substance, investigated at three different temperatures. We may state that every substance, when spread as a monolayer, has a critical temperature of liquefaction and that, at room temperature, tricaprylin is in the neighborhood of its critical temperature, tricaproin distinctly above, and tricaprin, and all the higher homologues, below.

Transformation of higher order in gaseous films

While the isotherm of tricaproin shows no discontinuity, the compressibility, the dipole

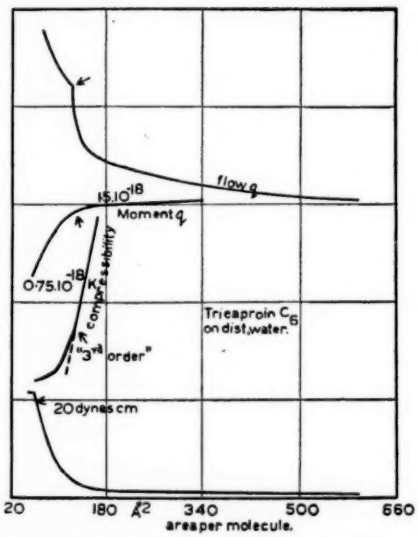

FIG. 4. Discontinuity of higher order in a highly compressed gaseous film (tricaproin C_6). There is a very marked kink in the fluidity curve at about 115–120A². The compressibility shows only an inflection at the same area; this would show a discontinuity on the dK/dA curve. According to definition, this corresponds to a discontinuity of the third order. There would also be a break in the derivative $d\mu/dA$ of μ.

perature. But, as this substance is slightly soluble, the curve is incomplete.

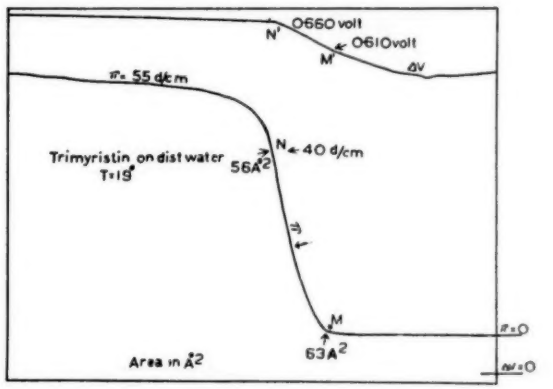

FIG. 5. Registered isotherm and ΔV curves of a solid film: Trimyristin (C_{14}) on distilled water at 19°. By placing a ruler along the curve one can easily see the marked changes of slope.

moment and especially the viscosity (actually the rate of flow) reveal a point of transformation at about 115–120A² as may be seen on Fig. 4. Tricaprylin behaves in the same way. The significance of this 115–120 point will be given later. Methyl-11-ceto-stearate and ethyl-11-oxy-stearate also show very distinct points of transformation of high order in the gaseous part of their isotherms. These are due to the presence of the supplementary polar groups of the molecules.

The two-dimensional solid state

A monolayer of trimyristin at room temperature is a representative solid monolayer. Besides cohesion, it shows another characteristic of solids: rigidity.[22] Fig. 5 reproduces the registered isotherm of this monolayer spread on distilled water at 19°. At any temperature below 21°, the same diagram is obtained. Discontinuities are seen on both the pressure (π) and the surface potential (ΔV) isotherms. The pressure curve is an isotherm of sublimation. The area at M is the area occupied by a molecule in the solid under its saturated vapor pressure. We find for this molecular area, values between 62.5 and 63.5 (average of 63A²). By further compression, the pressure rises rapidly, then at a certain minimum area the film collapses. With trimyristin, there is a sudden discontinuity only on the potential curve at N', the isotherm showing only an inflection starting at N, whence the slope decreases

[22] For the study of the rigidity see: Mouquin and Rideal, Proc. Roy. Soc. **A114**, 690 (1927); for the resistance to shearing, see: M. Joly, J. de phys. et rad. [7] **8**, 471 (1937).

with the appearance of the three-dimensional phase. This point (N or N') corresponds to a minimum area of 55–56A². With the C_{16} and C_{18} triglycerides, the same curve and areas of 63 and 56A² are found. These areas are independent of the molecular volume.

Solid films can be obtained by compression of a fluid film, we are concerned in this paragraph only with those films which are already solid under their saturated vapor pressure. At room temperature, normal fatty acids give such films only when the number of carbon atoms is at least 18. For the C_{18}, C_{20} and C_{22} acids, the area at the sublimation point M is very nearly 20.5A² and remains constant over large range of temperature as long as the film is solid. The minimum area is indicated in these cases by a sudden break, the isotherm showing a very sharp point after which the pressure falls (Fig. 14). This occurs at *ca.* 18.5A². It is remarkable that the minimum area of 55–56A² found for the triglycerides is equal to 3×18.5.

Discontinuities of second-order in solids

The isotherms of the solid triglycerides show two changes of slope, which correspond to sudden changes in the compressibility. It is difficult to find evidence for any corresponding singularities in the dipole moment. But, on the trimyristin potential curve, recorded at 19°, two breaks are noticed. These breaks as well as the change in compressibility occur at 57.5A²($=3\times19.2$) and 60.6($=3\times20.2$). The solid fatty acids show the same discontinuities at about 19.3A² and 20.3A².

Discussion on Data Given by X-Ray Analysis of Fatty Substances

Fatty acids

X-ray crystal analysis reveals that, according to conditions of solidification, a fatty acid may show three or four different values for the long spacing. These correspond to one of the A, B, C or D crystalline varieties.[23] In each of these polymorphous varieties, the spacing varies linearly with the number of carbon atoms, and the slope of the variation enables us to calculate the angle of tilt of the molecule on the plane of stratification. Whatever the chain length, this angle is the same and has values of about 70°, 60° or 50°[24] for the A, B, or C form, respectively. Thus the different intervals found with the same acid correspond to the different "heights" of the molecule, which has a constant length but is more or less tilted. A consequence of this is that if we calculate the area available per molecule on each plane of stratification[25] (ratio of the molecular volume by the height), the same values of 19.5, 20.5 and 23–24A² are found for the A, B and C varieties of all the acids from C_{10} to C_{26}. We can consider these three values of the molecular area as the horizontal section of a more and more inclined molecule, the cross section remaining constant. One finds 18.5A² for this cross section; that is the area which the molecule would have if it was completely erect. Müller has studied a single crystal of stearic acid and found the following dimensions of the unit cell:

$$a=5.546, \quad b=7.381, \quad c=48.84.$$

a and b are the sides of the rectangular base. The average number of molecules for each unit rectangle being 2 (1 central $+\frac{1}{4}$ of each of the four corners), the area per molecule is $ab/2=20.5$A². This was a B crystal. It has been possible to prepare single crystals belonging to the different varieties and to study the conditions of passage from one to the other.[26]

Triglycerides

Triglycerides have two crystalline forms: one stable, where the chains are inclined, the other unstable with the molecules vertical to the stratification plane. The density being 1.03, one finds for all the homologues between C_{10} and C_{18}, a molecular area of 64A² for the stable and 56A² for the unstable form.[27] The first value is about 3×21A² (form B of the acids) while the second approaches 3×18.5 (cross section of the chains). It must be emphasized that long chain paraffins which have generally vertical molecules, give a

[23] See for example: Francis, Piper and Malkin, Proc. Roy. Soc. **A128**, 124 (1930).

[24] More exactly: 53°, 63° and 71° for stearic acid.

[25] This calculation is based on the fact that the fatty acids have a monoclinic structure (the unit cell being a parallelopiped with a rectangular base) and the molecules fixed at each corner and at the center of the base are parallel to the tilted sides of the cell.

[26] Dupré La Tour, Ann. de physique [10] **18**, 199 (1932).

[27] The data for the spacing have been taken from Trillat and Nowarowski, Ann. de physique [10] **15**, 463 (1931) and Clarkson and Malkin, J. Chem. Soc. 666 (1934).

calculated cross section of 18.5A². This shows that the packing in the acids and triglycerides is governed mainly, if not completely, by the chains.

Interpretation of the Molecular Areas Found in the Solid Monolayers

The simple comparison of the x-ray data with those obtained from solid films allows us to derive some conclusions as to the state of the molecules in the films. First, the 18.5A² area found at the breaking point of the acids, and the minimum area of 55–56A² found at the collapsing point of the triglycerides, show that at these points the molecules are vertical. It is certainly not a simple coincidence that the 63A² found with the triglyceride solid layers as well as the 20.5 measured at the point of sublimation *M* of the acid (Fig. 5) agree with the x-ray data of both the stable form in triglycerides and the *B* form of acids.[28] Likewise, as will be seen with the mesomorphous films, in a certain well-defined range of temperature, acids give the molecular area of 23–24A² which corresponds to the *C* form. These later films when compressed show a very distinct break at 19.5A², showing the transition to the *A* form (Fig. 14). Triglycerides give also in a well-defined range of temperature a new form with a molecular area of 71A² (Fig. 13) which may be related to the *C* form of the acids ($71=3\times23.7$).

Since the molecular area is the same in the film and in the crystal, and undergoes a parallel modification, we are led to believe that *the lattice structure and the tilt of the molecules in the different forms are the same both in two and three dimensions.* It should be emphasized that once we admit this identity of structure, the only way we can interpret the variation of the area in the film on compression is by a progressive change of the tilt. We can no longer make use of the assumption

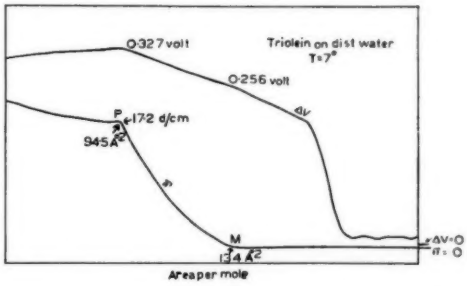

FIG. 6. Registered curves of a liquid film: triolein on distilled water at 7°.

that the molecules are always vertical and that the changes in area are due to changes in packing with "closed packed chains" or "closed packed heads" (Adam). As we have shown, the changes are due entirely to the tilt of the *chains* in the lattice, the cross section of the molecule remaining the same in acids and paraffins.

Liquid films

Let us consider the case of monolayers formed from substances which are liquid in three dimensions at the experimental temperature: for example oleic acid or triolein. Fig. 6 (triolein) shows a typical isotherm given by such films. At all pressures the film appears to be fluid and surface viscosity measurements reveal no anomalies or rigidity. The mean compressibility is 10 to 15 times greater than that of a solid film. In this case, as will be shown, the point *M* corresponds to the end of the condensation of the vapor phase into a two-dimensional liquid.[29] The point *P* indicates the limit of compression of the liquid monolayer: as the substance is liquid in three dimensions, the molecules which leave the surface collect into droplets or spots.

Some *solid substances*, such as stearic acid and trimyristin, form *solid films* at room temperature. But, provided the temperature is greater than a critical temperature of crystallization T_{cc} (different for different substances), it is possible to form, from solid substances, fluid films with isotherms similar to those of oleic acid and triolein (Fig. 1, V). Table I presents, for a series of substances, this minimum temperature T_{cc} and the areas at *M* and *P*.

[28] Lyons and Rideal (Proc. Roy. Soc. **A99**, 33 (1921)) have attempted to explain the value 20.5A², as well as that occasionally observed at about 26A², on the supposition that they correspond, respectively, to two inclinations which permit different modes of interlocking of the zigzag chains. This hypothesis does not, however, explain the other characteristic values (19.5 and23.5A²). In any case, we are not concerned here with explaining the different modes of crystallization, but merely with showing the correspondence of the several forms in two and three dimensions.

[29] On the graph, the horizontal part corresponding to condensation is indistinguishable from the axis.

TABLE I.

	T_{cc}	AREA AT P	AREA AT M	$V^{2/3}$/(CALC.)
Lauric Acid C_{12}	<0°	26A²	—	—
Myristic Acid C_{14}	34°	27–28A²	57–58A²	57A²
Palmitic Acid C_{16}	55	27	61	62
Oleic Acid C_{18}	<0°	26.5(4°), 29(20°)	56	64
Elaidic Acid C_{18}	·	·	·	64
Tariric Acid C_{18}	·	28–30	·	64
Trilaurin C_{39}	21°	78–80	110–115	111
Trimyristin C_{14}	43°	85–86	120–124	121
Triolein C_{18}	<0°	95–97	132–137(20°)	138
Taririn C_{18}	<0°	84(6°)88(20°)	132–134	130
Glycol dilaurate*	<0°	55	83	86 (∂=0.87)
Tribenzoin	<0°	60	75(3°)	69 (∂=1.16 at 80°)

* From Adam, Proc. Roy. Soc. **A126**, 366 (1930)

Structure of the liquid film at the point P

One notices that the areas per chain at the point P do not vary much with the chain length[30] indicating the molecules are standing on the surface; but the area of 27 to 30A² per chain proves that they are not vertical and close packed.

Proceeding from Langmuir's fundamental notion that the polar and nonpolar ends of the long chain molecules act independently, we shall describe the structure of liquid films at the points P and M, without making the further assumptions which he introduced in his theory of duplex films.[31] Whereas in that paper, Langmuir was principally interested in obtaining an equation of state, we are here concerned with finding the structural correspondence between the two- and three-dimensional liquid states.

Let γ_b be the surface tension of the liquid which is spread and γ_{ab} its interfacial tension with water. If we represent by γ' the surface tension of water covered with a film at the point P, we find *experimentally*[32] that:

$$\gamma' = \gamma_b + \gamma_{ab}. \tag{8}$$

As γ' represents the surface free energy, we may regard it as the sum of two different surface free energies ($\gamma_b' + \gamma_{ab}'$) localized at the upper and lower face, respectively, of the monolayer. It follows then from (8) that

$$\gamma_b' + \gamma_{ab}' = \gamma_b + \gamma_{ab}.$$

We now assume that this equality is a consequence of the identity of the two members, that is $\gamma_b' = \gamma_b$ and $\gamma_{ab}' = \gamma_{ab}$.

From this it follows that, on one hand at the water interface of the film as well as under a thick oil layer, the polar groups occupy the same space and relative positions and, on the other hand, at the air interface, the orientation and packing of the chains are the same in the film and *at the surface* of a three-dimensional liquid.

This basic assumption ($\gamma_b' = \gamma_b$ and $\gamma_{ab}' = \gamma_{ab}$) is justified by a series of facts. First of all, experiments of the difference in wettability between the two faces of a slab of fatty acid solidified at the surface of water (A. Pockels, H. Devaux), lead to the view that the molecules of the lower part of the oil thick layer have their COOH groups turned to the water, while those at the surface turn their paraffin chains towards the air.

Using the ordinary method, we have measured the change of the water-air interface potential affected, not by a monolayer, but by a layer of several millimeters of oil. Practically the same value as that at the point P was found. As the potential lowering depends on the surface concentration, we may deduce that the number of COOH groups in contact with the water is the same in both cases.

As to the air-oil surface, it is generally accepted that liquids show a surface orientation. For fatty substances more particularly, both x-ray spectroscopy (method of the tangent drop),[33] and the elliptical polarization of the reflected light[34] give us conclusive evidence. Consideration of the correction of Eötvös constant leads us to infer that the molecules at the surface of liquid alcohols and acids occupy an area of about 25A².[35]

We thus assume that in its structure and concentration, *the liquid monolayer at the point P is a reproduction of the surface of the three-dimensional liquid.*

[30] Tribenzoin which gives a definitely different area is not a long chain compound.

[31] I. Langmuir, reference 9.

[32] This is another way of stating that at the point P, the surface pressure π is equal to the spreading coefficient $\pi = \gamma_a - (\gamma_b + \gamma_{ab})$ for $\pi = \gamma_a - \gamma'$ (where γ_a is the surface tension of pure water). This is an important deduction, since (8) indicates that the contact angles of the first droplets are zero when the equilibrium is stated in terms of Neumann's triangle, $\gamma' = \gamma_b \cos a + \gamma_{ab} \cos b$.

[33] Trillat and Nowarowski, Ann. de physique [10] **1**, 467 (1931).

[34] Ch. Bouhet, Ann. de physique [10] **15**, 5 (1931).

[35] E. K. Rideal, *Surface Chemistry* (1930), p. 38, and D. G. Dervichian, Comptes rendus **200**, 2065 (1935).

Definition of an isotropic monolayer

At the surface of a liquid, the area occupied by a molecule is relatively small in comparison to the height: the space occupied by each molecule being a long prism or cylinder. In the bulk of the isotropic liquid, however, all directions are equivalent and thus the mean space per molecule is a cube whose volume is the molecular volume $V=M/N\partial$. We can imagine an isotropic monolayer in which all the possible *directions* of the molecules would be equally distributed at random. For such an isotropic layer, the *mean thickness* and the *mean base area* per molecule would be the height and the base of the cube V (i.e., $V^{\frac{1}{3}}$ and $V^{\frac{2}{3}}$). For example, the thickness of an isotropic liquid film of palmitic acid would be 7.9A instead of the 17.8 found at the point P, and the molecular area $62A^2$ instead of the $27A^2$. Thus the degree of anisotropy of liquid films can be defined by comparing the areas measured at different points of the isotherms to the area $A=V^{\frac{2}{3}}$ corresponding to the molecular volume of the isotropic liquid.

Structure of the liquid film at the point *M*

The last column of Table I gives the calculated values of $V^{\frac{1}{3}}$. It can be seen how close these values are to those found for the area at the point M.[36] We can at least conclude that at any rate the packing of the molecules in this type of film is not looser than in the three-dimensional liquid and the name of "expanded liquid" given to them is not justified. We shall adopt the simple terminology of "liquid film" and say that, *at the point of vaporization M, the state of the molecules is similar to what it is in the bulk of the three-dimensional isotropic liquid.*

Interpretation.—We can express the pressure π_P at the point P in terms of the work of cohesion ($W_b=2\gamma_b$) of the spreading liquid and of its work of adhesion ($W_{ab}=\gamma_a+\gamma_b-\gamma_{ab}$) to the water. From the definition of the surface pressure ($\pi_P=\gamma_a-\gamma'$[32]) and from (8), we find:

$$\pi_P=W_{ab}-W_b. \tag{9}$$

This expression has an immediate physical significance. It shows that if the affinity of the fatty substance for water is greater than the cohesion between its own molecules, these will leave the deposited drop with a pressure which depends on the difference between the two free energies.

Let us again consider the film at P as a very flat drop, one molecule thick, to which may still be applied the notion of a work of cohesion and a work of adhesion. These free energies always refer to an area of 1 sq. cm. Then, if starting from P, we go down the isotherm by expanding the film, the free energy of cohesion and the free energy of adhesion will gradually decrease, not only on account of the decrease of molecular concentration per sq. cm, but also as a consequence of the variation of the intermolecular actions which are also related to the concentration. W_{ab} and W_b being particular values at the point P, let w_{ab} and w_b be the variable quantities corresponding at each given surface concentration. Whatever is the variation law of these two functions, we can write for every surface concentration:

$$\pi=w_{ab}-w_b \tag{10}$$

and note that this difference decreases with increasing the area per molecule. At the point M, π is practically negligible[37] and $w_{ab}=w_b$. This means that, at the point M, actions due to cohesion and those due to adhesion counterbalance one another, although both are still important. As the molecules are submitted on the average to isotropic actions, the state of the film will reproduce the state of a liquid in the bulk.

If $l_0=V^{\frac{1}{3}}$ represents the mean intermolecular distance in the three-dimensional isotropic liquid, the relation $A_m=V^{\frac{2}{3}}$, which relates the area at M to the molecular volume, can also be written $A_M=l_0^2$. This expresses the fact that l_0 is a critical intermolecular distance which occurs both in fluids in bulk and in monolayers.

[36] The early investigators used to measure the area at the point M (maximum extension). They considered the molecules isotropic in shape and taking M for the point where they come into contact, they tried to compare the thickness of the film with the calculated value $V^{\frac{1}{3}}$ (which comes to $A=V^{\frac{2}{3}}$). Very satisfactory agreement was thus found (Lord Rayleigh, Devaux, Labrouste). It is curious to notice how, when Langmuir established that the molecules in question were elongated, these results were forgotten or considered as a meaningless coincidence. Langmuir's determinations were concerned more especially with solid or mesomorphous films whilst these dealt with liquid films.

[37] The pressure at the transition is generally less than 0.2 dyne/cm, while it has 20 or 30 dynes at P.

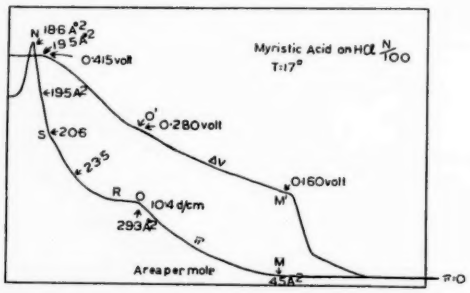

FIG. 7. Registered curves of a liquid film solidifying under compression: Myristic acid on HCl $N/100$ at 17°. Between M and O the film is liquid. OR is the crystallization transition which leads to the expanded mesomorphous state. On further compression, the mesomorphous ($23.5A^2$) and then the solid S (20.5, 19.5) states are reached. The film *breaks* at $18.6A^2$ (cross section of the vertical molecule).

Isotherms without discontinuous vapor-liquid transition (Fig. 1 or 2, VI).—In some cases, the expansion may gradually decrease w_{ab} and w_b but their difference $w_{ab}-w_b$ may remain relatively important. Then the film will be transformed into the gaseous state in a continuous manner giving an isotherm similar to a fluid which is above its critical temperature. This happens: 1.—with molecules having a second attractive group for water, which increases w_{ab}; 2.—with short chain molecules, which possess a relatively higher thermal agitation and consequently a smaller w_b.

Solidification of liquid films by compression ($T<T_{cc}$)

This case is illustrated by Fig. 7 which reproduces the registered isotherm of myristic acid at 17°C ($T_{cc}=34°$). This curve has a lower part similar to the isotherm of a liquid film and an upper part analogous to that of a solid film of stearic acid (Fig. 14); an intermediate more or less horizontal transition, followed by a rounded part, joins these two regions. The isotherm of trilaurine at 7.7° ($T_{cc}=21°$) shows also an intermediate transition (Fig. 9). Both films are fluid between M and O and show viscosities comparable to those of films spread from liquid substances like oleic acid or triolein. Between S and N, the films are solid. This is shown by the break at N with myristic acid and the values of the area and the ΔV at S and N (20.5 and 18.5 for the acid, 64 and 56 for the triglyceride) compared with Figs. 5 and 14.

The end of the liquid state is indicated by a marked discontinuity at O showing the beginning of the transformation. As will be proved, the rounded part RS corresponds to the mesomorphous state through which the film passes before reaching the solid state. The flat part OR will be termed "crystallization transition." Theoretically the isotherm from O to R should be flat. In fact, since the transformation takes place between a highly oriented liquid and a liquid crystal and is accompanied by a change in area of only a few A^2, one cannot expect to observe a marked transition (Figs. 7, 8 and 9). On the other hand, for some substances of the type illustrated by Fig. 2 (for examples see reference 14) the difference in area $O-R$ between the two phases is much larger and the corresponding portion of the experimental isotherm is very nearly horizontal. When the temperature is lowered, this transition occurs at lower pressures and, under a certain temperature T_l the liquid state disappears. Conversely, above a well determined temperature T_{cc}, after the

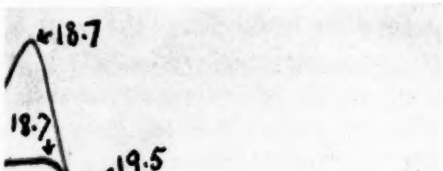

FIG. 8. Photographic reproduction at the actual size of part of a registered graph for myristic acid on HCl $N/100$. On the ΔV curve, the transition is particularly well marked. All the points of discontinuities of higher order are indicated. They correspond to changes of slope on both curves and are readily discerned. One of the curves is always slightly shifted with respect to the other. This is due to the recording system.

transition region has shortened and risen it eventually disappears, the film remaining liquid at any pressure (Fig. 1, V and Fig. 2, VI).

The triple point

The classical series of isotherms obtained by Adam and Jessop with myristic acid are summarized by curves III, IV and V of Fig. 1.[38] It will be noticed, that with decreasing temperature, the domain of existence (MO) of the liquid

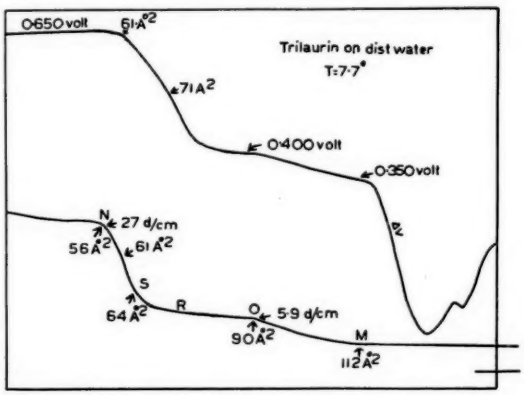

FIG. 9. Registered curves of a liquid film solidifying under compression: trilaurin on distilled water at 7°.7. See remarks of Figs. 7 and 8.

shortens. In Fig. 10 are plotted the corresponding areas of the M and O end points of the liquid state at different temperatures. The upper line AB represents the expansion of the liquid under its own vapor pressure. The lower part AC gives, for every temperature, the area at which the liquid is transformed into the mesomorphous phase. The temperature corresponding to the point A is that which we have previously denoted by T_l and termed the temperature of liquefaction under the saturated vapor pressure. From Figs. 1 and 2, one can see that this is a triple point, being the point of junction of three domains: the liquid, the vapor and the mesomorphous phases. The area at that point is 38–39A² for one chain molecules and 110–115 for triglycerides. It will be noticed that this later value is equal to three times 38–39.

Transformations of higher order in liquid films

At temperatures above T_l, and an area of 38–39A² per chain, we note a discontinuity of

[38] Similar isotherms have been obtained with trilaurine and trimyristine by D. G. Dervichian, Ann. de physique, reference 1.

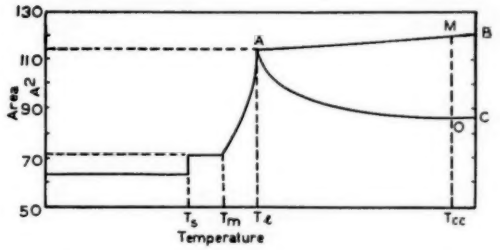

FIG. 10. Expansion of the film *under its own vapor pressure* with increasing temperature, T_s, T_m, T_l being the different transition temperatures. After the point A, the upper part AB refers to the expansion of the liquid phase under its saturated vapor (point M of the preceding graphs), while the part AC records the variation of the point O: i.e., the smallest area compatible with the liquid state at different temperatures. The region between AB and AC is the domain of existence of the liquid state. A is the triple point.

higher order. This was already found in highly compressed gaseous films (see above), but exists also in films like oleic acid, triolein ($T>T_{cc}$) or myristic acid ($T_l<T<T_{cc}$). The same area per chain is found for both saturated and unsaturated chains, acids or triglycerides (triolein, tricaproin, tricaprylin). Figs. 11 and 12 show that, for this area, the compressibility, viscosity and apparent moment curves have a singularity, while the isotherm is quite smooth. Even for substances like triricinolein, in addition to the particular higher order point due to the presence

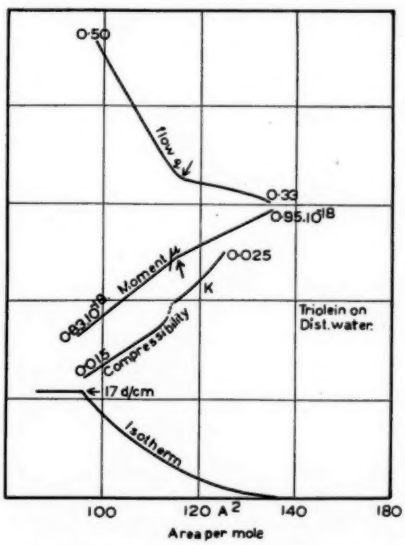

FIG. 11. Higher order transformation point in a liquid film ($T>T_{cl}$): Triolein on distilled water at room temperature. The fluidity, moment and compressibility curves show the existence of a second-order transformation at about 115A² (corresponding to the triple point area).

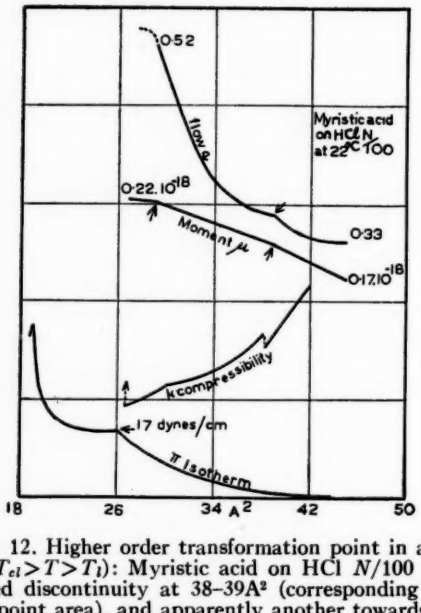

FIG. 12. Higher order transformation point in a liquid film ($T_{el} > T > T_l$): Myristic acid on HCl $N/100$ at 22°. Marked discontinuity at 38–39A² (corresponding to the triple point area), and apparently another towards 28–29 (corresponding to the point P).

of the supplementary alcoholic group, the 39A² point is found.

Liquid films of trilaurin and trimyristin, do not seem to present any higher order discontinuity; but it will be noticed that the maximum area of these substances as liquid films is 110–120A² (point of vaporization M), so that it may be confused with the point of higher discontinuity if it exists.

The mesomorphous state

When the temperature is gradually increased, solid films pass by a well-defined intermediate state before reaching the liquid state. We have previously called this the mesomorphous state. We shall try to identify it with a three-dimensional corresponding state.

1. Transition from the solid to the mesomorphous state.—At any temperature below 21°, the film of trimyristin is solid and gives at the point M the characteristic area of 63A². But at about 21° the area at M changes suddenly to 71A² and remains constant over another range of temperature. The isotherm then appears as in Fig. 13. The same state is found with the higher homologs of the triglycerides at higher temperatures. But the range of existence of this state is much more extended with acids on dilute HCl. Fig. 14 depicts stearic acid spread on HCl $N/500$. The C_{16}, C_{18}, C_{20} and C_{22} acids give the same curve on dilute HCl. The area at the point M is 23.5A² which is the third of 71A². For the lower members of the series (myristic acid or trilaurine), the range of existence of this form is certainly below 0°.[39] The film is fluid and stays so up to the point M' where it turns into solid.

2. Labrouste's transformation.—The expanded mesomorphous state.—The isotherms given by Adam and Jessop bring into prominence the

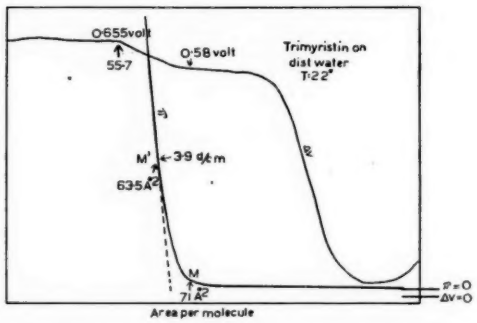

FIG. 13. Registered curves of a film showing the mesomorphous state ($T_m > T > T_s$): Trimyristin on distilled water at 22°. Compare with Fig. 5. The characteristic area of 63.5 appears here at M' as a transition of higher order.

evolution of the films after the liquid state has made its appearance. But before the real melting occurs and starting from the 23.5A² state, another transformation which has been more specially studied by Labrouste takes place. Labrouste's experiments were confined to variations of the area at the point M with the temperature. No measurements of pressure were made at that time and some important points could not be noted without a record of the complete isotherm. Fig. 10 has been plotted from results drawn from a great number of isotherms registered at different temperatures. They refer to trimyristin. As abscissa are indicated the temperatures and ordinates the corresponding areas at the vaporization point M (except the part AC). We note the discontinuous transition from the 63 to the 71 form at the temperature T_s(21°). This area remains constant up to a new point T_m(24°). Then a gradual expansion commences: the expansion coefficient goes on increasing and

[39] For the range of existence of this state, it must be noticed that besides the temperature, the nature of the substrate has to be considered, specially in the case of the acids (Adam and Miller Proc. Roy. Soc. **A142**, 401 and 416 (1933)).

finally attains a very high value when liquefaction is reached. Beginning from that point, the expansion at the point M proceeds more slowly following a slightly inclined straight line.

On the isotherms the lower part becomes more and more rounded and lengthens (Fig. 15); then suddenly at a temperature $T_l(29°)$ the characteristic type of curve of the liquid state appears. Over this range of temperature the film is still fluid. Films which give isotherms similar to Fig. 15 will be said to be in the expanded mesomorphous state.

3. Transition from the expanded mesomorphous to the liquid state.—The transition from the expanded mesomorphous to the liquid phase by increase of temperature occurs under its own vapor pressure at the point T_l. Above this temperature, the transition may be obtained by compression along the different flats of the Adam and Jessop's isotherms (Figs. 7, 8 and 9). The assumption of Langmuir[9] of the formation of "micelles" of a small number of molecules to explain these flats cannot be supported if we consider that, even with the relatively large dimensions of the electrode used, the inhomogeneity of the film in this region is detected on the registered potential curve. Corresponding to the kink point O of the isotherm, on this appears a flat horizontal part which varies from diagram

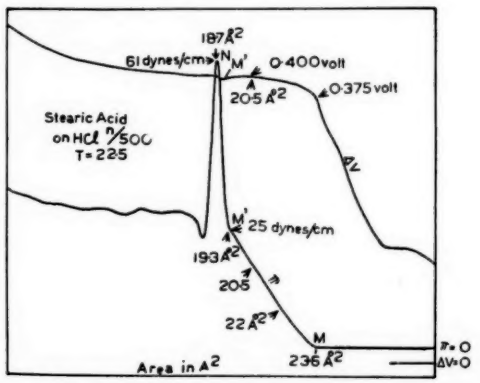

FIG. 14. Registered curves of a film showing the mesomorphous state ($T_m > T > T_s$): Stearic acid on HCl $N/500$ at 22.5°. The 22A² point can be noticed on the isotherm by a slight change of slope. The 19.5 point is clearly marked; above it the film is in an unstable state. After the break at 18.7A², the pressure falls approximatively to the value corresponding to the 19.3 point (the film is no longer homogeneous). Note the maximum value of the ΔV at 20.5A² and the minimum corresponding to 19.3A². On many graphs the isotherm itself shows a slight kink at 20.5Å².

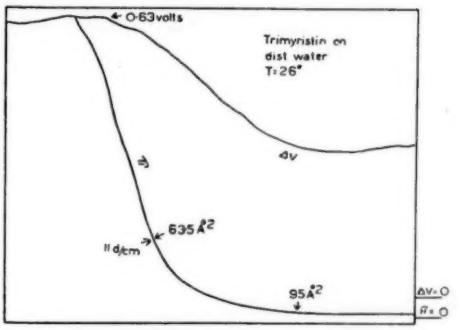

FIG. 15. Registered curves showing the expanded mesomorphous state ($T_l > T > T_m$): trimyristin on distilled water at 26°.

to diagram according to the fluctuations of relative concentrations of both phases under the electrode.[40] There is an ordinary transition probably from a state of disorder—or at least very similar to the liquid state—to a crystalline state. The crystalline state is the *expanded* mesomorphous, since this is the last form we meet before the liquid phase. The rounded part RS after the kink corresponds to the compression of the expanded mesomorphous phase and leads continuously to the solid. In other words, it is the reproduction at a higher pressure of the isotherm of Fig. 14.

Identification of the mesomorphous state

On the mesomorphous phase isotherms (Figs. 13, 14, 15), the transition from the C form (23.5) to the A form (19.5) is continuous from M to M'. There is only a discontinuity in the compressibility at M'. This is a transformation of the second order and shows that the change which occurs is from a given state of order to another state of order. We conclude, from this and from the fact that the area of 23.5A² corresponds to a well-defined crystalline form, that the mesomorphous films have a crystalline structure and must correspond to three-dimensional liquid crystals. We note also that the expansion curve in Fig. 10 is similar to that found in studying, in three dimensions, the change of volume of substances such as para-azoxy-phenetol or para-azoxy-anisol in their

[40] This unquestionably confirms once more the existence of transition even on the electrical curve, as was first detected by Schulman and Rideal, reference 3, and questioned by N. K. Adam (Proc. Roy. Soc. **A138**, 411 (1932)).

transition from the liquid crystal to the isotropic liquid phase.[41]

Mesomorphous films are able to form built up multilayers by the Langmuir-Blodgett technique, whilst liquid films cannot be superposed and solid films break. As is well known on the other hand, some of the liquid crystals (smectic state) give stratified drops (Grandjean terraces). The mesomorphous film can consequently be considered as representing one of the elementary layers of such drops or of Perrin's stratified soap films, which the Langmuir-Blodgett method enables us to build at will.[42]

Higher order transformations in mesomorphous films

Besides the 19.5 (transition to solid), two other second order points are found in the mesomorphous films. One at 20.5A²: this corresponds to the *B* form and to the sublimation area of the solid films (ordinary transformation point). Another discontinuity in the compressibility and specially in the viscosity is detected at 22A². This molecular area has no known correspondence in three dimensions and seems to be associated with the stability of the film.

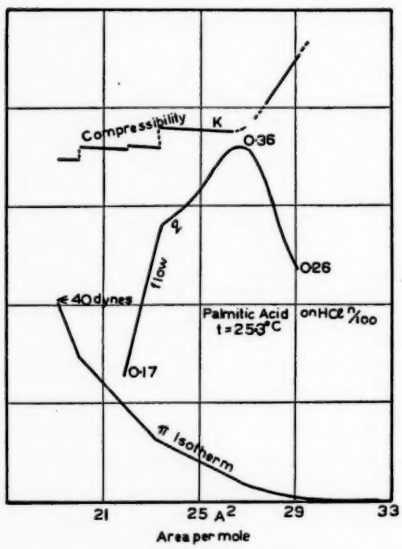

FIG. 16. Discontinuities of higher order in an expanded mesomorphous film: Palmitic acid on HCl *N*/100 at 25.3°. Commencing from the small areas, the compressibility and the fluidity curves show singularities at *ca.* 20.5, 22, 23.5 and 26.5A².

[41] See R. Schenck, Zeits. f. physik. Chemie **25**, 337 (1898), and Bauer and Bernamont, J. de phys. et rad. [7] **7**, 19 (1936).

[42] See J. J. Bikermann, Proc. Roy. Soc. **A170**, 130 (1939).

TABLE II.

	MELTING IN FILMS		MELTING IN THREE DIMENSIONS	
	BEGINNING OF MESOMORPHOUS T_s	REAL LIQUEFACTION T_l	VITROUS STATE	STABLE STATE
Tristearin	46–47°	55°	54.5–55°	70.8–71.5
Tripalmitin	35°	45°	45 –46.2	64.8–65.6
Trimyristin	21	29	32 –33	55 –57
Trilaurin	<0	2–14*	14 –16	44.3–46.4
Tricaprin	<0	<0	–15	31.0–31.6
Cetyl alcohol	32–33°	ca 50°		49.5
Stearic acid	(on dilute HCl)	50°		69°
Palmitic acid	(on dilute HCl)	29–30°		62°
Myristic acid	(on dilute HCl)	5°		54°
Lauric acid	(on dilute HCl)	<0°		44

* Trilaurin gives different temperatures; the samples used by the different investigators being presumably different.

In the expanded mesomorphous state are found, not only the 19.5, 20.5 and 22A² points, but also the 23.5 point which now appears as a second order discontinuity. We also find a new point of transformation with a *variable* area increasing with temperature. In the case of palmitic acid, it extends from 24.5 (17°) to 26.5A° (25°). The upper limit of this point is probably confused with the minimum area of 28A² of the liquid state (point *P*, Fig. 6).

Fig. 16 gives the compressibility and fluidity curves showing these different discontinuities. They both reveal that for areas above the 26.5 point the film behaves like a liquid monolayer and below this point as a mesomorphous (compare with Figs. 11, 12 and 13, 14).

Relations Between Melting Points in Two Dimensions and Three Dimensions

We have termed the melting temperature T_l, the temperature at which the liquid state appears, i.e. the end of Labrouste's transformation. For cetyl alcohol, this temperature (*ca.* 50°) is similar to the melting temperature of the substance in three dimensions. For triglycerides and acids, the melting point in films is much lower than the ordinary melting temperature. But, even in three dimensions, triglycerides have another melting point which corresponds to the one observed in monolayers.

It is well known, that triglycerides show two melting points: the higher one is commonly

known and corresponds to the stable form, the other, about twenty degrees lower, corresponds to an unstable form. Clarkson and Malkin who have carried out a systematic x-ray study of the triglycerides, call this second variety the *vitrous form*. The diagrams of this form do not show any large spacing periodicity. The stable form of tripalmitin, for example, melts at 65°. If the melt be suddenly cooled, a solid is obtained which, on increasing the temperature, melts at 45°, remains fluid for a while and then solidifies to melt again at the normal temperature of 65°. In Table II are listed the melting points in monolayers with those of the ordinary and vitrous forms in three dimensions (where known).

As far as the triglycerides are concerned, we note that T_l is practically the same as the melting point of the vitrous form in three dimensions. Labrouste has clearly established that the substance spread in monolayer form is the vitrous variety. The triglyceride was spread, then compressed till particles visible under the microscope were obtained and placed on a slide. By raising the temperature, these particles melted at the melting point of the vitrous form and after a while gave the stable form. Moreover, the vitrous solid form spreads spontaneously on the water up to very high pressures, while the crystal spreads with greater difficulty.

It may be concluded, that *the vitrous form of the triglycerides, while unstable under ordinary conditions, is the stable state in surface layers.* For the acids and alcohols, we may say that the vitrous form which is unknown in three dimensions, can exist only in monolayers.

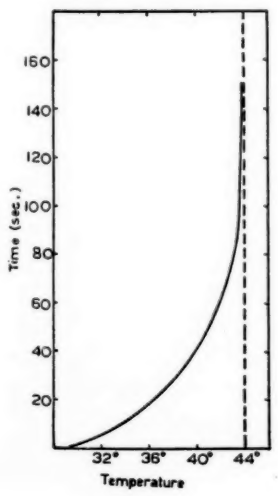

FIG. 17. Period of persistence of the melted vitrous form of trimyristin as a function of the temperature (redrawn from the data of Labrouste).

TABLE III. *Different characteristic areas.*

CHARACTERISTIC AREAS	SOLID FILMS	MESOMORPHOUS FILMS	EXPANDED MESOMORPHOUS	LIQUID FILMS	GASEOUS FILMS
18.5 (cross section)	**18.5**	**18.5**	**18.5**		
19.5 (form *A*)	19.5	19.5	19.5		
20.5 (form *B*)	**20.5**	20.5	20.5.		
22 (?)		22	22		
23.5 (form *C*)		**23.5**	23.5		
27–30 (surf. of liq.)			24.5 to 26.5	**27–30**	**27–30**
38–39 (triple point)				38–39	38–39
V' (isotropic layer)				V'	

SIGNIFICANCE OF THE CRITICAL TEMPERATURE OF CRYSTALLIZATION T_{cc}

Labrouste carried out a series of experiments on the vitrous form of the triglycerides which have a direct bearing on the behavior of monolayers. We have noted that when melting at the lower temperature, the vitrous form persisted for a while before solidifying again. This period in the metastable state increases with the temperature at which the fused vitrous form is kept (e.g. for trimyristin: 10 seconds at 34°, 100 sec. at 43°). Fig. 17 gives a curve redrawn from the data of Labrouste for trimyristin. Times have been plotted against the temperature. As was noticed by Labrouste, 30–31° is the melting point of the vitrous form and the temperature at which it is spontaneously transformed to the stable form without melting. But we also note that the curve is asymptotic towards 44–45°, indicating that over this temperature the substance can remain indefinitely melted. It is interesting to note that this temperature coincides with the critical temperature of solidification T_{cc} in the films of trimyristin. When Labrouste carried out his experiments, the critical phenomena in monolayers were not yet known.

It is to be noticed that retarded solidification is also found in surface films[43] and thus qualita-

[43] D. G. Dervichian, Ann. de physique [11] **8**, (1937).

tively corroborates Labrouste's results in three dimensions.

List of possible singular areas

It has been noticed that *some of the characteristic areas corresponding to higher order transitions in phases which exist at higher temperatures are precisely those which correspond to ordinary phase transition of the first order at lower temperatures.*

The Table III summarizes this general relation. Areas corresponding to discontinuities of the first order (ordinary change of phase) are printed in heavy type. Those referring to higher order discontinuities are printed in ordinary type.

Conclusions

(1) From the fact that different substances give different types of isotherms conclusions are frequently drawn on the influence of molecular constitution on the force area characteristics. This is likely to lead to erroneous results unless care is taken to compare the monolayers in corresponding physical states.

(2) We are naturally led to inquire whether there exist, *in three dimensions*, relations analogous to those illustrated by Table III. That such relations do in fact exist is confirmed by the data of Schroer[43] on the compressibility of ether over a wide range of temperature including the critical temperature. Discontinuities of higher order appear at temperatures well above the critical, when the volume reaches values near the critical volume. Furthermore x-ray analysis indicates traces of organization in the same region.[44]

Published data on the compressibility of three-dimensional liquids are unfortunately not sufficient to show up corresponding discontinuities in the neighborhood of the triple point volume.

I wish to express my sincere thanks to Professor E. K. Rideal for much help and criticism during the writing of this paper.

[44] Schroer, Zeits. f. physik. Chemie **140**, 381 (1929).
[45] Cybotactic condition. See W. Noll, Phys. Rev. **42**, 336 (1932); R. D. Spangler, Phys. Rev. **46**, 698 (1934); Benz and Stewart, Phys. Rev. **46**, 703 (1934).

OCTOBER, 1939 JOURNAL OF CHEMICAL PHYSICS VOLUME 7

Partition Functions for Partly Classical Systems

E. Bright Wilson, Jr.
Mallinckrodt Chemical Laboratory, Harvard University, Cambridge, Massachusetts

(Received June 27, 1939)

A method is described for calculating the partition function of systems whose Hamiltonian operator separates into three terms of the following types. The first and second terms are functions of different sets of coordinates while the third is a small coupling term. The energy levels of the first term by itself are widely spaced compared to kT while those of the second are closely spaced. In the result given, the partition function becomes a sum over the widely spaced levels and a phase integral for the contribution of the other levels, as in the case with no coupling term, but here the effect of the coupling term is included in the integral. As an illustration it is shown that the coupling of rotational and vibrational angular momentum in a polyatomic molecule has no appreciable effect on the thermodynamic properties even though it has a marked effect on the energy levels.

IN many systems it is possible to separate the Hamiltonian operator into two terms, each involving different coordinates, such that one term leads to closely spaced and the other to widely spaced energy levels. The partition function for a separable system can be written as a product of two factors and in this case the factor involving closely spaced energy levels can often be accurately approximated by an integral related to the classical phase integral.

In other cases, however, the Hamiltonian contains a third term, small but not negligible, which is a function of both sets of coordinates so that a strict separation cannot be carried out. It is the purpose of this note to show how such cases may be handled, retaining the phase integral ap-

proximation but bringing in the effect of the coupling term by a perturbation method.

Perturbation Technique

Suppose that the Hamiltonian operator or matrix is

$$\mathbf{H}=\mathbf{H}'+\mathbf{H}''+\epsilon\mathbf{H}''', \tag{1}$$

where $\mathbf{H}'$ leads to widely spaced energy levels, $\mathbf{H}''$ to closely spaced levels, and $\epsilon\mathbf{H}'''$ is the coupling term, ϵ being a parameter of smallness. In giving the elements of $\mathbf{H}$ it is convenient to use the wave functions of the unperturbed problem $\mathbf{H}'+\mathbf{H}''$ as basis functions so that two sets of quantum numbers, v (from H') and r (from H''), will be employed as indices. Then the only terms in $\mathbf{H}$ nondiagonal in v will be of order ϵ, arising from $\epsilon\mathbf{H}'''$. In this case Van Vleck has shown[1] that $\mathbf{H}$ may be transformed so that the terms off-diagonal in v are reduced to order ϵ^2; they can then be neglected if energies accurate to terms in ϵ^3 are desired. Van Vleck's result is that the new matrix $\mathfrak{H}$ has the elements

$$\mathfrak{H}_{vr,\,v'r'}=\text{order }\epsilon^2 (v\neq v')$$

$$\mathfrak{H}_{vr,\,vr'}=W^0{}_v+H''_{rr'}+\epsilon H'''_{vr,\,vr'}+\epsilon^2\sum_{v'',\,r}{}' H'''_{vr,\,v''r''}H'''_{v''r'',\,vr'}/(W^0{}_v-W^0{}_{v''}), \tag{2}$$

where $W_v{}^0=H'_{vv}$ and the sum is over all states $v''r''$ except those with $v''=v$. Let the coupling term H''' have the form

$$\mathbf{H}'''=\sum_i {}_i\mathbf{A}'\,{}_i\mathbf{A}'', \tag{3}$$

in which ${}_i\mathbf{A}'$ is a function only of the variables of $\mathbf{H}'$ and ${}_i\mathbf{A}''$ is a function only of the variables of $\mathbf{H}''$. Then the elements of $\mathfrak{H}$ diagonal in v may be represented as submatrices:

$$\mathfrak{H}_{vv}=W^0{}_v\mathbf{E}+\mathbf{H}''+\epsilon\sum_i {}_iA'_{vv}\,{}_i\mathbf{A}''+\epsilon^2\sum_{ij}\{\sum_{v''}{}' {}_iA'_{vv''}\,{}_jA'_{v''v}/(W^0{}_v-W^0{}_{v''})\}\,{}_i\mathbf{A}''\,{}_j\mathbf{A}''. \tag{4}$$

Here $\mathbf{E}$ is the unit matrix.

[1] J. H. Van Vleck, Phys. Rev. **33**, 484 (1929); O. M. Jordahl, *ibid.* **45**, 87 (1934). The terms of order ϵ^3 can also be found.

The Partition Function

If W_{vr} is an energy level for the complete problem, the partition function Z is

$$Z=\sum_{v,\,r}\exp(-W_{vr}/kT), \tag{5}$$

where k is Boltzmann's constant and T the absolute temperature. In the case given here this may be approximated by the expression

$$(1/\sigma h^s)\sum_v \exp(-W_v{}^0/kT)\int\cdots\int\exp(-\mathfrak{H}''_v/kT)dqdp, \tag{6}$$

in which σ is the so-called symmetry number, h is Planck's constant, s is the number of coordinates involved in $\mathbf{H}''$, q represents these coordinates, p represents the corresponding conjugate momenta, and $\mathfrak{H}_v''$ is the classical analogue of the double-primed part of $\mathfrak{H}_{vv}$; that is,

$$\mathfrak{H}''_v=H''+\epsilon\sum_i {}_iA'_{vv}\,{}_iA''+\epsilon^2\sum_{ij}\{\sum_{v''}{}' {}_iA'_{vv''}\,{}_jA'_{v''v}/(W^0{}_v-W^0{}_{v''})\}\,{}_iA''\,{}_jA''. \tag{7}$$

In using this, H'' and ${}_iA''$ are regarded as classical functions of q and p analogous to the operator functions $\mathbf{H}''(\mathbf{p},\mathbf{q})$ and ${}_i\mathbf{A}''(\mathbf{p},\mathbf{q})$. Since $\mathfrak{H}_v''$ may be a function of v, it is necessary to include the integral inside the summation over v. In going over to Eq. (6) the sum over the quantum-mechanical levels determined by the matrix $\mathfrak{H}_{vv}-\mathbf{W}_v{}^0E$ has been replaced by an integral involving a classical Hamiltonian function which is the classical analog of $\mathfrak{H}_{vv}-W_v{}^0\mathbf{E}$.

An Illustration: Rotation-Vibration Coupling

A good approximation for the Hamiltonian operator for the vibration and rotation of a symmetrical top molecule is[2]

$$\mathbf{H}=\mathbf{H}'+\mathbf{H}''-(1/C)\mathbf{p}_z\mathbf{P}_z. \tag{8}$$

Where $\mathbf{H}''$ is the ordinary rotational operator for

[2] J. H. Van Vleck, Phys. Rev. **47**, 487 (1935); M. Johnston and D. M. Dennison, Phys. Rev. **48**, 868 (1935); E. B. Wilson, Jr., and J. B. Howard, J. Chem. Phys. **4**, 260 (1936).

a rigid symmetrical top, $\mathbf{H}'$ is the vibrational operator, and $\mathbf{p}_z$, $\mathbf{P}_z$ are the components of vibrational and total angular momenta along the symmetry axis. C is the moment of inertia about the symmetry axis.

Applying the general method, one gets

$$\mathfrak{H}_v''=H''-(1/C)(p_z)_{vv}P_z+(1/C^2)\times\{\sum_{v''}{}'(p_z)_{vv''}(p_z)_{v''v}/(W_v^0-W_{v''}^0)\}P_z^2. \quad (9)$$

Since many of the vibrational energy levels $W_{v''}^0$ of a symmetrical top molecule are degenerate, the term in P_z^2 requires further discussion. It is necessary to use the proper linear combinations of the wave functions for a degenerate level in calculating $(p_z)_{vv''}$, the correct combinations being those which make $(p_z)_{vv''}$ zero when v and v'' represent the same energy level but different states. When this is done it is seen that the term in P_z^2 is probably quite small in ordinary cases. Its effect is to modify the moment of inertia C which would occur in the rigid case.

$\mathbf{H}''$ has the form

$$\mathbf{H}''=\frac{1}{2A}(\mathbf{P}_x^2+\mathbf{P}_y^2)+\frac{1}{2C}\mathbf{P}_z^2, \quad (10)$$

where A is the moment of inertia about the x and y axes (perpendicular to the symmetry axis z) and $\mathbf{P}_x$, $\mathbf{P}_y$ are the components of total angular momentum about these axes, so that

$$\mathfrak{H}_v''=\frac{1}{2A}(P_x^2+P_y^2)+\frac{1}{2C'}P_z^2-\frac{1}{C}(p_z)_{vv}P_z, \quad (11)$$

where

$$\frac{1}{C'}=\frac{1}{C}+\frac{2}{C^2}\sum_{v''}{}'(p_z)_{vv''}(p_z)_{v''v}/(W_v^0-W_{v''}^0). \quad (12)$$

This can be inserted directly in the phase integral if the volume element $8\pi^2dP_xdP_ydP_z$ is used instead of $dqdp$, since P_x, P_y, P_z are momentoids, not true momenta.[3] To evaluate the integral it is convenient to make a transformation which eliminates the linear term in P_z; *viz*;

$$P_z=\mathcal{P}_z+(C'/C)(p_z)_{vv}. \quad (13)$$

The resulting integral is

$$(8\pi^2/\sigma h^3)\int_{-\infty}^{\infty}\int\int e^{-\mathfrak{L}/kT}dP_xdP_yd\mathcal{P}_z, \quad (14)$$

with

$$\mathfrak{L}=\tfrac{1}{2}\{[(P_x^2+P_y^2)/A]+(\mathcal{P}_z^2/C')-(C'/C^2)(p_z)_{vv}^2\}.$$

The complete partition function is therefore

$$Z=(8\pi^2/\sigma h^3)(2\pi kT)^{\frac{3}{2}}AC'^{\frac{1}{2}}\sum_v \exp\{-[W_v^0-\tfrac{1}{2}(C'/C^2)(p_z)_{vv}^2]/kT\}. \quad (16)$$

The effect of the coupling term is twofold: first it changes C to C' and second it adds a small correction to some of the excited vibrational energy levels. In practice both these effects are probably negligible. Certainly if the best values available for W_v^0 are those calculated by a simple normal coordinate treatment, there will be other corrections to W_v^0 of the same or greater magnitude. However, it is interesting to show that the thermodynamic properties are not much affected even though this coupling term produces a major change in the observed rotational spacing, up to 300 percent, in fact, in methane.

I should like to thank Dr. Fred Stitt and Dr. B. L. Crawford, Jr. for reading the manuscript. Another application of this method has been made by Dr. Crawford to the problem of molecules having several attached symmetrical tops.

[3] J. H. Van Vleck, *Electric and Magnetic Susceptibilities* (Oxford, 1932), p. 35.

Electrostatic Effects on Ionization Constants

E. C. BAUGHAN*
Princeton University, Princeton, New Jersey
(Received May 8, 1939)

The equation of Born for the self-energy of an ion is applied to the heats of ionization of acids and bases, following a treatment by Gurney. In this way the variations in these heats with temperature are quantitatively explained, and approximate ionic radii predicted. Further applications to the ionization of amino acids and the variation of dissociation constants as between different solvents are discussed.

I

IN a recent paper R. W. Gurney[1] has discussed the temperature variation of ionization constants. It is the object of this paper to point out that the theoretical considerations advanced by him may be developed in a more exact and simple way to allow of stricter comparison with experiment. His views may be summarized as follows: If we consider as typical ionization processes:

(1) $C_6H_5NH_3^+ + H_2O \rightleftarrows C_6H_5NH_2 + H_3O^+$,

(2) $CH_3COOH + H_2O \rightleftarrows CH_3COO' + H_3O^+$,

(3) $NH_3^+CH_2COOH + H_2O \rightleftarrows NH_3^+CH_2COO' + H_3O^+$,

(4) $H_2PO_4' + H_2O \rightleftarrows HPO_4'' + H_3O^+$.

Dissociations of type (1) do not involve the creation of a new electric field, but only the shift of charge from one ion to another ("isoelectric" dissociations). Type (2) requires the formation of the field due to the pair of ions, type (3) of the field due to the Zwitterion, and type (4) of the field due to a pair of ions with further electrical work necessary to separate the positively charged proton from the negative ion.

Now it appears from modern accurate measurements that dissociations of type (1) vary with temperature in the simple way:

$$\log K = A - B/T \qquad (1)$$

(where K is the ionization constant, T the absolute temperature, and A, B constants), which implies that the heat of ionization is constant. This appears from the measurements of Pedersen[2] on anilinium and *o*-chloranilinium, and of Everett and Wynne-Jones[3] on ammonium ions.

Dissociations of the other three types vary with temperature in a different way. Harned and Embree[4] have analyzed the data for several such reactions, and shown that the ionization constants rise with temperature to a maximum, and then decrease. The curves of log K against T are approximately parabolae, and the curves for the different acids and bases are superposable. These conclusions may be written:

$$\log K = \log K_m - p(t-\theta)^2, \qquad (2)$$

where K_m is the maximum value of the dissociation constant, attained at temperature θ, K is the value at temperature t, and p a constant for all acids and bases. That this equation, although a surprisingly good approximation, is not exact and p has not precisely the same value for all systems, is apparent from more detailed investigation.[5]

Gurney has supposed that in ionizations of these three types the work done in creating the field is given by the formula of Born:[6]

$$W = \frac{e^2}{2D}\left(\frac{1}{r_+} + \frac{1}{r_-}\right), \qquad (3)$$

where W is the work done to create the field due to the charges e on the two ions of radii r_+ and r_- in a medium of dielectric constant D. This very simple view has already led to a valuable interpretation of variations in dissociation constants from solvent to solvent,[7] and to an

* Former Jane Eliza Procter visiting Fellow at Princeton University. Now in London, England.

[1] R. W. Gurney, J. Chem. Phys. **6**, 499 (1938).

[2] Pedersen, Kgl. Danmske Vidensk. Selsk. Math-fys. Medd **14**, No. 9, **15**, No. 3 (1937).

[3] Everett and Wynne-Jones, Proc. Roy. Soc. (London) **169A**, 190 (1938).

[4] Harned and Embree, J. Am. Chem. Soc. **56**, 1050 (1934).

[5] Walde, J. Phys. Chem. **39**, 478 (1935).

[6] Born, Zeits. f. Physik **1**, 45 (1920).

[7] Wynne-Jones, Proc. Roy. Soc. (London) **140A**, 440 (1933).

TABLE I.

$T°C$	D	$1/D$	$-T\frac{\partial \ln D}{\partial T}$	X ($\times 10^3$)
0	88.31	0.01133	1.2886	3.270
5	86.28	.01159	1.3122	3.618
10	84.25	.01187	1.3358	3.986
15	82.30	.01215	1.3594	4.367
20	80.35	.01244	1.3830	4.765
25	78.50	.01274	1.4066	5.180
30	76.73	.01304	1.4303	5.611
35	74.89	.01335	1.4539	6.050
40	73.12	.01368	1.4775	6.532
45	71.44	.01400	1.5011	7.015
50	69.85	.01432	1.5247	7.514
55	68.14	.01467	1.5483	8.044
60	66.62	.01502	1.5719	8.590

approximate theory of solubility in various solvents.[8]

Gurney is thus able to provide a qualitative interpretation of the relationship found by Harned and Embree (Eq. (2)). His subsequent development does not allow of any exact test. These hypotheses will now be developed by the methods of classical thermodynamics, and it will be shown that they are in complete agreement with the experimentally observed variations in heats of ionization with temperature, and permit of comparison of the values of the ionic radii r_+ and r_- with those obtained by other methods.

II

We may put:

$$\Delta F^0 = -RT \ln K$$

(where K refers to infinite dilution so that all species are in their standard states, and ΔF^0 is the free energy difference in this state). Then

$$-RT \ln K = -RT \ln K_x + (\epsilon^2/2D)(1/r_+ + 1/r_-)$$

for an acid or base giving two ions, where this equation serves to define K_x. Hence

$$\ln K = \ln K_x - (\epsilon^2/2DRT)(1/r_+ + 1/r_-),$$

by differentiation

$$\frac{\partial \ln K}{\partial T} = \frac{\partial \ln K_x}{\partial T} + \frac{\epsilon^2}{2R}\left(\frac{1}{r_+}+\frac{1}{r_-}\right)\left(\frac{1}{DRT^2}+\frac{1}{D^2RT}\frac{\partial D}{\partial T}\right)$$

and since

$$\partial \ln K/\partial T = \Delta H/RT^2,$$

if $$\partial \ln K_x/\partial T \equiv \Delta H_x/RT^2$$

(ΔH = heat of reaction at constant pressure)

$$\left\{\begin{array}{l}\Delta H = \Delta H_x + c \cdot 1/D(1+T\partial \ln D/\partial T) \\ \text{where} \quad c = (\epsilon^2/2)(1/r_+ + 1/r_-)\end{array}\right. \quad (4)$$

A more rigorous derivation should contain a small term for the expansion of the solvent, which is, however, negligible compared with the uncertainties in $\partial \ln D/\partial T$. This equation may then be tested as follows: The experimentally determined values of ΔH for a given acid or base are plotted against $1/D(1+T\partial \ln D/\partial T)$ $(=X)$. If ΔH_x is independent of temperature over the ranges involved, as would be expected by analogy with dissociations of type (1), and the r's are also independent of temperature, the graph should be a straight line and the r's could be calculated from its slope.

The values for $X = 1/D(1+T\partial \ln D/\partial T)$ for water between 0° and 60° were taken from the data of Åkerlöf and Short.[9] These are in good agreement with other recent data given in Landolt-Börnstein's tables. (See Table I.)

The results of comparison of this Eq. (4) with experiment will now be given. For the exact test of the functional form we are confined to the very accurate data of Harned and his collaborators on the ionization constants of carboxylic (all of the aliphatic series) and some inorganic and amino acids. These were obtained

TABLE II. HCOOH = 2518 + 485,300X; H_2O = 16,045 + 490,200X; H_2PO_4' = 3090 + 454,000X.

	HCOOH		H_2O		H_2PO_4'	
T °C	ΔH_{OBS}	ΔH_{CALC}	ΔH_{OBS}	ΔH_{CALC}	ΔH_{OBS}	ΔH_{CALC}
0	+931	931	14,513	14,442	—	—
5	755	762	14,312	14,271	—	—
10	573	584	14,109	14,091	—	—
15	384	389	13,901	13,904	—	—
20	+189	206	13,692	13,709	+903	881
25	−13	+4	13,481	13,506	731	738
30	−221	−205	13,267	13,294	546	543
35	−436	−418	13,051	13,079	347	343
40	−657	−652	12,833	12,843	134	124
45	−884	−886	12,612	12,606	−92	−94
50	−1118	−1129	12,390	12,362	−334	−321
55	−1358	−1386	12,164	12,102	—	—
60	−1602	−1650	11,936	11,834	—	—

[8] Bjerrum and Larsson, Zeits. f. Physik. Chemie **127**, 358 (1927); Brönsted, Delbanco and Volqvartz, *Ibid.* **162A**, 128 (1932).

[9] Åkerlöf and Short, J. Am. Chem. Soc. **58**, 1241 (1936).

TABLE III.

ACID	$pK_{25}°$	ΔH_x	c	R (A)	REF
Formic	3.754	2,518	$4.85_2 \times 10^5$	0.68	10
Acetic	4.757	1,948	$3.90_3 \times 10^5$	0.85	a
n-Propionic	4.874	2,169	$4.44_3 \times 10^5$	0.75	b
n-Butyric	4.820	1,975	$5.14_0 \times 10^5$	0.65	c
Mono-chloracetic	2.861	1,135	$4.39_0 \times 10^5$	0.76	d
Glycollic	3.831	2,588	$4.65_7 \times 10^5$	0.71	e
Lactic	3.862	2,628	$5.18_0 \times 10^5$	0.64	f
Water	15.741	16,045	$4.90_2 \times 10^5$	0.68	g
H_2PO_4'	7.206	3,090	$4.54_0 \times 10^5$	0.74	h
HBO_2	9.236	5,966	$5.06_5 \times 10^5$	0.66	i
o-Chlorbenzoic	2.943	−1,868	$1.83_6 \times 10^5$	1.84	11, j
o-Nitrobenzoic	2.173	−2,284	$2.15_8 \times 10^5$	1.56	11, j

[a] Harned and Ehlers, J. Am. Chem. Soc. **55**, 652 (1933).
[b] Harned and Ehlers, J. Am. Chem. Soc. **55**, 2383 (1933).
[c] Harned and Sutherland, J. Am. Chem. Soc. **56**, 2039 (1934).
[d] Wright, J. Am. Chem. Soc. **56**, 314 (1934).
[e] Nims, J. Am. Chem. Soc. **58**, 987 (1936).
[f] Nims and Smith, J. Biol. Chem. **113**, 148 (1936).
[g] Harned and Hamer, J. Am. Chem. Soc. **55**, 2198 (1933).
[h] Nims, J. Am. Chem. Soc. **55**, 1946 (1933).
[i] Owen, J. Am. Chem. Soc. **56**, 1695 (1934).
[j] $pK_{25}°$ values from Dippy and Lewis, J. Chem. Soc. (London) 1426, (1937).

by an e.m.f. method involving no liquid junctions. Of these data perhaps the most accurate are those for formic acid, the heats for which were calculated by fitting the log K–T curves to empirical equations involving several parameters.[10]

These values for ΔH were plotted against X, and the best straight line drawn. The values of ΔH_{calc} were then taken from this line. Since $T\partial \ln D/\partial T$ is negative and greater than unity, ΔH decreases with temperature as required by experiment.

The values of ΔH_{calc} and ΔH_{obs} are given in Table II as are also the data for water and $H_2PO_4^-$ (type (4)). The agreement is practically perfect. In Table III are given the values of ΔH_x and c appropriate for all the dissociations of types (2) and (4) measured by this technique. The individual agreement is in all cases about as good as for the examples given. The scatter of the individual points is worst for monochloracetic acid, for which the less accurate quinhydrone electrode was used.

Of the earlier data, those of Schaller[11] are perhaps the only ones sufficiently systematic to test Eq. (4). These were done by the conductivity technique at several temperatures from 0° to 100° for various benzoic and cinnamic acids. Of these most have maxima in or near the range of experiment, and their variations in K are, therefore, small and of the same order as the experimental error. Some, *o*-nitro and *o*-chlor benzoic acids in particular, have maxima at much lower temperatures, and so the changes in the observed range are considerable. The heats were then estimated graphically for these two acids and plotted against X. Good straight lines were obtained, and hence the ΔH_x's and c's given in Table III.

The relationship between the empirical equation of Harned and Embree (Eq. (2)), and the equation for ΔH_x here developed may be most clearly shown by expressing ΔH_T (at a temperature T) in terms of θ, the temperature at which K is a maximum.

Eq. (2) yields at once

$$\Delta H = +2pRT^2(\theta - T). \tag{5}$$

Eq. (4) gives

$$\Delta H_T = \Delta H_x + c1/D_T\left(1+T\frac{\partial \ln D}{\partial T}\right)_T,$$

whence

$$\Delta H_\theta = 0 = \Delta H_x + c1/D_\theta\left(1+\theta\frac{\partial \ln D}{\partial T}\right)_\theta,$$

so that

$$\Delta H_T = c\left\{1/D_T\left(1+T\frac{\partial \ln D}{\partial T}\right)_T - 1/D_\theta\left(1+\theta\frac{\partial \ln D}{\partial T}\right)_\theta\right\}.$$

To get this into a comparable form, we must know the variation of D with temperature Åkerlöf and Short[9] find their results to be expressible by

$$\ln D = A - BT,$$

whence

$$\Delta H_T = ce^{-A}\{e^{BT}(1-BT) - e^{B\theta}(1-B\theta)\}.$$

Expanding the exponentials, and collecting terms, we get

$$\Delta H = ce^{-A}\sum_{n=2}^{\infty}\frac{B^n(\theta^n - T^n)}{n(n-2)!}. \tag{6}$$

By substituting the appropriate values of A, B and taking $\theta = 300°\text{K}$, $T = 320°$, it can easily be shown that this is given to within 1

[10] Harned and Embree, J. Am. Chem. Soc. **56**, 1042 (1934).
[11] Schaller, Zeits. f. physik. Chemie **25**, 497 (1898).

percent by the first term, so that

$$\Delta H \doteq ce^{-A}B^2(\theta^2 - T^2)/2. \qquad (6^1)$$

We may now consider the predictions of these two equations in the immediate neighborhood of θ (i.e. $T^2 \doteq \theta^2$, $\theta + T \doteq 2\theta$).

Eq. (5) gives

$$\Delta H = 2pR\theta^2\Delta\theta$$

and Eq. (6^1)

$$\Delta H = ce^{-A}B^2\theta\Delta\theta \qquad (7)$$

(where $\Delta\theta = \theta - T$), so that, if Harned and Embree's equation is to be approximately valid, c must increase proportionally to θ. The low values for c for the substituted benzoic acids support this roughly. But it can be seen that p depends on c and θ, and so cannot be simply interpreted in terms of either. Most of the acids in Table III have θ between 270° and 320° Absolute, so that the approximate validity of Eq. (2) can be understood. As, however, p is not exactly the same for all acids,[5] further discussion is hardly profitable.

It is clear then that a formula

$$\log K = A - B/T - C/DT \qquad (8)$$

(where A, B, C are constants for each acid) fits the data well and is, at any rate, a valuable interpolation formula. We may now consider the values of the ionic radii which these graphs would predict. The individual radii r_+ and r_- are not, in general, known. But we may define a mean radius R by $2/R = 1/r_+ + 1/r_-$, and obtain this from the appropriate values of c. (In Table III, c is in calories per mole; taking the proper values for the electronic charge and Avogadro's number, and remembering that W in Eq. (1) is in ergs per molecule, then $2/R = 602c$, where R is in cm.)

By this means the values (in A) of R given in the fourth column of Table III were calculated. These values, though probably too small, are of the right order. It is remarkable that R should vary so little over the series formic -*n*-butyric acids. This would suggest that the charge is localized on one oxygen atom, or, at any rate, on the carboxyl group only.

Other estimates of the radii may be obtained in the following ways:

(1) From crystal lattice data the radius of the O'' ion is about 1.40A. The covalently linked $=O$ has, in the gas phase, a radius 0.60A. The ion $-O'$ should presumably be intermediate in size, i.e. of radius about 1.0A. If the charge were "smeared" over the whole carboxyl group, the radius would be larger.[12] It is possible that the high values of R for the two *o*-substituted benzoic acids are due to some such resonance "ortho-effect."

(2) The data on activity coefficients of acetic acid in salt solutions[13] are well represented by the Debye-Huckel equation with the mean distance of closest approach 3.5A, i.e. a radius of 1.75A. This is not strictly comparable with the radii here defined and is probably larger, particularly if collision between ions is frequently prevented by intervening water molecules.

(3) Carboxylate ion mobilities are, in general, about 35 in the conventional units at 25°. This would, assuming Stokes' law, imply a radius of 2.6A, which should represent the maximum cross section of the ion, not the radius of the charge bearing group. This value is, therefore, again not strictly comparable with the values in Table III. It follows that, although the ionic radii there given seem rather small, no independent estimate of their value is obtainable.

The possibility of using Born's equation implies the neglect of the effects due to covalent forces between the ions and solvent molecules, and to dipole saturation. The first of these would affect only the ΔH_x in formula (4), unless the specific heat differences involved were large. The simple behavior observed for "isoelectric" dissociations makes this improbable. It is, however, clear that such effects enter directly, and not, as here, simply through specific heat effects, into expressions for heats of transfer and integral heats of dilution for ions. These heats could hardly be expected, therefore, to be given by the simple Born equation.

The dipole effects have been considered by Webb.[14] His treatment predicts that Born's equation could not be valid for any ion of radius less than about 10A, and that the self-energy should be larger by a factor depending on the

[12] Radii from Sidgwick, *The Covalent Link in Chemistry* (Cornell University Press, 1933), p. 85.

[13] Harned and Robinson, J. Am. Chem. Soc. **50**, 3157 (1928).

[14] Webb, J. Am. Chem. Soc. **48**, 2589 (1926).

size of the ion, which would be about 10 for 1A radius. These conclusions depend, however, on the assumption that the solvent dipoles are free to rotate without doing any work except against the electric field. It has since been shown by Debye[15] that this assumption yields a value for the change of dielectric constant with field strength for water about 3500 times as large as that observed. For ether the agreement is almost quantitative. Debye accounts for this abnormal behavior of water by assuming a barrier of about $10kT$ which must be surmounted on rotation, and this value is supported by the abnormal orientation polarization. It has also been pointed out that the same assumption of restricted rotation will account well for the thermodynamic peculiarities of typical "associated" solvents.[16]

It is clear, therefore, that Webb's treatment would exaggerate enormously the effects in "associated" solvents while for normal solvents his conclusions should, presumably, be valid. Hence, Born's equation should be more nearly exact the smaller the "free angle ratio" of the solvent. Unfortunately no data on the variation of heats of dissociation with temperature exist for systems in any pure solvents other than water, so that this conclusion cannot be tested. The results obtained for acetic acid in water-dioxane and water-methanol mixtures[17] can simply be explained by assuming preferential concentration of water around the ions.

This view, that saturation effects may be neglected, has received further support from the recent work of Kirkwood and Westheimer[18] on the ratio of the two dissociation constants of a dicarboxylic acid. They have shown that, if a correction be applied to Bjerrum's simple treatment to take into account the field strength inside the cavity in the solvent caused by the molecule, the lengths of hydrocarbon chains predicted are in excellent agreement with those to be expected from free rotation, even if the chain length is small. This again suggests that the electric saturation and similar effects are not very large.

III

We may now attempt to extend these conclusions to the data for the two ionizations of aminoacids. The two processes are (for glycine):

$$(K_a)\ NH_3{}^+CH_2COOH + H_2O \rightleftharpoons NH_3{}^+CH_2COO' + H_3O^+$$

$$(K_b)\ NH_3{}^+CH_2COO' + H_2O \rightleftharpoons OH_3{}^+ + NH_2CH_2COO'.$$

Calculation on the lines of the preceding treatment would require the estimation of the electrostatic field energy due to the dipole Zwitterion. For the work done in establishing the dipole μ in the center of a sphere of radius a, Martin[19] has derived the formula:

$$W = \mu^2/3a^3(1/D). \qquad (9)$$

This formula neglects the field in the dipole sphere itself, which has been taken into account in later treatments,[20] and assumes also that the dipole is located at a point, and so is only approximate. These more correct formulae involve the "internal dielectric constant" of the sphere, about which little is known, various values from 1 to 3 having been suggested for it. Since it has been shown[21] that the formula of Martin is in as good agreement with the experi-

TABLE IV. *Heats of first dissociation of amino acids.*

	GLYCINE*		*dl*-LEUCINE†	
$T°$	ΔH_{OBS}	ΔH_{CALC}	ΔH_{OBS}	ΔH_{CALC}
1	—	—	1510	1524
10	1562	1596	—	—
12.5	—	—	1210	1188
15	1439	1453	—	—
20	1305	1304	—	—
25	1159	1149	800	784
30	1000	987	—	—
35	829	827	—	—
37.5	—	—	320	337
40	646	642	—	—
45	449	460	—	—
50	—	—	−250	−154

* glycine, reference 22.
† *dl*-leucine, reference 24.

[15] Debye, Physik. Zeits. **36**, 193 (1935). Cf. also Malsch, *Ibid.* **30**, 837 (1929); Gundermann, Ann. d. Physik **6**, 545 (1930).
[16] Kincaid and Eyring, J. Chem. Phys. **6**, 620 (1938).
[17] Harned and Embree, J. Am. Chem. Soc. **57**, 1669 (1935); Harned and Kazanjian, J. Am. Chem. Soc. **58**, 1812 (1936).
[18] Kirkwood and Westheimer, J. Chem. Phys. **8**, 506, 513 (1938).
[19] Martin, Phil. Mag. **8**, 547 (1929).
[20] R. P. Bell, J. Chem. Soc. (London), p. 1371 (1931); Trans. Faraday Soc. **27**, 297 (1931); Kirkwood, J. Chem. Phys. **2**, 351 (1934).
[21] W. H. Banks, Trans. Faraday Soc. **33**, 215 (1937).

TABLE V. *Values of ΔH_x, c for first dissociations of amino acids.*

	ΔH_0	c	REF.
Glycine	3091	3.75×10^5	22
dl-alanine	2365	3.27	23
dl-alanine	2866	4.02	24
dl-amino *n*-butyric	2700	4.66	24
dl-amino *n*-valeric	2800	4.40	24
dl nor-leucine *dl* aminoiso-butyric	2850	4.53	24
dl valine	2500	4.72	24
dl leucine	2770	4.66	24
dl isoleucine	2770	4.90	24

mental data on free energies of transference of acetic acid, monochloracetic acid, and ammonia between various solvents as are these more complex formulae, with the internal dielectric constant taken as unity, it has been adopted for the provisional calculations which follow.

For the first process (K_a), it is evident that this formula leads to Eq. (4) valid for dissociation into a pair of ions, but with $c=\mu^2/3a^3$ instead of $(e^2/2)(1/r_+ + 1/r_-)$. The data for the ΔH's can, therefore, be plotted precisely as before. We have available data for glycine,[22] for alanine[23] and for alanine and seven other α-amino acids.[24] The test of the Eq. (4) with experiment for glycine and *dl*-leucine is shown in Table IV, and in Table V are given the values of ΔH_x and c appropriate for all these aminoacids. The considerable discrepancy between the two sets of values for alanine indicates that these data are perhaps not sufficiently accurate in themselves for a crucial test of the functional form of ΔH with respect to T. The following further points may be noticed:

(1) If we take $\mu=15\times10^{-18}$ e.s.u. for glycine, then we arrive at $a=1.45\times10^{-8}$ cm for glycine instead of the proper value 3×10^{-8}.[25] This is perhaps as good agreement as could be expected in view of the theoretical uncertainties mentioned.

(2) The dipole moment of the α-aminoacids will probably remain constant when the chain is sufficiently long. It follows that the radius a must remain about the same, since the c's in Table V are all approximately equal, for aminoacids with chains longer than that of alanine. This points to localization of the dipole at the end of the molecule. Banks[21] has pointed out that this conclusion is necessitated by the data on the transference energies of some aminoacids between water and *n*-butyl alcohol, and of several α-bromoacids between various solvents. The agreement of these two methods of approach supports the view that the theory here developed is essentially correct—even if too crude for exact numerical prediction of the size of the dipole sphere. It would be of great interest to measure the temperature coefficients of ionization of β, $\gamma\cdots$ aminoacids.

(3) In the ionization of a carboxylic acid the two dipoles RCOOH and H_2O disappear. The corresponding electrostatic term in the free energy, and hence in the heat of ionization, can then be estimated from the known values of the μ's. Taking the a's as 1A, this involves only a 2 percent correction to the c's, and as this correction varies inversely as the cube of the a's, and as they are certainly considerably larger than 1A, it is negligible for the ionization of these acids.

The more accurate treatment of Kirkwood and Westheimer[18] gives the electrostatic energy of a dipole as $f_1/D+f_2/D_2$, where f_1/D is the term corresponding to the effect of the solvent (of dielectric constant D) and f_2/D_2 the term for the electrostatic effect of the cavity (internal dielectric constant D_2) in the solvent due to the molecule. For explicit expressions for f_1, f_2 see their papers.

The first of these terms we have replaced by Martin's approximation. The second, and larger (since f_1, f_2 are of the same order, and $D_2 \ll D$), will be independent of temperature if D_2 is. Hence, the dipole effects will be very much larger than here estimated, but will affect the ΔH_x's of our formula (4) almost exclusively. Examination of the ΔH_x, c values in Table III for acetic and monochloracetic acids shows the c's to vary by only 10 percent, although the ΔH_x's vary by a factor of two. Since the difference between the pK's of these acids is well accounted for by Kirkwood and Westheimer's detailed electrostatic theory, our conclusion, that the

[22] Owen, J. Am. Chem. Soc. **56**, 24 (1934).
[23] Nims and Smith, J. Biol. Chem. **101**, 401 (1933).
[24] Smith, Taylor and Smith, J. Biol. Chem. **122**, 109 (1937).
[25] E. J. Cohn, Chem. Reviews **19**, 241 (1936).

dipole effects on the c's in Eq. (4) are small for carboxylic acids, is justified even on their more detailed picture.

(4) We may now consider the heats ΔH_b of the second stage of ionization of aminoacids. Here the Zwitterion disappears, and a pair of ions is formed. Examination of the c's in Tables III and V shows that the electrostatic work done in these processes will be almost equal. Hence, the ΔH for the second process will vary but slightly with temperature. This conclusion is supported by the data of Smith, Taylor and Smith,[24] which show the deviations from constancy to be small for all six aminoacids measured. Thus they give for alanine at 1°, 12.5°, 25°, 37.5°, 50° the pK_b values 10.586, 10.225, 9.866, 9.548, 9.256; a constant ΔH of $-10{,}920$ cal. would predict 10.579, 10.228, 9.877, 9.554, 9.256. This very small variation in ΔH, which these results establish (the constant heat predictions are probably within the experimental error), is just what the theory here developed would predict.

IV

Since $\ln K = \ln K_x - c/DRT$ at any one temperature T, K_x can be calculated from a knowledge of c and D, and has the significance of a dissociation constant at infinite dielectric constant. The K_x's so predicted have not the significance of dissociation constants where no electrostatic work is done on separating the ions for the following reasons. We may regard the ionic sphere (carboxyl or oxygen) as surrounded to an extent q by the solvent of dielectric constant D, and to an extent s by the rest of its own molecule. The dielectric constant Z of this will presumably be roughly that of a paraffin, and so independent of temperature. Hence, the simple Born expression must be replaced by

$$\frac{e^2}{2}\left(\frac{1}{r_+}+\frac{1}{r_-}\right)\left(\frac{q}{D}+\frac{s}{Z}\right).$$

This will then, if Z is independent of temperature give agreement with Eq. (4), but with $1/R$ replaced by q/R. A simple geometric interpretation of q/s as the ratio of solid angles subtended at the center of the ion by the solvent and the rest of the molecule, should give $q=0.7$–0.8. This would make the ionic radii in Table III too large by about 20 percent. As however

TABLE VI.

	log $K_{H_2O,\ 25°}$	log $K'_{25°,\ H_2O}$	log K_x	log K_x'	log K_∞'	log K_{II}'
Acetic	−4.757	0	−1.11	0	0	0
Formic	−3.754	+1.00	+0.79	1.90	0.75	0.88
Glycollic	−3.831	+0.93	+0.52	1.63	0.70	0.83
Mono-chloracetic	−2.861	+1.90	+1.25	2.36	1.83	1.83
o-chlorbenzoic	−2.943	+1.82	−0.12	0.99	2.05	2.09
o-nitrobenzoic	−2.973	+2.58	−1.23	−0.12	2.75	2.81

All K_∞' values from Minnick and Kilpatrick (reference 26), except formic and *o*-nitrobenzoic from Wynne-Jones (reference 7).

$Z \ll D$, $1/Z \gg 1/D$, and the true dissociation constants for zero electrostatic work will be mainly determined by the unknown s/Z term.

This simple picture would make this correction independent of solvent. The values of K_x should, therefore, be directly comparable with the K_∞ values of the theory of Wynne-Jones.[7] He has shown that $\log K_{A,D} - \log K_{B,D}$ should be linear in $1/D$ where $K_{A,D}$, $K_{B,D}$ are the dissociation constants of the acids A, B in a solvent of dielectric constant D. Extrapolation to $1/D=0$ gives K_∞. This equation follows from the equation of Born if the ionic radii of the anions are independent of solvent, and if "exchange" forces can be neglected. By considering, as he does, only the differences in the log K's one avoids the difficulties due to chemical solvation of the proton, and to uncertainty as to the concentration scale on which free energy differences should be expressed to be comparable in different solvents, and the exchange effects are reduced to the differences as between various acids. This equation has been recently investigated by Minnick and Kilpatrick,[26] who show it to be valid for similar solvents such as water, the alcohols and dioxane-water mixtures if $D>25$ or so, but to fail for solvents of different chemical type or lower D, in agreement with the conclusions of Section II.[27]

In Table VI are given the values of log K_∞' (referred to acetic acid as a standard; taking Minnick and Kilpatrick's value of log K_∞ benzoic $-\log K_\infty$ acetic as $+0.65$), log K_x predicted from the data in Table III, and log K_x' these adjusted to log K_x acetic as zero. It can be seen that the agreement is bad, and a more exact treatment of the whole problem is needed. (In the

[26] Minnick and Kilpatrick, J. Phys. Chem. **43**, 259 (1939).

[27] Cf. also the data of Verhoek, J. Am. Chem. Soc. **58**, 2577 (1936) on acid strengths in formamide.

second column are given the log K's for water at 25° adjusted to this standard for comparison). In view of this discrepancy which might be expected from the discussion in Section II, it is surprising that a single value Y can be found for the dielectric constant for which the differences between the log K's predicted from the equation $\log K_Y = \log K_X - c/YRT$, are equal to the differences between the log K_∞'s. These values (with $Y=87.7$) are given in the last column of Table VI.

This correlation implies that the shift in the ratio of two dissociation constants in water on going at 25° ($1/D=0.01274$) to an imaginary solvent of $1/D=0.0114$, the slope of the $\log K - 1/D$ graphs being obtained from the temperature coefficients in water, is the same for all the dissociation constants listed, as the shift on going from water at 25° to an imaginary solvent with $1/D=0$, if the slopes are taken from the differences in log K' for different hydroxylic solvents. In terms of the Born equation, this means that the ionic radii to be obtained from the solvent shifts, are greater by a factor of about 9 than those from the temperature coefficients in water, and that this factor is the same for all acids. In this connection, it is suggestive that the values for ionic radii obtained from the ratio of the differences in log K for uncharged and singly positively charged acids in water and *m*-cresol, would have to be given the high value 5A, if this ratio were interpreted by Born's equation.[28] Further data are needed to be sure that this correlation is not numerical coincidence.

The views advanced by Gurney provide therefore a valuable approximation to the problem of electrostatic influences on ionic dissociation, and predict values of the ionic radii of the correct order of magnitude. Exact test of these values is not at present possible. The equations deduced for the variation in heats of ionization with temperature are supported by the experimental data to within their probable error. The radii so obtained do not, however, account for changes in dissociation constant from solvent to solvent.

The author wishes to express his thanks to Princeton University for a Procter Visiting Fellowship during his tenure of which this paper was written, to Professor H. S. Taylor for extending to him the hospitality of his Institute, and to Professors H. Eyring and H. S. Harned, and Dr. F. H. Westheimer for discussion of the points raised.

[28] Brönsted, Delbanco and Tovborg-Jensen, Zeits. f. physik. Chemie **169A**, 361 (1934).

OCTOBER, 1939 JOURNAL OF CHEMICAL PHYSICS VOLUME 7

The Effect of Temperature on the Structure of Mercury

ROBERT NEILSON BOYD* AND HELMUT R. R. WAKEHAM
Department of Chemistry, University of California, Berkeley, California

(Received May 29, 1939)

X-ray diffraction patterns of mercury at eight temperatures ranging from −36°C to 250°C have been obtained using Mo $K\alpha$ radiation. The x-ray beam was diffracted from an open mercury surface using the small angle of incidence of 4° 11′, thus permitting observation of a previously unreported peak at a diffraction angle of about 10°. Fourier analyses of the intensity curves gave distribution functions showing the expected shifting and broadening of the maxima with increasing temperature. A small subsidiary peak, which changes position with temperature more rapidly than the others, occurs between the first and second main concentrations of atoms.

INTRODUCTION

THE atomic distribution functions for liquid sodium[1] and potassium[2] have been investigated over a considerable portion of their liquid ranges, but no attempt has been made to investigate mercury above room temperature. Coster and Prins[3, 4] and Debye and Menke[5, 6]

* Abraham Rosenberg Research Fellow.

[1] F. H. Trimble and N. S. Gingrich, Phys. Rev. **53**, 278 (1938).

[2] C. D. Thomas and N. S. Gingrich, J. Chem. Phys. **6**, 411 (1938).

[3] D. Coster and J. A. Prins, J. de phys. et rad. **9**, 153 (1928).

[4] J. A. Prins, Physik. Zeits. **30**, 525 (1929).

[5] P. Debye and H. Menke, Erg. D. Tech. Röntgenkunde, II.

[6] H. Menke, Physik. Zeits. **33**, 593 (1932).

made studies of the structure of mercury at room temperature, and Danilov and Neimark[7] took x-ray photographs near the freezing point (−38.87°C) but made no determination of the atomic distribution. Since mercury is frequently considered as a classical example of a monatomic liquid, it is of interest to investigate this function at various temperatures for the information it may give concerning interatomic forces and for the data it may supply to assist in evaluating existing theories of the liquid state. Such information promises to be very enlightening.[8]

Analysis of x-ray diffraction patterns gives a direct determination of the atomic distribution function. It is necessary, however, to have reliable values of corrected relative scattering intensities at large angles for which interferences no longer play a large part in the pattern; the observed pattern may then be placed on the basis of units of intensity per electron. From this point straightforward calculations using the methods outlined by Zernike and Prins[9] and Debye and Menke[5] lead to the distribution of atoms about a given central atom.

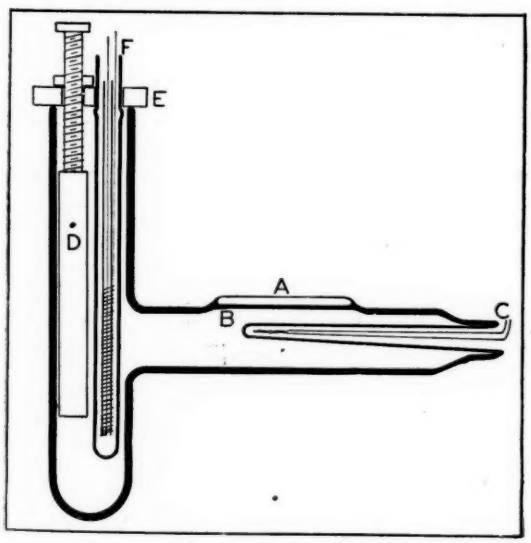

FIG. 1. Mercury container with open surface at *A*.

[7] V. I. Danilov and V. E. Neimark, J. Exp. Theoret. Phys. (U.S.S.R.), **5**, 724 (1935).
[8] J. H. Hildebrand and S. E. Wood, J. Chem. Phys. **1**, 817 (1933); J. H. Hildebrand, J. Chem. Phys. **7**, 1 (1939).
[9] F. Zernike and J. A. Prins, Zeits. f. Physik **41**, 184 (1927).

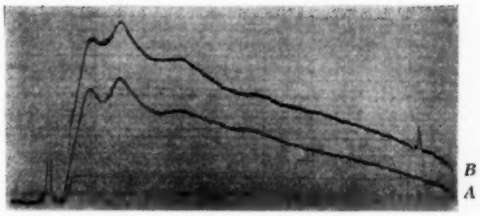

FIG. 2. Microphotometer tracings for mercury diffraction at 30°C. *B*, curve for eight-hour exposure; *A*, curve for four-hour exposure.

EXPERIMENTAL

Diffraction patterns of liquid mercury at −36°C, −34°C, 0°C, 30°C, 75°C, 125°C, 175°C and 250°C have been obtained using Mo $K\alpha$ radiation filtered through a ZrO_2 layer. The method used was essentially the same as that employed by the previous workers,[3, 5] that is, diffraction was obtained by allowing the x-ray beam to impinge on the mercury surface. The angle of incidence on the level mercury surface was carefully measured and found to be 4° 11′. This angle was considerably smaller than that used by all previous investigators and made possible the observation of an intensity maximum appearing at an angle of diffraction of about 10°, not previously reported. (See peak on intensity curve in vicinity of $(\sin\theta)/\lambda = 0.1 - 0.15$, Fig. 3.)

Mercury samples were contained in the tube shown in Fig. 1, and diffraction occurred in the mercury which was made to bulge out of the open part, *A*, by means of the plunger, *D*. The opening was roughly rectangular, about 3 cm by 5 cm in dimensions, and was large enough to give a flat mercury surface. This was necessary for application of the absorption correction calculated by Debye and Menke.[5] The temperature was measured by means of a copper-constantan thermocouple with one junction in the small tube, *B-C*, in the mercury. An electrical heating element, *F*, used for high temperatures was replaced for the low temperatures by a U-tube attached to a refrigerating system in which circulated acetone cooled in an acetone-solid CO_2 mixture. The mercury tube was mounted in front of a specially constructed x-ray camera so that the x-ray beam was diffracted from the mercury at the exact center of curvature of the film in the camera. The

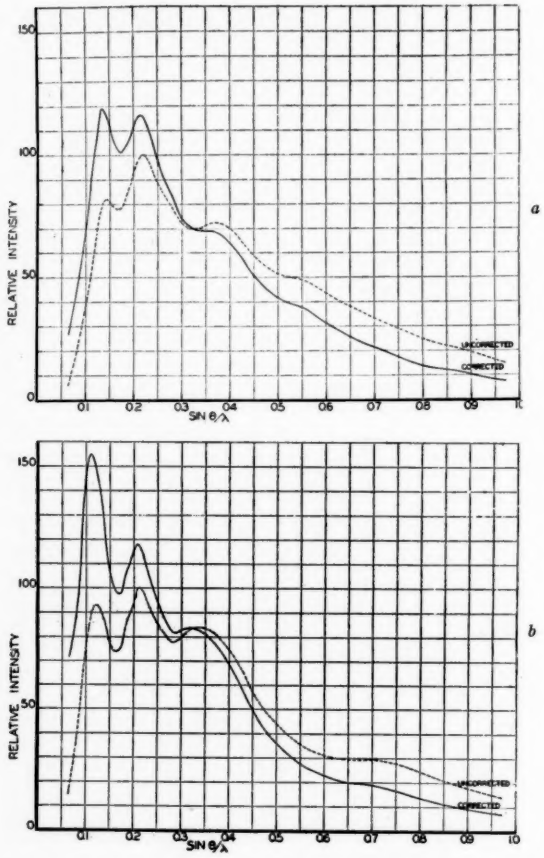

FIG. 3. Relative intensity distribution for mercury diffraction at 34°C and 175°C. Uncorrected (broken line) and corrected for polarization and absorption (solid line). (a) Temperature 34°C. (b) Temperature 175°C.

radius of curvature of the film was 7.00 cm. A nickel foil placed halfway between the sample and the film served to cut out the L radiation from the mercury.

The formation of dew or frost on the mercury was prevented at the lower temperatures by blowing on the surface a stream of air dried by by passing through a liquid-air trap. At high temperatures mercury vapor was removed by means of a funnel-shaped tube inverted a short distance over the mercury and attached to a vacuum. Mercury oxide which was formed was sucked off periodically with a tipped tube and the level restored by means of the plunger.

Using new type Agfa film[10] exposures of eight or ten hours gave photographs of proper densities when the tube was operated at 30 kv and 20 ma. Half the film was given half the exposure to facilitate relative intensity conversion with a correction of variations of film development, and the microphotometer tracing all in one step. Both parts of the film were microphotometered on the same plate, as shown in Fig. 2, which is for mercury at 30°C (A is four hours, B is eight hours); and intensity measurements were made with a ratiometer described by Langstroth,[11] using the half-time tracing to make the calibration curve. The relative intensity curves were corrected for absorption and polarization in the usual manner. Sample uncorrected and corrected curves for mercury at −34°C and 175°C are shown in Fig. 3.

Application of the Fourier Method

The application of the Fourier method requires that the experimental scattering intensity curves, corrected for polarization and absorption, be placed on an absolute basis, in electron units per atom. To do this it is considered that the scattering becomes independent at a large value of $(\sin\theta)/\lambda$ and equal to the sum of the modified and independent unmodified scattering of N atoms. This sum is readily determined from tables of f and Σf_n^2,[12] in electron units per atom.

The experimental curve is then placed on an absolute basis by multiplying the arbitrary units

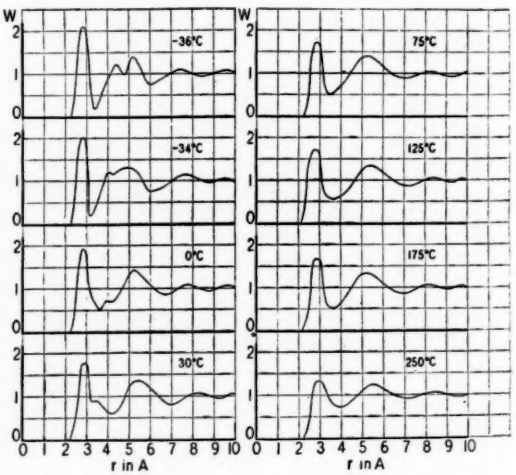

FIG. 4. Menke's W function for mercury.

[10] C. Gamertsfelder and N. S. Gingrich, Rev. Sci. Inst. **9**, 154 (1938).

[11] G. O. Langstroth, Rev. Sci. Inst. **5**, 255 (1934).

[12] A. H. Compton and S. K. Allison, *X-Rays in Theory and Experiment* (D. Van Nostrand, 1935), pp. 781, 782.

by a constant. This constant is the ratio of the sum of the modified and independent unmodified intensities (in electron units per atom) at a large value of $(\sin\theta)/\lambda$ to the experimental intensity (in arbitrary units) at the same point. The correction for modified scattering was almost negligible due to the high atomic number of mercury. The value $(\sin\theta)/\lambda=0.971$ was chosen in practically all cases.

Warren and Gingrich[13] have outlined the theory of the mathematical treatment. The equation used is

$$4\pi r^2\rho(r)=4\pi r^2\rho_0+(2r/\pi)\int_0^\infty si(s)\sin rs\,ds, \quad (1)$$

where $4\pi r^2\rho(r)dr$ is the number of atoms between the distances r and $r+dr$ for a given central atom, ρ_0=average density of scattering matter in atoms per unit volume, $s=4\pi(\sin\theta)/\lambda$, $i(s)=(I/N-f^2)/f^2$, I/N=unmodified intensity per atom, and f=atomic scattering factor.

The function $si(s)$ was plotted against various scales of s, and the integral in Eq. (1) evaluated by means of a Bardsley harmonic analyzer. Any variations caused by the choice of $(\sin\theta)/\lambda$ would be long period ones affecting only the first few harmonics, which are known to be zero from the almost complete impenetrability of the atoms. From these values, the probability function of Menke, W,[6] was determined (Fig. 4) and finally values of $4\pi r^2\rho(r)$ as a function of r were obtained (Fig. 5).

Discussion

Since no calculation has been made for the distribution of mercury atoms at any other temperature than room temperature, it is not possible to make a direct comparison between the results appearing here and those of other authors. The distribution obtained for 30°C corresponds approximately to that obtained by Coster and Prins[3] and Debye and Menke,[5] with the exception of the small subsidiary peak which appears in the vicinity of 4A. The first maximum in the experimental intensity pattern has not been mentioned by investigators on this liquid; their experimental arrangements appear to be such that it was impossible or unlikely for them to observe such a peak in the intensity pattern.

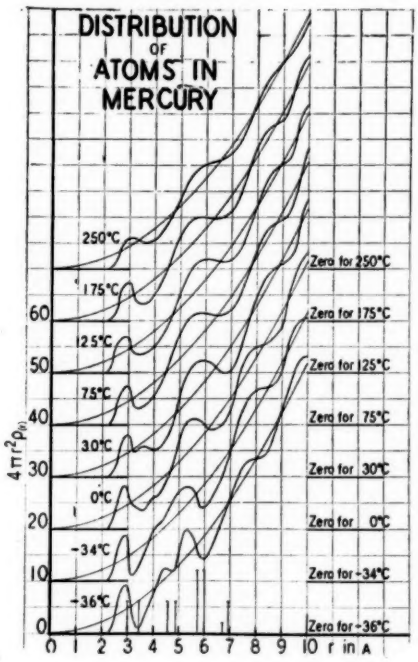

FIG. 5. Radial density distribution of atoms about any one atom in mercury. Solid lines below −36°C curve show distribution in the solid.

The fact that this first maximum had not been reported was known when it was first observed and attempts were made to eliminate it. The suggestion that it might have been due to gas scattering led to taking photographs with a stream of helium passing through the camera, but this failed to solve the discrepancy. The convincing argument in favor of its being due to scattering from the liquid mercury was that the peak was found to shift in relation to the other peaks when the temperature was changed. (See Fig. 3.)

In Fig. 5 are given the atomic distribution curves for the various temperatures, together with the corresponding $4\pi r^2\rho_0$ curves. It can be seen in every case that the actual distribution approaches the average at the larger distances, and more rapidly as the temperature increases. The peaks become broader and less pronounced for the higher temperatures, and the positions of the maxima shift to larger distances in accordance with the increased expansion of the liquid.

[13] B. G. Warren and N. S. Gingrich, Phys. Rev. **46**, 368 (1934).

The area under the first peak gives the number of atoms which may be considered as closest neighbors of any given atom, though there is a constant interchange of atoms in the liquid. The rhombohedral structure of solid mercury[14] gives six atoms as closest neighbors, as is shown by the solid distribution indicated by the vertical lines in Fig. 5. As might have been expected, six atoms were found for the liquid for $-36°$C, and likewise for all the higher temperatures. However, in considering the structure of a liquid, a distribution curve as presented here should be regarded as a measure of the probability of finding an atomic center at some particular distance.

This probability, and the changes with temperature, are very clearly shown in the curves of Fig. 4. The line, $W=1$, corresponds to $4\pi r^2\rho_0$. Again, it can be seen that the peaks broaden and decrease in height, while the minima rise, as the temperature increases, indicating a less pronounced structure as the atomic motions become more violent. All the curves are similar in displaying a trend toward a value of unity at large distances, and for the high temperatures the trend is evident at smaller distances. A W curve for a completely random arrangement of the atoms would show a rapid rise to unity, and outside of a possible small peak would remain unity. The curve for 250°C, at least, indicates an approach to this condition.

In Fig. 5 a subsidiary peak is observed between the first and second main maxima at the lower temperatures. The position of this small maximum changes in a regular manner with change in temperature although its direction of displacement is contrary to that for the other peaks. This fact, together with the further one that all the low temperature atomic distributions showed this subsidiary maximum, indicate that the effect is real and not one arising out of mathematical discrepancies in the Fourier analysis. A possible reason for its shift is that the "defence" of the volume of the first shell by the closest neighbors breaks down as the temperature is raised, permitting the closer approach of a few atoms, an effect which is observable until finally the broadening of the principal peak obscures the minor one.

A consideration of the mathematical theory behind the calculation of a distribution function such as that plotted in Fig. 5 will indicate that no simple relationship exists between the positions of maxima or minima in the experimental intensity pattern and the peaks in the final atomic distribution function. Determination of a most probable distance, d, by means of the Bragg equation from the intensity peak positions gives values which do not correspond at all to those obtained by the Fourier method. Most probable interatomic distances in a liquid cannot be determined by a gross inspection of an intensity pattern for this reason, and a more careful mathematical analysis should be made before far-reaching conclusions concerning liquid structures are drawn.

Some applications of the results reported here will be presented in a later paper.

The authors are indebted to Professor J. H. Hildebrand for his suggestion of the problem and for his continued encouragement throughout the experimental work. They also wish to thank Professors F. A. Jenkins and Robert B. Brode of the Department of Physics who made possible the use of the microphotometer, the ratiometer and the Bardsley harmonic analyzer; the latter, also, for his many helpful suggestions in experimental details.

[14] L. W. McKeehan and P. P. Cioffi, Phys. Rev. **19**, 444 (1922); H. Terrey and C. M. Wright, Phil. Mag. **6**, 1055 (1928); M. Wolf, Zeits. f. Physik **53**, 72 (1929).

The Variation of the Differential Diffusion Constant of Hydrochloric Acid with Temperature

W. A. JAMES* AND A. R. GORDON
Chemistry Department, University of Toronto, Toronto, Ontario, Canada

(Received June 29, 1939)

The differential diffusion constant of hydrochloric acid has been determined at temperatures ranging from 10°C to 35°C. At 10° and at 15°, the variation of the diffusion constant with concentration is given by the relation $k=k_0(1+c\partial \ln f/\partial c)\cdot(\eta_0/\eta)$ only up to about 0.2 normal. The activation energy of diffusion for concentrations less than $0.2N$ is practically independent of acid concentration; it decreases with increasing temperature, and is of the order of magnitude of the activation energy of viscous flow. For higher concentrations, the activation energy increases with increasing acid concentration.

A RECENT communication[1] from this laboratory reported the values of the differential diffusion constants for hydrochloric and sulphuric acids at 25°C, obtained by means of measurements carried out in Northrop-McBain diffusion cells. The present paper gives the results of similar measurements on hydrochloric acid carried out at temperatures ranging from 10°C to 35°C; our reason for undertaking this work was the comparative lack[2] of information in the literature as to the temperature coefficients of differential diffusion constants. Such information is definitely needed in the light of recent theories[3, 4] of solutions and of the liquid state in general.

The apparatus, the technique of the measurements, and the method of analysis by interferometer were previously described;[1] the only difference in the work reported here was that heavy rubber rings were inserted between the diffusion cell and its surrounding vessel containing the weaker solution, in order to minimize chance of evaporation. As in the previous work, the cells were recalibrated after every three or four runs with acid by allowing $0.1N$ KCl at 25°C to diffuse into water; as before, the value of $\bar{k}$ used for calibration[5] was 1.842×10^{-5} cm²/sec.

Table I summarizes the results; the second column gives the mean value of the initial concentration of the stronger solution inside the cell, expressed in moles per liter; the third, the initial concentration of the weaker solution in the outer compartment; the fourth gives the square root of the mean concentration of the experiment, i.e., the concentration for which the differential diffusion constant has been measured. The fifth column gives the mean diffusion constant, computed by the McBain relation (Eq. (2), reference 1); the entries in this column are in each case the average obtained from four measurements each with a different cell; as a rule, the individual measurements showed a mean absolute deviation from the mean of considerably less than one percent.

TABLE I.

°C	c_0'	c_0''	$((c_0'+c_0'')/2)^{\frac{1}{2}}$	$10^5\cdot k$	$F(f,\eta)$	$10^5\cdot k_{\text{CALC}}$
10	0.0392	0	0.140	2.05	0.951	2.05
10	.0866	0	.208	2.03	.942	2.03
10	.1471	0.0548	.318	2.05	.940	2.03
10	.405	0.308	.597	2.11	.998	2.16
15	.0466	0	.153	2.34	.948	2.35
15	.0988	0	.222	2.33	.940	2.33
15	.1519	0.0521	.320	2.33	.938	2.33
15	.202	0.103	.390	2.35	.945	2.34
15	.403	0.306	.596	2.37	.991	2.46
15	.705	0.603	.809	2.51	1.071	2.66
15	1.015	0.914	.982	2.67	1.161	2.88
35	0.0501	0	.158	3.62	0.943	3.65
35	.0936	0	.216	3.64	.935	3.62
35	.1000	0	.224	3.60	.934	3.61
35	.1205	0.0346	.279	3.63	.931	3.60
35	.153	0.051	.320	3.61	.932	3.61
35	.204	0.103	.392	3.68	.936	3.62
35	.226	0.127	.420	3.64	.939	3.63
35	.405	0.302	.595	3.76	.975	3.77

* Holder of a bursery granted by the National Research Council of Canada.

[1] W. A. James, E. A. Hollingshead and A. R. Gordon, J. Chem. Phys. **7**, 89 (1939).
[2] H. S. Taylor, J. Chem. Phys. **6**, 331 (1938).
[3] H. Eyring, J. Chem. Phys. **4**, 283 (1936).
[4] M. J. Polissar, J. Chem. Phys. **6**, 833 (1938).
[5] A. R. Gordon, J. Chem. Phys. **5**, 522 (1937); G. S. Hartley and D. F. Runnicles, Proc. Roy. Soc. **A168**, 401 (1938); see also reference 1.

TABLE II. $10^5 \cdot k$ *for hydrochloric acid.*

c	10°	15°	25°	35°
0	2.16	2.48	3.14	3.87
0.02	2.05	2.35	2.97	3.66
.05	2.02	2.33	2.93	3.61
.10	2.03	2.33	2.92	3.60
.20	2.05	2.35	2.98	3.65
.35	2.11	2.40	3.06	3.77
.50		2.45	3.18	
0.75		2.56	3.37	
1.00		2.68	3.58	

The relation previously proposed by one of us[6]

$$k = (k_0/2RT) \cdot (c\partial\mu_2/\partial c) \cdot (\eta_0/\eta) = k_0 \cdot (1 + c\partial \ln f/\partial c) \cdot (\eta_0/\eta) = k_0 \cdot F(f, \eta) \quad (1)$$

has been shown to represent the variation of the diffusion constant of hydrochloric acid with concentration at 25° reasonably closely, although the value of k_0 (the diffusion constant at infinite dilution) required to fit the data was six percent less than the Nernst value. The sixth column of Table I gives the values of the thermodynamic-viscosity factor $F(f, \eta)$ for the concentrations and temperatures of the table. Values of $(1 + c\partial \ln f/\partial c)$ were obtained from the data of Harned Ehlers[7] (see Eq. (3), reference 2). The viscosity data for the lower temperatures are from *International Critical Tables;* for 35°, there are apparently no data as to relative viscosities for hydrochloric acid solutions in this range of concentration. Since for the present purpose no high precision in the viscosity was required, the relative viscosity at 35° for solutions 0.516 and 1.041 molal was determined in an Ostwald viscosimeter, the resulting values being 1.038 and 1.071; measurements with this apparatus at 25° gave results agreeing with those in *International Critical Tables* within the estimated limit of error of the tables. From these results (after conversion to volume concentrations) the values of η_0/η for the concentrations of Table I were obtained by graphical interpolation.

If k_0 of Eq. (1) be computed from the observed values of k by means of the relation $k_0 = k/F(f, \eta)$, it is found that at the higher concentrations for both 10° and 15° there is a definite drift in k_0. If only the lower concentrations are considered at these two temperatures, the values of k_0 listed in the first line of Table II are obtained. This drift is illustrated in the last column of Table I where, under the heading k_{calc}, are recorded the values of k computed from these k_0 by the relation $k_{calc} = k_0 \cdot F(f, \eta)$. Fig. 1 shows graphically the data of the table, as well as the previous results[1] obtained for 25°C; here the broken lines correspond to the last column of Table I. Whether this deviation from Eq. (1) is due to the increasing abnormality of water as a solvent with decreasing temperature, or whether the agreement found at 25° for the higher concentrations is fortuitous, can only be settled by further experimental work. Table II gives for round values of the concentration values of k corresponding to the continuous curves of Fig. 1.

According to modern theories of solutions, the tangent to a plot of log k against $1/T$ should yield a value of the activation energy of diffusion. Results of such plots of our data show that up to $0.2N$, the activation energy is (for a given temperature) independent of the acid concentration within the limit of error of the measurements. As Taylor[8] found in the case of mannitol solutions, the plots are definitely curved towards the $1/T$ axis, the corresponding mean activation energies for the ranges 10°–15°, 15°–25°, 25°–35° being 4.4, 4.0 and 3.8 kcal., respectively. Thus, just as with mannitol, there is a decrease in activation energy with rising temperature, the decrease being less rapid the higher the temperature. It is also of interest to note that the

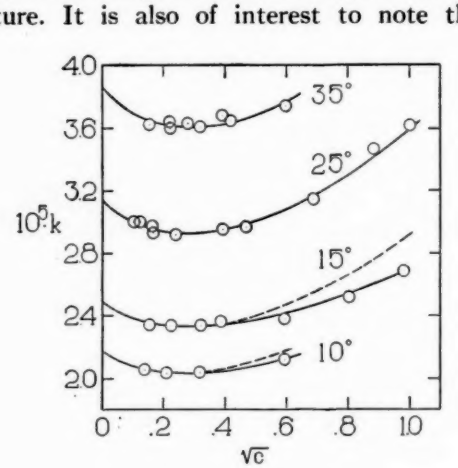

FIG. 1.

[6] A. R. Gordon, J. Chem. Phys. **5**, 522 (1937). The notation is that of Eq. (3) of reference 1.

[7] H. S. Harned and R. W. Ehlers, J. Am. Chem. Soc. **57**, 27 (1935).

activation energies for hydrochloric acid are from 0.5 to 1.0 kcal. less than are the corresponding values for mannitol, and in fact are approximately those for the activation energy of viscous flow.[8] At higher concentrations, however, the activation energy depends on concentration; thus for the range 15°–25°, the values are 4.2, 4.4, 4.7_5 and 5.0 kcal. for 0.35, 0.50, 0.75 and 1.00 normal solutions, respectively.

In conclusion, we wish to express our thanks to the National Research Council of Canada for the grant to one of us (W.A.J.) of a bursery.

[8] R. H. Ewell and H. Eyring, J. Chem. Phys. **5**, 726 (1937).

OCTOBER, 1939 JOURNAL OF CHEMICAL PHYSICS VOLUME 7

The Vibrational Spectra of 1,2 Dihalogen Ethanes and the Question of Internal Rotation

TA-YOU WU
Department of Physics, National South-West Associated University, Kun-ming, China
(Received July 10, 1939)

On symmetry considerations, it is shown that a satisfactory assignment can be given to *all* the observed infra-red and Raman frequencies of the 1,2 dihalogen ethanes provided both the *cis*- and the *trans*-forms are assumed to exist. The potential functions for the internal rotation in such molecules derived from the temperature variation of the electric moments and from electron diffraction measurements are such, however, as to give a negligibly small number of molecules in the *cis*-configuration which is unstable. A suggestion is made to account for the apparent difference between the spectroscopic and the other evidences.

IN view of the interest in the question concerning the internal rotation in the 1,2 dihalogen ethanes, the study of the temperature variations of the electric moments,[1, 2] the electron diffraction measurements of the intramolecular distances[3] and the investigations of the Raman and the infra-red spectra of these molecules[4, 5] have been taken up by a number of workers. Both the electric moment and the electron diffraction data seem to be consistent with a potential $V(\varphi)$ for the relative orientation φ of the two CH_2X groups having a minimum at the *trans*-position which is about 6–7 kcal./mole below the maximum at the *cis*-position. On the other hand, both the Raman and the infra-red data show that in liquids at ordinary temperatures, both the *trans*- and the *cis*-forms exist—the *cis*-form in a proportion which is far greater than is given by the Boltzmann factor corresponding to the above difference between the energies of the configurations. As the assignments of the frequencies given by Cheng and Lecomte[4] and also Cabannes[5] are based on regarding the CH_2X-CH_2Y molecule as a four-particle system $X-(CH_2)-(CH_2)-Y$ possessing only six fundamental frequencies in the region between 500 and 1400 cm^{-1}, objection might be raised against the incompleteness of the identification of the spectra of the two forms. In fact, the assignments given by these and other authors will be shown to be not entirely correct. In the following, we shall show, however, that the existence of both forms can be even more definitely established by a more detailed classification of all the observed frequencies.

On treating the XCH_2-CH_2X molecule as an eight-atomic system, we obtain readily the symmetrical properties and the selection rules for the normal vibrations of both the *trans*- and the *cis*-forms. They are given in Table I.

[1] C. T. Zahn, Phys. Rev. **38**, 521 (1931); **40**, 291 (1932); E. W. Greene and J. W. Williams, *ibid.* **42**, 119 (1932).
[2] W. Altar, J. Chem. Phys. **3**, 460 (1935); J. Y. Beach and D. P. Stevenson, *ibid.* **6**, 635 (1938).
[3] J. Y. Beach and K. J. Palmer, J. Chem. Phys. **6**, 639 (1938); J. Y. Beach and A. Turkevich, J. Am. Chem. Soc. **61**, 303 (1939).
[4] H. C. Cheng and J. Lecomte, J. de phys. et rad. **6**, 477 (1935).
[5] H. C. Cheng, J. chim. phys. **32**, 715 (1935); Kohlrausch and Ypsilanti, Zeits. f. physik. Chemie **B29**, 79 (1935); B. Trumpy, Zeits. f. Physik **93**, 624 (1935); Ananthakrishnan, Proc. Ind. Acad. Sci. **A5**, 285 (1937); J. Cabannes, J. chim. phys. **35**, 1 (1938); S. Mizushima and Y. Morino, Bull. Chem. Soc. Jap. **13**, 182 (1938).

TABLE I.

C_{2v} (*cis*)					C_{2h} (*trans*)			
SYMMETRY CLASS σ^*		v	NO. OF VIBS.	RAM. INF.	SYMMETRY CLASS σ	$i\dagger$	NO. OF VIBS.	RAM. INF.
A_1	s	s	6	p act.	A	s s	6	p ina.
B_1	s	a	5	d act.	B	s a	5	ina. act.
B_2	a	s	3	d act.	B'	a s	3	d ina.
A_2	a	a	4	d ina.	A'	a a	4	ina. act.

* σ is the plane of XCCX.
† i is the center of symmetry.

An important difference between the spectra of the two forms is the complementary nature of the infra-red and the Raman spectra of the *trans*-form. On consideration of these selection and polarization rules and also of the observation by Mizushima and Morino[5] that certain frequencies (marked with * in Table II) do not disappear in passing from the liquid to the solid state at −40°C and are to be ascribed to the *trans*-form of the molecules,[6] it is possible to give a classification of the observed frequencies summarized in Table II.[7] The suggested assignments are given in Tables III and IV.

The assignments of the frequencies in Tables III and IV are guided by the following rough considerations of the nature of the various normal vibrations. In class A or A_1, one vibration is roughly a symmetrical valence vibration in the C−C bond, one in the C−X bonds, one the symmetrical valence vibration ν_1 in the CH_2 group, one the deformation vibration ν_2 in CH_2, one the deformation of the (CH_2) group with respect to C−C and C−X, and the last is the deformation of the (CH_2X) group with respect to the C−C axis. In class B or B_1, the five vibrations are essentially the same as the last five vibrations in the A or A_1 class, except that the vibrations in the two CH_2X groups are opposite in phase. In class B' or B_2, one vibration is roughly the antisymmetrical valence vibration ν_3 in the CH_2 group, one a turning of the CH_2 group about the bisector of the H−C−H angle, and one a bending of the molecule in directions perpendicular to the plane of X−C−C−X, each CH_2X group acting more or less as a rigid group. In class A' or A_2, three of the vibrations are the out-of-phase vibrations of the three in the class B' or B_2, and the last is a torsional oscillation of the two CH_2X groups relative to each other.

It is seen from Tables III and IV that the data are incomplete, especially in the case of the C_2H_4ClI and $C_2H_4I_2$. The line 3002 in $C_2H_4Cl_2$ and that at 3012 cm in $C_2H_4Br_2$ have been assigned to more than one normal vibrations because these two lines were found to be broad and it is possible that they are really due to more than one lines whose frequencies are very close together. The strong line at 2956 cm^{-1} in $C_2H_4Cl_2$ is also broad. The presence of the weak and polarized lines 2872 in *trans*-$C_2H_4Cl_2$ and 2852 in *trans*-$C_2H_4Br_2$ (i.e., in the solid at −40°C) can be explained as arising from a resonance between the A fundamental and the harmonic of the B' fundamental at *ca.* 1440 cm^{-1}. Apart from the incompleteness, the assignments given here seem satisfactory from the view of the selection rules, the order of magnitude of the frequencies, and the trend in passing from $C_2H_4Cl_2$ to $C_2H_4I_2$.[8]

From the Raman and the infra-red spectra, it seems that both the *trans*- and the *cis*-configurations are populated in the liquids at ordinary temperatures; and from the intensities of the Raman lines and absorption bands, it appears that the number of molecules in the *cis*-configura-

[6] That only the *trans*-form is present at low temperatures s supported by the observation of A. H. White and S. O. Morgan, J. Chem. Phys. **5**, 655 (1937), that there are sudden drops in the values of the dielectric constants of the molecules at low temperatures.

[7] Cheng and Lecomte, reference 4, gave for $C_2H_4Br_2$ an infra-red frequency at 650 cm^{-1} in the diagram and tables in their paper. However, no trace of this absorption band can be found from their reproduced absorption curve for this molecule. Instead, an intense band is shown at 750 cm^{-1}. It seems that the value 650 resulted from an error in the calculation. Here we take the value 750 cm^{-1}. Because of the low dispersion in their work, the bands in the 1400 cm^{-1} (7μ) region in these molecules have only been approximately located. Hence the round number 1400 cm^{-1} is given in Tables II, III and IV. Similarly for the absorption bands in the region 3000 cm^{-1}.

[8] Y. Morino, Bull. Chem. Soc. Jap. **13**, 189 (1938), assigned the Raman lines 2956*p*, 1440*d*, 1301*p* in $C_2H_4Cl_2$ and 2970*p*, 1436*d*, 1256*p* in $C_2H_4Br_2$ to the totally symmetrical A fundamentals in the *trans*-molecules, and cited the work of Wu, J. Chem. Phys. **5**, 392 (1937), and of Trumpy, Nature **135**, 764 (1935), on C_2H_4 and *trans*-$C_2H_2Cl_2$. While the order of magnitude of the deformation frequencies is correct, his assignment cannot be correct in view of the polarization data. The lower values for these deformation frequencies suggested in Table III can be easily understood when one takes into consideration the coupling of the motions of all the atoms in the molecule and remembers that in C_2H_4, the deformation frequencies of CH_2 are 1344 for the symmetrical and 1444 for the antisymmetrical vibrations. It is true that the 1051-cm^{-1} line in Table III does not have the correct polarization character, but it was marked doubtful by Trumpy so that a re-examination of this line may be desirable.

TABLE II. *Vibrational spectra of 1.2 dihalogen derivatives of ethane. Numbers in parentheses are the relative intensities; p = polarized; d = depolarized; s = strong; m = medium; w = weak; vw = very weak.*

$C_2H_4Cl_2$		C_2H_4ClBr		$C_2H_4Br_2$		C_2H_4ClI		$C_2H_4I_2$	
RAMAN	INFRA	RAMAN	INFRA	RAMAN	INFRA	RAMAN	INFRA	RAMAN	INFRA
123(4)*d*				92(2)*d*					
263(2)*p*		246(8)*p*		230(1)*p*					
*302(8)*p*		211($\frac{1}{2}$)*p*		*189(10)*p*					
411(3)*d*		386(1)*d*		359(2)*d*		365			
654(10),	656*s*	568(8)*p*	569*s*	551(8)*p*	550*s*	510			
675(3)*d*	676*s*	630(8)*p*	631*s*	583(2)*d*	587*s*	574	576*s*	512	
	707*s*	662(2)*d*	664*w*			655	655*s*		635*s*
*754(15)*p*		720(15)*p*	722*s*	*659(15)*p*		703	702*s*	582	
	759*w*		756*w*		750*s*		740*w*		720*s*
880(1)*d*	878*m*	852	858*m*	834($\frac{1}{2}$)*d*	834*s*		817*m*		778*m*
940(2)*p*	940*m*	919(1)*p*	917*m*	897(1)*p*	896*m*	904	896*w*		840*w*
*989(1)				*930(1)*p*					
1031(1)	1015*w*		1020*w*	1019($\frac{1}{2}$)?					
*1052(1)*p*		1050		*1052(6)*d* ?		1040	1030*w*		
	1092*vw*		1090*vw*		1075*vw*				1040*w*
1144($\frac{1}{2}$)*d*		1120		1086 ?					
1206(2)*d*		1180				1150			
	1243*m*	1200	1201*m*		1191*s*		1132*m*		1128*s*
*1262(1)*d*				*1169($\frac{1}{2}$)*d*					
*1302(3)*p*		1280		*1256(10)*p*		1270			
1393($\frac{1}{2}$)				1295(1)*p*					
1429(3)*d*	1400*m*		1400*m*	1419(1)*d*	1400*m*		1400*m*		1400*m*
*1440($\frac{1}{2}$)*d*				*1436(2)*d*					
2844(1)?									
*2872(1)*p*				*2852(1)*p*					
				2950(6)*p*					
*2956(12)*p*	3000		3000	*2970(8)*p*	3000		3000		3000
*3002(4)*d*				*3012(2)*d*					
				132(2)?					
				320($\frac{1}{2}$)?					
				470($\frac{1}{2}$)?					
				790(0)?					

tion is not very much smaller than that in the trans-configuration. That the *trans*-form is more stable is consistent with the observation of Mizushima and his co-workers[9] that the ratio of the intensities of the Raman lines at 653 and 750 cm^{-1} in $C_2H_4Cl_2$ increases as the value of the dielectric constant of the solvent increases. But the existence of a definite spectrum satisfying the selection rules for the symmetry C_{2v} requires that the *cis*-position be a stable position of equilibrium.

From the observed increase of the electric moments of $C_2H_4Cl_2$, C_2H_4ClBr and $C_2H_4Br_2$ with the rise of temperature, Altar[2] and more recently Beach and Stevenson[2] have tried to determine the constants in a two-term Fourier series and a cosine function, respectively, for the potential $V(\varphi)$, it being assumed that the number of molecules with the two CH_2X groups at an angle φ is proportional to the Boltzmann factor $\exp(-V/kT)$. The potential so obtained has a minimum at the *trans*-position which is about 4–5 kcal./mole below the maximum at the *cis*-position. On the same assumption concerning the distribution of molecules according to the Boltzmann factor, Beach, Palmer and Turkevich[3] have calculated the intensity patterns of the diffracted electrons with a potential obtained by the method of Eyring for the calculation of the exchange repulsions in the ethane molecule,[10] and compared them with the observed intensity patterns. They found that after a semi-empirical correction that raises the potential near the *cis*-position by *ca.* 2 kcal./mole, the calculated patterns for $C_2H_4Cl_2$, C_2H_4ClBr, $C_2H_4Br_2$ approximate the observed ones quite well. These resulting potentials have minima at the *trans*-position at about 6–7 kcal./mole below the maxima at the *cis*-position. With these potentials, however, the appearance of the Raman

[9] S. Mizushima *et al.* Physik. Zeits. **35**, 905 (1934); **36**, 600 (1935).

[10] E. Eyring, J. Am. Chem. Soc. **54**, 3191 (1932).

TABLE III. *Fundamental frequencies of trans 1,2 dihalogen ethanes. The notations for the vibrations in parentheses are those of Cheng and Lecomte.*

A	ν_{C-C} (ω_1') Raman	Infra	ν_{C-X} (ω_2') Raman	Infra	ν_1 in CH_2 Raman	Infra	ν_2 in CH_2 Raman	Infra	δ (CH_2) Raman	Infra	δ (CH_2X) (ω_3') Raman	Infra
Br−Br	930*p*	—	658*p*	—	2970*p*	—	1256*p*	—	1051*d*?	—	187*p*	—
Br−Cl			720*p*	722			1280		1050		211*p*	
Cl−Cl	990	—	750*p*	—	2956*p*	—	1302*p*	—	1052*p*	—	300*p*	—
Cl−I			703	702			1270		1040	1030		
I−I		—	582	—		—		—		—		—

B	ν_{C-X} (ω_4')		ν_1 in CH_2		ν_2 in CH_2		δ (CH_2)		δ (CH_2X) (ω_5')
Br−Br	—		—	3000	—	1400	—	1075	—
Br−Cl	662*d*	664	—	3000	—	1400	—	1090	
Cl−Cl	—	707	—	3000	—	1400	—	1092	—
Cl−I	655	655		3000		1400			
I−I	—	635	—	3000	—	1400	—	1040	—

B'	ν_3 in CH_2		Turning of CH_2		$\delta'(CH_2X)$	
Br−Br	3012*d*	—	1436*d*	—	1169*d*	—
Br−Cl						
Cl−Cl	3002*d*	—	1440*d*	—	1265*d*	—
Cl−I						
I−I		—		—		—

A'	ν_3 in CH_2		Turning of CH_2		$\delta(CH_2X)$		Torsion (ω_6')
Br−Br	—	3000	—	1191	—	750	—
Br−Cl		3000	1200	1201		756	
Cl−Cl	—	3000	—	1243	—	760	—
Cl−I		3000		1132		740	
I−I	—	3000	—	1128	—	720	—

TABLE IV. *Fundamental frequencies of cis 1,2 dihalogen ethanes.*

A_1	ν_{C-C} (ω_1) Raman	Infra	ν_{C-X} (ω_2) Raman	Infra	ν_1 in CH_2 Raman	Infra	ν_2 in CH_2 Raman	Infra	$\delta(CH_2)$ Raman	Infra	$\delta'(CH_2X)$ (ω_3) Raman	Infra
Br−Br	897*p*	896	551*p*	550	2950*p*	3000	1295*p*		1019?	1000	230*p*	
Br−Cl	919*p*	917	568*p*	569		3000					246*p*	
Cl−Cl	940*p*	940	653*p*	653	2956*p*	3000	1393?	1400	1031?	1015	264*p*	
Cl−I	904	896	510			3000						
I−I		840				3000						

B_1	ν_{C-X} (ω_4)		ν_1 in CH_2		ν_2 in CH_2		$\delta(CH_2)$		$\delta(CH_2X)$ (ω_5)
Br−Br	583*d*	587	3012*d*	3000	1419*d*	1400	1086?		358*d*
Br−Cl	630*p*	631		3000		1400	1120?		386*d*
Cl−Cl	675*d*	675	3002*d*	3000	1429*d*	1400	1144*d*		411*d*
Cl−I	574	576		3000		1400			365
I−I	512			3000		1400			

B_2	ν_3 in CH_2		Turning of CH_2	$\delta'(CH_2X)$	
Br−Br	3012*d*	3000		834*d*	834
Br−Cl		3000		852	858
Cl−Cl	3002*d*	3000		880*d*	880
Cl−I		3000			817
I−I		3000			778

A_2	ν_3 in CH_2		Turning of CH_2		$\delta'(CH_2X)$		Torsion (ω_6)	
Br−Br	3012*d*	—			1187?	—	92*d*	—
Br−Cl					1180			
Cl−Cl	3002*d*	—		—	1206?	—	123*d*	—
Cl−I					1150			
I−I		—		—		—		—

lines and absorption bands in Table IV becomes difficult to understand. The Boltzmann factor at room temperatures for the energy difference of 6–7 kcal./mole is so small that no Raman lines of the *cis*-form should have been observable at all.

To understand this apparent contradiction, one may suppose that in the liquid, the high value of the dielectric constant (*ca.* 10 at 22°C) of $C_2H_4Cl_2$ considerably reduces the electrostatic repulsion between the two halogen atoms so that the potential energy difference between the *trans*- and the *cis*-position is somewhat lower than the above value demanded by the electron diffraction data for the vapor. In fact, Mizushima and his co-workers[9] found that the electric moments of the dihalogen ethanes increase as the dielectric constant of the solvent increases. But any great change in the potential energy of the two CH_2X groups would imply some shifts in the frequencies of certain vibrations in passing from the liquids to the vapors, or in fact from solutions of these molecules in one solvent to solutions in a different solvent. It is also possible, however, that the theoretical potentials calculated by Beach, Palmer and Turkevich may not be correct, since the same method of calculation is now known to lead to a result in complete disagreement with evidences from specific heat and entropy measurements in the case of the ethane molecule.[11] The calculated potential in this case has minima in the D_{3d} configuration, which are about 300 cal./mole below the maxima in the D_{3h} configuration, while the thermal data at low temperatures (down to 100°K) require a potential barrier of the order of 3000 cal./mole between the D_{3d} and the D_{3h} configurations. Evidences from the vibrational spectrum seem to prefer the D_{3h} symmetry for the molecule in contradiction to the calculated potential.[12] It is true that the cause for the great discrepancy between the calculated and the empirical potentials is not yet understood. But if we accept the high value 3000 cal./mole for the potential barrier and the D_{3h} symmetry for the molecule, and if we apply a fraction of this empirical potential as a "correction" to the one calculated for the dihalogen ethanes,[13] then there would result a relative minimum at the *cis*-position, which is still very much higher than the minimum at the *trans*-position. Such a potential can still be consistent with the temperature variation of the electric moment and the electron diffraction data, since these are essentially determined by the Boltzmann factor and the value of this factor is still small for small values of the angle φ with this "corrected" potential. There are the following differences, however, namely, that the *cis*-configuration is one of stable equilibrium and molecules in this configuration will give rise to a vibrational spectrum characteristic of the symmetry C_{2v}. This enables us to explain the depolarized Raman lines at 92 cm^{-1} in $C_2H_4Br_2$ and 123 cm^{-1} in $C_2H_4Cl_2$ as the torsional frequencies in these molecules about the *cis*-position.[14] These frequencies also place the heights of the potential barriers in these molecules at *ca.* 300–400 cm^{-1} (*ca.* 1000 cal./mole) above the minimum at the *cis*-position, in agreement with the empirically corrected potentials estimated above.[13]

Also, because of the potential barrier between the *cis*- and the *trans*-configurations, an activation energy is necessary to transform one form into the other. Consequently, in a liquid at ordinary temperature the relative numbers of molecules in the two configurations may not necessarily be the equilibrium ratio given by the Boltzmann factor for that temperature. Rather one may expect a dependence of the relative populations of the two forms, and hence of the electric moment, at a given temperature, on the previous treatment of the liquid such as by irradiation with ultraviolet radiations or other activating agents. The discrepancies in the values

[11] Cf. K. Schäfer, Zeits. f. physik. Chemie **B40**, 357 (1938); J. D. Kemp and K. S. Pitzer, J. Am. Chem. Soc. **59**, 276 (1937); E. B. Wilson, J. Chem. Phys. **6**, 408, 740 (1938); Kistiakowsky, Lacher and Stitt, *ibid.* **6**, 407 (1938); and references given in these papers.

[12] For a discussion of the Raman and infra-red spectra of C_2H_6, see Avery and Linnett, J. Chem. Phys. **6**, 682 (1938); Karweil and Schäfer, Zeits. f. physik. Chemie **B40**, 382 (1938).

[13] In 1,2 $C_2H_4Cl_2$, there are only 4 pairs of interacting H atoms while there are 9 pairs in C_2H_6. We may quite arbitrarily reduce the maxima at the $\pi/3$ and $5\pi/3$ positions in C_2H_6 by one-half and the maximum at π by a still somewhat greater amount, and regard the resulting potential as the "empirical" potential arising from the interactions between the H atoms in $C_2H_4Cl_2$.

[14] That these lines are not present in the crystals at −40°C forces one to ascribe them to the *cis*-forms; and as seen from Table IV, there is no other place for such a low frequency fundamental besides the torsional vibration. There is no simple way of assigning them to difference frequencies; in fact their intensities seem too great for scattering by molecules already in an excited state.

of the electric moments of $C_2H_4Cl_2$, C_2H_4ClBr, $C_2H_4Br_2$ as observed by different authors[1] may of course be due to experimental errors; but it is not impossible that they have their origin in the different conditions under which the substances have been previously treated. It would be desirable to have accurate measurements of the electric moment of such a liquid at a definite temperature after treating it with different activating agents, or to study the relative intensities of the *trans*- and the *cis*-bands of the vapor and the liquid after similar treatments.

OCTOBER, 1939 JOURNAL OF CHEMICAL PHYSICS VOLUME 7

The Significance of Activation Entropy in Catalytic Mechanisms

ALLEN E. STEARN, H. P. JOHNSTON AND CHAS. R. CLARK
University of Missouri, Columbia, Missouri

(Received April 10, 1939)

IN absolute reaction rate theory the rate depends in a specific way on two important quantities, the heat of formation of the activated complex, and its entropy of formation.[1] The equation is formulated

$$k' = \kappa \frac{kT}{h} e^{\Delta S^{\ddagger}/R} e^{-\Delta H^{\ddagger}/RT} = \kappa \frac{kT}{h} e^{-\Delta F^{\ddagger}/RT}. \quad (1)$$

The symbols have been repeatedly defined. Confining oneself to homogeneous reactions and excluding chain mechanisms, it is evident that any rate of reaction measures the concentration of the activated complex, which always decomposes with a frequency $\kappa kT/h$. In general, then, any catalyst must either affect the activity coefficients of the reactants or must become a part of the activated complex of the rate-determining step (or may do both). In no other sense do preliminary equilibria matter.[2] It has already been pointed out[3] that in the case of certain reactions in mixed solvents of varying dielectric constant $\Delta H^{\ddagger}$ may vary greatly but there is a compensating change in $\Delta S^{\ddagger}$ so that $\Delta F^{\ddagger}(=\Delta H^{\ddagger}-T\Delta S^{\ddagger})$ is held more nearly constant. The less effective this compensating mechanism is, the greater the catalytic effect of that particular solvent with respect to some reference solvent. The chemical mechanism of this type of action by any catalyst may be crudely pictured by the following set of equilibria. The symbol R refers to reactant, X is catalyst, A is activated complex in absence of catalyst, and P is reaction product. Two general cases arise: (1) The catalyst is more strongly bound to R than to A. Here the formation of the activated complex involves the breaking of catalyst-reagent bonds with consequent increase in $\Delta H^{\ddagger}$. The freeing of the catalyst will, however, cause a compensating increase in $\Delta S^{\ddagger}$. (This is shown by path "b" in the diagram.) (2) The

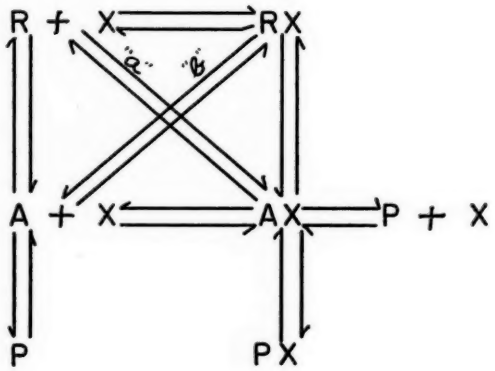

catalyst is more strongly bound to A than to R. Here the formation of catalyst bonds with the ordinary activated complex will lower $\Delta H^{\ddagger}$ but the tying up of catalyst will involve a compensating decrease in $\Delta S^{\ddagger}$ (path "a" in the diagram). When these compensating factors are equal, i.e., the changes in $\Delta H^{\ddagger}$ and in $T\Delta S^{\ddagger}$, there will be no net change in $\Delta F^{\ddagger}$ and thus no effect on reaction rate. Otherwise there is catalysis. Whether it is positive or negative depends on which factor predominates. In case 1 when the effect on $\Delta H^{\ddagger}$

[1] W. F. K. Wynne-Jones and H. Eyring, J. Chem. Phys. **3**, 492 (1935).

[2] A possible exception might be a large shift in a preliminary equilibrium which is *maintained* during the reaction.

[3] Allen E. Stearn and H. Eyring, J. Chem. Phys. **5**, 113 (1937).

predominates, we have negative catalysis. (Taylor's theory[4] of negative catalysis implies this condition.) When $\Delta S^{\ddagger}$ is predominantly affected we have positive catalysis. For case 2 just the opposite is true. The above scheme covers the effect of catalyst both on the activity of the reactant and on the activated complex.

A few examples of these conditions are collected in Table I. Here the values of $\Delta H^{\ddagger}$ were obtained from the relation

$$\Delta H^{\ddagger} = RT^2 \frac{d \ln k'}{dT} - RT,$$

and those of $\Delta S^{\ddagger}$ from values of $\Delta H^{\ddagger}$ substituted in Eq. (1). k' is the rate constant in reciprocal seconds. The four sets of conditions are exemplified as follows: (a) Case 1 with increase in $\Delta H^{\ddagger}$ predominating, and negative catalysis, the example is reaction 5b. Even here the compensation shown in the increase in $\Delta S^{\ddagger}$ is nearly complete. Were it not for this we would calculate a value of k' of the order of 10^{-35} for the catalyzed reaction in place of the observed 10^{-5}. (b) Case 1 with increase in $\Delta S^{\ddagger}$ predominating, and positive catalysis, examples are 5a and 1. Reactions 5a and 5b are of interest as in both cases the catalyst, as given in the table, increases $\Delta H^{\ddagger}$ by almost exactly the same amount, 43,000 calories. This by itself, at 60°C would correspond to a decrease in k' by about 10^{28}. In 5b this is slightly undercompensated by the factors involved in $\Delta S^{\ddagger}$ so that a net decrease in k' of 14 times results. In 5a the same effect is highly overcompensated so that the catalyzed reaction at 33°C proceeds at about the same rate as the uncatalyzed reaction at 60.5°C. (If it were legitimate to extrapolate from 60.5 to 33°, we should find a catalytic effect of about 10^4.) Reaction 1 shows a positive catalytic effect of about 6000 with slight change (if anything an increase) in $\Delta H^{\ddagger}$. The entire effect is thus born by the $\Delta S^{\ddagger}$ factor. (c) Case 2 with decrease in $\Delta H^{\ddagger}$ predominating, and positive catalysis, is exemplified by the extreme case of reaction 4. These conditions represent the mechanism of catalysis ordinarily pictured. (d) Case 2 with decrease in $\Delta S^{\ddagger}$ predominating, and negagive catalysis, is exemplified by reactions 2 and 3. They show a decrease in k' produced by catalyst, accompanied by a small though, it is thought, a real decrease in $\Delta H^{\ddagger}$. The positive catalytic effect which would be ordinarily expected from the decrease in $\Delta H^{\ddagger}$ is more than compensated by the decrease in $\Delta S^{\ddagger}$.

[4] H. S. Taylor, J. Phys. Chem. **27**, 332 (1923).

TABLE I.

No.	Reaction	Order	Catalyst	Catalyst Conc.	pH	T°C	$k'_{sec.^{-1}}$	$\Delta H^{\ddagger}$	$\Delta S^{\ddagger}$	Ref.
1	Xanthogenic acid decomposition	1	alcohol	0.00	—	25.	2.7×10^{-7}	13,290	−44.0	5
				1.0	—	25.	1.6×10^{-3}	13,670	−25.4	
2	Decomp. of malic acid by H_2SO_4	1	H_2O	0.00	—	30	4.8×10^{-4}	24,010	5.6	6
				0.93	—	30	1.2×10^{-4}	21,550	−5.3	
3	Addition of amylene to CCl_3COOH	2	acetone	0.00	—	20	1.5×10^{-5}	17,350	−21.3	7
				1.04	—	20	5.5×10^{-7}	17,050	−28.6	
4	Denaturation of egg albumin	1	urea	0.00	5.9	65	2.5×10^{-4}	135,000	325.	8
				0.6 g/cc	5.9	23	$3.\times10^{-4}$	−3,000	−85.	9
5a	Denaturation of oxyhemoglobin	1	alcohol	0.0	6.5	60.5	2.3×10^{-4}	76,500	154.	10
				30 vol.%	6.5	33.	6.8×10^{-4}	120,100	319.	
5b	Denaturation of oxyhemoglobin	1	$(NH_4)_2SO_4$	0.001 *N*	6.76	64.	3.4×10^{-4}	76,500	153.	11
				3.03 *N*	6.76	64.	2.4×10^{-5}	119,800	276.	

[5] H. von Halban and A. Kirsch, Zeits. f. physik. Chemie **82**, 325 (1913).
[6] E. L. Whitford, J. Am. Chem. Soc. **47**, 953 (1925).
[7] Unpublished data from University of Missouri Dissertation by C. R. Clark.
[8] P. S. Lewis, Biochem. J. **20**, 978 (1926).
[9] F. G. Hopkins, Nature **126**, 383 (1930).
[10] N. Booth, Biochem. J. **24**, 1699 (1930).
[11] P. S. Lewis, Biochem. J. **20**, 984 (1926).

LETTERS TO THE EDITOR

This section will accept reports of new work, provided these are terse and contain few figures, and especially few halftone cuts. The Editorial Board will not hold itself responsible for opinions expressed by the correspondents. Contributions to this section should not exceed 600 words in length and must reach the office of the Managing Editor not later than the 15th of the month preceding that of the issue in which the letter is to appear. No proof will be sent to the authors. The usual publication charge ($3.00 per page) will not be made and no reprints will be furnished free.

The Effect of Baffles on the Thermal Separation of Gases

Various experiments have been carried out in this laboratory to determine the effect of chamber design on the efficiency of the thermal mechanism for the separation of gases and isotopes. A tube was used of the same general design as that described previously[1] except that it was equipped with a ground glass joint to permit the insertion of baffles. The chamber was made from concentric glass tubes 110 cm in length; the inner heated tube was 1 cm O. D. and the clearance between the hot and cold surfaces was 2 cm. The power input was 500 watts. Under these conditions a 50–50 ammonium-methane mixture gave a negligible separation. However, by the use of baffles it was possible to materially enhance the value of the separation factor.

One set of baffles was made by soldering 100 copper washers, 4 cm O. D. and 2 cm I. D. on three $\frac{1}{16}$" brass rods with a clearance of 1 cm between washers. The unit was mounted symmetrically between the hot and cold surfaces. In this chamber the separation factor was 1.18. Another type of baffle was made from 1-inch brass washers machined to fit tightly on the inner heated tube; the clearance between washers was 2.2 cm. The separation factor in this case was 1.35, a greater separation than any previously obtained with a tube of similar length.

An idea of the movement of the gases within the tube was obtained by depositing a uniform film of ammonium chloride on the walls before admitting the ammonium-methane mixture. Fig. 1 shows the condition of the deposit after several hours of operation. The ammonium chloride is now deposited on the outer wall in clearly defined striations placed symmetrically with respect to the baffles. The position of the striations shows that the hot gas moves directly across the tube from the heated to the cold surface and then back in well-defined swirls. The net effect of these movements is that the tube is crossed by a series of streams of hot gas, each contiguous to cold streams moving in the opposite direction. The character of the deposits excludes the possibility of any general mass movement down along the cold wall. Similar striations were observed in some of the concentric glass tubes already tested but were not noted in a tube with a fine heated wire extending down the center. The results indicate that the separation factor is enhanced by the definition of the swirls. A detailed account of this mechanism will be presented shortly.

FIG. 1. Striated deposit of ammonium chloride on the cold wall.

A. KEITH BREWER
ARTHUR BRAMLEY

Bureau of Agricultural Chemistry and Engineering,
U. S. Department of Agriculture,
Washington, D.C.,
September 4, 1939.

[1] Bramley and Brewer, J. Chem. Phys. **7**, 553 (1939).

Heterophase Fluctuations and Pretransition Phenomena

In a recent paper[1] J. Frenkel proposes a theory of fluctuations in the neighborhood of the melting point and other transition points. The phenomenon of "premelting" of crystals is defined as to the formation of small nuclei of the second (liquid) phase below the melting point. The author states that "The appearance of small nuclei of a new phase within a practically homogeneous substance (liquid or gaseous) has been admitted hitherto only in the case of undercooling or overheating, i.e., a thermodynamically unstable state." I wish, however, to draw attention to the fact that I have discussed this question already in a paper in 1922.[2] In the papers quoted by Frenkel in a preliminary note[3] attempts were made to treat the question with kinetic methods. On account of the difficulty of such a treatment, I—like Frenkel—used a thermodynamical reasoning using Einstein's method for calculation of fluctuations. The result of my considerations (formulae 1 and 2) were similar to those expressed in Eqs. (7*b*) and (8*a*) of Frenkel. A further development of the problem by Frenkel was done by taking into account the surface energy of the nuclei.

J. BRODY

Tungsram Research Laboratory,
Ujpest, Hungary,
August 3, 1939.

[1] J. Frenkel, J. Chem. Phys. **7**, 538 (1939).
[2] E. Brody, Physik. Zeits. **23**, 197 (1922).
[3] J. Frenkel, J. Chem. Phys. **7**, 200 (1939).

Fluorescence of Diacetyl: Quantum Yield and Quenching by Iodine

A considerable amount of work has been done on the fluorescence of diacetyl,[1, 2] but no measurements of quantum efficiency have been reported. Preliminary measurements of this quantity have just been completed. In the experiments the diacetyl was irradiated with filtered light from a small high pressure mercury arc at λλ4358, 4047 and 3650. The energy of the fluorescence was measured with a photo-cell and electrometer tube and the incident energy with a photronic cell. Both detectors were calibrated at appropriate wave-lengths against a thermopile whose sensitivity had been determined with the use of a standard lamp.

Absorption coefficients for the diacetyl and tube windows were determined at the appropriate wave-lengths and the energy absorbed in the region seen by the photo-cell calculated. The absorption coefficients per cm path per cm pressure, and the quantum yields, in quanta of fluorescence per quantum absorbed, are listed below. The probable error in quantum yield is about 10 percent at λ4358 and is somewhat higher for the shorter wave-lengths. Between 2 and 5 cm the yield is independent of pressure.

Exciting Wave-length	Abs. Coeff. Diacetyl	Quantum Yield
4358	0.0158	0.033
4047	0.0103	0.0058
3650	0.0042	0.029

The absorption spectrum of diacetyl exhibits discrete structure between 4600A and about 4100A; below 4100A it becomes continuous. Since this change of structure may be due to the onset of predissociation it is not surprising that the fluorescence yield at 4047A should be sharply less than at 4358A. It is surprising that the yield rises again at 3650A.

Iodine has been found to be very effective in the quenching of irradiated diacetyl. With the addition of only 0.007 mm pressure of iodine to 49 mm of diacetyl the intensity of the fluorescence excited by λ4358 was reduced to less than 3 percent of the fluorescence without iodine. From this and other similar observations it appears that the effective cross section for quenching by iodine is at least 50 to 100 times greater than for quenching by oxygen which also strongly quenches the fluorescence.[2]

With continued radiation the fluorescence showed a recovery. Upon irradiating the described mixture of diacetyl and iodine for 3 hours the fluorescence recovered to about 15 percent of the intensity without iodine. In another experiment with a low undetermined pressure of iodine (order of magnitude, 0.001 mm) complete recovery was obtained in 30 minutes.

Diacetyl at a pressure of 49 mm absorbs energy from the source used at the rate of about 2×10^{13} quanta per sec. per cc. Assuming that in 3 hours practically all of 0.007 mm of iodine is used, one can calculate that the total number of excited molecules quenched is 20 to 30 times the number of iodine molecules originally present. One interpretation of this result is that the iodine molecule can quench many excited molecules before it loses its identity. Iodine, which shows discrete absorption at wave-lengths greater than 5000A, may very well be excited by collision with a molecule which fluoresces in the same region. Close resonance may be responsible for the large effective cross section for quenching the diacetyl fluorescence. In further experiments we shall look for sensitized fluorescence of iodine.

H. Q. Fuller*
L. W. Phillips
G. M. Almy

Physics Department,
University of Illinois,
Urbana, Illinois,
August 31, 1939.

* At Albion College, Albion, Michigan.

[1] Matheson and Noyes, J. Am. Chem. Soc. **60**, 1857 (1938).
[2] Almy, Fuller and Kinzer, Phys. Rev. **55**, 238 (1939); more complete report of these experiments now in process of publication.